5-2021

Susceptibility of Riverine Fishes to Anthropogenically-linked Trauma: Strikes from Hydropower Turbine Blades

Ryan K. Saylor
University of Tennessee, Knoxville, rsaylor6@vols.utk.edu

To the Graduate Council:

I am submitting herewith a dissertation written by Ryan K. Saylor entitled "Susceptibility of Riverine Fishes to Anthropogenically-linked Trauma: Strikes from Hydropower Turbine Blades." I have examined the final electronic copy of this dissertation for form and content and recommend that it be accepted in partial fulfillment of the requirements for the degree of Doctor of Philosophy, with a major in Energy Science and Engineering.

Mark S. Bevelhimer, Major Professor

We have read this dissertation and recommend its acceptance:

Debra L. Miller, Ryan A. McManamay, Elizabeth D. Barker, Brenda M. Pracheil

Accepted for the Council:

Dixie L. Thompson

Vice Provost and Dean of the Graduate School

(Original signatures are on file with official student records.)

Susceptibility of Riverine Fishes to Anthropogenically-linked Trauma: Strikes from Hydropower Turbine Blades

A Dissertation Presented for the

Doctor of Philosophy

Degree

The University of Tennessee, Knoxville

Ryan Kurt Saylor

May 2021

DEDICATION

To my mother and father, Marcia and Lyndon, for always being supportive in every way that matters my entire life, thank-you. To my sons, Walter and Lyndon, never give up on your dreams, ever. I will always be here to support you both in exactly the same way as my parents. I hope you are proud to call me dad, because I am very proud to call you both my sons.

ACKNOWLEDGEMENTS

First and foremost, I must acknowledge Dr. Mark Bevelhimer for his continued, steadfast support and guidance throughout my dissertation research and writing—he was the best PhD adviser you could hope for. With his mentorship, I have been able to find my voice as a biologist, scientist, and teacher. He has truly shaped the scientist I am today: he helped guide me through a master's degree, and has now assisted with the completion of my PhD. I truly appreciate his willingness to communicate openly and often, such that our conversations always started with: "How are your sons?" or "How is the family?" He also insisted that I think for myself and allowed me remarkable freedom to design this dissertation, especially the last chapter, thank you for everything.

I must also acknowledge Dr. Debra Miller for her absolute commitment to scientific curiosity and willingness to always collect a "few samples" for histopathological analysis. She is truly a remarkable person and fantastic scientist, a genuine inspiration in every sense of the word. I wish to thank my remaining committee members as well, including Dr. Ryan McManamay, Dr. Elizabeth Barker, and Dr. Brenda Pracheil for their role in my dissertation journey these last few years.

I am also deeply grateful to Dr. Teresa Mathews for her role as my new mentor at Oak Ridge National Laboratory, especially her assistance with the Gelfish project which would be impossible without her guidance. She is also a fantastic scientist and inspirational leader that I aspire to emulate in my own scientific career. I must acknowledge Dr. Brennan Smith, Dr. Eric Pierce, and Dr. Stan Wullschleger for their fervent support of the Gelfish, which would have never come to fruition without their advocation for time and resources to help prove the concept was viable. I must also thank Dr. Brian Post and Dr. Peter Wang for their assistance with the state-of-the-art equipment and expertise at ORNL's Manufacturing Demonstration Facility, which made production of the Gelfish prototype possible.

I wish to thank the Bredesen Center, specifically Lee Riedinger and Suresh Babu, for their continued support during my collegiate pursuits at UT. Without Lee's support, I would have likely left the program years ago when I was requesting a leave of absence. I extend many thanks to other Bredesen Center graduate students including Piet Jones,

Armin Gieger, Ishita Ray, Edward Jones, and Carissa Blekker for their friendship and willingness to listen when I needed it the most.

I am very thankful to Dustin Sterling for all his help collecting most of the data described in this dissertation. I must also acknowledge all the interns, students, and staff within the Biodiversity and Ecosystem Health Group at ORNL for their constructive feedback and friendly demeanor, which made my long days in the laboratory a bit little easier. Successful completion of this dissertation was only possible because I was surrounded by some of best scientific minds available within my field. Luckily, these folks are also genuinely good people in every sense of the word as well.

Finally, I must thank my parents for remaining supportive of my career journey since I left Pennsylvania nearly 20 years ago. I know they do not always understand my motivation or even what I actually do, but they always remained supportive through all my ups and many downs. I also extend my love, support, and thanks to my sons who inspire me every day.

My success is your success, and was only possible because I had your support. Thank-you all for helping me achieve this career goal.

ABSTRACT

Hydropower accounts for nearly 40% of renewable electricity generation in the US; however, dams significantly impact the surrounding aquatic ecosystems. One of the most visible impacts of hydropower—beyond the dam itself—is the direct negative impacts (injury or death) to fish populations that must pass through hydropower turbines to access desired downstream habitat. During passage, fishes face many potential stressors that can cause severe injuries and often leads to high rates of mortality. In this dissertation, I have focused on quantifying how fishes respond to impacts from turbine blades that may occur during turbine passage. Laboratory research into blade strike impact has a nearly 30-year publication record and observed trends in injury and mortality rates are generally true for most species. Additional research on untested species (American eel, bluegill, paddlefish, American shad, blueback herring, and brook trout) was successfully completed and new biological response models are also available. Quantitative support of surrogacy—applying biological response models for blade strike from one species to represent another species or group of species—was also confirmed. For example, *Oncorhynchus* and *Salvelinus* species had approximately the same biological response curves suggesting data from one could be used to infer mortality for the other. Live animal response data are invaluable, but the paucity of data on actual physical forces of turbine blade strike necessitated developing novel technology. A new biomimetic model (i.e., Gelfish) was successfully created using additive manufacturing techniques, ballistic gelatin as a tissue surrogate, and a sensor to detect changes in acceleration during blade strike. Importantly, preliminary blade strike testing also suggested the Gelfish prototype responded in a similar way to live fish. Finally, I compiled an anatomical and morphological fish traits dataset that was used to delineate species into functionally relevant groups. The resulting anatomorphic functional guilds were also found to account for variation in relative flexibility better than purely taxonomic groups among the riverine species studied. Combined, these results suggest that the available biological response models can be used to represent untested species within the same anatomorphic functional guilds, and will help calibrate/validate newer versions of Gelfish that maximize biofidelity.

TABLE OF CONTENTS

LIST OF TABLES

LIST OF FIGURES

INTRODUCTION

Background

Dams are designed to help humanity contain and harness one of the most powerful and potentially destructive forces of nature—moving water. In the United States, there are greater than 90,000 dams that serve a multitude of functions including flood control, water diversion, transportation, and electric power generation [1]. Hydropower dams generate only 6.6% of the total electrical power in the USA, but that equates to 38% of the entire renewable energy portfolio [2]. The most recent inventory of dams in the USA suggests just 7% of all dams generate hydroelectric power with most generating capacity found in Washington, Oregon, New York, California, and Alabama, respectively [2,3]. Collectively, these facilities have impounded most large rivers in the conterminous USA including the Missouri, Ohio, and Colorado Rivers. Generation of hydroelectricity on these impounded systems carries a hefty ecological toll because dams disrupt riverine connectivity and alter hydrologic flows [4,5]. Passage through hydropower turbines can also be directly injurious to fishes that may become entrained during annual (spawning) migrations or movement throughout impounded riverine systems [4,6–8]. The negative effects of hydropower dams can also lead to changes in biodiversity, species abundances, distribution, or localized extinctions in extremely degraded systems [5,9,10]. Disruption of riverine systems was identified as a major concern as early as the 18th century when the first fishway passage structure was installed to help restore connectivity in the Northeastern USA [5]. Fishways are usually designed to facilitate movement of fish upstream and are rarely beneficial for all impacted species or those at greatest risk of downstream entrainment [5,11]. To that end, exclusion devices (e.g., racks or grates) or active collection and transportation operations are also implemented to help reduce downstream entrainment of fishes at hydropower facilities [12]. These solutions may provide some benefit to otherwise disconnected systems, but none are 100% effective and turbine passage remains a direct threat to many riverine fishes.

In most/many systems, passage through turbines is likely unavoidable and has been confirmed during field studies [4,8,13,14]. In addition to death, field trials of turbine

passed fish identified highly prevalent, non-lethal injuries (e.g., lacerations, contusions, descaling and fin tears) as well as low prevalence, lethal injuries including amputations [8]. Understanding what causes these injuries and death is problematic because fish face a suite of stressors during turbine passage including barotrauma from rapid decompression, hydraulic shear, cavitation, turbulence, blade strike, or collisions with structures [7,15–17]. Linking exact causes of traumatic injury and death to a specific stressor is difficult because the precise exposure conditions and path through the turbine are variable and largely unknown. Exposure risk is also linked to site-specific operational requirements and seasonal changes in water flow or temperature making inferences gained at one facility or one operational regime difficult to translate to other facilities that may be on the same river. Fishes at the highest risk of turbine passage are those that undergo long distance migrations to (adult) or from (juvenile) freshwater or marine spawning habitat, respectively, to fulfill their life history. In addition, risk of turbine passage also depends on the number of encounters a migrating population of fish may experience throughout the entire impounded system that contains multiple dams [18,19]. For example, salmonid smolts traveling from upper reaches of the Snake River may have to pass through 10 or more hydropower dams on their journey to the Pacific Ocean [19,20]. The risk to an entire riverine community is also largely dependent on fish species, timing of migration events, and turbine passage stressor.

Physical impact of turbine blades striking fish represents one of the most obvious avenues of injury or mortality during passage through hydropower turbines. The risk and severity of injury from blade strike has been linked to turbine type, with Francis and Kaplan types being the most common turbines found in hydropower dams in the USA [21]. Francis turbines are often associated with higher rates of mortality because they generally have more turbine blades and operate at higher RPMs than Kaplan turbines [22,23]. In addition to turbine type, leading-edge thickness and strike velocity are two important turbine blade characteristics, yet knowledge of both is limited because these data are often considered proprietary by turbine manufactures. The movement and orientation of the fish, in combination with location and angle of blade strike, must also be accounted for to accurately predict injury and mortality. Aspects of the fish itself is

also of concern because of differential probability of injury or death linked with size and body shape. Fish size also affects risk of entrainment with smaller individuals more likely to pass through exclusion devices like trash racks, thereby increasing the potential for passage related injury [24]. Laboratory trials on blade strike identified a fish length to blade thickness ratio (i.e., L/t ratio) which suggests larger fish struck with thinner blades are most susceptible [25,26]. Fish species is also an important variable to consider because of the diversity of shapes that also impart different probability of injury. Though blade strike data for most species are not available, prior research suggests clupeids are highly susceptible, while anguillids and acipenserids are the most resistant, and salmonids and moronids are moderately susceptible based on species tested to date [25–28]. Ideally, one could account for all blade strike variables at once (e.g., turbine blade and fish characteristics) and provide a multiplicative probability estimate of injury or mortality for each species. However, blade strike represents one of multiple stressors, each with its own suite of exposure conditions, that would factor into estimates of total turbine passage mortality. Logistical constraints would also prohibit investigating every exposure condition for every stressor (including blade strike) across all species at risk. The exact species of interest varies by project, which must assign risk and prioritize research efforts that accurately reflect the diversity of riverine fish communities.

There are some 30,000 to 40,000 described species of fish world-wide [29,30], and 41% of this diversity is found in freshwater systems that make-up only 1% of earth's entire water supply [31]. The extensive network of freshwater streams, rivers, and lakes of the USA are also remarkably diverse and host nearly 1000 species of fishes [30,32]. One can observe this diversity firsthand due in part to the wide range of unique shapes, sizes, and other physical adaptations that have allowed these fishes to thrive. Diversity of riverine fish communities within the USA is not the same across every freshwater system because of speciation brought about by geographic isolation through geologic time [33]. It is not surprising, perhaps, that biodiversity of freshwater systems is now threatened because many rivers in the USA are also impacted by hydroelectric power production as well [34]. The fact that most rivers are impounded indicates that many 100s of freshwater species in the USA are likely impacted by loss of riverine connectivity or potential

passage through hydropower electric facilities. Fishes at the highest risk of entrainment include anadromous (acipenserids, clupeids, salmonids, or moronids), catadromous (anguillids), and potamodromous (cyprinids or catostomids) species or common reservoir inhabitants such as centrarchids [4,11,35]. Less information is available related to the relative risk to lepisosteids or percids (among other groups) that are common in impounded systems but do not undertake long distance spawning migrations; however, notable kilometer-scale home range movements have been observed [36,37]. Potamodromous and non-migratory species have largely been overlooked in the literature in favor of studying high-profile migratory species like Pacific coast salmonids or Atlantic coast anguillids and clupeids. The astounding diversity of fishes is also a limitation because insights from one species does not necessarily apply to another and researching all impacted species within a riverine community is not possible.

The desire to avoid researching every species of fish has led to the development of a traits-based approach that combines fishes into groups using shared traits [38,39]. Part of this prioritization begins by identifying species within an impacted riverine community followed by their underlying classification and evolutionary relatedness. Taxonomic groupings form the basis of this understanding by placing species into hierarchical groups (i.e., genera, family, etc.) based on shared genetic, behavioral, physiological, or ecological traits [29]. Alternatively, taxonomically unrelated species have been placed into feeding, reproductive, life history, and environmental guilds (among others) for community analyses [40–45]. Both taxonomic and functional grouping of fishes seek to learn as much as possible about multiple species by investigating a few, representative or umbrella species [38]. This aspect of a traits-based approach is also useful because certain species are studied more heavily because they are abundant, economically valuable, easy to obtain and care for, or have a long publication history. Another hallmark of both approaches is the use of surrogate species—any species used to represent another or group of species [46]—because the targeted species is rare, difficult to collect, or protected by law [38]. Use of a surrogate ensures each species or group is well represented in community analyses, especially for data deficient species or river systems. More importantly, a study using fish life history data found that trends

predicted for surrogates were similar to overall trends observed in the analysis that included all species, which suggests surrogacy is a viable option using traits-based data [42]. Of course, caution must be exercised when selecting a surrogate to ensure the associated data accurately represents the community of interest [47]. Most studies using traits-based analyses rely on ecological data and few if any have used fish physical traits to create functional guilds. The functional traits of interest to assess susceptibility to blade strike would be linked to anatomical, morphological, and biomechanical data that could be readily quantified. A more challenging question is determining which grouping method (taxonomic or functional) is best suited to describe an entire community of fishes with differential risks of entrainment and susceptibility to passage through hydropower turbines.

Overview & Objectives

The focus of this dissertation is to better understand how strikes from hydropower turbine blades affect rates of injury and mortality of riverine fishes passing through turbines. This fundamental, individual-based knowledge is useful to quantify a specific response (i.e., probability of mortality); however, the applicability of these data must also account for other aspects of turbine passage to accurately predict the population-level effects. For example, population-level consequences would also include the probabilities of entrainment and adverse interactions with each passage stressor, which includes barotrauma, hydraulic shear, as well as pinching or grinding [4,24,39]. Thus, the probability of an adverse effect from turbine passage is a multiplicative combination of all probabilities including blade strike impacts. Natural variation in fish demographics like the number of reproductive events, generation time, recruitment, and overall mortality rate also directly affect population growth, age structure, and density [48]. So, the overall effect of turbine passage represents one the many anthropogenic stressors that may impact fish populations within impounded systems [39]. Previous work has provided robust estimates of entrainment risk [24] and probability of being struck [49,50] for fish communities, and fisheries biologists often publish data on natural demographic trends as well. The narrative discussed herein is focused on quantifying responses of blade strike

impact specifically to better predict how this turbine passage stressor effects fish populations and the ecology of impounded systems at hydropower dams.

Research rationale and objectives are provided below to establish specific goals and describe how each chapter pertains to the dissertation. Insights from each chapter are used to inspire and direct research of subsequent chapters, with specific emphasis and importance placed on the design of the last chapter (Chapter V). The last chapter is the culmination of all insights from previous chapters and represents the ultimate research question to establish how disparities in anatomy, morphology, and biomechanical phenomena may help predict susceptibility to blade strike among diverse riverine fishes. To that end, a testable research hypothesis is directly stated for Chapter V following its overview described below.

Chapter I

Biological responses of fishes exposed to simulated blade strike impacts—A review.

The first chapter provides a review of fish biological responses to blade strike impact including contributed research from in Chapters II and III. The overall motivation is to produce a document that synthesizes what is currently known about blade strike impact and how it affects rates of injury and mortality among riverine fishes. This chapter represents one section of a report on the current state of knowledge related to biological responses to turbine passage stressors that also includes sections for shear forces and barotrauma. Overall trends in susceptibility are provided across species whenever possible but most of the narrative related to species focuses on dose-response relationships derived for each species and passage stressors. Dose-response relationships are then used to parameterize the Biological Performance Assessment (BioPA) tool [50] or Hydropower Biological Evaluation Toolset (HBET) [51] which can be used to better predict risk of injury and mortality when combined with turbine-specific operational parameters. The targeted audience for this report is turbine manufacturers and dam owners/operators for which the data can be used to inform design of new turbines or operational regimes that increase survival without significantly impacting electric generating capacity. In addition, a review of sufficient depth will also help us better

understand gaps in current knowledge and understanding of blade strike impact and more poignantly directly future research endeavors.

The main purpose of this chapter is to synthesize the current state of understanding linked to the mathematical relationships used to derive biological responses of fish to blade strike impact. To meet this end, there were several objectives including 1) a historical overview of blade strike testing apparatuses and methods used to date, 2) definitions of biological responses used in laboratory testing and underlying mathematical relationships used to derive dose-response models, 3) general trends in rates of injury and mortality as functions of turbine- and fish-specific variables, 4) descriptions of species responses including comparisons of dose-response models among species tested to date, 5) identify gaps in knowledge and research that would best complement available data, and 6) provide overall conclusions related to fish biological responses to blade strike impact.

Chapter II

Quantifying mortality and injury susceptibility for two morphologically disparate fishes exposed to simulated turbine blade strike

The second chapter seeks to broaden our understanding of how blade strike impact affects riverine fishes passing through hydropower turbines. Responses to blade strike include rates of injury and mortality as a function of blade leading edge width and strike velocity, as well as the location, orientation, impact angle, and size of the fish. To date, previous work focused mainly on mid-body, lateral strikes, perpendicular to the fish body which is often considered the worst-case scenario for blade strike impact [25–28,52]. Initially, impacts to the head and tail or dorsal and ventral surfaces were mostly considered incidental strikes in the experimental design with little emphasis on dedicated study of different strike angles [25,28]. More recent work included multiple treatment groups with combinations of major exposure variables (e.g., blade width, strike velocity, location, orientation, and impact angle) to better estimate susceptibility to blade strike [26,27]. Exact exposure conditions of fish struck by a turbine blade are unknown so information on as many potential interactions between the blade and fish are needed

when possible. Most available data relate to salmonid species [52] but live fish trials on American eel, white sturgeon, gizzard shad, and striped bass hybrid responses are also now available [26,27]. The effect of size on rates of injury and mortality among fishes exposed to blade strikes also remains unresolved, though previous work has argued longer fish struck with thinner blades (i.e., a large L/t ratio) are at greatest risk to injury and death [25,26]. If the L/t ratio relationship is true across a variety of disparate species, one could argue that species identity is not as important as fish total length. In contrast, injury and mortality rates may be linked to the proximity of the strike to its center of mass, which would vary by size and among species [27,28]. Lack of predictable trends across all blade strike conditions may be linked to limitations with univariate statistics used to compare treatments groups [27], though earlier work placed no emphasis on statistical inferences in their discussion and no dose-response relationships were presented [25,26,28].

The main purpose of this chapter is to build upon the basic knowledge of how blade strike impact affects injury and mortality rates of riverine fishes. More specifically, bluegill sunfish, *Lepomis macrochirus,* and American eel, *Anguilla rostrata*, were studied because of their morphologically distinct body shapes compared with previously tested species. American eel represents a distinct anguilliform body shape and is a catadromous species impacted by dams on the Atlantic coast of the USA [53–55]. Bluegill has a stout, laterally compressed body shape and does not undergo migrations; however, it is often abundant in reservoirs [30] suggesting it has a high risk of entrainment [55]. Experimental treatment conditions and protocols for these species followed those described in Bevelhimer et al. [27,56]. New methods of data analyses were performed using regression techniques that simultaneously models mortality according to all treatment conditions (including body size) and also includes the use of model selection criteria. The specific objectives were 1) estimate instantaneous mortality of bluegill sunfish and American eel exposed to multiple blade strike treatment conditions including changes in blade leading edge thickness, impact velocity, strike location, impact angle, and orientation of the fish itself, 2) determine how bluegill size effects rates of injury and mortality, 3) use log-logistic dose-response analyses to model mortality according to

blade strike velocity and fish size, and 4) perform logistic regression analysis and model selection on data sets containing all treatment scenarios including fish total length to better predict mortality caused by blade strike impact.

Chapter III

Within and among fish species differences in simulated turbine blade strike mortality: Limits on the use of surrogacy for untested species

The third chapter is designed to quantifiably assess the applications of surrogacy using blade strike impact data and dose-response models. Using one species to represent many is not a new concept and has been used to help prioritize species research because studying all species is logistically impractical. Furthermore, the surrogates and groups of species they represent, were established using a traits-based method of assessing entrainment risk through hydropower turbines [38,39]. Traits-based analyses and expert opinion were used to prioritize species and life stages for direct dose-response studies on turbine passage stressors including blade strike impact. A total of seven groups were created based on similarities in distribution, life history, and risk of entrainment in the USA. Whenever possible, groups were created at the family level while other groups were based on similarities shared by species within the same order. Within these groups, multiple target species were identified for study linked mostly to conservation status or perceived risk of entrainment. Additionally, a surrogate species was identified whenever possible to be used in place of the target species which are often protected, difficult to collect in sufficient numbers, problematic to keep in captivity, or a combination of factors. In many cases, the surrogate is a different species found in the same genus, a different genus in the same family, or a member of different family within the same order. Regardless, surrogates are identified for use in experimental studies without empirical evidence to support their use in laboratory studies of turbine passage stressors. Recent research by Beirão et al. [57] indicates that multiple species within the *Oncorhynchus* genus (rainbow trout, *O. mykiss*; kokanee, *O. nerka*; and chinook, *O. tshawytscha*) had similar dose-response curves when exposed to a range of rapid decompression scenarios. Similarities in response to barotrauma among *Oncorhynchus*

spp. suggest that one dose-response curve from one species could be used as a surrogate for all species in this genus, or that data for all species could be pooled according to treatment conditions; however, responses between species differed at high ratios of decompression (i.e., the ratio of acclimation compared to nadir pressure) which may limit use of surrogacy to lower ratios of rapid decompression [57]. Rapid decompression studies have provided the first empirical support of surrogacy for use in the application of dose-response relationships associated with turbine passage stressors. The previous study only applies to juvenile *Oncorrhynchus* species such that dose-response for smaller or larger fish may not follow the same trends. While surrogacy appears to be supported for rapid decompression data, no such evidence is available to date to support its use with blade strike dose-response data.

The main purpose of this chapter is to provide empirical support for use of surrogacy with blade strike dose-response data. Two different taxonomic levels will be tested to assess application of surrogacy among species within the same genus or family. To test species within the same genus, two species of juvenile clupeids were selected within the *Alosa* genus including American shad, *A. sapidissima*, and blueback herring, *A. aestivalis*. Gizzard shad, *Dorosoma cepedianum*, were also included to test disparities between different genera within the same family (i.e., Clupeidae). Finally, rainbow trout, *O. mykiss* and brook trout, *Salvelinus fontinalis*, were used to provide additional opportunity to test different genera within the same family (i.e., Salmonidae). Clupeids and salmonids were chosen because of their risk of entrainment through hydropower turbines, anadromous behavior, and availability of multiple genera for testing [11,35]. Furthermore, genera-level taxonomy represents the first taxonomic level below family where disparities in body shape, physical attributes, or other ecological life history may affect application of surrogacy. Comparable data for blade strike are important because surrogacy seems to be confirmed within the *Oncorhynchus* genus for barotrauma dose-response data [57]. Blade strike trials and dose-response analyses were similar to those described in Bevelhimer et al. [27,56] and Chapter I here. Surrogacy was tested in two ways including logistic regression analyses where taxonomic category (species or genus) was included and model selection criteria was used to determine if and at what level

taxonomic variables are important predictors of mortality. A second method will include multivariate statistical analyses of morphometric data measured from all three clupeids to determine how best to categorize these species for logistic regression analysis. The specific research objectives were to 1) estimate instantaneous mortality and dose-response relationships for rainbow trout, brook trout, gizzard shad, American shad, and blueback herring, 2) use morphometric data to determine which taxonomic level best captures fish shape among clupeids 3) test the role of taxonomic level (species or genus) as a predictor of mortality, 4) test the application of intraspecies surrogacy by comparing small and large rainbow trout, and 5) compare uncertainty in dose-response models (i.e., 95% confidence bands) between taxonomic groups to better assess the application of surrogacy in these species.

Chapter IV

Creation of a biomimetic fish to better understand impact trauma caused by hydropower turbine blade strikes

The fourth chapter is dedicated to the description and testing of a novel, biologically-realistic, physical fish model that will provide additional insights into the physical forces imparted on fishes during blade strike impact. Current knowledge of blade strike impact and risk of injury or death of turbine-passed fishes relies on computational fluid dynamic (CFD) models or field and laboratory research on live animals. CFD models have been used extensively to track water flow through turbines and estimate probability of exposure to injurious conditions during turbine passage [17,50,58]. Unfortunately, these models are poorly suited to estimate rates of injury or mortality of fishes exposed to specific stressors like blade strike impact. Field studies offer the most realism when estimating rates of injury or mortality and have shown that passage through turbines may be detrimental [8,14], yet linking observed injuries to the exact stressor that caused it is also not possible. To understand the effects of a specific turbine passage stressor, live fish must be brought into the laboratory so that bioassays can be conducted to create dose-response curves. For blade strike, the dose is either blade strike velocity or leading-edge thickness and the response is rate of injury or mortality.

Generating dose-response curves requires sacrifice of 100s of fish which limits studies to common, highly abundant species that are generally easy to obtain and keep in captivity. Beyond the ethical issues of using live organisms, most injuries linked with blade strike can only be confirmed post mortem during necropsies which limits the amount of useful data provided from each fish. Thus, creation of a realistic biomimetic model fish that contains an array of sensors and could be used on multiple occasions would be especially useful. The model must be designed to mimic the biomechanical (whole-body flexibility, tissue firmness, etc.) responses of live fishes to blade strike impact and be validated against laboratory-derived biological response data. Successful creation of a biofidelic model fish could preclude the need for live animal testing and would also provide data on the physical forces of blade strike impact which have yet to be linked to fish biological response data.

The main goal of this chapter is to produce an initial version of the biofidelic model that incorporates sensors and is exposed to simulated blade strike testing. There were many objectives for this chapter that can be linked with scanning fish, model composition, sensor development, and simulated impact testing. High performance laser scanners were used to create 3D scans of recently euthanized fish to capture the general shape and as many external surface features as possible. Multiple species were scanned to test our ability to create high fidelity images of bluegill sunfish, rainbow trout, gizzard shad, hybrid striped bass, *Morone saxatilis* × *Morone chrysops*, and American eel. Initial advice from additive manufacturing experts suggested that using 3D scans to create a reusable mold would be more cost effective then printing the model directly. Additional development included modifying scanned data based on proportional changes in fish morphology to create additional models without the need to scan larger fish. We chose ballistic gelatin as a surrogate for fish tissue because of its extensive use in ballistics testing as a human tissue simulant [59,60], it is easy to handle, and procedures used to create it are well established. Tissue durometer (material hardness) using Shore-OO scale was used to test initial material properties of ballistic gelatin and compared to actual animal tissue, which has been used in similar capacities to confirm tissue firmness in the field of medicine [61–63]. Ballistic gelatin concentration, preparation temperature, and

warming time were also investigated to determine the durometer range of this material and to establish consistent testing protocols. Surrogate skin and skeletal structures were also included; however, vertebral elements in the initial model were not included because of their small size and associated challenges with recreating these structures. Sensor development focused on inclusion of up to three, 3-axis accelerometers embedded into the model, though initial versions only included one accelerometer. Finally, the ballistic gelatin model created was exposed to similar simulated blade strike impact scenarios as those investigated during live animal testing. Flexibility of the model was compared to live fish exposed to the same simulated blade strike scenarios to make initial comparisons between whole-fish and whole-model responses following contact with the blade. Impact testing of the model was also used to help determine the relationship between changes in three-dimensional acceleration and biological response data gathered from laboratory tests.

Chapter V

A Traits-based Approach to Assess Susceptibility of Riverine Fishes to Hydropower Turbine Blade Strike

The fifth and final chapter was inspired by the need to create a novel method to categorize riverine fishes into functional guilds based on anatomical and morphological traits for the purpose of inferring susceptibility to blade strike impact. Tennessee rivers hold the highest diversity of temperate fishes in North America [33,64] and this concentrated biodiversity is ideally suited for research queries requiring access to multiple species. Fish diversity includes living relics like sturgeon and paddlefish to more highly derived perciform white bass and largemouth bass. In addition, many Tennessee rivers have been impounded and used to generate hydroelectric power as far back as the 1930s when the Tennessee Valley Authority was formed [65]. While hydroelectric power has undoubtedly helped bolster Tennessee economic development and prosperity, it has also negatively impacted the remarkable aquatic biodiversity found there. While the methods described in this chapter best applies to fishes found in Tennessee and the Southeastern USA, creation of functional guilds for fish communities in the Pacific

Northwest or Northeastern USA would be useful as well. Functional traits of interest include anatomical and morphological metrics as well as how these traits relate to biomechanical nature of fishes exposed to blade strike impact. Center of gravity relative to blade strike, tissue durometer, and whole-fish flexibility likely factor into how a species responds to simulated impact conditions. Insights from previous research suggests that location of center of gravity relative to blade strike location is likely an important predictor of susceptibility to blade strike [27,28]. Durometer, or firmness of fish integument (mucus, scales, and skin) and muscle tissues may also factor into susceptibility through the combined material properties of these complex biological tissues. Flexibility is linked to vertebral anatomy and morphology including the number and length of vertebrae as well as changes in joint angle between vertebrae [66–70]. In addition, most but not all riverine species are covered in a layer of protective scales that overlap one another and will also affect flexibility [71–73]. To best create these guilds, physical traits that represent or describe each species must be identified and compared between multiple species to determine the most influential and important traits. Creation of these new functional guilds based on shared anatomorphic traits (e.g., anatomorphic functional guilds; AFGs) would also make selection of surrogates more specific to blade strike (Chapter III). Successful identification of functional guild members would also support the development of fewer biomimetic models (Chapter IV) which could be linked to a species that best represents each AFG. Creating similar functional traits-based guilds to more thoroughly study fishway passage structure design and efficacy or to better model the effects of non-lethal exposure to thermoelectric effluent would also be useful.

The primary purpose of this chapter is to create a method for placing riverine fishes into traits-based AFGs as opposed to taxonomic groups (genus to order level) with respect to flexibility. Anatomorphic insights included morphometric measurements of body landmarks (i.e., fins and other structures commonly used in species identification) to estimate fish 3D shape and followed methods employed in Chapter III. Anatomical data were broken into categories related to the scales (type, area, embedding depth, etc.) and vertebral structures (number of vertebrae, centra dimensions, etc.). Biomechanical measurements were made including center of gravity, tissue durometer, and whole-body

flexibility. Principal component analysis was used to select variables with the most influence on fish shape and flexibility, which in turn was used in cluster analyses to help create AFGs. Anatomorphic functional guilds were compared to taxonomic groups using model selection criteria and multiple linear regression statistics to determine which grouping best captures variation and trends in fish flexibility. The specific objectives of this chapter were to 1) measure anatomorphic traits and create a dataset for impounded riverine fish communities in Eastern Tennessee, 2) use the traits dataset to help identify anatomorphic functional guilds that may contain taxonomically unrelated species, 3) test which anatomorphic variables best predict relative flexibility among fishes, and 4) determine which grouping method (functional or taxonomic) best accounts for variation in relative flexibility.

Research Hypothesis

In the chapters that follow, I will add to and expand upon current knowledge of blade strike impact which will culminate with direct hypothesis testing in the last chapter. The last chapter will investigate the best method to group fishes and apply insights across an entire riverine community as it relates to susceptibility to turbine passage and blade strike impact specifically. Susceptibility was defined in terms of whole-fish relative flexibility which could be linked to unique anatomical and morphological traits among riverine fishes that may infer differential risk of injury and mortality to blade strike impacts. The competing methods in question would include grouping species based on shared traits that are either 1) consistent with accepted taxonomic dogma only, 2) coincident among unrelated, yet functionally similar species, or 3) a combination of both that depends on level of taxonomic classification to be used. Taxonomic classification makes sense phylogenetically because traits are shared among evolutionarily related species; however, biogeographical processes have also shaped current fish communities in North America [33], suggesting that adaptive convergence of shared functional traits occurs separately from phylogenetic influences [42,43,45]. Additionally, susceptibility to turbine blade strike impacts is an anthropogenic (artificial) selective force from which fishes have no comparable natural process to adapt, suggesting that shared traits among

groups would likely not be taxonomic [38]. To that end, I hypothesize that using anatomorphic functional guilds will model (i.e., according to model selection criteria) susceptibility to simulated blade strike impact as well or better than strictly taxonomic groups of riverine fishes.

References

1. ASCE, (American Society of Civil Engineers) 2017 American Infrastructure Report Card: Dams. *ASCE Infrastruct. Rep. Card* 2017, 1–5.

2. EIA, (Energy Information Administration) Hydropower Explained Available online: https://www.eia.gov/energyexplained/index.php?page=hydropower_home (accessed on Dec 23, 2020).

3. USACE, (United States Army Corp of Engineers) National Inventory of Dams Available online: http://nid.usace.army.mil/cm_apex/f?p=838:5:0::NO (accessed on Dec 23, 2020).

4. Pracheil, B.M.; DeRolph, C.R.; Schramm, M.P.; Bevelhimer, M.S. A fish-eye view of riverine hydropower systems: The current understanding of the biological response to turbine passage. *Rev. Fish Biol. Fish.* **2016**, *26*, 153–167.

5. Silva, A.T.; Lucas, M.C.; Castro-Santos, T.; Katopodis, C.; Baumgartner, L.J.; Thiem, J.D.; Aarestrup, K.; Pompeu, P.S.; O'Brien, G.C.; Braun, D.C.; et al. The future of fish passage science, engineering, and practice. *Fish Fish.* **2018**, *19*, 340–362.

6. Čada, G.F. Fish passage mitigation at hydroelectric power projects in the United States. In *Fish Migration and Fish Bypasses*; Jungwirth, Mathias; Schmutz, Stefan; & Weiss, S., Ed.; Fishing New Books: Malden, Massachusetts, **1998**; pp. 208–219.

7. Čada, G.; Loar, J.; Garrison, L.; Fisher, R.; Neitzel, D. Efforts to reduce mortality to hydroelectric turbine-passed fish: Locating and quantifying damaging shear stresses. *Environ. Manag.* **2006**, *37*, 898–906.

8. Mueller, M.; Pander, J.; Geist, J. Evaluation of external fish injury caused by hydropower plants based on a novel field-based protocol. *Fish. Manag. Ecol.* **2017**, *24*, 240–255.

9. Larinier, M.; Marmulla, G. Fish passes: Types, principles and geographical distribution - An overview. *Proc. Second Int. Symp. Manag. Large Rivers Fish. Vol. Il.* **2004**, *II*, 22pp.

10. Limburg, K.E.; Waldman, J.R. Dramatic declines in North Atlantic diadromous fishes. *Bioscience* **2009**, *59*, 955–965.

11. Binder, T.R.; Cooke, S.J.; Hinch, S.G. Physiological specializations of different fish groups: Fish migrations. In *Encyclopedia of Fish Physiology: From Genome to Environment*; Farrell, A.P., Cech Jr., J.J., Richards, J.G., Stevens, E.D., Eds.; Elsevier Inc.: San Diego, California, **2011**; pp. 1921–1952 ISBN 9780123745538.

12. Čada, G.F. The development of advanced hydroelectric turbines to improve fish passage survival. *Fisheries* **2001**, *26*, 14–23.

13. Kostecki, P.T.; Clifford, P.; Gloss, S.P.; Carlisle, J.C. Scale Loss and survival in smolts of Atlantic salmon (Salmo salar) after turbine passage. *Can. J. Fish. Aquat. Sci.* **1987**, *44*, 51–52.

14. Hostetter, N.J.; Evans, a. F.; Roby, D.D.; Collis, K.; Hawbecker, M.; Sandford, B.P.; Thompson, D.E.; Loge, F.J. Relationship of external fish condition to pathogen prevalence and out-migration survival in juvenile steelhead. *Trans. Am. Fish. Soc.* **2011**, *140*, 1158–1171.

15. Neitzel, D. a; Dauble, D.D.; Cada, G.F.; Richmond, M.C.; Guensch, G.R.; Mueller, R.R.; Abernethy, C.S.; Amidan, B. Survival estimates for juvenile fish subjected to a laboratory-generated shear environment. *Trans. Am. Fish. Soc.* **2004**, *133*, 447–454.

16. George, S.D.; Baldigo, B.P.; Smith, M.J.; McKeown, D.M.; Faulring, J.W. Variations in water temperature and implications for trout populations in the Upper Schoharie Creek and West Kill, New York, USA. *J. Freshw. Ecol.* **2015**, *31*, 93–108.

17. Colotelo, A.H.; Goldman, A.E.; Wagner, K.A.; Brown, R.S.; Deng, Z.D.;

Richmond, M.C. A comparison of metrics to evaluate the effects of hydro-facility passage stressors on fish. *Environ. Rev.* **2017**, *25*, 1–11.

18. Norrgård, J.R.; Greenberg, L.A.; Piccolo, J.J.; Schmitz, M.; Bergman, E. Multiplicative loss of landlocked Atlantic salmon Salmo salar L. smolts during downstream migration through multiple dams. *River Res. Appl.* **2013**, *29*, 1306–1317.

19. Rechisky, E.L.; Welch, D.W.; Porter, A.D.; Jacobs-Scott, M.C.; Winchell, P.M. Influence of multiple dam passage on survival of juvenile Chinook salmon in the Columbia River estuary and coastal ocean. *Proc. Natl. Acad. Sci. U. S. A.* **2013**, *110*, 6883–6888.

20. Williams, R.N.; Stanford, J.A.; Lichatowich, J.A.; McConnaha, W.E.; Whitney, R.R.; Mundy, P.R.; Bisson, P.A.; Powell, M. s. Conclusions and strategies for salmon restoration in the Columbia River Basin. In *Return to the River: Restoring Salmon to the Columbia River*; Williams, R.N., Ed.; Elsevier Academic Press, **2006**; pp. 627–664 ISBN 9780120884148.

21. Uria-Martinez, R.; Johnson, M.M.; O'Connor, P.W.; Samu, N.M.; Witt, A.M.; Battey, H.; Welch, T.; Bonnet, M.; Wagoner, S. *2017 Hydropower Market Report*; Oak Ridge, Tennessee, **2018**.

22. Fu, T.; Deng, Z.D.; Duncan, J.P.; Zhou, D.; Carlson, T.J.; Johnson, G.E.; Hou, H. Assessing hydraulic conditions through Francis turbines using an autonomous sensor device. *Renew. Energy* **2016**, *99*, 1244–1252.

23. Martinez, J.J.; Deng, Z.D.; Titzler, P.S.; Duncan, J.P.; Lu, J.; Mueller, R.P.; Tian, C.; Trumbo, B.A.; Ahmann, M.L.; Renholds, J.F. Hydraulic and biological characterization of a large Kaplan turbine. *Renew. Energy* **2019**, *131*, 240–249.

24. Coutant, C.C.; Whitney, R.R. Fish behavior in relation to passage through hydropower turbines: A review. *Trans. Am. Fish. Soc.* **2000**, *129*, 351–380.

25. EPRI, (Electric Power Research Institute) *Evaluation of the effects of turbine*

blade leading edge design on fish survival; Palo Alto, CA, **2008**.

26. EPRI, (Electric Power Research Institute) *Tests examining survival of fish struck by turbine blades*; Palo Alto, CA, **2011**.

27. Bevelhimer, M.S.; Pracheil, B.M.; Fortner, A.M.; Saylor, R.; Deck, K.L. Mortality and injury assessment for three species of fish exposed to simulated turbine blade strike. *Can. J. Fish. Aquat. Sci.* **2019**, *76*, 2350–2363.

28. Turnpenny, A.W.H.; Davis, M.H.; Fleming, J.M.; Davies, J.K. *Experimental studies relating to the passage of fish and shrimps through tidal power turbines*; Southampton, United Kingdom, **1992**.

29. Nelson, J.S.; Grande, T.C.; Wilson, M.V.H. *Fishes of the World*; 5th ed.; John Wiley & Sons: Hoboken, New Jersey, **2016**.

30. Froese, R.; Pauly, D. Fishbase. *Fishbase* **2020**.

31. Helfman, G.S.; Collette, B.B.; Facey, D.E.; Bowen, B.W. *The Diversity of Fishes: Biology, Evolution, and Ecology*; 2nd ed.; Wiley-Blackwell Publishing: West Sussex, UK, **2009**.

32. Page, L.M.; Burr, B.M. *A Field Guide to Freshwater Fishes, North America North of Mexico*; 2nd ed.; Houghton Mifflin Company: Boston, Massachusetts, **2011**.

33. Ross, S.T.; Matthews, W.J. Evolution and ecology of North American freshwater fish assemblages. In *Freshwater Fishes of North America Volume 1: Petromyzontidae to Catostomidae*; Warren Jr., M.L., Burr, B.M., Eds.; Johns Hopkins University Press: Baltimore, Maryland, **2014**; pp. 1–49.

34. Pracheil, B.M.; Mestl, G.E.; Pegg, M.A. Movement through dams facilitates population connectivity in a large river. *River Res. Appl.* **2015**, *31*, 517–525.

35. Grubbs, R.D.; Kraus, R.T. Fish Migration. In *Encyclopedia of Animal Behavior*; Breed, M.D., Moore, J., Eds.; Elsevier Academic Press: San Diego, California,

2010; pp. 715–724.

36. Echelle, A.A.; Grande, L. Lepisosteidae: Gars. In *Freshwater Fishes of North America Volume 1: Petromyzontidae to Catostomidae*; Warren Jr., M.J., Burr, B.M., Eds.; Johns Hopkins University Press: Baltimore, Maryland, **2014**; pp. 243–298.

37. Strainer, A. Seasonal movement and angler exploitation of an adfluvial walleye population in the Missouri River, Montana. *Intermt. J. Sci.* **2018**, *24*, 14–25.

38. Pracheil, B.M.; McManamay, R.A.; Bevelhimer, M.S.; DeRolph, C.R.; Čada, G.F. A traits-based approach for prioritizing species for monitoring and surrogacy selection. *Endanger. Species Res.* **2016**, *31*, 243–258.

39. Čada, G.F.; Schweizer, P.E. *The application of traits-based assessment approaches to estimate the effects of hydroelectric turbine passage on fish populations*; Oak Ridge, Tennessee, **2012**.

40. Frimpong, E.A.; Angermeier, P.L. Fish traits: A database of ecological and life-history traits of freshwater fishes of the United States. *Fisheries* **2009**, *34*, 487–495.

41. Frimpong, E.A.; Angermeier, P.L. Trait-based approaches in the analysis of stream fish communities. *Am. Fish. Soc. Symp.* **2010**, *73*, 109–136.

42. Winemiller, K.O.; Rose, K.A.; Rose, K.A. Patterns of life-history diversification in North American fishes: Implications for population regulation. *Can. J. Fish. Aquat.* **1992**, *49*, 2196–2218.

43. Balon, E.K. Reproductive guilds of fishes: A proposal and definition. *J. Fish. Res. Board Canada* **1975**, *32*, 821–864.

44. Balon, E.K.; Momot, W.T.; Regier, H.A. Reproductive guilds of percids: Results of the paleogeographical history and ecological succession. *J. Fish. Res. Board Canada* **1977**, *34*, 1910–1921.

45. Mims, M.C.; Olden, J.D.; Shattuck, Z.R.; Poff, N.L. Life history trait diversity of native freshwater fishes in North America. *Ecol. Freshw. Fish* **2010**, *19*, 390–400.

46. Caro, T.M. *Conservation by proxy: Indicator, umbrella, keystone, flagship, and other surrogate species*; 2nd ed.; Island Press: Washington, D.C., **2010**.

47. Hermoso, V.; Januchowski-Hartley, S.R.; Pressey, R.L. When the suit does not fit biodiversity: Loose surrogates compromise the achievement of conservation goals. *Biol. Conserv.* **2013**, *159*, 197–205.

48. Rubach, M.N.; Ashauer, R.; Buchwalter, D.B.; Lange, H.J. De; Hamer, M.; Preuss, T.G. Framework for traits-based assessment in ecotoxicology. *Integr. Environ. Assess. Manag.* **2011**, *7*, 172–186.

49. Deng, Z.; Carlson, T.J.; Dauble, D.D.; Ploskey, G.R. Fish passage assessment of an advanced hydropower turbine and conventional turbine using blade-strike modeling. *Energies* **2011**, *4*, 57–67.

50. Richmond, M.C.; Serkowski, J.A.; Radowski, C.; Strickler, B.; Weisbeck, M.; Dotson, C. Computational tools to assess turbine biological performance. *Hydroreview* **2014**, *33*, 1–6.

51. Hou, H.; Deng, Z.; Martinez, J.; Fu, T.; Duncan, J.; Johnson, G.; Lu, J.; Skalski, J.; Townsend, R.; Tan, L. A Hydropower Biological Evaluation Toolset (HBET) for characterizing hydraulic conditions and impacts of hydro-structures on fish. *Energies* **2018**, *11*, 990–1002.

52. Turnpenny, A.W.H. Mechanisms of fish damage in low head turbines: An experimental appraisal. In *Fish Migration and Fish Bypasses*; Jungwirth, M., Schmutz, S., Weiss, S., Eds.; Blackwell Publishing Ltd: Malden, Massachusetts, **1998**; pp. 300–314 ISBN 0-85238-253-7.

53. Haro, A. Anguillidae: Freshwater Eels. In *Freshwater Fishes of North America: Petromyzontidae to Catostomidae*; Warren Jr., M.L., Burr, B.M., Eds.; Johns Hopkins University Press: Baltimore, Maryland, **2014**; pp. 313–331.

54. Jager, H.I.; Elrod, B.; Samu, N.; McManamay, R.A.; Smith, B.T. *ESA Protection for the American Eel: Implications for U.S. Hydropower*; Oak Ridge, Tennessee, **2013**.

55. Bevelhimer, M.S.; Derolph, C.R. *Market assessment for hydropower turbine design tools using integrated datasets of dams, turbines, owners, and fish*; **2019**.

56. Bevelhimer, M.S.; Pracheil, B.M.; Fortner, A.M.; Deck, K.L. An overview of experimental efforts to understand the mechanisms of fish injury and mortality caused by hydropower turbine blade strike. *ORNL/TM-2017/731* **2017**, 29.

57. Beirão, B.; Pflugrath, B.; Harnish, R.A.; Harding, S.F.; Richmond, M.C.; Colotelo, A.H. Empirical investigation into the applicability of surrogacy for juvenile salmonids (Oncorrhynchus spp.) exposed to hydropower induced rapid decompression. *Ecol. Indic.* **2020**, *121*.

58. Harding, S.F.; Richmond, M.C.; Mueller, R.P. Experimental observation of inertial particles through idealized hydroturbine distributor geometry. *Water (Switzerland)* **2019**, *11*, 471.

59. Jussila, J. Preparing ballistic gelatine - Review and proposal for a standard method. *Forensic Sci. Int.* **2004**, *141*, 91–98.

60. Maiden, N.R.; Fisk, W.; Wachsberger, C.; Byard, R.W. Ballistics ordnance gelatine - How different concentrations, temperatures and curing times affect calibration results. *J. Forensic Leg. Med.* **2015**, *34*, 145–150.

61. Falanga, V.; Bucalo, B. Use of a durometer to assess skin hardness. *J. Am. Acad. Dermatol.* **1993**, *29*, 47–51.

62. Belyaev, O.; Herden, H.; Meier, J.J.; Muller, C.A.; Seelig, M.H.; Herzog, T.; Tannapfel, A.; Schmidt, W.E.; Uhl, W. Assessment of pancreatic hardness — Surgeon versus durometer. *J. Surg. Res.* **2010**, *158*, 53–60.

63. Murphy, T.; Brown, S.; Brown, T.; Plast, F.; Plast, F. A durometer

(mammometer) for objective measurement capsular contraction following breast implant surgery. *Am. J. Cosmet. Surg.* **2020**, 1–6.

64. Etnier, D.A.; Starnes, W.C. *The Fishes of Tennessee*; 1st ed.; The University of Tennessee Press: Knoxville, Tennessee, **1993**.

65. TVA, (Tennessee Valley Authority) Hydroelectric Available online: https://www.tva.gov/Energy/Our-Power-System/Hydroelectric (accessed on Dec 23, 2020).

66. Brainerd, E.L.; Patek, S.N. Vertebral column morphology, C-start curvature, and the evolution of mechanical defenses in tetraodontiform fishes. *Copeia* **1998**, 971–984.

67. Long, J.H.; Koob-Emunds, M.; Koob, T.J. The mechanical consequences of vertebral centra. *Bull Mt Desert Isl. Biol Lab* **2004**, *43*, 99–101.

68. Ward, A.B.; Azizi, E. Convergent evolution of the head retraction escape response in elongate fishes and amphibians. *Zoology* **2004**, *107*, 205–217.

69. Porter, M.E.; Roque, C.M.; Long, J.H. Turning maneuvers in sharks: Predicting body curvature from axial morphology. *J. Morphol.* **2009**, *270*, 954–965.

70. Nowroozi, B.N.; Brainerd, E.L. Regional variation in the mechanical properties of the vertebral column during lateral bending in Morone saxatilis. *J. R. Soc. Interface* **2012**, *9*, 2667–2679.

71. Long, J.H.; R, J.; Hale, M.E.; Henry, M.J.M.C.; Westneat, M.W. Functions of fish skin: Flexural stiffness and steady swimming of longnose gar Lepisosteus osseus. *J. Exp. Biol.* **1996**, *199*, 2139–2151.

72. Bruet, B.J.F.; Song, J.; Boyce, M.C.; Ortiz, C. Materials design principles of ancient fish armour. *Nat. Mater.* **2008**, *7*, 748–756.

73. Yang, W.; Chen, I.H.; Gludovatz, B.; Zimmermann, E.A.; Ritchie, R.O.; Meyers, M.A. Natural flexible dermal armor. *Adv. Mater.* **2013**, *25*, 31–48.

CHAPTER I

BIOLOGICAL RESPONSES OF FISHES EXPOSED TO SIMULATED BLADE STRIKE IMPACTS—A REVIEW

A version of this chapter was originally published by Ryan Kurt Saylor, et al:

Ryan Saylor[*1,2], Mark Bevelhimer[2], and Brenda Pracheil[2]. "Chapter 2: Predicting the Effects of Exposure to Blade Strike on Fish." In: The Development of Biological Response Models for Predicting Injury and Mortality of Fish During Downstream Passage Through Hydropower Facilities. Pacific Northwest National Laboratory. Technical Report. (2021) pgs. 4-35.

Affiliations:
[1] Bredesen Center for Interdisciplinary Research and Graduate Education, University of Tennessee, Knoxville, Tennessee 37996
[2] Environmental Science Division, Oak Ridge National Laboratory, Oak Ridge, Tennessee 37830
*Corresponding Author: Ryan K. Saylor
1 Bethel Valley Road
Oak Ridge National Laboratory
Oak Ridge, Tennessee 37830
Phone: 865-974-7709
E-mail: saylorr@ornl.gov

Author Contributions:

Content layout – RKS, with assistance from MB
Literature review – RKS
Table and Figure Preparation – RKS
Composition of review – RKS, with input from MB
Revisions and draft reviews – RKS, with input from MB and BP
Project management – MB and BP

Abstract

Hydropower remains an important component of renewable energy portfolios globally, but negative consequences of these facilities on riverine fish communities remains a concern. Loss of connectivity between rearing and spawning habitat means many fishes must migrate around (if fishways are present) or pass through turbines to reach desired habitat. Passing through hydropower turbines can be especially stressful and may cause high incidences of mortality when fishes. While field trials have confirmed injuries and mortality does occur as a result of turbine passage, it is impossible to link the exact stressor to damage or mortalities observed. Rather, laboratory trials are used to better understand how stressors like blade strike affect rates of injury and mortality by precisely controlling exposure conditions. These research efforts began in the early 1990s with Turnpenny's original studies, continued at the Electrical Power Research Institute in the 2000s, and were undertaken at Oak Ridge National Laboratory in 2010s as part of the Department of Energy's HydroPASSAGE project. All three have provided useful insights into blade strike and a brief perspective on each is provided in this review. Work at ORNL specifically focused on understanding as many exposure scenarios as possible, while earlier research mostly investigated changes in blade characteristics only. Treatment conditions include aspects of the turbine (i.e., blade leading-edge thickness and realized impact velocity) or the fish itself (strike location or angle, orientation of fish, fish size, etc.). Biological response models are produced from multiple treatments groups using dose (impact velocity) response (mortality) analyses to determine the underlying relationship. The resulting models provide a useful means for comparing species' responses to blade strike and to help inspire new turbine designs. Inspiration into the design of said turbines relies heavily on biological response models that are used to parameterize software and other toolsets available for use by the hydropower industry. For nearly 30 years, research into stressors like blade strike has been undertaken and is reviewed in this article along with data limitations and suggestions for future research to augment currently available data.

Introduction

When fish pass downstream through hydropower facilities, either through turbines, spillways, or other pathways, they may be exposed to physical and hydraulic stressors. There are three main stressors of concern: fluid shear, rapid decompression, and strike or collision [1]. Turbine blade strike can be a significant source of fish injury and mortality during passage through hydroelectric turbines, particularly for larger fish [2,3]. Physical blade strike discussed here is considered separate from other collisions of the fish with non-rotating structures (e.g., stay vanes, wicket gates) or pinching between the tip of a turbine blade runner and a discharge ring wall. Field trials have confirmed that fish passing through turbines experience a wide range of traumatic injuries [4–7], but linking the exact stressor to each injury is not often possible because some stressors cause similar injuries. For example, scale and mucus loss may result from both shear stress and blade strike impact [8,9] or exophthalmia, which has been linked to exposure to fluid shear, barotrauma, and blade strike impact [8,10,11]. Scale turbine models are also used to test passage survival, and the ability to control passage conditions may provide additional insights about passage injuries not possible from field trials [12–14]. Amaral et al. [12] were able to remove wicket gates from their model so that injuries and mortalities were more directly linked to the physical impacts of the runner. Injuries included contusions, lacerations, amputations, eye damage, and descaling, but contusions were the most common injury observed in all species tested [12]. All injuries for both field and scale-model hydropower studies are limited to post passage assessments, which makes it difficult to determine the exact cause of death. Furthermore, field and scale-model studies are unable to control every aspect of the exposure conditions (stressor magnitude), including exposure to non-blade strike stressors. Therefore, inferences about fish injuries in these studies must be confirmed by controlled laboratory experiments that include internal necropsies.

Controlled laboratory experiments involving blade strike form the bulk of current knowledge about injuries caused by blade strike impact. Early insights from laboratory

studies confirmed that scale and mucus loss, contusions, and eye trauma could be linked to blade strike impacts [15,16]. Other signs of severe trauma included internal hemorrhaging, crushing of the body, and spinal damage assumed to be fractures [15]. Likewise, research performed more than 15 years later found similar external injuries, confirmed contusions were the most prevalent, and also observed lacerations [17]. More detailed injury descriptions have now been published and also include internal necropsies to better link mortality with a specific cause. Similar external injuries were also observed in these studies, but hyperpigmentation near the impact site, damage to the gills, and eye amputation were noted as well [9,11,18]. Traumatic injuries to internal organs are often observed as well including hemorrhaging, clotting, lacerations, and in severe cases avulsion or rupture. The most common organ injuries were linked to the liver, heart, gas bladder, and kidney; damage to other organs have been observed but are rare [9,18]. Skeletal fracture of the ribs was common but non-lethal, whereas vertebral fractures and internal decapitation (separation of atlas vertebrae from the cranium) occurred frequently and were often associated with moribund individuals or immediate mortality [11,18]. In most cases, rib and vertebral fractures also led to more severe damage to the kidney and surrounding musculature [9]. The most severe injuries noted were in fish with up to three or more separate vertebral fractures, which may also include internal decapitation [11,18]. While many injuries have been noted, nearly every fish that was considered dead had a broken vertebral column, suggesting these fractures were the most likely cause of death. No other general injury trends were apparent among species that have been examined during laboratory testing and species-specific descriptions are provided later in this review.

Other trends can be inferred from laboratory-derived data in order to make predictions if mathematical relationships can be successfully applied to the treatment dose (impact velocity) and organismal responses (mortality). The result is a biological response model that can predict the rate of mortality given the impact velocity and also infers the velocity range describing 0% to 100% mortality. Biological response models represent a useful means from which turbine designers or dam operators can realistically

infer probability of injury or death based on design or operation parameters. Ideally, response models would be available for every species and exposure condition possible, but logistically constraints of laboratory trials (e.g., number of individuals, space to hold and care for fish, etc.) make this prohibitive. To overcome these limitations, two software tools were developed, the Hydropower Biological Evaluation Toolset (HBET) [19] and Biological Performance Assessment (BioPA) [20], to increase the usefulness and predictive ability of the available biological response data. Biological response models are a key component to each toolset and are parameterized according to species-specific data for each of the three major stressors. Both tools have similar functions as they combine the probability that fish will be exposed to various magnitudes of a stressor (i.e., in addition to blade strike) during turbine passage with biological response models generated from laboratory data. The results for individual stressors from the toolset, and the performance score from BioPA, are used to compare different designs or operations of turbines, spillways, or other hydropower facilities while considering fish survivability. Thus, HBET and BioPA can be used to aid with the design of new turbines or enhanced operation regimes that maximize fish survival without significantly impacting electric generating capacity.

Herein, this review will survey nearly 30 years of simulated blade strike testing and provide a synthesis of fish responses to blade strike impacts. All biological response data and subsequent dose-response models are described for each species tested to date; however, trends that appear to be consistent for multiple species are also highlighted to broaden the inference space of these data. The specific objectives of this review were to 1) describe apparatuses and procedures used in controlled laboratory tests of blade strike impact, 2) define biological response metrics and mathematical models used to describe a species response, 3) synthesize trends in biological responses to blade strike impact across multiple species according to major factors linked to the hydropower turbine and the fish itself, and 4) discuss the application space, limitations, and research needs of blade strike response data available currently. The narrative of the review ends with a

brief summary and major conclusions associated with biological response data generated from blade strike impact testing.

Simulated Blade Strike Testing Apparatuses

National Power Marine and Freshwater Biology Unit

The first apparatus designed to simulate blade strike impact was used by Turnpenny et al. [15] and enabled controlled exposure of blade strike impact for individual fish (Figure 1). The setup included a linear platform and used stored energy in springs to power blade movement along guide rails through an open, water filled flume to impact fish [15]. Trials also included blades of different shapes, leading-edge thicknesses between 10 to 100 mm, and the realized strike velocity was 5 to 7 m/s [15,16]. The blade moved along a linear trajectory from left to right and impact was viewed through an observation window on the left side. All impacts were video-recorded for later analysis and fish were held in place along the mid-sagittal plane with the snout pointing toward the viewing window with a fine thread, though it was not possible to control fish orientation completely during impact [21]. In this orientation, the blade would make contact with the fish along the frontal plane (Figure 1), which was considered a positive strike [15]. Two different trial types were performed: (1) mortality estimates for live brown trout (*Salmo trutta*), European eel (*Anguilla anguilla*), and European bass (*Dicentrarchus labrax*), and (2) probability of strike trials on freshly euthanized fish including the previous species as well as rainbow trout (*Oncorhynchus mykiss*) and sand smelt (*Atherina presbyter*; Table 1). Mortality estimates were made during a 1-hr observation period after blade strike impact to measure instantaneous mortality. No biological response models are available for this work because there were too few treatment groups to properly model mortality.

Electric Power Research Institute

Work at Alden Laboratories was similar to Turnpenny et al. [15] work, but their system used larger blades and could attain faster impact velocities. The system employed

by Alden also used blades that moved in a linear trajectory through a water-filled flume until they impacted fish at the opposite end (Figure 2). Early work tested elliptical and semicircular leading-edge shapes, but most studies focused on semicircular blades with leading-edge thicknesses between 10 to 150 mm for live fish trials. The blade was attached to a carriage that moved along a track on the back wall of the flume, but unlike the system used by Turnpenny et al. [15], the blade was moved by a motorized belt-driven mechanism [21]. The new modification allowed the thickest, 100- and 150-mm blades to achieve velocities >7.0 m/s and provided a blade strike velocity range of 3.0 to 12.2 m/s [17,22,23]. This study also used view windows and high-speed videography to film impacts for later visual inspection to confirm exact strike impact characteristics. Fish were held in a head-up, ventral surface outward (toward view window) position using monofilament line and Styrofoam braces that were designed to allow the fish to move freely after contact with the blade [17]. The exact position was also difficult to maintain using this method and, in some cases, led to mortal injuries as a result of interactions with the monofilament line [17]. In all studies using this apparatus, only live fish were tested including rainbow trout, white sturgeon (*Acipenser transmontanus*), and American eel (*Anguilla rostrata*; Table 1) [17,22,23]. Both instantaneous (1-hr) and delayed (96-hr) mortality were estimated for each treatment group and for all species tested. Adjusted mortality rates were reported for each species that included delayed mortality and were adjusted for control deaths if observed [17]. Biological response models were based on adjusted mortality rates and grouped according to fish body length to blade thickness ratio (L/t ratio). Linear relationships were assumed across a range of blade strike velocities but no formal regression analysis (e.g., with regression coefficients or tests of statistical significance) were applied to these models which limits interpretation.

Oak Ridge National Laboratory

The apparatus used at Oak Ridge National Laboratory (ORNL) for blade strike experiments was designed based on insights gained from all previous work. More specifically, the overall size of the blade strike apparatus reduced and the addition of

mounting brackets allowed for more precise control of fish positioning. The system also relied on stored energy from a single extension spring that could be easily was loaded and released within a few seconds. The spring assembly was attached to the blade arm that extended down into a 0.324 m3 stainless-steel tank that could hold up to 320 L of water (Figure 3). Simulated turbine blades used with this system were made of aluminum, had a semicircular cross section, and contained a blade shaft that extended upward from the blade itself. The blade shaft slid inside the blade arm where it was securely fastened. The blade was "loaded" by extending the spring until safety release trigger was engaged. Once triggered, the blade moved in an arc toward the front side of the tank where it would hit a rubber stopper and come to rest. Blades with leading-edge thicknesses of 19, 26, 52, and 76 mm were used, although most trials used the 26- and 52-mm blades. Blade strike velocity ranged from 4.9 to 15.3 m/s (Figure 4), but the exact velocity range generated was dependent on blade leading-edge thickness. Velocity was changed by adjusting the tension on the spring using the bolt tensioner or changing the slot position where the spring attached to the blade arm. In addition, up to three pieces of flexible tubing could be secured around the blade arm to further reduce blade strike velocities. Standard curves were created for 26-, 52-, and 78-mm blades according to bolt setting, slot position, and average strike velocity for quick reference during experimentation (Figure 4). Fish were held in place on two mounting brackets that hung down into the tank along the front wall at a shallow angle such that the blade would make contact with the fish body perpendicular to its mid-sagittal axis. Fish were loosely secured to the brackets using flexible tubing that gently held the fish in place while still allowing the fish to move freely once struck. Modifying the brackets also allowed angle of strike to be changed and to better accommodate each species. Impacts on the fish were filmed through a viewing port using high-speed videography at 1,000 frames per second to confirm exact strike conditions and estimate blade strike velocity. To date, live tests have been conducted on nine species including rainbow trout and American eel, but new species like American paddlefish (*Polyodon spathula*), gizzard shad (*Dorosoma cepedianum*), American shad (*Alosa sapidissima*), blueback herring (*Alosa aestivalis*),

brook trout (*Salvelinus fontinalis*), hybrid striped bass (*Morone saxatilis* × *M. chrysops*), and bluegill sunfish (*Lepomis macrochirus*) were also investigated (Table 1). Instantaneous (1-hr) mortality rates were estimated but inferences linked to major injuries like vertebral fractures were also used to assess more conservative estimates of mortality [9,11,18]. Biological response models were reported as rates of mortality versus blade strike velocity using log-logistic dose-response analyses.

Biological Responses to Blade Strike

Mortality Rates

The baseline estimate of mortality includes any fish that is moribund or dies during a 1-hr observation period, though this may underestimate actual mortality. Early work at ORNL found little difference in mortality rates for 1 and 48-hr post exposure so only 1-hr mortality rates were assessed for most species [9,21]. In contrast, research performed by EPRI [17,22] observed that some fish held up to 96-hr would die after blade strike impact. Delayed mortality could increase the overall mortality rate (or decrease survival) by up to 25% for some treatments where fish were exposed to higher strike velocities [17,22]. Mortality estimates at ORNL did not include delayed mortality; however, internal necropsies were used to further refine estimates and account for severe injuries like vertebral fractures. Vertebral fractures including internal decapitation were assumed to be severe enough to limit the ability of fish to escape predators, acquire sufficient food, or reproduce, so they were classified as functional or ecological (i.e., the individual has no chance to contribute to the species genetic pool) mortalities. While not linked directly to blade strike impacts, predation on entrained fish have been observed in the field by piscine, avian, or mammalian predators following turbine passage [24–28]. More importantly, field confirmation of functional death could be assessed during the post-passage observation period using reflex impairment indices which have been significantly correlated with elevated stress levels and increased instances of delayed mortality [29–31]. To that end, a new combined mortality metric was created using

instantaneous and functional mortalities because it was a more conservative estimate of mortality, much like the EPRI-adjusted rates of survival which included delayed mortalities [17,22]. Combining these two metrics is supported by the observation that the combined mortality rates for American eel were similar to adjusted survival rates reported by EPRI [17,18]. Both estimates are likely comparable because spinal damage was observed in American eel during the 96-hr observation period, but this was not confirmed by necropsy [17]. Direct statistical comparisons between treatment group mortality rates (within or between studies) is possible using sample-size corrected Chi-square tests [9], but these tests lack the ability to detect trends across multiple exposure conditions [11,18].

Dose-response Models

Generating biological response models that can predict a response (i.e., mortality) as a function of the dose (i.e., blade strike velocity; m/s) offers the most useful form of these data for turbine designers or dam operators [32]. Biological response models for blade strike were initially linear models of mortality versus blade strike velocity for each fish body length to blade thickness (L/t) ratio group (Figure 5) [17,22]. These linear models did not separate treatment conditions (location, orientation, or impact angle), the number of treatment groups for each L/t ratio were low, and no linear regression analyses were reported. Combined, these limitations suggest use of linear models to estimate mortality may actually underestimate survival for each L/t ratio group in some circumstances. The biological response models produced at ORNL regressed combined mortality rates against blade strike velocity for fish exposed to mid-body, lateral strikes at 90°. These conditions usually caused the highest mortality rates and were used to generate baseline biological response models for each species. Models were generated from four-parameter log-logistic regression given by the following equation [33]:

$$f(x; b, c, d, e) = c + \frac{d-c}{1+\left(\frac{x}{e}\right)^b} \quad (1)$$

where *f(x)* is the estimated mortality rate, *x* is the strike velocity (m/s), *b* is the inclination point, *c* is the lower boundary for mortality rate and was fixed a 0.0, *d* is the upper boundary for mortality rate and was fixed at 1.0, and *e* is the effective dose (ED_{50}) of velocity that would be expected to cause 50% mortality. Ideally, separate curves would be created for each treatment scenario but it is logistically challenging and impractical to test all possible exposure conditions. Rather, biological response models were created for mid-body, lateral strikes at 90° (i.e., worse-case scenario) which could be modified based on any data generated from different treatment conditions. One limitation of this method is higher levels of uncertainty of the model associated with smaller samples sizes used in each group. At the least, these models clearly indicate the range of velocity where 0 to 100% mortality would be expected during worst-case scenarios for each species.

Factors Affecting Mortality—Turbine Characteristics

Turbine Type

Rates of injury and mortality among fish are closely linked to the type of turbine installed at each hydroelectric dam, and the Francis and Kaplan turbines represent the most common types installed in the United States [34]. Francis turbines have the most installed capacity to date (~66%), but are installed less frequently at new hydropower plants (~33%) [34]. Francis turbines are ideal for locations with 10 to 550 m or greater of head and are best for systems with water flows between 0.5–25 m3/s [35,36]. Design characteristics include 9 to 25 fixed runner blades [35] with radial water flow entering and axial flows exiting the turbine [36]. Blade leading-edge thickness and velocity varies along the meridional length of the runner with a range of thickness between 10 to 25 mm [37] and velocities between 3.0 to 23.0 m/s (Andritz Hydro, *personal communication*). All these design characteristics are likely why Francis turbines have the highest incidences of fish passage mortality; however, exact mortality varies by project based on operation regimes and local hydrology. Nonetheless, estimates of mortality for Francis

turbines can be as low as 5% but as high as 75% for some projects and fish species [3,36,38–40].

Kaplan-type turbines actually form a group of slightly different but related turbines, most notably characterized by fewer blades and considered to be more fish friendly overall. Kaplan turbines (including both horizontal and vertical units) are mostly installed at sites that have low head (i.e., 2 to 50 m) over a much wider range of flow rates between 0.2 to 50 m3/s [35]. In addition to fewer runner blades (i.e., 3 to 8), wicket gates and runners may be adjustable, which allows dam operators to optimize performance [35,41]. Additional modifications, such as minimum gap runners designed to avoid grinding-type injuries, are becoming standard features in new turbine designs to increase fish survival [42]. The blades of modern Kaplan turbines are also larger and have more pronounced variation in leading-edge thickness along the meridional length—the thickest part of the blade is located near the hub and the thinnest at the tip [9]. In addition, the velocity of the blade also changes along the same continuum because of the rate of rotation and change in radius from the center of rotation. Thus, the thicker portion of the blades moves slower than the fast-moving, thin sections of the blade at the periphery at the maximum extent of the radius and therefore risk to fish increases as they pass further from the hub. Modifications like fewer, adjustable blades or minimum gap runners are likely why Kaplan turbines have noticeably higher fish survival rates (88 to 96%) than Francis turbines [36]. Strikes of sufficient magnitude do occur and are likely responsible for some instances of mortality among fish passing through them [41].

Blade Leading-Edge Thickness

One of the most prominent factors linked to differential rates of injury and mortality among fish is blade leading-edge shape and thickness. The exact shapes of turbine blades are proprietary, but previous laboratory studies have shown blades that have semicircular leading edges limit hydrodynamic drag, which suggests they are better suited to simulating turbine blades than elliptical shapes [17]. Information regarding leading-edge blade thicknesses is also not widely distributed because industry developers

consider blade geometry to be proprietary as well. In addition, insights from one turbine are difficult to apply to all turbines of a specific type because each has been engineered according to project-specific parameters [9]. While available information is lacking related to blade design in turbines, valuable insights have been gained about the biological response of fish to leading-edge blade thickness and design. In general, regardless of species, controlled laboratory studies have shown that thinner blades tend to have higher rates of fish injury and mortality [9,15,17]. To date, laboratory studies involving blade strike have found the same trends across a range of leading-edge thicknesses from as low as 10 mm and up to 150 mm [17,22]. The disparity between 0% and 100% mortality is quite dramatic over small increases in blade thickness when strike velocity is the same. High-speed video footage has shown that a zone of displaced water (i.e., a bow wave) is formed in front of the simulated blade caused by differential pressure distribution [17], which has the effect of causing the fish body to begin bending before actual contact with the blade. For example, the bow wave of a thicker blade (≥ 52 mm) is associated with higher levels of pre-bending, while maximum curvature around the blade is notably less compared to a thinner blade (Figure 6). In contrast, the bow wave of thinner blades (≤ 26 mm) is less pronounced and does not cause as much pre-bending or movement of the fish body prior to actual blade strike (see Figure 3-5 in EPRI [17]). Curvature of thin blades also occurs over a smaller section of the fish body and the maximum curvature of impact is more pronounced at the point of contact [15,17]. Thinner blades would also cause the energy of the strike to be transferred over a much smaller surface relative to thicker blades, which would also lead to higher rates of injury and mortality. The presence of a strong bow wave effect that decreases maximum body curvature and dissipates energy over a larger surface area may explain why mortality is significantly lower with thicker blades when impact velocity is held constant.

Realized Impact Velocity

The second characteristic of the turbine blade to consider is realized impact velocity, i.e., the velocity at which the blade makes physical contact with the fish body.

The actual or realized impact velocity is determined by accounting for both the angular velocity of the blade at the radius where the strike occurs and that of the fish. Because the velocity of a fish passing through the turbine is difficult to obtain or model, the water velocity is often used as a surrogate. Rotational velocity is a function of turbine revolutions per minute (RPMs), which in turn varies by turbine, operational conditions, and the radius from the center of rotation. Across all turbine types, RPMs may range from 50 to 900 with Francis turbines operating at higher RPMs than Kaplan-type turbines [9]. Water velocity is related directly to flow rate (discharge), which can range from 0.2 to 50 m^3/s [35], cross-sectional surface area of the turbine inlet, and subsequent water passage through the distributer, runner, and draft tube. Water velocity is important because we assume fish move in the same direction as water flow after reaching critical swimming speeds, fatigue, and succumb to water movement. The orientation of the fish entering the turbine is not known and is also assumed that the water (and fish) moves in the same direction as the turbine blades, which simplifies realized impact velocity calculations. If these assumptions are true, the realized impact velocity would be the difference in the runner compared to water velocity vectors; however, this may be a low estimate, which would increase as angular velocity vectors of water flow changes direction relative to the turbine runner [9]. Like blade width, realized impact velocity would change along the meridional length of each turbine blade. In Francis turbines, the velocity may increase in the crown (uppermost portion) to band (lowermost portion) direction, and velocities as low as 3.0 m/s near the crown or in excess of 20.0 m/s near the band may be possible (Andritz Hydro, *personal communication*). In contrast, Kaplan turbines would have the slowest velocities near the hub, fastest near the tip, and form a continuum in between the hub and tip along the leading edge of the blade. In general, higher impact velocities cause significantly higher rates of injury and mortality—impact velocity becomes especially lethal as it reaches 10.0 m/s for most species during direct hits, though the exact velocity range depends on species and blade thickness.

Factors Affecting Mortality—Fish Characteristics

Location of Impact

When a fish enters a turbine, impact could occur anywhere along the length of the fish, from head to tail, and risk of injury or mortality is dependent on the location of impact. Estimates of injury and mortality are often first linked to strikes that occur on the head, mid-body, or tail (Figure 7). The head refers to the area between the snout and posterior margin of the operculum, but the exact proportion of the head relative to total length varies by species. The "mid-body" or trunk generally includes the fish body between the posterior margin of the operculum and anterior margin of the anal fin. Caudal or tail regions of fish were considered any location posterior of the anal fin for most fishes at risk to pass through turbines. For most species this breaks the body surface into roughly equal thirds (except American eel and paddlefish). Injury and mortality rates are generally higher in individuals struck on the mid-body for all species tested to date [9,11,15,17,18,22,23]. Mid-body strikes are likely worse because this area includes the location of most internal organs, ribs, as well as the vertebral column. The center of mass is also found in the mid-body region of most species which would cause the blade to remain in contact with the body longer and lead to greater changes in acceleration during blade strike impact [15,23]. Thus, strikes near the center of gravity would transfer more of the impact force onto sensitive tissues or organs causing higher incidences injury and mortality. In contrast, tail strikes are associated with low rates of mortality (generally <20%) at velocities up to 12.0 m/s because the fish body deflects away from the blade following impact [9,15,23]. Low injury rates in the caudal region are likely because it has less mass which lead to more deflections [15,23] and is dominated by the musculoskeletal system with very few internal organs found in this region (i.e., posterior edge of kidney or swim bladder). Head strikes lead to higher rates of mortality than tail strikes because of greater relative mass of the head, which may often lead to internal decapitation. Strikes to the head may also be deflected away from the blade when the impact occurs at angles other than perpendicular to the body (Figure 7).

Body Orientation During Impact

The orientation of the fish body when it is struck is also an important factor in injury and mortality risk. Fish orientation can be defined by three distinct body surfaces—dorsal, lateral, and ventral (Figure 7). The dorsal (upper side or back) and ventral (bottom side or belly) surfaces correspond to less surface area than the two lateral (side) surfaces of laterally compressed fishes. Furthermore, each surface may be distinguished by the relative proximity to, and differential interactions with, the musculoskeletal system or abdominal cavity organs during blade strike impact. As fish dimensions change the amount of surface area also changes and may become more equally distributed between all three surfaces. Similarly, the probability of strike at any orientation is assumed to be equal for all three orientations; however, lateral strikes are more likely because fish have two sides. Strikes on the left versus right lateral surface were considered to have the same effect on fish injury and mortality because fish are bilaterally symmetrical along the medial or mid-sagittal plane. Strikes on the lateral surface were also associated with the highest rates of severe injury and mortality, which often reached 100% at or below 10.0 m/s strike velocity across all species regardless of blade leading-edge thickness [9,17,18,22]. Lateral strikes often correspond to the highest incidence of rib and vertebral fractures, though damage to the liver and kidney are also common [9,18]. Dorsal strikes also cause injury (e.g., vertebral fractures) but mortality is typically lower than lateral strikes. Ventral strikes caused injuries to soft tissues (organs and musculature), observations of skeletal fractures were uncommon, and had the lowest incidence of mortality among species tested.

Angle of Impact

Like location and orientation, the exact angle at which the turbine blade impacts passing fishes is not known, but rates of severe injury and death are affected by impact angle. The angle of impact is a more challenging variable to define because each fish could conceivably be struck at any angle (0–180°) on each surface and location (Figure 8). The total number of exposure conditions a fish may encounter is nearly infinite, which

makes it impossible to test them all. After initial trials, 0 and 180° (i.e., direct head and tail strikes, respectively) were not considered because of the low probability of a blade contacting the fish from these angles and the high likelihood of deflection for these strikes. Further testing revealed that strikes perpendicular to the mid-sagittal axis (i.e., 90°) were the most injurious impact angles for all species [9,18,22]. Mortality at this angle often reaches 100% and is also associated with the highest incidence of severe injuries including spinal fractures at velocities near 10.0 m/s. Additional trials included 45 and 135° blade strike impacts to better approximate the probability of mortality associated with blade strike [9,18,22]. Strikes at 45° are defined by any impact that occurs in a head to tail direction. Excluding hits to the tail, head strikes at 45° caused more severe injuries because the blade traveled toward the mid-body after contact where it could transfer more energy to the soft tissue and the musculoskeletal system. Most 45° strikes to the mid-body did not cause severe injuries or mortalities because the body of the fish deflected toward the caudal fin and away from the blade after initial contact. The opposite was true for 135° strikes because mid-body strikes had the highest incidence of severe injury and death. These strikes were likely more injurious because the blade travels toward the head after initial contact, where it may transfer energy to the mid-body, operculum, and gills. All 135° strikes to the head caused the fish to immediately deflect away from the blade after initial contact. Recently, Amaral et al. [23] reported that 60° and 75° strikes had rates of mortality between estimates for 45° and 90°, which suggests mortality rate may increase in a predictable way with impact angle; however, these angles have not been tested extensively and the previous study did include 120° or 150° strikes and used an experimental blade design with markedly different shape. It is assumed that most strikes other than 90° would probably result in deflections based on how the fish body moved following strikes from a blade at 45° or 135°.

Fish Length

Fish size, and how it affects injury and mortality rates, is also of critical importance but the exact relationship is unknown. Fish size plays a role in nearly every

part of fish passage starting with entrainment risk, which is highest for small fish [2,42]. Unlike other fish characteristics, there is no clear trend in injury or mortality rates linked with fish size that is true for every species tested. Turnpenny et al. [15] described a size effect linked to standard length but also emphasized fish mass and related variation in the inertial effect to higher probability of impact in larger versus smaller fish. More importantly, small fish were often pushed out of the way and to the side of the blade by its approaching bow wave because these fish had masses < 20 g [15,16]. Rainbow trout and *Alosa* spp. with an average mass below 20 g also moved more dramatically than larger individuals as the largest diameter blade (i.e., 76 mm) approached each fish [11]. Center of gravity and the movement of fish after blade strike impact are linked with inertia, which may partially explain why rates of injury and mortality differ among fish according to size. Susceptibility to blade strike impact is undoubtedly dependent on size, but size-based trends in one species does not necessarily translate to the other species.

More recent experimentation by EPRI [17] built upon work by Turnpenny et al. [15], but also directly tested size effects. One of the main comparative metrics of this study was the L/t ratio (the ratio between fish length and blade thickness) that accounted for size within each treatment group of fish. As the L/t ratio increases, i.e., as the size of the blade decreases relative to the fish or as the size of fish increases relative to the size of the blade, estimated survival decreases (Figure 5). In a similar way, smaller blades that impact relatively larger fish were specifically injurious because released energy and body curvature after strike is dissipated over a smaller area of the fish body [17,22]. Treatment groups with L/t ratios near or below 1.0 correlate with blade thicknesses that nearly match fish length and also have notably higher survival [17]. Fish struck with blades comparable to their own length bend less after impact and the energy of strike would be dissipated over a larger section of the fish body. This trend was true for species like rainbow trout, white sturgeon, and American eel for L/t ratios of 25.0 and velocities up to 12.2 m/s [17,22]. While trends in L/t ratio seem well supported, the estimates of mortality for some groups contained fish that were decapitated as a result of the apparatus design and not blade strike specifically [17]. Furthermore, there is no indication about how many

individuals or for what treatments this was true, but the authors included these fish as a conservative estimate of mortality [17]. Work by EPRI [17,22] also did not explicitly separate survival rates based on specific treatment conditions (i.e., location, orientation, and impact angle) so that survival rates for each L/t ratio include all fish in that group. Estimated survival did include individuals that experienced delayed mortality within 96 hours of strike, but no internal necropsies were performed to determine the actual cause of death of those fish. All L/t ratios for each treatment group were based on average body length, which may dilute the effect of size because individual variation was not analyzed. Lastly, no regression analyses were applied to each L/t ratio data and no statistical tests were used to compare treatment groups to controls or other groups, which would help strengthen observed trends discussed by these authors.

Trials at ORNL performed from 2016 to 2020 were designed to control all aspects of blade strike and also investigated the effects of size using a variety of statistical methods [9,11,18]. The L/t ratios for rainbow trout [9] and American eel [18] were also estimated during these trials, but these data are difficult to compare because location and orientation were not explicitly controlled in EPRI's original work (Figure 5). Furthermore, trials at ORNL suggested that responses of fish to other blade strike treatment combinations infer differential rates of injury and must be separated along with fish size to better estimate survival [9,11,18]. Size affects in a new species (bluegill sunfish) and additional analyses on rainbow trout were also investigated in more detail. Trials including small (~11 cm) versus medium (~16 cm) bluegill sunfish struck with the 52-mm blade over a range of exposure velocities suggested smaller fish were as susceptible, if not more so, to blade strike injury and mortality than larger fish [18]. This disparity is apparent when comparing dose responses produced from immediate mortality versus mortality estimates that also included fish that survived exposure with vertebral fractures. These individuals were considered functionally dead and added to our combined mortality rates which is similar to adjusted survival reported in EPRI [17,22]. Research on rainbow trout also found that large trout may experience slightly higher mortality than small rainbow trout, but the disparity between the curves is small and

confidence intervals overlapped, suggesting responses are not significantly different [11]. In addition, this work included a logistic regression of mortality against blade width, velocity, and total length. In this way, individual variation in total length was included in regression analysis as a continuous covariate used to predict mortality. Logistic regression indicated that bluegill and rainbow trout size was not a significant predictor of mortality compared to blade width or realized impact velocity [11,18]. Confidence intervals for our biological response curves suggest that bluegill size relationships may be more significant compared to size effects detected in rainbow trout. Low sample sizes of ORNL trials are also associated with more uncertainty (larger 95% confidence intervals) which limits comparisons between dose-response models based on size. Interpretation of logistic regression is also limited by the number of treatment scenarios included in the analysis, which mainly focused on the worst-case scenario (mid-body, lateral strikes at 90°) and did not include as many other treatment conditions. To that end, the opposing trends between fish size and mortality described in ORNL's studies suggests that species is also an important factor and must be considered when estimating mortality.

Fish Species

To date, blade strike trials have been performed on a total of 17 species in nine families of fishes (Table 1), but biological response models have only been developed for eight species and six families. The blade strike data for most species has at least provided a baseline understanding of how physical impact affects mortality rates and has informed the general trends discussed here. Rainbow trout has served as the foundation of most blade strike studies because it has been included in most laboratory experiments completed in the last 25 years. Gizzard shad, hybrid striped bass, and bluegill sunfish are also well represented in terms of number of treatments and range of blade strike impact velocities tested (Table 2). The remaining species data for American paddlefish, American eel, American shad, blueback herring, and brook trout did not include as many treatment scenarios, but biological response models were successfully created for these species (Table 2; Figure 9). In the sections below, species accounts are provided for

biological response models built from baseline (i.e., worst-case scenario) treatment groups (Figure 9). Species accounts are presented in phylogenetic order and are meant to provide general trends observed during blade strike trials that have not been discussed in previous sections. In addition, species accounts may contain descriptions of unique injuries observed during testing that do not apply to other species tested to date. Please note, biological response curves reported for each species are associated with a specific size known to pass through turbines; however, because size is often a variable that affects susceptibility, modeling biological responses of an entire population (of all sizes) using one curve should be approached with caution in certain species.

American paddlefish (average mid-eye to fork length = 27.8 cm; 21.2 – 33.8 cm) were especially interesting because of their mostly cartilaginous endoskeleton, large protruding rostrum, and mostly scale-less body. Resistance to blade strike impact for paddlefish appears to be nearly the same as that for subadult rainbow trout because the predicted ED_{50} (e.g., 6.44 m/s) and velocity exposure range (5.0 to 8.0 m/s) nearly overlapped (Figure 9). Damage to the notochord was rarely observed in paddlefish, but forceful avulsion of the muscle from around the notochord was often observed in moribund or mortally wounded fish. Paddlefish were also observed to have severe damage to their rostrum, which was nearly amputated when struck on the lateral surface of the head at 90° with the 52-mm blade moving at 7.3 m/s. Similar injuries have been observed in the field and many paddlefish collected in large rivers in the Midwest are often missing rostrums [43,44]. Interestingly, while the damage to the rostrum was quite severe, most of these individuals did not die from the trauma, suggesting their survivability is high. This is the first instance where laboratory results have been directly observed in the field, suggesting this trauma may be linked to blade strikes specifically during turbine passage.

American eel (average total length [TL] = 53.9 cm; range = 45.7 – 67.5 cm) was the most resistant species tested, which is likely a result of their unique, anguilliform body shape, that is mostly tail. Mortalities in eels were not observed until velocities reached at least 12.0 m/s, but insufficient treatment groups were tested to determine the

complete velocity exposure range [18]. No biological response model could be created directly for American eel though inferences were made so it could be included in HBET and BioPA. For example, eel was considered in fifths instead of thirds like other species because of the large tail region of this species suggesting velocities in excess of 13.6 m/s would be required to cause 100% mortality. Interestingly, dorsal strikes to the head were associated with much higher mortality rates than both mid-body lateral and dorsal strikes in eel, which was not observed in other species. Lateral and ventral mid-body strikes also caused traumatic injuries to the liver (e.g., tissue became friable) and in a few cases ruptured the gall bladder, which is probably related to lack of ribs to protect internal organs.

Young of the year (average TL = 7.6 cm; range = 6.1 – 10.3 cm) American shad and blueback herring were analyzed and reported together as Alosa spp. because of the remarkable similarities in their body shapes and sizes that are at highest risk of turbine passage [11]. These clupeids are also notably resistant to blade strike impact with an ED_{50} value of 7.87 m/s and formed the upper limit of biological response models with hybrid striped bass (Figure 9). The overall velocity exposure range was only about 2.0 m/s, and steepness of the curve suggests the rate of mortality increased faster than other species tested to date [11]. Vertebral fractures were by far the most common injury observed, but eye amputation also occurred at the highest impact velocities with the thinnest blade. Review of high-speed video showed that the approaching blade and bow wave had a profound effect on these fishes, which would begin to curve well before being struck. The bow wave effect was especially prominent for the largest (76-mm) blade which would often push the fish aside and out of the impact zone completely. Turnpenny et al. [15] observed similar phenomenon in fish less than 20 g—both Alosa spp. tested were also well below 20 g in mass and have comparably high surface area-to-body ratios.

Gizzard shad (average TL = 16.0 cm; range = 14.3 – 17.2) were one of the most susceptible species to blade strike impact (Figure 9). The ED_{50} for gizzard shad was 5.66 m/s, which was the second lowest value recorded when compared to other species tested at ORNL. The velocity exposure range was between 5.0 to 8.0 m/s, which is comparable

to most other species but a noticeably wider range than *Alosa* spp. [11]. Direct comparison with *Alosa* spp. was not possible because the gizzard shad tested were two times longer on average. Much like other species, vertebral fractures were the most common severe wound observed. Interestingly, in nearly every individual tested hemorrhaging, clotting, and sometimes avulsion of gill tissue was observed within the buccal cavity and operculum chamber as well.

Rainbow trout remains the most tested species with blade strike data over the last 25 years, but many insights are based on mid-body lateral strikes at 90° only [9,11,15,17,22,23]. The most recent study at ORNL included biological response data for both small (average TL = 11.6 cm; range = 10.1 – 14.9 cm) and large (average TL = 16.1 cm; range = 20.1 – 31.6 cm) fish to directly test the effect of fish size. The predicted ED_{50} value for large trout was 6.59 m/s, which was slightly lower than small trout with 7.08 m/s [11]. Both small and large trout have a velocity exposure range of ~3.0 m/s, though the slope of the small trout curve indicates that the increase in mortality after 7.0 m/s occurs quickly (Figure 9). Differences in the frequency and number of spinal fractures were also detected when small rainbow trout were not observed to have internal decapitation but large fish were.

Brook trout (average TL = 24.8 cm; range = 19.3 – 29.3 cm) fell in the mid-range susceptibility of all the species tested and the biological response model covers a slightly wider velocity exposure range of 4.0 – 9.0 m/s (Figure 9). The ED_{50} for brook trout was ~6.0 m/s, which places it within the same range as medium-sized bluegill and gizzard shad [11]. Dorsal, mid-body strikes at 90° had a higher rate of mortality than mid-body lateral strikes, which differs from all other species tested to date. Mortality was observed in at least 13 brook trout exposed to lateral strikes to the head at 90°, but no apparent cause of death could be confirmed and none of these fish suffered vertebral fractures. Inflammation or other aspects of a potential stress response to blade strike impact was suspected as the likely cause of death in these individuals (Debra Miller, DVM/PhD, *personal communication*) and was not observed in any other species tested. Inclusion of biochemical indicators, such as cortisol, glucose, or lactate, of stress could be used to

further elucidate mortality estimates in fish that have no obvious signs of impact-related trauma.

Hybrid striped bass was the second most resistant to blade strike of all the species tested, after American eel. This species had a predicted ED_{50} value of 8.32 m/s, could potentially survive velocities above 9.0 m/s, and had a velocity exposure range of nearly 3 m/s (7.2 – 9.6 m/s), but only one size group (average TL = 18.0 cm; range = 15.6 – 21.3 cm) was investigated (Figure 9). Also of note, is that the biological response curve for hybrid striped bass was inferred from the 26-mm blade [9] to approximate the 52-mm curve shown in Figure 9. This curve was created by adjusting the 26-mm curve by adding +1.0 m/s to the ED_{50} value and translating the entire curve to the right. For the purposes of comparison, we included because Chi-square tests suggested that the 26-mm blade had significantly higher mortality (i.e., lower ED_{50}) than the 52-mm blade and this simple adjustment created a curve that fit available treatment data for the thicker blade well. Regardless, this species was still quite resistant to blade strike considering few trials with the 52-mm blade were performed because of low observed mortality.

Bluegill sunfish was the most susceptible species tested to date and size effects were exactly opposite of those described for rainbow trout. In fact, small bluegill (average TL = 11.8 cm; range = 9.0 – 14.7 cm) were markedly more susceptible than medium bluegill (average TL = 16.1 cm; 12.2 – 17.7 cm) and mortalities were observed at velocities below 4.0 m/s [18]. The ED_{50} values for both sizes also differed by more than 1.0 m/s, which was greater separation than observed for any other analysis that included within-species comparisons (Figure 9). Bluegill was also the first species for which multiple vertebral fractures were confirmed; i.e., up to three separate fractures was not uncommon. Functional mortality rates were especially high among bluegill because many of the individuals of all sizes tested did not die as a result of skeletal fractures. Other injuries of note included lacerations and rupture of gonads for both sexes, but especially gravid females. This species is also the best represented relative to the number of different treatment scenarios investigated because many experiments were conducted

on fish struck on the head, dorsal and ventral surfaces, and 45° and 135° strike angles [18].

Fish Shape and Body Morphology

Fish are the most taxonomically diverse group of extant vertebrates with nearly 40,000 species described to date [45]. Fish have evolved into a variety of unique shapes that are best adapted to suit their needs (e.g., interacting with the environment, use of resources, and other life history requirements). In biological terms, fish shape is most often linked with swim type—proportion of the body and fins involved with propulsion—which in turn relates to swimming performance based on the biomechanics of movement [46]. Fish shape likely plays an important part in susceptibility to turbine passage-related injuries including blade strike impact as well. For example, many riverine species, including clupeids (shad/herring), centrarchids (sunfishes), moronids (temperate basses), and percids (perch-like fishes), have laterally compressed bodies that are much deeper than they are wide. In contrast, acipenserid (sturgeons), anguillid (true eels), ictalurid (North American freshwater catfishes), and catostomid (suckers) fishes are more rotund so that the disparity between body depth and width is reduced. The salmonid (salmon/trout), cyprinid (minnows), and esocid (pikes/muskellunge) fishes have shapes that fall somewhere between these other groups. Regardless, it seems reasonable to assume that each shape, and the inherent biomechanical traits linked with shape, would also have unique susceptibility to blade strike. Laterally compressed fish have much less musculature along their lateral flanks than other groups, which would not absorb as much energy after impact. Less muscle may cause more energy to transfer directly onto the skeletal system and organs, thereby causing higher rates of injury or mortality in these fishes. The exact relationship between body shape and susceptibility to blade strike injury or mortality has not been explicitly tested.

Center of Gravity (Mass)

Another species-related difference is consideration of fish as a physical object and variation in susceptibility to blade strike linked to proximity of impact to the center of gravity. Strike events occurring near the center of gravity would transfer more energy to vital organs and the axial skeleton, which may explain the higher injury and mortality rates observed from mid-body strikes. Early work by Turnpenny et al. [15] found that impacts from a turbine blade were always deflections unless the blade contacted the body close to the center of gravity. Bevelhimer et al. [9], showed similar trends in hybrid striped bass for which the highest number of mortalities were associated with strikes to the head and mid-body near what is likely the center of gravity for this species. More recently, Alden Laboratories found that fish struck near the center of gravity also interacted with the blade longer which likely exerted more of the impact force onto the fish and decreased survival [23]. To investigate this directly, two different groups of rainbow trout were exposed to blade strike impact with a 52-mm blade at velocities known to be nearly 100% lethal. Fish were struck along their entire body length (head to tail) to link vertebral fractures to location of strike relative to center of gravity. In general, vertebral fractures were more likely and severe (i.e., more than one fracture) as the impact occurred closer to the center of mass for both small and large rainbow trout (Figure 10). Interestingly, a separate cluster of internal decapitations was observed in large rainbow trout linked with impacts to the head, but similar impacts did not cause the same injuries in small rainbow trout. Internal decapitations were likely observed in large fish because their head has more mass compared to small fish, suggesting strikes near vulnerable points (e.g., the connection of vertebral column to the cranium) may also cause fractures as well. While the latter may be true, uncertainty remains because the experiment was not replicated which limits its interpretation, especially for other species. For example, the proximity of major organs to the center of gravity of paddlefish and American eel would be markedly different compared to salmonids. Center of gravity is generally between 35 to 50% of standard length [15,23], but the underlying relationship

between center of gravity, blade strike impact, and severity of injury or mortality has not been directly tested.

Biomechanical Traits

The biomechanical traits of fish, or the inherent physical properties related to the mechanical behavior of their entire body or vertebral column, may also account for differences in blade strike injury and mortality susceptibility among species. Fish are a complex, well-adapted, mixture of mucus, scales, skin, muscle, and skeleton—the exact size, shape, and proportion of each structure also varies by species. To date, data from blade strike trials suggest that mid-body, lateral strikes at 90° causes the highest incidence of severe injury and death compared to other conditions [9,11,17,18,22]. The high rates of mortality from lateral strikes are surprising considering dorso-ventral flexion of the body and vertebral column is minimal even in particularly flexible anguillid eels. Likewise, medial-lateral movement of the fish body about the center of gravity is normal and may be quite profound for certain species. There are contrasting demands at play with fish that have evolved efficient shapes and rigid musculoskeletal systems to maximize swimming efficiency; however, the same adaptations also allow for extraordinary flexibility during escape responses from predators. The startle or escape response is characterized by the formation of a "C-shape" of the fish body when the head and tail curve toward one another prior to a spring-like motion in a new direction [46,47]. Escape responses of fish occur within a few milliseconds during which the body returns to normal orientation but in the direction perpendicular to the stressful stimulus [48]. The exact dimensions of the C-shape (i.e., how close the head gets to the tail) varies by species and condition of the fish tested [48,49]. These disparities among species have prompted use of this behavioral phenomena as a latent indicator of stress caused by turbine passage [48–50], but no such link has been made with blade strike impact to date. Of particular interest is gaining a better understanding of how flexibility observed during the startle response compares to the curvature caused by blade strike impact. Both the startle response and impact curvature appear to be approximately the same (R. Saylor,

personal observation) and occur over comparable time scales, but resistance to blade strike may only be partially related to flexibility.

Discussion

Use of Species Surrogacy

All laboratory work performed at ORNL was directed via prioritization of species analysis and use of surrogates to represent the most at-risk groups of fishes. Most prioritization relies on traits-based analyses that link common biological, ecological, or life history traits to groups of taxonomically related fish and estimated entrainment risk [51,52]. Species were chosen because they were affected by hydropower, broadly representative of each taxonomic group, easy to collect or purchase, were not considered threatened, and were reasonably easy to maintain in captivity. While the latter is justifiable from a logistical standpoint, more quantitative evidence is needed to support using surrogacy for blade strike biological response models. Recent experiments at ORNL were directed at this very problem and tested surrogacy directly for salmonids and clupeids. Results suggested that surrogacy among salmonids was possible at the genus level, i.e., *Oncorhynchus* (rainbow trout) and *Salvelinus* (brook trout), because responses to blade strike were not significantly different from one another and impact variables were more important predictors of mortality [11]. In contrast, however, size-based surrogacy within a species was ill-advised because the exact relationship between size and mortality has yet to be broadly applied to all species. Surrogacy among clupeids was also deemed possible so that species within the *Alosa* and *Dorosoma* genera could be represented by one biological response model for each genus. This was the first instance of quantifiable support for blade strike surrogacy using biological response data and suggests that the biological response models can potentially be applied to other groups beyond the nine species tested to date.

Data Limitations

In this review, we have highlighted many insights gained from laboratory trials for determining blade strike impact over more than 25 years of active research. This summary would not be complete without discussion of limitations associated with potential application and use of the biological response data. To start, at least half of the tested species are still in need of additional research to increase the understanding of trends beyond worst case scenarios (i.e., mid-body, lateral strikes at 90°) available for species tested to date (Table 2). Methods employed at ORNL allowed the effects of strikes at different locations, orientations, and impact angles to be studied more extensively than previous studies. There are two potential limitations: determining which trials to prioritize and deciding how to balance uncertainty in the estimates with knowledge gained by having more treatment groups. Ideally, blade strike testing could continue for all species to confirm the assumptions about impact characteristics across a wider range of strike velocities. Small samples ($n < 25$ fish per treatment) may be viewed as a limitation, but treatment groups with at least 20 individuals were found to be sufficient with an estimated 95% confidence range of ~0.5 m/s for ED50 values from biological response models (Figure 11). Moreover, using 100 fish to investigate five treatment scenarios is better than using them all in just one experiment that seeks to limit uncertainty at the cost of gaining more relevant knowledge by including more treatment groups. Obviously, uncertainty is an important consideration when factoring into turbine design, but the blade strike apparatus and experimental procedures discussed in this review are designed to maximize the replicability and utility of these biological response data. Surrogacy and its use with blade strike data specifically is only limited by how well one can argue two or more groups of species are similar or different. Most assumptions about surrogacy are based on similarities in biology or ecology and how other researchers have used surrogacy and trait-based data to successfully group related fishes. One important limit of surrogacy in the context of blade strike dose-response models is that size-based substitution within the same species is not advised unless no other data are available.

Research Needs

Though significant advancements have been made, more research is needed to better understand how blade strike impact affects fish survival. To start, key gaps in available knowledge for species like American eel and paddlefish need to be filled to more completely to understand how susceptible both species are to blade strike. It would be beneficial to test more American eel at much higher velocities (up to 15.0 m/s or more) to determine the velocity and leading-edge blade width that causes 100% mortality for 90° lateral strikes. These data would be especially useful because eels are often severely injured by turbine passage and currently there is a lack of sufficient evidence to rule out blade strike impact as the main cause. Alternatively, no one has attempted to design a study of the pinching or grinding of eel between the stators and rotors, which is presumed to be the main cause of amputation and mortality observed in subadult yellow- and silver-phase eels [18]. Research on American eel has broad international appeal because of comparable species like the European eel, which often becomes entrained in hydropower dams located throughout Europe as well. Paddlefish are of particular interest at dams throughout the Mississippi River watershed because this species is often captured with obvious signs of turbine passage-related trauma, such as rostrum damage, disfigurement, or complete amputation [44]. Observations of similar injuries during laboratory experimentation suggest blade strike is the most likely cause; however, previous experimental work was based on only ~100 individuals and additional research focused on effects of blade strikes to the head and paddle would be informative. The paddlefish reference biological response model was only based on three treatment groups and investigation of more scenarios would also be ideal to help reduce uncertainty in its biological response model.

Research efforts at ORNL have focused on species that are broadly representative of passage concerns in the U.S. However, only minimal laboratory testing of turbine passage-related stressors has been performed on cypriniform fishes (carps, minnows, suckers, and chubs) and no blade strike data are currently available. More laboratory studies on cypriniform fishes are especially important because they represent the most

diverse order of freshwater fishes globally [45]. While migratory patterns of most freshwater fishes are unknown, many cypriniform suckers and some large-bodied minnows are likely potamodromous—fish that migrate between upper and lower reaches of rivers and lakes but do not travel at any time to the marine environment [53,54]. Most efforts to understand passage concerns at dams focus on anadromous salmonids, clupeids and catadromous anguillids, but largely ignore potamodromous cyprinids and catostomids [55]. Both families have unique body shapes, morphological traits, and attain a variety of sizes that likely make them very susceptible to turbine passage-related stressors as well. To date, none of these species have been tested and their distinct cross-sectional profiles and large cycloid scales suggests a profoundly different response to blade strike impact compared to other fishes tested so far. Outside of North America, groups of fish belonging to the Characiform (e.g., piranha and tetras) and Siluriform (catfishes) orders should also be investigated because their unique body shapes and marked diversity in South American and Southeast Asian rivers where new hydropower development is occurring rapidly.

Lastly, there is a need for novel research into the biomechanics of blade strike impact and how differences in fish size, shape, and morphological characteristics affect estimates of mortality. Studies of this nature would also allow us to use traits-based approaches by defining and grouping fish based on shared biomechanical characteristics. The resulting functional guilds or groups of fishes would provide additional opportunity to more broadly test the use of surrogacy among diverse assemblages of riverine fishes. Each species is uniquely suited to its riverine environment because of its unique anatomorphic adaptations; however, little is known about how the same adaptations may affect risk of mortality to a completely unnatural stressor like turbine passage. The effect of size also remains mostly unconfirmed for every species tested to date, and even well-studied species like rainbow trout have provided conflicting trends. We are most curious to determine if size-based disparities are related simply to methodological differences, are truly a biological phenomenon based on changes in center gravity and other physical characteristics, or a combination of both. Regardless, it is quite clear that fish size is an

important variable given how rainbow trout and bluegill exhibited differences in size-effected mortality. While additional trials would be useful, the biological response data discussed previously will help inspire new technologies that simultaneously optimize power generation and maximize fish survivability during turbine passage.

Conclusions

The purpose of this review was to clarify general trends for all current biological response data such that it may be a useful reference guide. We have also discussed each species' biological responses in slightly more detail and refer the readers to the publications cited throughout for more specific detail if desired. To conclude this review of blade strike testing, we reiterate important trends highlighted previously and make the following recommendations:

- Mid-body lateral strikes at 90° are generally the most injurious and lethal and thus should always be included in laboratory experiments that aim to assess blade strike impacts.
- Thinner faster blades are always more detrimental than thicker slower blades, which is true even when evaluating differences in blade leading-edge thicknesses that may only be 10 mm.
- All species we have tested so far generally do not survive mid-body, lateral blade strike impacts at 90° above 10.0 m/s (except American eel), which makes testing faster velocities unnecessary.
- Blade strike is likely the main cause of paddlefish injury because significant damage to the rostrum observed in the field was nearly replicated during laboratory tests of blade strike impact.
- Young of the year *Alosa* spp. (i.e., American shad) may survive impacts up to 8.0 m/s but their small size, presence of many dams throughout their native range, and annual downstream migrations suggest these clupeids have a high likelihood of passage and interactions with hydropower turbines.

- American eel seems resistant to blade strike impacts, yet observations of whole-body amputations do occur, which may be caused by strikes from thinner blades (< 19 mm) moving at higher velocities (> 20 m/s), or is perhaps linked to pinching or grinding: both scenarios remain untested.
- Surrogacy of blade strike response data is possible, but justification for use should also be based on shared functional traits between species.
- Use of surrogacy between size groups is not recommended unless no other biological response data are available for the species of concern.
- If possible, turbines with fewer, minimum-gap runners containing thicker leading-edge widths (> 52 mm) and slower realized velocities (< 10 m/s), should be considered to mitigate risk of injury.
- Modifications to turbines should include designs with shallower impact angles, which would likely result in more strikes being deflected away from the center of mass, thereby decreasing the rate of severe injury and increasing passage survival [23].
- Currently available tools like HBET and BioPA include the most relevant biological response data for all species and passage stressors tested to date, which should make these tools a useful reference to turbine manufacturers and/or dam operators.

Many of assumptions related to experimental design and model derivation need to be supported by actual data. For example, we still lack data about the fundamental relationship of blade width to blade velocity that fish may encounter when passing through Francis and Kaplan turbines because this type of turbine design data are often proprietary. Our data are meant to be broadly applicable to all turbines given trends in blade leading-edge width and strike impact velocity; however, more precise estimates based on actual blade geometry and operational specifications would be especially useful. Mutual data sharing of this nature will create stronger partnerships and allow researchers to provide more useful response data to turbine manufacturers. Collaborations of this nature will help researchers overcome data limitations and ensure that biological response

data remain useful for an industry seeking to design new, more efficient, biologically-inspired hydropower turbine technologies.

Acknowledgments

The authors thank our collaborators at Pacific Northwest National Laboratory including Brett Pflugrath, Alison Colotelo, Marshall Richmond (retired), Daniel Deng, John Stephenson, and Lysel Garavelli as well as Dana McCoskey (Department of Energy, Water Power Technologies Office) for their thorough review of earlier versions of this document. We must also thank Paul Matson (Biodiversity and Ecosystem Health Group, ORNL) for his insightful technical review of this article as well. All reviews strengthened the overall quality, technical merit, and potential utility of this article for the hydropower industry. We also thank Lara Aston (PNNL), Alison Colotelo (PNNL), and Shelaine Curd (ORNL) for project management.

References

1. Cada, G.F. Shaken, not stirred: The Recipe for a fish-friendly turbine. In Proceedings of the Waterpower ’97; Mahoney, D.J., Ed.; American Society of Civil Engineers: Atlanta, Georgia USA, **1997**; p. 11.

2. Coutant, C.C.; Whitney, R.R. Fish behavior in relation to passage through hydropower turbines: A review. *Trans. Am. Fish. Soc.* **2000**, *129*, 351–380.

3. Pracheil, B.M.; DeRolph, C.R.; Schramm, M.P.; Bevelhimer, M.S. A fish-eye view of riverine hydropower systems: The current understanding of the biological response to turbine passage. *Rev. Fish Biol. Fish.* **2016**, *26*, 153–167.

4. Mathur, D.; Heisey, P.G.; Terry Euston, E.; Skalski, J.R.; Hays, S. Turbine passage survival estimation for chinook salmon smolts (Oncorhynchus tshawytscha) at a large dam on the Columbia River. *Can. J. Fish. Aquat. Sci.* **1996**, *53*, 542–549.

5. Mathur, D.; Heisey, P.G.; Skalski, J.R.; Kenney, D.R. Salmonid smolt survival relative to turbine efficiency and entrainment depth in hydroelectric power generation. *J. Am. Water Resour. Assoc.* **2000**, *36*, 737–747.

6. Hostetter, N.J.; Evans, a. F.; Roby, D.D.; Collis, K.; Hawbecker, M.; Sandford, B.P.; Thompson, D.E.; Loge, F.J. Relationship of external fish condition to pathogen prevalence and out-migration survival in juvenile steelhead. *Trans. Am. Fish. Soc.* **2011**, *140*, 1158–1171.

7. Mueller, M.; Pander, J.; Geist, J. Evaluation of external fish injury caused by hydropower plants based on a novel field-based protocol. *Fish. Manag. Ecol.* **2017**, *24*, 240–255.

8. Neitzel, D. a; Dauble, D.D.; Cada, G.F.; Richmond, M.C.; Guensch, G.R.;

Mueller, R.R.; Abernethy, C.S.; Amidan, B. Survival estimates for juvenile fish subjected to a laboratory-generated shear environment. *Trans. Am. Fish. Soc.* **2004**, *133*, 447–454.

9. Bevelhimer, M.S.; Pracheil, B.M.; Fortner, A.M.; Saylor, R.; Deck, K.L. Mortality and injury assessment for three species of fish exposed to simulated turbine blade strike. *Can. J. Fish. Aquat. Sci.* **2019**, *76*, 2350–2363.

10. Brown, R.S.; Carlson, T.J.; Gingerich, A.J.; Stephenson, J.R.; Pflugrath, B.D.; Welch, A.E.; Langeslay, M.J.; Ahmann, M.L.; Johnson, R.L.; Skalski, J.R.; et al. Quantifying mortal injury of juvenile chinook salmon exposed to simulated hydro-turbine passage. *North Am. J. Fish. Manag.* **2012**, *141*, 147–157.

11. Saylor, R.; Sterling, D.; Bevelhimer, M.; Pracheil, B. Within and among fish species differences in simulated turbine blade strike mortality: Limits on the use of surrogacy for untested species. *Water* **2020**, *12*, 1–27.

12. Amaral, B.S.; Hecker, G.; Metzger, M.; Cook, T. 2002 Biological Evaluation of the Alden/Concepts NREC Turbine. In Proceedings of the Waterpower XIII; HCI Publications: Buffalo, NY, **2003**; pp. 1–12.

13. Cook, T.C.; Hecker, George, E.; Amaral, S. V.; Stacy, P.S.; Lin, F.; Taft, E.P. *Pilot Scale Tests Alden/Concepts NREC Turbine*; Holden, MA, **2003**.

14. Hecker, G.E.; Cook, T.C. Development and evaluation of a new helical fish-friendly hydroturbine. *J. Hydraul. Eng.* **2005**, *131*, 835–844.

15. Turnpenny, A.W.H.; Davis, M.H.; Fleming, J.M.; Davies, J.K. *Experimental studies relating to the passage of fish and shrimps through tidal power turbines*; Southampton, United Kingdom, **1992**.

16. Turnpenny, A.W.H. Mechanisms of fish damage in low head turbines: An

experimental appraisal. In *Fish Migration and Fish Bypasses*; Jungwirth, M., Schmutz, S., Weiss, S., Eds.; Blackwell Publishing Ltd: Malden, Massachusetts, **1998**; pp. 300–314 ISBN 0-85238-253-7.

17. EPRI, (Electric Power Research Institute) *Evaluation of the effects of turbine blade leading edge design on fish survival*; Palo Alto, CA, **2008**.

18. Saylor, R.; Fortner, A.; Bevelhimer, M. Quantifying mortality and injury susceptibility for two morphologically disparate fishes exposed to simulated turbine blade strike. *Hydrobiologia* **2019**, *842*, 55–75.

19. Hou, H.; Deng, Z.; Martinez, J.; Fu, T.; Duncan, J.; Johnson, G.; Lu, J.; Skalski, J.; Townsend, R.; Tan, L. A Hydropower Biological Evaluation Toolset (HBET) for characterizing hydraulic conditions and impacts of hydro-structures on fish. *Energies* **2018**, *11*, 990–1002.

20. Richmond, M.C.; Serkowski, J.A.; Radowski, C.; Strickler, B.; Weisbeck, M.; Dotson, C. Computational tools to assess turbine biological performance. *Hydroreview* **2014**, *33*, 1–6.

21. Bevelhimer, M.S.; Pracheil, B.M.; Fortner, A.M.; Deck, K.L. An overview of experimental efforts to understand the mechanisms of fish injury and mortality caused by hydropower turbine blade strike. *ORNL/TM-2017/731* **2017**, 29.

22. EPRI, (Electric Power Research Institute) *Tests examining survival of fish struck by turbine blades*; Palo Alto, CA, **2011**.

23. Amaral, S. V; Watson, S.M.; Schneider, A.D.; Rackovan, J.; Baumgartner, A. Improving survival: Injury and mortality of fish struck by blades with slanted, blunt leading edges. *J. Ecohydraulics* **2020**.

24. Poe, T.P.; Hansel, H.A.L.C.; Vigg, S.; Palmer, D.E.; Prendergast, L.A. Feeding of

predaceous fishes on out-migrating juvenile salmonids in John Day Reservoir, Columbia River. *Trans. Am. Fish. Soc.* **1991**, *120*, 405–420.

25. Blackwell, B.F.; Krohn, W.B.; Dube, N.R.; Godin, A.J. Spring prey use by double-crested cormorants on the Penobscot River, Maine, USA. *Colon. Waterbirds* **1997**, *20*, 77–86.

26. Blackwell, B.F.; Juanes, F. Predation on Atlantic salmon smolts by striped bass after dam passage. *North Am. J. Fish. Manag.* **1998**, *18*, 936–939.

27. Keefer, M.L.; Stansell, R.J.; Tackley, S.C.; Nagy, W.T.; Gibbons, K.M.; Peery, C.A.; Caudill, C.C. Use of radiotelemetry and direct observations to evaluate sea lion predation on adult pacific salmonids at Bonneville Dam. *Trans. Am. Fish. Soc.* **2012**, *141*, 1236–1251.

28. Hawkes, J.P.; Saunders, R.; Vashon, A.D.; Cooperman, M.S. Assessing efficacy of non-lethal harassment of double-crested cormorants to improve Atlantic salmon smolt survival. *Northeast. Nat.* **2013**, *20*, 1–18.

29. Davis, M.W. Simulated fishing experiments for predicting delayed mortality rates using reflex impairment in restrained fish. *ICES J. Mar. Sci.* **2007**, *64*, 1535–1542.

30. Davis, M.W. Fish stress and mortality can be predicted using reflex impairment. *Fish Fish.* **2010**, *11*, 1–11.

31. Raby, G.D.; Donaldson, M.R.; Hinch, S.G.; Patterson, D.A.; Lotto, A.G.; Robichaud, D.; English, K.K.; Willmore, W.G.; Farrell, A.P.; Davis, M.W.; et al. Validation of reflex indicators for measuring vitality and predicting the delayed mortality of wild coho salmon bycatch released from fishing gears. *J. Appl. Ecol.* **2012**, *49*, 90–98.

32. Colotelo, A.H.; Goldman, A.E.; Wagner, K.A.; Brown, R.S.; Deng, Z.D.; Richmond, M.C. A comparison of metrics to evaluate the effects of hydro-facility passage stressors on fish. *Environ. Rev.* **2017**, *25*, 1–11.

33. Ritz, C.; Baty, F.; Streibig, J.C.; Gerhard, D. Dose-response analysis using R. *PLoS One* **2015**, *10*, 1–13.

34. Uria-Martinez, R.; Johnson, M.M.; O'Connor, P.W.; Samu, N.M.; Witt, A.M.; Battey, H.; Welch, T.; Bonnet, M.; Wagoner, S. *2017 Hydropower Market Report*; Oak Ridge, Tennessee, **2018**.

35. Ghosh, T.K.; Prelas, M.A. Energy Resources and Systems. In *Energy Resources and Systems*; Spring Science+Business media, LLC: New York, **2011**; Vol. 2, pp. 157–215 ISBN 9789400714021.

36. Fu, T.; Deng, Z.D.; Duncan, J.P.; Zhou, D.; Carlson, T.J.; Johnson, G.E.; Hou, H. Assessing hydraulic conditions through Francis turbines using an autonomous sensor device. *Renew. Energy* **2016**, *99*, 1244–1252.

37. Çelebioğlu, K.; Kaplan, A. Development and implementation of a methodology for reverse engineering design of Francis turbine runners. *Pamukkale Univ. J. Eng. Sci.* **2019**, *25*, 430–439.

38. Calles, O.; Greenberg, L. Connectivity is a two-way street - The need for a holistic approach to fish passage problems in regulated rivers. *River Res. Appl.* **2009**, *25*, 1268–1286.

39. Martinez, J.; Deng, Z.D.; Tian, C.; Mueller, R.; Phonekhampheng, O.; Singhanouvong, D.; Thorncraft, G.; Phommavong, T.; Phommachan, K. In situ characterization of turbine hydraulic environment to support development of fish-friendly hydropower guidelines in the lower Mekong River region. *Ecol. Eng.* **2019**, *133*, 88–97.

40. Serrano, I.; Rivinoja, P.; Karlsson, L.; Larsson, S. Riverine and early marine survival of stocked salmon smolts, Salmo salar L., descending the Testebo River, Sweden. *Fish. Manag. Ecol.* **2009**, *16*, 386–394.

41. Martinez, J.J.; Deng, Z.D.; Titzler, P.S.; Duncan, J.P.; Lu, J.; Mueller, R.P.; Tian, C.; Trumbo, B.A.; Ahmann, M.L.; Renholds, J.F. Hydraulic and biological characterization of a large Kaplan turbine. *Renew. Energy* **2019**, *131*, 240–249.

42. Čada, G.F. The development of advanced hydroelectric turbines to improve fish passage survival. *Fisheries* **2001**, *26*, 14–23.

43. Pracheil, B.M.; Mestl, G.E.; Pegg, M.A. Movement through dams facilitates population connectivity in a large river. *River Res. Appl.* **2015**, *31*, 517–525.

44. Hoover, J.J.; Bailey, P.; Januchowski-Hartley, S.R.; Lyons, J.; Pracheil, B.; Zigler, S. Anthropogenic obstructions to paddlefish movement and migration. In *Paddlefish: Ecological, Aquacultural, and Regulatory Challenges of Managing a Global Resource*; American Fisheries Society: Bethesda, Maryland, **2019**; pp. 1–36.

45. Froese, R.; Pauly, D. Fishbase. *Fishbase* **2020**.

46. Blake, R.W. Review Paper: Fish functional design and swimming performance. *J. Fish Biol.* **2004**, *65*, 1193.

47. Webb, P.W. Fast-start performance and body form in seven species of teleost fish. *J. Exp. Biol.* **1978**, *74*, 211–226.

48. Cada, G.F.; Ryon, M.G.; Wolf, D.A.; Smith, B.T. *Development of a new technique to assess susceptibility to predation resulting from sublethal stresses (indirect mortality)*; Oak Ridge, Tennessee, **2003**; Vol. August.

49. Ryon, M.G.; Cada, G.F.; Smith, J.G. *Further tests of changes in fish escape*

behavior resulting from sublethal stresses associated with hydroelectric turbine passage; Oak, **2004**.

50. Čada, G.F.; Ryon, M.G.; Smith, J.G.; Luckett, C.A. *The effects of turbine passage on C-start behavior of salmon at the Wanapum Dam, Washington Wind and Hydropower Technologies*; Oak Ridge, Tennessee, **2006**; Vol. June.

51. Čada, G.F.; Schweizer, P.E. *The application of traits-based assessment approaches to estimate the effects of hydroelectric turbine passage on fish populations*; Oak Ridge, Tennessee, **2012**; Vol. April.

52. Pracheil, B.M.; McManamay, R.A.; Bevelhimer, M.S.; DeRolph, C.R.; Čada, G.F. A traits-based approach for prioritizing species for monitoring and surrogacy selection. *Endanger. Species Res.* **2016**, *31*, 243–258.

53. Grubbs, R.D.; Kraus, R.T. Fish Migration. In *Encyclopedia of Animal Behavior*; Breed, M.D., Moore, J., Eds.; Elsevier Academic Press: San Diego, California, **2010**; pp. 715–724.

54. Binder, T.R.; Cooke, S.J.; Hinch, S.G. Physiological specializations of different fish groups: Fish migrations. In *Encyclopedia of Fish Physiology: From Genome to Environment*; Farrell, A.P., Cech Jr., J.J., Richards, J.G., Stevens, E.D., Eds.; Elsevier Inc.: San Diego, California, **2011**; pp. 1921–1952 ISBN 9780123745538.

55. Silva, A.T.; Lucas, M.C.; Castro-Santos, T.; Katopodis, C.; Baumgartner, L.J.; Thiem, J.D.; Aarestrup, K.; Pompeu, P.S.; O'Brien, G.C.; Braun, D.C.; et al. The future of fish passage science, engineering, and practice. *Fish Fish.* **2018**, *19*, 340–362.

Appendix

Table 1. Review of simulated blade strike laboratory experiments on all live fishes published to date between 1992 and 2020.

Family	Scientific name	1-hr Mortality?	Functional Mort?	Latent Mortality?	External Assess?	Internal Necropsy?	Fish Length (cm) (Standard, Fork, or Total; mean)	Blade Width (mm)	Realized Blade Strike Velocity (m/s)	Strike Location			Impact Angle			Fish Orientation			Source
										H	M	T	90	45	135	D	L	V	
Polydontidae	*Polyodon spathula*	✔	✔		✔	✔	5.10 – 10.3	26, 52	5.3 – 9.4	✔	✔		✔			✔	✔		up
Acipenseridae	*Acipenser transmontanus*	✔		✔	✔		10.5 – 16.8	50, 100	10.7, 12.2	✔	✔	✔	✔			✔	✔	✔	17
	A. transmontanus	✔		✔	✔		20.6 – 21.7	25, 50	12.0, 12.2	✔	✔	✔	✔	✔		✔	✔	✔	22
Anguillidae	*Anguilla anguilla*			✔	✔	✔	32.0 – 70.0	10, 20, 40 & 100	5.2 – 7.1	✔	✔	✔	✔				✔		15
	A. rostrata	✔	✔		✔	✔	53.9	19, 26	12.0, 13.6	✔	✔		✔			✔	✔	✔	18
	A. rostrata	✔		✔	✔		28.5 – 79.5	25, 50 & 150	10.7, 12.2	✔	✔	✔	✔			✔	✔	✔	17
Clupeidae	*Alosa aestivalis*	✔	✔		✔	✔	7.2	26, 52, 76	7.1 – 9.7		✔		✔				✔		11
	A. sapidissima	✔	✔		✔	✔	8.5	52	7.1 – 9.7		✔		✔				✔		11
	Clupea harengus				✔	✔	7.0	10, 20, 40 & 100	5.2 – 7.1		✔		✔				✔		15
	Dorosoma cepedianum	✔	✔		✔	✔	19.3	26, 52	7.4 – 8.3	✔	✔	✔	✔	✔	✔	✔	✔	✔	9
	D. cepedianum	✔	✔		✔	✔	16.0	52	4.7 – 8.1		✔		✔				✔		11

Table 1 continued…

Salmonidae	*Oncorhynchus mykiss*	✔	✔		✔	✔	17.4	26, 52	8.0, 8.3	✔	✔	✔	✔				✔		9
	O. mykiss	✔		✔	✔		10.7 – 26.4	10, 25, 50, 100 & 150	3.0 – 12.2	✔	✔	✔	✔			✔	✔	✔	17
	O. mykiss	✔		✔	✔		12.7 – 25.5	25, 50 & 100	7.3, 12.2	✔	✔	✔	✔	✔		✔	✔		22
	O. mykiss				✔	✔	50.2 – 61.6	10, 20, 40 & 100	5.2 – 7.1		✔		✔				✔		15
	O. mykiss	✔	✔		✔	✔	11.4, 25.8	26, 52	5.5 – 9.4	✔	✔		✔		✔	✔	✔	✔	11
	Salmo salar				✔	✔	15.0 – 100.0	10, 20, 40 & 100	5.2 – 7.1		✔		✔				✔		15
	S. trutta			✔	✔	✔	18.0 – 23.8	10, 20, 40 & 100	5.2 – 7.1	✔	✔	✔	✔				✔		15
	Salvelinus fontinalis	✔	✔		✔	✔	24.2	52	4.9 – 7.3	✔	✔		✔		✔	✔	✔		11
Gadidae	*Merlangius merlangius*				✔	✔	20.0	10, 20, 40 & 100	5.2 – 7.1		✔		✔				✔		15
Atherinidae	*Atherina presbyter*				✔	✔	6.1 – 9.0	10, 20, 40 & 100	5.2 – 7.1		✔		✔				✔		15
Moronidae	*Dicentrarchus labrax*			✔	✔	✔	15.0 – 38.0	10, 20, 40 & 100	5.2 – 7.1	✔	✔	✔	✔				✔		15
	Morone saxatilis × *M. chrysops*	✔	✔		✔	✔	17.1	26, 52	6.4 – 10.1	✔	✔	✔	✔	✔	✔	✔	✔	✔	9
Centrarchidae	*Lepomis macrochirus*	✔	✔		✔	✔	11.8, 16.0 & 17.5	26, 52	4.7 – 9.1	✔	✔	✔	✔	✔	✔	✔	✔	✔	18

Note: Variable questions are answered yes with a check mark. External assessments include visual inspection of fish but do not include internal necropsy in their protocol. ORNL [9,11,18] reported fish length as total length (TL) for every species except paddlefish which used fork length. EPRI [17,22] reported fork length for fish size and Turnpenny [15] used standard length. Unpublished data from ORNL [up]. Work from Amaral et al. [23] was not included because it was generated from laboratory trials using an experimental turbine design with novel leading-edge shape profile.

Table 2. Current level of understanding by species according to available biological response data derived from laboratory experiments.

Species	Data	Citation (s)
Paddlefish (*Polyodon spathula*)	●	*Unpublished data**
American Eel (*Anguilla rostrata*)	○●	EPRI [17]; Saylor et al. [18]
American shad (*Alosa sapidissima*)	●	Saylor et al. [11]
Blueback herring (*Alosa aestivalis*)	●	Saylor et al. [11]
Gizzard shad (*Dorosoma cepedianum*)	●●	Bevelhimer et al. [9]; Saylor et al. [11]
Rainbow trout (*Oncorhynchus mykiss*)	○○●●	EPRI [17]; Bevelhimer et al. [9]; Saylor et al. [11]
Brook trout (*Salvelinus fontinalis*)	●	Saylor et al. [11]
Hybrid Striped Bass (*Morone saxatilis* x *M. chrysops*)	●●	Bevelhimer et al. [9]
Bluegill sunfish (*Lepomis macrochirus*)	●●	Saylor et al. [18]

Grey = Electric Power Research Institute experimental data
Blue = Oak Ridge National Laboratory experimental data
** Paddlefish data available through BioPA/HBET software and technical report*
● Dose-response available; mortality includes individuals that survived exposure with severe injuries, i.e., functional or ecological mortality
○ No dose-response relationships were generated; project specific metrics were described
● Baseline understanding; biological response based mostly on worst-case scenario treatments
●● Complementary understanding; biological response also includes additional treatment scenarios
●●● Comprehensive understanding; biological response covers most expected exposure scenarios

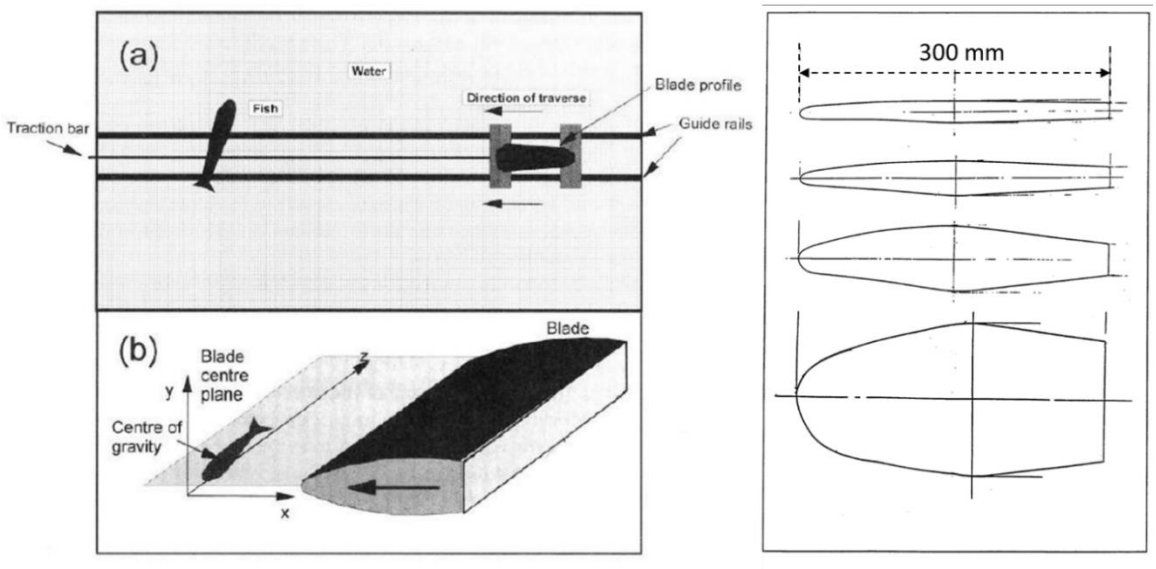

Figure 1. Blade strike apparatus used by Turnpenny et al. [15] and described by Turnpenny [16]. The left panel includes a diagram that highlights fish location and orientation relative to the blade that is guided along tracks. The right panel includes diagram schematics of the blades tested in this study with a reference length of 300 mm. Original Source: Turnpenny [16].

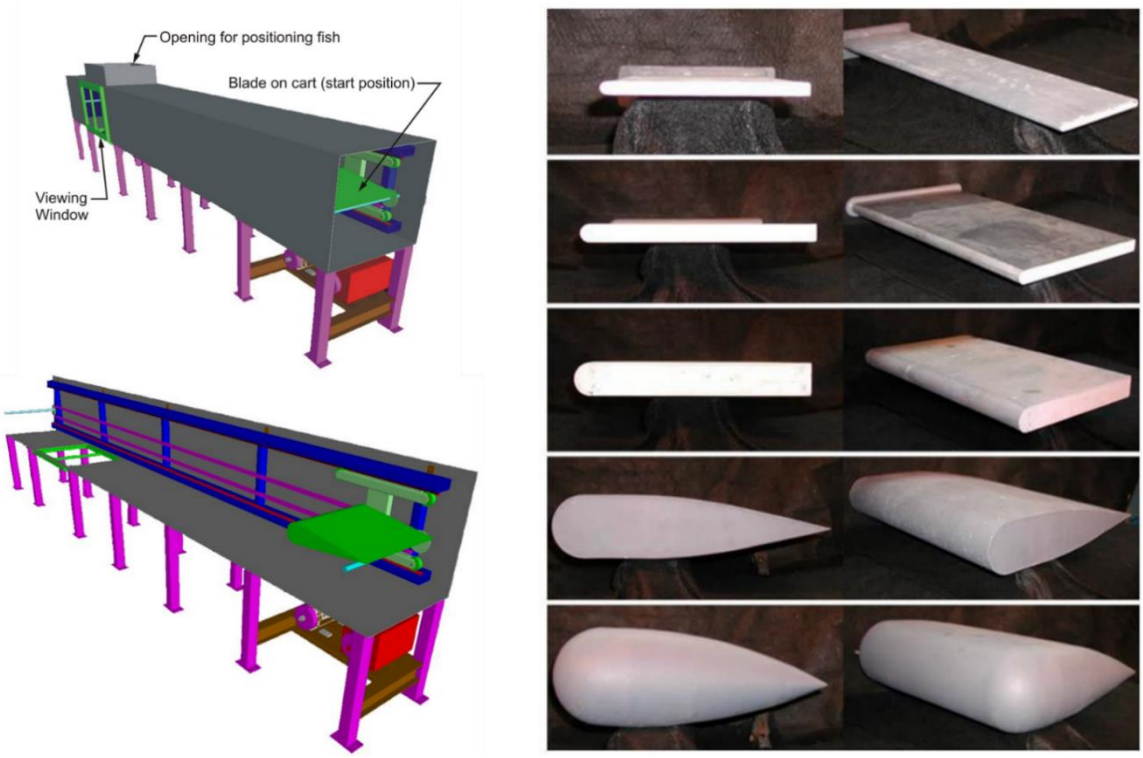

Figure 2. Blade strike apparatus used by Alden Laboratories and reported by EPRI [17,22] and Amaral et al. [23]. The left panel includes a labeled diagram of major features including the viewing window and guide rail that held and moved the blade. The right panel is a compilation of pictures showing the blades of varying leading-edge thicknesses. Original Source: EPRI [17].

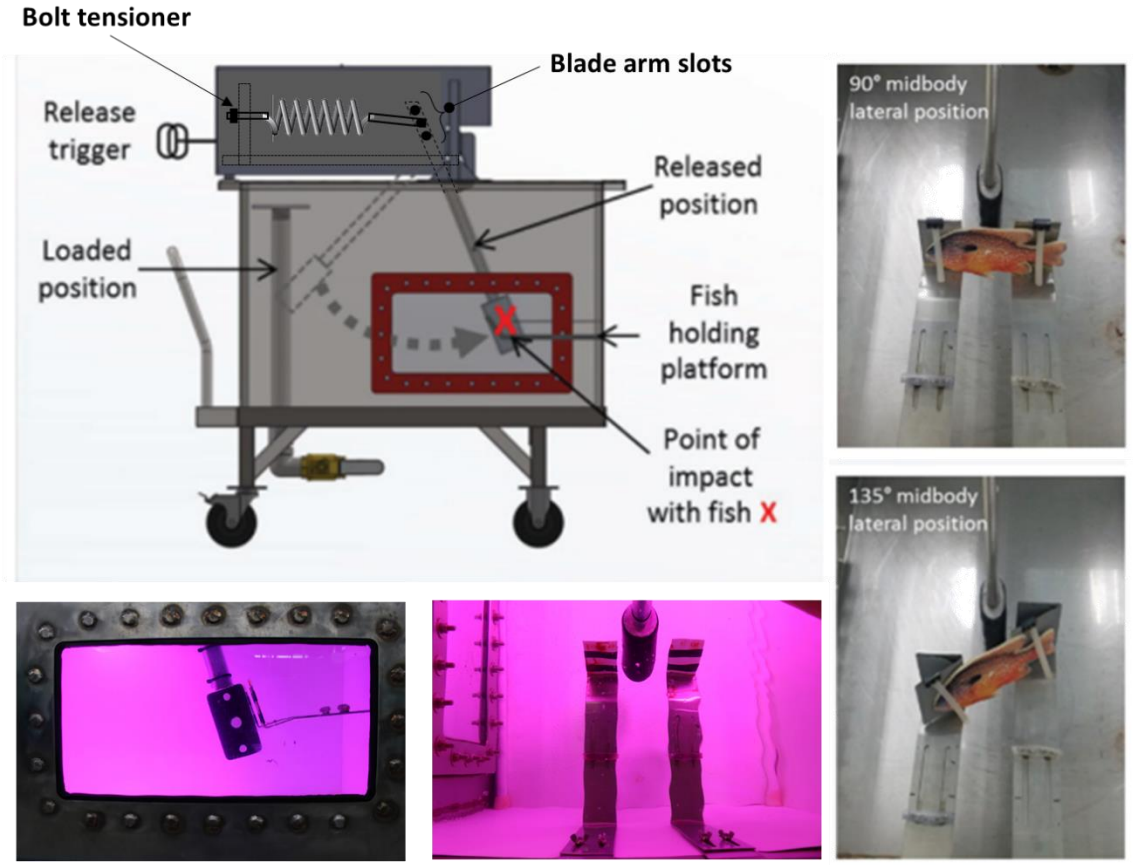

Figure 3. Blade strike apparatus used by researchers at ORNL and reported by Bevelhimer [9] and Saylor et al. [11,18]. The top-left panel is a diagram showing the spring assembly, test tank, and mobile carriage that enabled the system to be moved as needed. The bottom left pane shows the viewing port; the middle panel is a top-down look at the brackets designed to hold fish and relative location of approach for the blade. The right-most panels also showcase the holding brackets that secure fish and also allowed for easy modification of the impact angle.

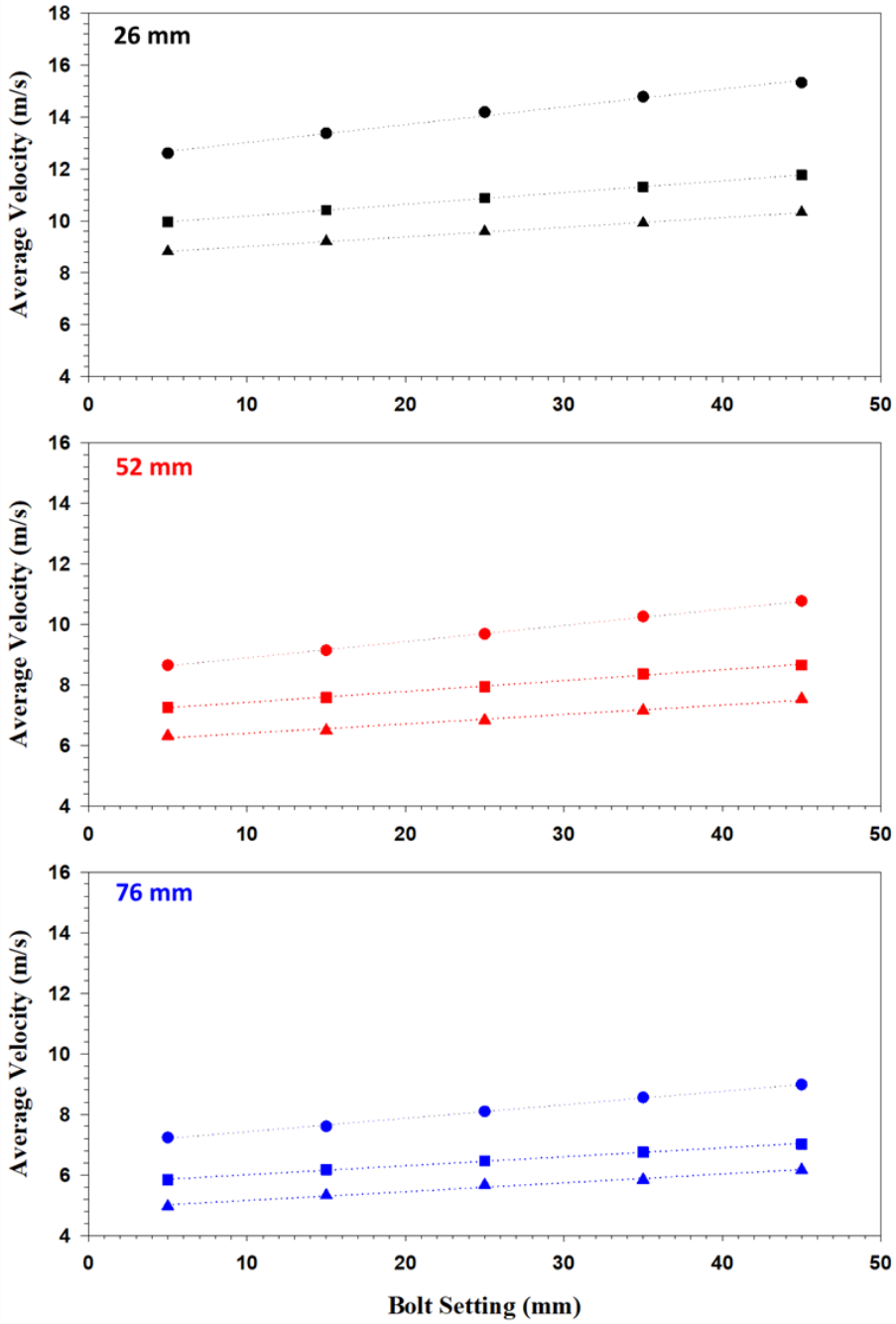

Figure 4. Standard curves of average velocity (m/s) against bolt setting (mm) for each of three blade leading-edge thicknesses (26, 52, and 76 mm) used in ORNL laboratory studies of blade strike impact. Shapes correspond to different slot locations (middle or top) and/or springs (original or new) used to generate sufficient velocity. Triangles refer the original spring in the middle slot, squares represent original spring in the top slot, and circles represent the new spring in the top slot.

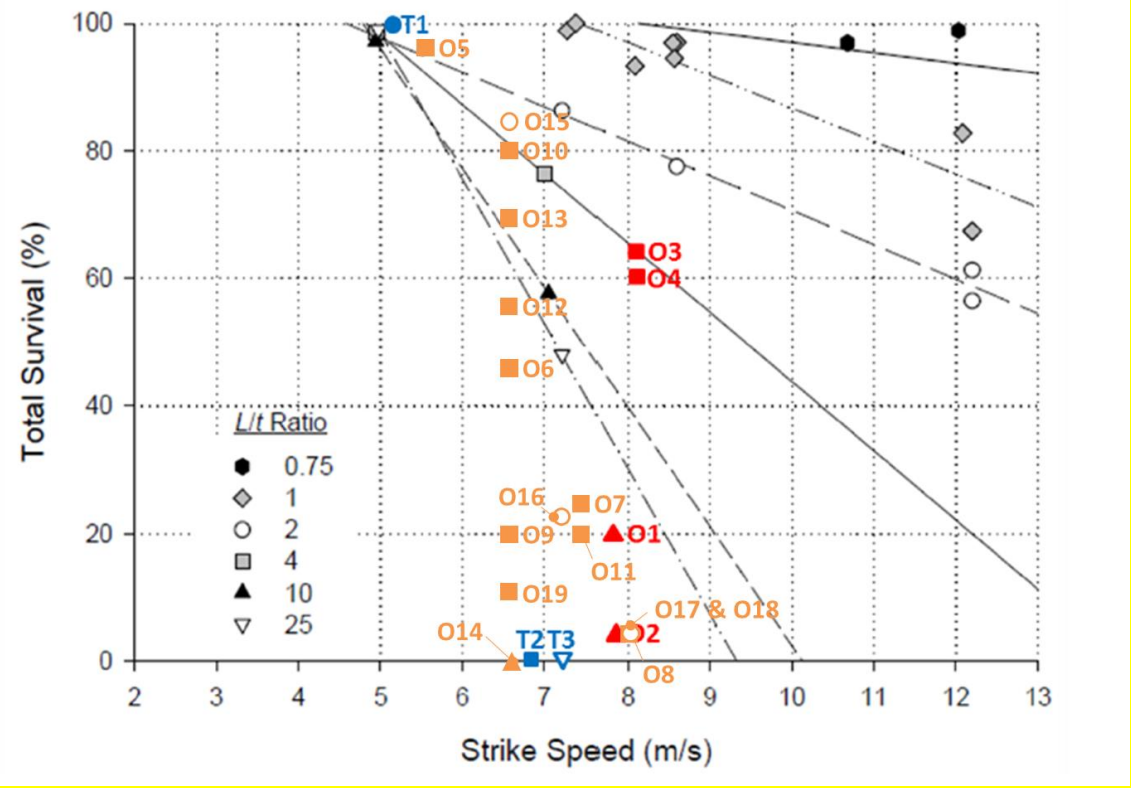

Figure 5. Comparison of all L/t ratio data for rainbow trout published to date and presented with original data from EPRI [17]. Symbol shapes are comparable to the L/t ratio legend presented with the original figure. Treatment groups included outside original EPRI source material are distinguished by location (head, H; mid-body, M; or tail, T), orientation (dorsal, D; lateral, L; or ventral, V), and impact angle (45°, 90°, or 135°). Colored symbols include (**red**) Bevelhimer et al. [9]; O1 (HL90; L/t=6.4), O2 (ML90, L/t=6.7), O3 (HL90; L/t=3.4), and O4 (ML90; L/t=3.3); (**orange**) Saylor et al. [11]; O5 – O8 (ML90; L/t=5.0), O9 (HD90; L/t=4.9), O10 & O11 (HL90; L/t=5.0), O12 (ML135; L/t=4.8), O13 (MV90; L/t=4.9), O14 (ML90; L/t=10.2), O15 – O18 (ML90; L/t=2.2), and O19 (ML90; L/t=4.4); and (**blue**) Turnpenny et al. [15] represents data for brown trout, which were all mid-body hits with L/t ratios of 2.0 (T1), 4.0 (T2), and 20.2 (T3).

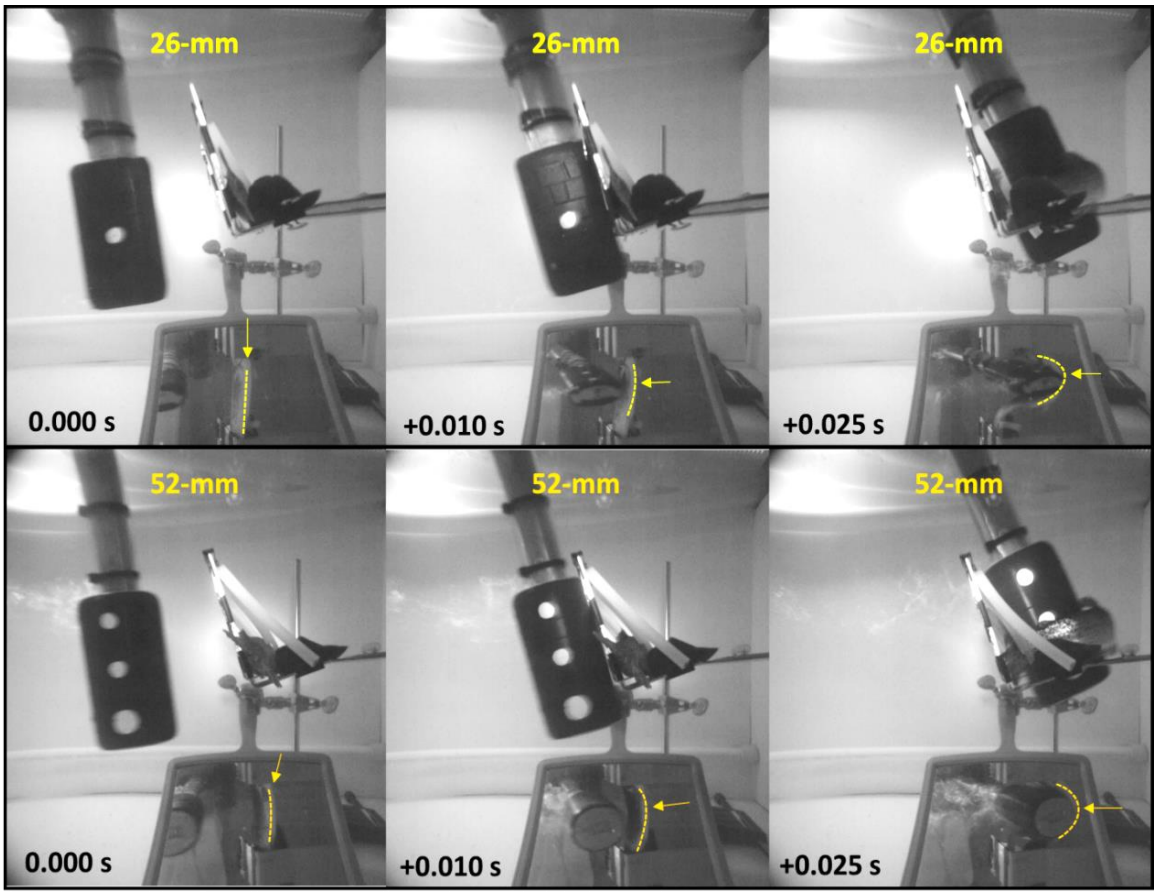

Figure 6. High-speed video images of sub-adult rainbow trout being struck with a 26 (top panel) and 52 mm (bottom panel) turbine blade. Dashed lines and arrows in the mirrored image were included to show the trout's body curvature along the ventral surface in each frame, including the blade approach (0.000 s; reference), just before contact (+0.010 s), and through the maximum curvature after impact (+0.025 s). Both fish were struck at approximately the same position on the mid-body, lateral surface at 90° with an impact velocity of 6.6 m/s.

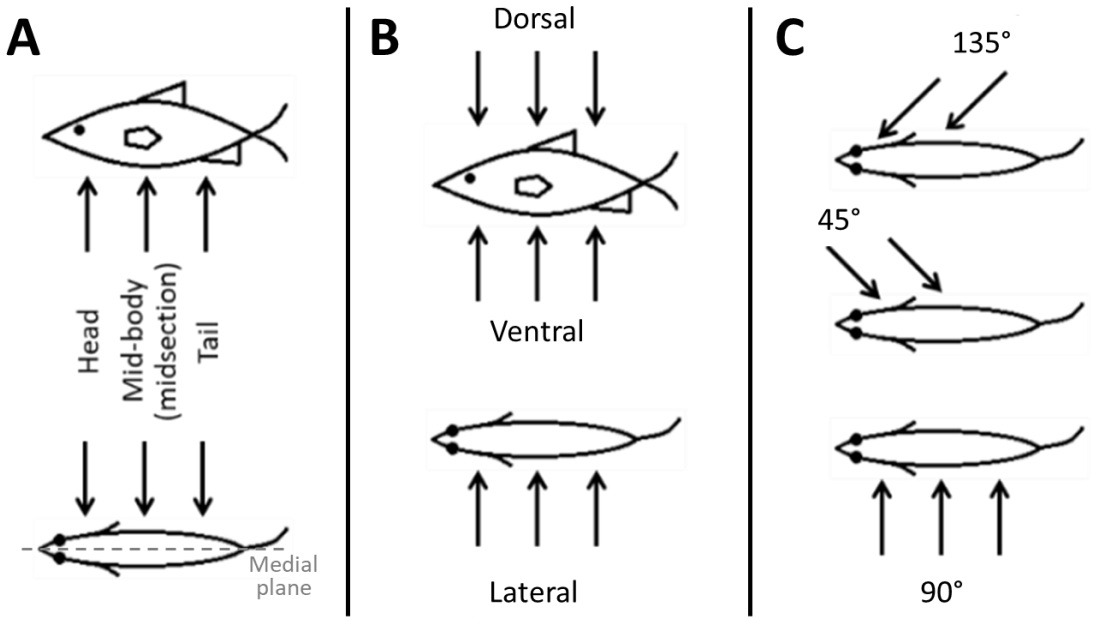

Figure 7. Simplified diagram showing blade strike impact characteristics related to the fish itself including (A) body location, (B) body orientation, and (C) angle of impact. The medial plane (i.e., mid-sagittal plane) is labeled in (A).

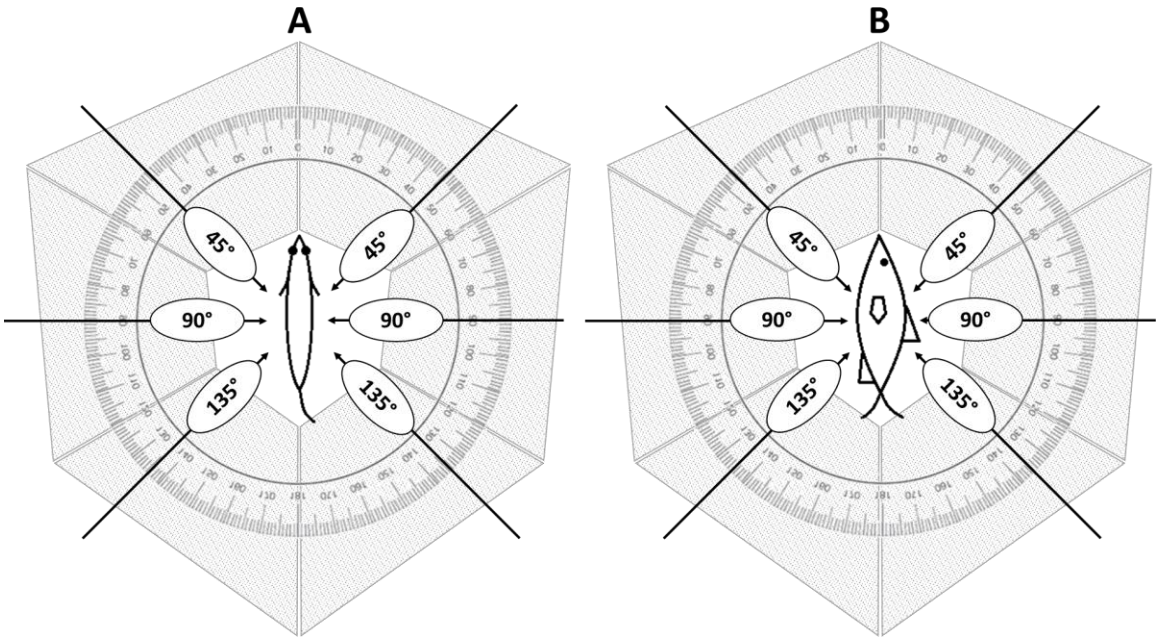

Figure 8. Diagram of potential blade strike impact angles according to the location (A) and orientation (B) of the fish. The impact angles that have been tested are indicated by black arrows. Strikes at 90° occurred perpendicular to the mid-sagittal axis of the fish. Strikes at 45° occurred in a head to tail direction, while 135° was defined by a tail to head strike. Not shown in this image are the same angled strikes for every location and orientation, which were also possible. The grey trapezoids indicate each of six, 60° areas that are represented by each 45, 90, or 135° strike angles.

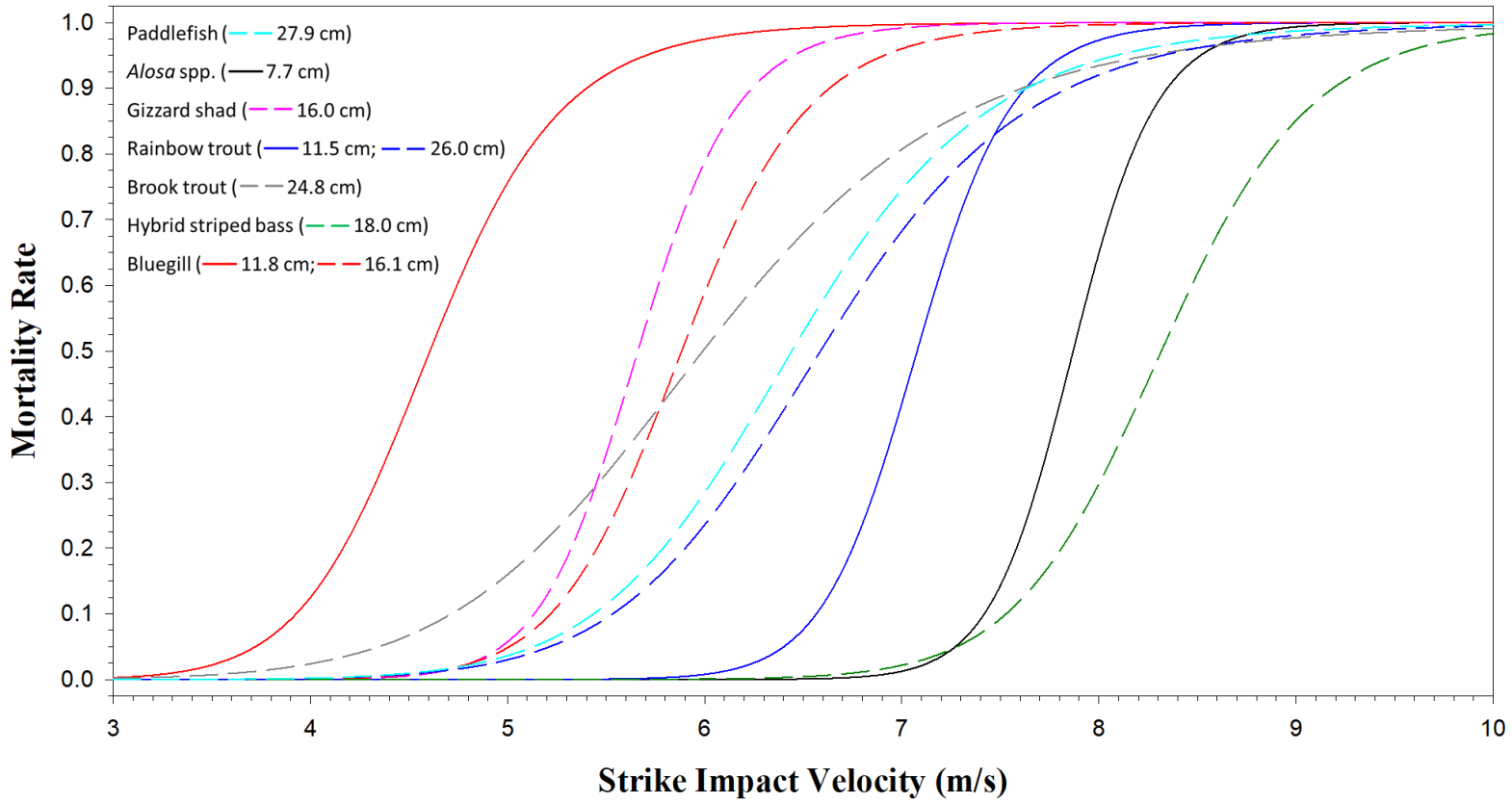

Figure 9. Summary plot of all species dose-response curves available to date for mid-body lateral strikes at 90° with a 52-mm blade. Similar colors correspond to the same species, while solid versus dashed lines represent smaller versus larger individuals, respectively. Note: The curve for hybrid striped bass was produced by modifying the log-logistic curve produced from 26-mm data to approximate the 52-mm curve for comparison purposes. All response models were produced from at least four treatment groups that varied by strike impact velocity, except paddlefish, which was only based on three treatment groups.

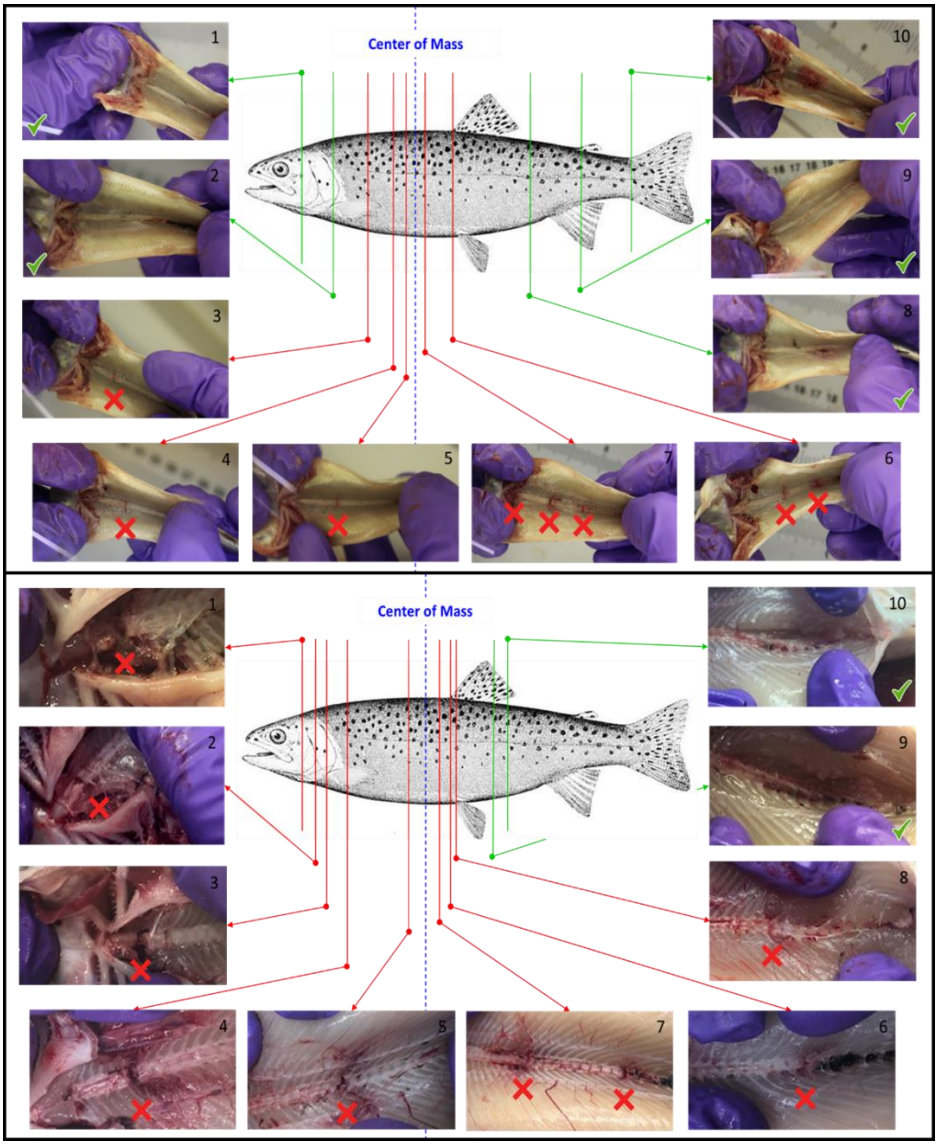

Figure 10. Results of blade strike impact trials on 10 small or juvenile (top panel; TL = 10.1–14.9 cm) or 10 large or subadult (bottom panel; 20.1–31.6 cm) rainbow trout. Trials include impacts to the mid-body, lateral surface at 90° with the 52-mm blade and ~9.0 m/s (small) or 8.2 m/s (large) impact velocity known to cause vertebral fractures. Center of mass was calculated as a proportion relative to standard length and was approximately 0.45 for small and 0.48 large rainbow trout. Red arrows and "X's" represent fish observed with vertebral fractures, while green arrows and "√s" correspond to fish that were not observed to have any vertebral fractures. Note: (1) Top panel; rib fractures, clotting, and muscle contusions on fish 6 & 10 were not caused by blade strike impact and was linked to pinching between the blade and holding brackets following tail strikes. (2) Bottom panel; internal decapitations were also observed in large rainbow trout (fish 1–3) and formed a separate cluster associated with head strikes.

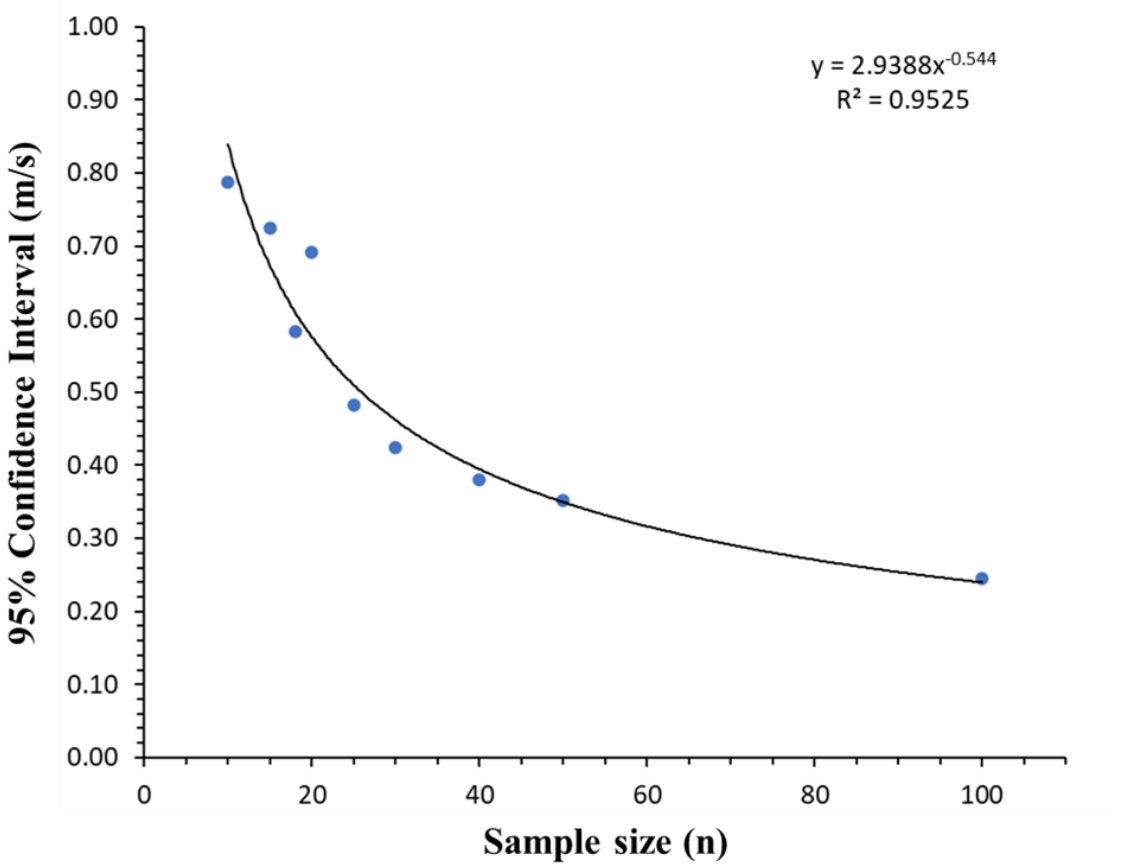

Figure 11. Estimated 95% confidence intervals versus relative sample size of each treatment groups. The resulting values were best described by a power function, which suggested sample size alone accounted for 95.3% of the total variation in this estimate. Use of 20 fish per treatment group is ideal because it will keep variability near 0.5 m/s but also allows for inclusion of more test scenarios compared to higher sample sizes.

CHAPTER II

QUANTIFYING MORTALITY AND INJURY SUSCEPTIBILITY FOR TWO MORPHOLOGICALLY DISPARATE FISHES EXPOSED TO SIMULATED TURBINE BLADE STRIKE

A version of this chapter was originally published by Ryan Kurt Saylor, et al:

Ryan Saylor[*1,2], Allison Fortner[2], Mark Bevelhimer[2]. "Quantifying mortality and injury susceptibility for two morphologically disparate fishes exposed to simulated turbine blade strike." *Hydrobiologia* 842(1), 2019, 55-75.

Affiliations:

[1] Bredesen Center for Interdisciplinary Research and Graduate Education, University of Tennessee, Knoxville, Tennessee 37996

[2] Aquatic Ecology Group, Environmental Science Division, Oak Ridge National Laboratory, Oak Ridge, Tennessee 37830

*Corresponding Author: Ryan Saylor

1 Bethel Valley Road

Oak Ridge National Laboratory

Oak Ridge, Tennessee 37830

Phone: 865-974-7709

E-mail: saylorr@ornl.gov

Author Contributions:

Conceived or designed experiments – RKS, with input from MB

Blade strike experimentation – RKS, with assistance from AF and MB

Fish necropsies – RKS, with assistance from AF

Analysis of data – RKS, with input from MB

Composition of paper – RKS, with input from AF and MB

Revisions and draft reviews – RKS, with input from MB

Project management – MB

Abstract

Passage of fishes through hydropower turbines and water pumping stations may cause mortal injury as the result of exposure to blade strike impact. Laboratory trials of simulated blade strike on two morphologically distinct fishes, American eel (*Anguilla rostrata*) and bluegill sunfish (*Lepomis macrochirus*) were undertaken to assess injury and mortality rates. We hypothesized that bluegill would have comparable rates of injury and mortality to other laterally compressed fishes while anguilliform American eel would be more resistant to injury. American eel had low observed mortality rates at the highest velocity tested (13.6 m/s), but many fish were observed with vertebral fractures which we categorized as functionally dead individuals. Bluegill were more susceptible to blade strike with high rates of mortality regardless of blade thickness, velocity, or impact conditions (location, angle, or fish orientation). These data have broadened our understanding of the range of responses among entrained fishes exposed to blade strike and represent species with low (American eel) and high (bluegill) susceptibility to injury and mortality. Our blade strike data can help inform safer turbine designs or prioritization of pumps that minimize traumatic injury and mortality of fishes during non-volitional passage through hydropower turbines or water pumping stations.

Introduction

Controlled movement of water to generate electricity, manage flooding, or provide irrigation are all important components of water management worldwide. These activities have also impacted riverine connectivity, altered stream hydrology, and sometimes have lethal consequences to fish passing through hydropower [1] or water pumping stations [2]. Field studies have confirmed that turbine passage is frequent at many dams [3–5] and at water pumping stations [6–8], so industry developers have been tasked with redesigning hydropower turbines to reduce the risk of major injury or death [9] or prioritizing use of safer pumps [6]. Fishes at the highest risk of passage are those that undergo migrations to (adults) or from (juveniles) spawning habitat including anadromous salmonids or clupeids, catadromous anguillids, and potamodromous fishes [10–12] although resident fish are also often entrained. The remarkable diversity of form

(shapes, size, and other morphometrics) among migratory fishes, and disparate geological and hydrological features at each dam or pumping station, make it impossible to design a one-size-fits-all strategy to reduce passage at all sites.

To reduce or eliminate passage, some facilities have installed fishway passage structures, exclusion devices, or actively collect and transport certain species (e.g., salmonids smolts) safely around the dam or pumping station [6,9]. Some fishways and operations may help fish avoid passage, but none of the current solutions are 100% effective making passage unavoidable at many sites. When fish do pass through turbines, they are faced with a suite of stressors that may cause traumatic injury or death including, barotrauma from rapid decompression, hydraulic shear, cavitation, turbulence, blade strike, or collisions with structures [13]. Similarly, traumatic injury caused by passage through water pumping stations has also been linked with mechanical damage, shear, and pressure fluctuations.[2]. Linking traumatic injury and death to a specific stressor following turbine passage during field trials is problematic because the exact exposure conditions of each fish are unknown. To that end, laboratory experimentation that investigates each stressor separately is the best alternative to better inform safer turbine designs that minimize injury and mortality during turbine passage.

Physical impact of blades striking fish represents one of the most likely avenues of injury or mortality when fish pass through hydropower turbines or water pumping stations. The risk and severity of injury from blade strike has been associated with turbine type, with Francis and Kaplan-types being the most common turbines found in hydropower dams globally [14]. Francis turbines are often associated with higher rates of mortality because they have more turbine blades and operate at higher RPMs than Kaplan turbines [15,16]. Mortality of fish passing through pumping stations is linked with pump type and operation conditions, with axial pumps have the highest mortality when flow rates exceed 200 m3/min [6]. In contrast, Hidrostal pumps often have low mortality which is likely a result of using lower flow rates and having fewer, thicker blades [7,17]. In addition, velocity and leading-edge thickness of the blades also factors into probability of mortality from strike impact. The movement, orientation, and size of passing fish in combination with location and angle of blade strike must also be accounted for when

predicting rates of injury and mortality. Ideally, one could account for all blade strike variables at once and provide a multiplicative probability estimate of injury or mortality for each species. However, probability of injury or mortality from blade strike is only one of multiple stressors, each with its own suite of exposure conditions, that would factor into estimates of total turbine passage mortality. Logistic constraints prohibit estimating injury and mortality rates for every exposure condition and stressor because both are also dependent on fish species [13].

Among species, marked variation in body shape, skeletal composition or architecture, muscle thickness, and integument quality (e.g., skin thickness or scale-type) are important factors influencing susceptibility to injury or mortality [18]. Laboratory data have shown that susceptibility to mortality in gizzard shad *Dorosoma cepedianum* (Lesuer, 1818) and rainbow trout *Oncorhynchus mykiss* (Walbaum, 1792) is markedly higher compared to hybrid striped bass (striped bass *Morone saxatilus* [Walbaum, 1792] × white bass *Morone chrysops* [Rafinesque, 1820]) or white sturgeon *Acipenser transmontanus* (Richardson, 1836), especially at higher blade strike velocities and thinner blade widths [19–22]. Injuries linked with blade strike trauma may include scale loss, trauma to internal organs and musculature (hemorrhage, lacerations, contusions, or rupture), and skeletal fractures including the vertebrae [19,22]. Within a species, injury susceptibility and mortality are also affected by size of entrained fish [23] making size an important covariate in blade strike studies. Previous work in EPRI (2008, 2011) showed that survival of fish was related to the L/t ratio (fish total length divided by the blade thickness) and blade strike velocity. For example, fish that were struck by blades as thick or thicker than their total length ($L/t \leq 1.0$) tended to have higher survival than fish struck by thinner blades ($L/t > 2.0$) moving at similar velocities [20,21]. The diversity of form among fishes likely impacts their susceptibility to injury or death from turbine blade strike and suggests each species (or guild representative) must be investigated to best inform turbine design.

American eel, *Anguilla rostrata* (Lesueur, 1817), is an elongate, migratory species that may be susceptible to turbine passage in the USA. Anguillid eels are well known catadromous species that migrate down freshwater rivers to reach spawning grounds in

the Sargasso Sea [10,11,24]. This species has a wide geographic range throughout Eastern North America where it is found as far north as coastal Canada, down into the Gulf coast states in the southeastern USA, and up the Mississippi River drainage [24,25]. Its distribution and migratory behavior increase the likelihood that eel will become entrained which has been observed in some rivers [26,27], especially coastal rivers of the eastern USA where many hydroelectric facilities are found [28,29]. American eel is an IUCN listed endangered species with documented declines in historical abundance as result of overfishing and habitat loss, but population decline is likely confounded by dams disrupting riverine connectivity [24]. Field studies have confirmed that anguillid eels (American and European eels) pass through turbines, and observations of eels that have been completely severed in half are not uncommon (B. Pracheil, *personal observation*). European eels, *Anguilla anguilla* [Linnaeus, 1758], a closely related species, is also known to pass through pumping stations and passage trials showed that this species did not experience mortality until velocity was >8.0 m/s [2]. Laboratory data suggest American eel are markedly resistant to blade strike impact up to 12.2 m/s, though no internal injury assessments were performed that might link specific injuries to death [20]. More information is needed for eels exposed to more strike conditions and detailed injury assessments would also be beneficial so trauma could be linked with blade strike characteristics to better elucidate the susceptibility of eels to blade strike.

Bluegill sunfish, *Lepomis macrochirus* [Rafinesque, 1819], is often found in the same freshwater habitat as eel, where its pelagic nature could increase its risk of turbine passage. Bluegill have a markedly wider distribution than American eel with a native range in Eastern and Central USA where it is an abundant representative of the ichthyofauna [25,30]. Unlike eel, sunfish do not make characteristic mass migrations of any notable distance or destination, but they are common in reservoirs [25] including dams with hydropower facilities [18]. Bluegill represent a typical centrarchid species: laterally compressed, with a deep body, relatively short total length, and pronounced spines on the dorsal, pelvic, and anal fins [30]. This species has a unique shape for which little information is available related to susceptibility to turbine passage including blade strike. The limited data from field trials showed that bluegill mortality may approach

57%, but entrainment appeared to be more haphazard and not because of volitional turbine passage [31]. To our knowledge, there is no other field or laboratory data available on bluegill or any centrarchid that relates turbine blade strike conditions to probability of injury or mortality.

This study aims to increase our knowledge about the effects of blade strike on susceptibility to injury and mortality through investigation of two fishes with high risk of turbine entrainment. Responses of American eel and bluegill to blade strike will vary as a result of their morphologically distinct nature; however, injury and mortality rates of both species will likely be higher when struck perpendicular to the blade on the mid-body, lateral surface, i.e., the worst-case-scenario relative to other strike locations [22]. To that end, the objectives of this study are: 1) assess short-term mortality of bluegill and American eel after exposure to multiple treatment combinations of blade width, velocity, strike location, orientation, and impact angle, 2) document external and internal injuries of all fish, and 3) analyze these data using univariate statistics and logistic regression to better model injury and mortality rates related to simulated blade strike.

Materials and Methods

Simulated Blade Strike Testing

The blade strike apparatus and protocol used to generate simulated blade strike followed methods reported in Bevelhimer et al., [22], though modifications were made to accommodate our study species. Briefly, we used a spring-powered blade arm that accommodated blades of different thicknesses and generated velocities up to 13.6 m/s. Major strike variables used for both species included strike location (head or mid-body), fish orientation (lateral, dorsal, or ventral), and impact angle (45, 90, or 135°; Figure 12). Tail strikes were not included in this study because previous work found low mortality across multiple species suggesting tail strikes would have negligible impacts on fish survival [20,22]. Blade widths of 19, 26, or 52 mm in this study and strike velocities used for both species represented conditions typical of velocities between the hub and blade tip, i.e., average turbine passage conditions [22]. A high-speed camera system (Model

IL4, Fastec Imaging, San Diego, California) filmed every impact at 1000 frames per second to confirm blade strike velocity, location, and impact angle as well fish orientation. Average blade strike velocity (± 0.10 m/s) was estimated from two velocity check videos (one before and one after each experimental group) and from three fish treatment videos in each group using Kinovea software (v0.8.15, www.kinovea.org). Treatment groups varied by blade width, velocity, location, orientation, and impact angle to cover as many exposure scenarios as possible because exact conditions of turbine passed fish are unknown. Upon arrival to laboratory, fish were evenly distributed into separate 680-liter, circular fiberglass tanks which received constant water supply, aeration, and were fed daily. Fish were not fed 24 hours prior to experimentation to avoid tank fouling. Our design used 20 fish per group though some groups contained <15 fish so that more scenarios could be included to provide additional inferences about injury and mortality rates of each species. In addition, each treatment group contained 2-3 fish used as experimental controls and were pooled together by species.

Study Species

Wild-caught American eel with an average mass of 266.7 g (141.0 – 422.3 g) and total length of 53.9 cm (45.7 – 67.5 cm) were purchased from a commercial supplier in Pennsylvania (Delaware Valley Fish Company, Norristown, Pennsylvania, USA). Preliminary trials suggested blade strike was not injurious until velocities reached 12.0 m/s which became the lowest blade strike velocity, so eel were exposed to 12.0 and 13.6 m/s using the 19- and 26-mm blades. Blade strike location for American eel was restricted to the anterior portion of the body (up to 22% of TL) using the pectoral fin to demarcate a head strike (4 – 11% TL) and mid-body strike (13 – 22% TL). A mid-body strike on an eel was closely associated with location of most internal organs including the heart, liver, gall bladder, stomach, swim bladder, and kidney. Due to the lower number of available fish, we did not include 45 or 135° strikes and prioritized impacts at 90°. A total of 156 treatment fish in 11 exposure groups and 20 control fish were used for eel analyses (N = 176; Table 3).

Bluegill sunfish were received from a commercial supplier in Alabama (Southeastern Pond Management, Saginaw, Alabama, USA) and sorted into three size groups: “small” (n = 73; average TL = 11.8 ± 1.49 cm; average mass = 30.4 ± 12.48 g), “medium” (n = 377; average TL = 16.0 ± 1.02 cm; average mass = 80.7 ± 10.28 g), and “large” (n = 19; average TL = 17.5 ± 1.18 cm; average mass = 113.6 ± 33.32 g). Preliminary trials on bluegill suggested use of 26- and 52-mm wide blades with blade strike velocities of 4.7 – 9.1 m/s. An impact to the head was considered at any point between the snout and trailing edge of the operculum (i.e., head length). A mid-body strike occurred between the operculum and leading edge of the anal fin which is also associated with most of the visceral mass. A total of 422 treatment fish in 26 exposure groups and 48 control fish were used for bluegill analyses (N = 470; Table 3).

Blade Strike Protocol

Pairs of fish were anesthetized in a 14-L water bath containing a solution of pure clove oil extract dissolved in 95% ethanol (1:10) and diluted with dechlorinated tap water. Concentrations of clove oil for anesthesia were 60 ppm for bluegill and 120 ppm for American eel [32] to ensure fish reached deep anesthesia (i.e., Stage III, Plane 3) denoted by loss of equilibrium, lack of movement, and rare gill ventilations [33]. Anesthetized fish were removed from the bath and visually inspected for external injuries or deformities. Following visual inspection, fish were randomly assigned treatment condition and placed on the strike platform at the intended treatment position. Neutrally buoyant fish were placed onto the strike platform and loosely held in place with flexible tubing designed to allow fish to move freely after blade impact. A final check of correct treatment conditions was proceeded by initiation of high-speed videography and the triggered release of the blade. Control fish were exposed to the exact same conditions as treatment fish but did not receive a blade strike. Following blade impact and removal from tank, the fish was tagged in the lower jaw with a numbered, T-bar anchor tag (Floy Tag & Mfg. Inc., Seattle, Washington), photographed, placed into a 450-liter fiberglass recovery tank containing freshwater with aeration, and observed for up to 1-hour. Individual observations of gill ventilation, maintenance of upright position, discoloration,

swimming ability, and hemorrhaging were noted every 15-minutes. Fish were categorized based on their condition including 1) individuals that appeared normal with no obvious signs of distress which were considered survivors, 2) early removal of any fish that appeared to be severely injured or moribund fish with irregular or labored gill ventilation, loss of equilibrium, or labored swimming, 3) fish that were removed right at the one-hour mark with signs of severe injury or appeared to be moribund, and 4) fish that were considered dead within hour observation (i.e., direct mortality). Observed mortality for each treatment group included direct mortalities (category 4) plus moribund individuals removed early (categories 2 and 3). All fish including those considered dead, were then placed in the euthanasia bath. Euthanasia was accomplished with a 250-ppm clove oil solution for bluegill and a 420-ppm solution for American eel. After gill ventilations were no longer observed (i.e., usually after 10 minutes) all fish were placed on ice prior to necropsy.

Detailed injury assessments were performed via external and internal necropsy on all fish following euthanasia. Mass (± 0.1 g) and total length (± 0.1 cm) of each fish was recorded. The external examination included identifying potential hemorrhaging, lacerations, contusions, or discoloration associated with the fins, snout, eyes, operculum, and integument. Degree of descaling was also noted when applicable. The internal examination began with a traverse cut using the cloaca (vent) and continued anteriorly until reaching the isthmus of the operculum. Next, another incision continued dorsally along the trailing edge of the operculum until reaching the vertebral column. The final incision cut along the spine posteriorly until reaching the area above the vent, followed by an incision in the ventral direction until the entire flank was removed. Sex was noted when it could be easily determined from existing gonad condition. Soft tissues assessed included the heart, liver, gall bladder, stomach, intestines, gonads, swim bladder, and kidney. Specific injuries were categorized as hemorrhage, laceration, contusion, clotting, edema, rupture, or avulsion. Partial or complete fracture of skeletal elements including the vertebral column, ribs (bluegill only), or haemal spines (eel only) were also noted. Spinal fractures, regardless of location, was considered a major injury for both species and was used as an indicator of functional death. Functional mortality (i.e., ecological

death) was considered for fish with spinal fractures as they would most likely be unable to escape conditions that would lead to their death or impair their ability to capture food. Combined mortality for each treatment group included functional and observed mortalities. The assessor performed necropsies without knowledge of which treatment individual fish had received.

Data Analysis

Mortality rates (observed and combined) were calculated for both species across all treatments groups and pair-wise comparisons were made using Chi-square test with Yate's correction according to the following equation:

$$\chi^2_{Yates} = \frac{(|ad-bc|-0.5N)^2 N}{mnrs} \quad (1)$$

where a and b are the number of mortalities for treatments 1 and 2, respectively, c and d are the number of survivors for treatment 1 and 2, respectively, m is the total number of mortalities and n is the total number of survivors for both treatments, r and s are the total number of fish for each treatment, and N is the total number of fish in the comparison [34]. The Yates corrections to Chi-square tests was used because it accounts for treatment groups with <5 expected mortalities or survivors [34]. Chi-square tests were used to compare groups that were similar in all but one category to assess effects of blade width, blade strike velocity, strike location, orientation, and impact angle on mortality. One-tailed p-values were used to test significance comparing treatment groups to controls, and two-tailed p-values for tests between treatment groups. We assumed $\alpha = 0.05$.

A second analysis was performed to determine the effect that velocity had on observed and combined mortality rates between groups of bluegill that only varied by average total length. We used a four-parameter log-logistic function to model the dose-response of velocity and mortality according to the following equation [35]:

$$f(x; b, c, d, e) = c + \frac{d-c}{1+\left(\frac{x}{e}\right)^b} \quad (2)$$

where *f (x; b, c, d, e)* is predicted proportion of fish that would not survive, *b* is the slope or inclination point, *c* is the lower bound which was fixed at 0.0, *d* is the higher bound which was fixed at 1.0, and *e* is the effective dose for 50% mortality of the population

(ED_{50}) or the blade strike velocity at which 50% of the population would not be expected to survive. The log-logistic dose response curve was used to analyze two subsets of bluegill that received mid-body, lateral strikes at 90° with at least four blade strike velocities. The subsets differed in average length – i.e., small (11.7 cm; n = 57) and medium-sized fish (16.1 cm; n = 70). Dose-response regression analysis and goodness of fit tests were performed using the "drc" package [35] in R *v3.5.1* [36].

Finally, a logistic regression analysis was performed using generalized linear model (glm) with a logit link function available in R *v3.5.1* [36]. The analyses were performed using observed or combined mortality as the binary predictor variable for both eel and bluegill. Logistic regression is well suited for data that contain a combination of continuous, discrete, categorical, or binary variables with a binary response bounded between 0 and 1 [37]. Continuous variables included, blade velocity (m/s), mass (g), and total length (cm). Categorical variables included blade width (19, 26, and 52), location (M; mid-body or H; head) of blade strike, fish orientation (L; lateral, D; dorsal, or V; ventral), and impact angle (45, 90, 135°). The last group of variables with binary outcomes were linked with injuries pooled together by anatomical structure. For example, if an individual was observed with hemorrhaging and contusions on the liver, it was considered a "1" for the liver category otherwise it was assigned "0" if no injuries were present. Injury categories found in both species included integument, head, fins (all paired and medial fins), gills, viscera (visceral mass as a whole), heart, liver, spleen, swim bladder, kidney, muscle, internal decapitation, and vertebral column. Mouth cavity (including the mouth, buccal surfaces, and palate), gall bladder, stomach, and haemal spines were included in the American eel analysis, whereas eye, opercula, intestines, gonads, and ribs were only included in the bluegill analysis. Only one size-based variable (mass or total length) was included in the analysis because of collinearity among these data. Outliers were detected by centering and scaling size data (mass or length) and removing values with z-scores less than -3.29 or greater than 3.29. Two statistical analyses were performed: 1) blade strike conditions regressed against combined mortality in treatment fish only (n = 151 eels and 400 bluegill) and 2) injury categories regressed against observed mortality including controls (n = 175 eels and 465 bluegill).

Akaike model selection criteria (AIC) and stepwise variable selection was used to select the best fitting model. We used a train to test data ratio of 80:20 for both species. Receiver operating (ROC) plots and area under the curve (AUC) estimates were used to test the ability of our models to predict injury or mortality.

Results

Confirmation of Blade Strike Velocity and Impact

High speed videography confirmed that blade velocity and strike impact conditions (location, orientation, and impact angle) were consistently replicated. Estimates of blade velocity indicated our system had a precision of ± 0.1 m/s within treatment groups. During video confirmation of strike impacts, we found that some fish were not struck as intended, either due to initial misplacement or drifting out of alignment as the blade approached the fish. As a result, about 5% (n = 9) of American eel were analyzed in a different than intended treatment group. Similarly, ~5% of bluegill (n = 25 fish) were not struck as intended. Twenty bluegill that moved could not be placed into one of the 26 original treatment groups, so they were excluded from Chi-square analyses; however, these individuals were included in the logistic regression relating injury to mortality because this model accommodated all variations of treatment conditions. The remaining five bluegill were excluded from all analyses because interaction with holding brackets may have caused injury unrelated to treatment conditions. Nearly all bluegill (n = 465) and every American eel (n = 176) were used in our statistical analyses.

Mortality

A total of 626 fish across both species were successfully exposed to one of 39 treatment conditions including controls (Table 3). No control fish of either species (20 American eel and 48 bluegill) died at any point in our experiment including brief handling, anesthesia, or tagging procedures (i.e., mortality rates = 0.0). Most observed mortalities were the result of removing moribund fish during the 1-hr post-strike observation and not direct death. Some moribund fish exhibited marked

hyperpigmentation on the skin that usually affected only one part of the body and was clearly demarcated from normal skin near the impact site. Hyperpigmentation was not a good predictor of survivorship for either species because abnormal pigmentation disappeared immediately during euthanasia and it was not observed in all fish. Moribund fish were often observed resting on the tank bottom and made few efforts to swim unless stimulated by the assessor. We also observed labored swimming with an inability to maintain upright position in the water column (for bluegill only) which prompted early removal.

American eel had low overall mortality across all treatment groups for fish exposed to velocities up to 13.6 m/s. The highest observed mortality rate was 45.5% when struck on the dorsal surface of the head with the 19-mm blade moving at 13.6 m/s and was the only group (trial #7; Table 3) with significantly ($p << 0.001$) higher mortality compared to control fish. One group (trial #4; Table 3) of eels had no observed instances of mortality, but this trial had a significantly higher combined mortality rate of 100% ($p << 0.001$). Mortality (observed and combined) for fish exposed to 19- and 26-mm blades (Trial #1 & #9; 12.0 m/s, mid-body, lateral strike) were statistically indistinguishable from one another (Table 4). Velocity groups (12.0 versus 13.6 m/s) tested had low observed mortality but high rates of combined mortality, though none of the comparisons differed significantly. Location had a modest effect when fish struck on the head experienced significantly higher observed mortality compared to mid-body strikes (Trial #4 & #7; 19 mm blade, 13.6 m/s; $p = 0.021$), though this was not true for combined mortality or any other comparisons (Table 4). All eel struck on the dorsal surface had significantly higher combined mortality rates compared to controls ($\geq 73\%$; $p << 0.001$) and to fish struck on the lateral ($p \leq 0.014$) or ventral surfaces ($p << 0.001$). No other comparisons yielded significant results (Table 4).

Overall rates of mortality (observed and combined) among bluegill were notably higher than American eel, and mortality was >90% on multiple occasions at moderately low velocities. Most observed and combined mortality rates among treatment groups were significantly higher than control fish (Table 3). Combined mortality rates of 100% were detected in at least five treatment groups at low velocities (i.e., 6.1 m/s). No

significant affect was detected between the 26- and 52-mm blades because mortality (observed and combined) was high in both groups. Significantly higher observed and combined mortality was not detected until velocity exposure groups differed by ≥ 1.0 m/s, though this was not true for all velocity treatment groups (Table 4). Mid-body strikes had significantly higher mortality (observed and combined) than head strikes at 7.1 and 8.0 m/s, but not at 9.0 m/s because mortality was high at both strike locations at this velocity (Table 4). Observed and combined mortality rates were significantly higher when fish were struck on the lateral compared to the ventral surfaces at velocities near 7.5 m/s, but rates were high at all orientations above 8.7 m/s. Mortality was high regardless of impact angle, though only combined mortality was significantly higher for lateral strikes to the head at 90° compared to 45° ($p << 0.001$). Large bluegill (trial #22; Table 3) had observed and combined mortality rates of 100% when exposed to a mid-body, lateral strike at 90° with the 52-mm blade moving at 6.4 m/s. In a comparable trial for medium-sized fish (trial #19; Table 3), observed mortality rate of 50.0% was significantly lower ($p = 0.002$) than large fish. The small size group (trial #19; Table 3) had a slightly higher observed mortality rate (71.4%) and was not significantly different from medium or large fish. Combined mortality rates increased to 83.3% in medium fish and was 100% for both small and large bluegill and did not vary significantly among groups.

Injury Assessment

Dissections of both species revealed that many individuals survived with major internal injuries which were not observed externally. Some moribund fish exhibited marked hyperpigmentation on the skin that usually affected only one part of the body and was clearly demarcated from normal skin near the impact site. In addition to hyperpigmentation, the most common external injury was hemorrhaging from the mouth or the opercular cavity of eel, while minor abrasions and descaling were common among bluegill. We observed fractures of the vertebral column in both species, which was considered a major injury and was used to indicate functional mortality. Nearly 15% of bluegill and 20% of American eel were observed with vertebral fractures but did not

exhibit any signs of stress to indicate it was moribund and should be removed early. The most severe vertebral fracture in both species was observed when the 1st pre-caudal vertebrae was forcefully separated from the posterior edge of the cranium, i.e., internal decapitation. In both species, internal decapitation was often associated with external and internal signs of hemorrhaging near the fracture site. Hemorrhaging or clotting within the visceral mass (i.e., internal organs excluding the heart and kidney) was used as an indication of internal bleeding and was detected in both species. No other general trends across both species were observed.

Though only 16 American eel died during this study, > 25% of all eel dissected showed some signs of severe trauma to the vertebral column. Only the internal decapitation injury group had significantly higher observed mortality (33.3%; $p = 0.002$) than the overall eel mortality rate of 9% (Table 5). Localized hemorrhaging in the buccal cavity and pooling of blood against the palate was also observed as result of internal decapitation when fish were struck on dorsal surface of the head. Gill hemorrhaging was observed from strikes to lateral or ventral surface of the head but had low observed mortality. The most common internal injury among eel was hemorrhaging, lacerations, or contusions to the liver for fish exposed to mid-body lateral and ventral strikes. Some livers were so severely damaged that the hepatic tissue became friable and fell apart during dissection. Fractures to the caudal vertebrae and haemal spines were also common for fish receiving mid-body lateral and dorsal strikes, but only one of these fish was confirmed dead. Five fish with vertebral fractures also had hemorrhaging from damaged kidney tissue which caused blood to pool inside the swim bladder. Muscle injuries (mainly contusions and clotting) where only found in fish that also had concurrent bone fractures in the mid-body region. Organ avulsion ($n = 1$) was only observed in the spleen, while rupture ($n = 5$) was observed in both the spleen and gall bladder, though only one fish was confirmed dead. Internal hemorrhaging and clotting of the viscera were likely from damage to the liver or spleen. One eel that died had no obvious external or internal injuries and was excluded from logistic regression.

Three-quarters of all bluegill tested were observed with one or more injuries. Damage to the eye, operculum, fins, and muscle had mortality rates statistically

indistinguishable from the overall rate 50.2% (Table 5). Mortality rates among fish observed with internal decapitation was also similar to the overall rate (58.3%) and nearly half of these survived the assessment period. Vertebral fracture was the most common injury observed in bluegill including the small fish exposed to the lowest velocity (i.e., 4.7 m/s). Nearly ¼ of all bluegill with vertebral fractures had two or three separate fractures along the entire vertebral column. While no external signs of fractures were evident, moderate to severe hemorrhaging and clotting along the vertebral column against the swim bladder was observed internally. Source of hemorrhaging was difficult to pinpoint, but may have originated from vessels along the spine, trauma to the kidney, or combination of both. Swim bladder damage had a significantly higher rate of mortality (82.1%; $p << 0.001$) and was the second most common injury observed. Rupture of gonadal tissue had significantly higher rates of mortality (71.7%; $p = 0.002$) and was observed in both sexes. Damage to the viscera did not have significantly higher levels of mortality and was only detected in 12% of bluegill. All fish observed with broken ribs ($n = 30$) also had at least one complete fracture of the vertebral column. Fish with gill damage had significantly higher mortality ($p = 0.011$) but this injury was only detected in nine fish. Damage to integument (e.g., minor descaling) was associated with significantly higher rates of mortality (72.3%; $p << 0.001$) but was most likely not the direct cause of mortality. All injuries with significantly higher rates of mortality were also observed with high incidence of vertebral fractures (≥ 75%) which was likely the cause of death for these fish. Injuries to the head and intestine were rare ($n = 2$ fish) and were excluded from logistic regression.

Dose-Response

The dose response analyses of mortality rate against blade strike velocity produced two significant models with good fit for both small ($p << 0.001$) and medium ($p = 0.004$) sized bluegill. The log-logistic models predicted 0 – 100% mortality over a 3 – 4 m/s range in velocity (Figure 13a). Both curves had approximately the same shape and slope (*b*), but smaller fish were expected to reach 50% mortality at a velocity 0.7 m/s lower than the medium-sized group. Predicted models fit our dose-response data better

than the fully parameterized model and one-way analysis of variance (ANOVA) of average mortality across velocity exposure groups ($p >> 0.05$).

The log-logistic models of combined mortality against blade strike velocity were also significant for both small and medium sized fish ($p << 0.001$). Both models predicted 0 – 100 percent mortality over a 3 – 4 m/s velocity range, but small and medium ED_{50} values decreased (Figure 13b). Functional death was predicted to occur at lower velocities overall compared to observed mortality, and small fish experienced major injuries at velocities ~1.0 m/s lower than medium bluegill. The shape of the small and medium curves was also similar but the separation between curves was greater than observed mortality data. Both predictive models fit combined mortality rate data better than the fully parameterized model and one-way ANOVA across velocity exposure groups ($p >> 0.05$).

Logistic Regression

Logistic regression of blade strike conditions against combined mortality found a significant effect among American eel and bluegill data. Stepwise variable selection chose the model containing only blade width and orientation for American eel (AIC = 85.81) while velocity, location, and orientation were the best predictors of combined mortality in bluegill (AIC = 270.62; Table 6). Eel struck on the lateral or ventral surface had higher odds of survival compared to individuals struck on the dorsal surface. Similarly, strikes with the 26 mm blade at fixed orientation would have 85% higher odds of survival compared to strikes with the 19 mm blade. At average velocity and fixed orientation, bluegill would be ~80X more likely to die when struck in the mid-body compared to the head. Similarly, fish struck on the lateral surface were ~45X more likely to die (at average velocity and fixed location), whereas individuals struck on the ventral surface were 77% more likely to survive. For every 1.0 m/s increase in blade strike velocity (at fixed location and orientation) fish would be ~3X more likely to perish. Fish size (e.g., total length, mass, or L/t ratio) did not have a significant impact on mortality for American eel or bluegill across the entire range tested; therefore, it was dropped from the most parsimonious model during stepwise regression. The ROC curves suggested our

logistic models had high specificity (high probability of correctly predicting combined mortality), and AUC values ≥ 0.882 indicated both eel and bluegill models properly classified combined mortality as a result of blade strike conditions (Figure 14a, b).
We only found a significant effect of injury category on observed mortality among bluegill data. Stepwise variable selection produced a model containing integument, operculum, viscera, liver, swim bladder, internal decapitation and vertebral fracture as the best predictors of observed mortality among bluegill (AIC = 275.92; Table 6). Fish with vertebral fractures or internal decapitations with fixed rates of integument, operculum, viscera, and liver injuries were >18X more likely to die. Fish with damage to the integument and fixed rates of operculum, viscera, liver, swim bladder, internal decapitation and vertebral fracture injuries were nearly 2X more likely to die as a result. Damage to the operculum and swim bladder were both important to our parsimonious model but neither were a significant predictor of mortality by itself (Table 6). The ROC curve suggested our logistic model had high specificity and an AUC score of 0.847 suggested the injury model properly classified observed mortality related to injury category.

Discussion

Pairwise comparisons were unable to clearly separate overall trends in our data which highlights the limitations of univariate statistics and not a lack of an actual relationship between blade strike conditions and mortality. For example, logistic regression indicated that thicker blades had higher odds of survival in eel but not in bluegill (Table 6), while results of chi-square tests were less conclusive for both species (Table 6). Lack of significance in bluegill was likely the result of high rates of mortality overall though only two widths were used in this study. Blade strike velocity is likely to have effect on eel mortality, but it was not detected in our study which included only a limited range of blade strike velocities (e.g., 12.0 and 13.6 m/s). In contrast, chi-square and logistic regression analyses indicated that mortality was significantly higher in bluegill when blade strike increased by ≥ 1.0 m/s. Orientation had a clear effect on American eel mortality while location did not – dorsal strikes had higher odds of

mortality than lateral or ventral strikes regardless of location. Mid-body lateral strikes were associated with higher odds of mortality in bluegill which was also shown in rainbow trout, gizzard shad, and hybrid striped bass [22]. Bluegill had high mortality (≥ 80.0%) at all impact angles with no obvious trend, and no other angles were tested or analyzed for American eel. In general, our data indicates that eel may resist blade strike at velocities near 12.0 m/s, though dorsal strikes at or below this velocity would still be severely injurious. Bluegill mortality data fit expected trends of higher mortality with mid-body lateral strikes, but the effects of blade width and impact angle were not obvious. Furthermore, while bluegill data covered more exposure scenarios, the effect of blade width should not be completely dismissed because only two widths were tested in our experiment. Furthermore, lack of significance among bluegill does not indicate lower susceptibility, rather mortality rates were high overall suggesting this species is more intolerant of blade strike conditions compared to eel.

American eel and bluegill data presented here fall within the lower and upper range of survival data published for other species. Bluegill exposed to 6.4 m/s and struck on the mid-body, lateral side at 90° experienced significantly higher mortality than hybrid striped bass which did not die from these conditions [22]. Mortality rates of bluegill and gizzard shad were both equivalently high (>60%) when exposed to a 52-mm blade moving at ~7.4 m/s, and impacting the mid-body, lateral surface at 90° [22]. Bluegill exposed to comparable strike conditions (~4.7 m/s, mid-body, lateral strikes at 90°) as rainbow trout had similarly low observed mortality rates [19,20]. Low rates of observed mortality were also found in American eel at velocities up to 12.2 m/s; however, overall mortality after a 96-hr observation period increased to 70% for mid-body strikes specifically [20]. White sturgeon had significantly higher mortality (~50%) from similar turbine blade strike conditions (12.0 m/s velocity, 26-mm blade, mid-body, lateral strike at 90°) suggesting sturgeon may be more susceptible to turbine passage than American eel [21]. Across all studies discussed so far, it appears bluegill and gizzard shad are the most susceptible, followed by rainbow trout and hybrid striped bass, while white sturgeon and American eel are the most resistant species tested to date.

The marked range in response to blade strike is mirrored by the anatomically and morphologically distinct body types of American eel and bluegill. American eel are elongate with total length far exceeding body depth and have incredibly flexible bodies that facilitate its anguilliform mode of swimming [24,38]. In contrast, bluegill is short with a laterally compressed body and high surface area to maximize acceleration, turning behavior, and maneuverability [39]. Review of highspeed video revealed that both species wrapped around the blade to some degree after contact, but eel wrapped more completely with seemingly minimal negative effect. The only instance this was not true for eel was during all dorsal strikes which often had low observed mortality but ≥ 73% were considered functionally dead due to spinal fractures, indicating dorso-ventral flexibility is limited. Bending in bluegill was exceedingly traumatic and many fish had more than one vertebral fracture at low velocities (~ 5.0 m/s). The exact degree to which each species can bend with minimal vertebral damage was not measured; however, vertebral morphology has been linked with C-start curvature and swimming performance [40,41]. More specifically, the number of, and angle between, each vertebra influences maximum curvature and is one measure of stiffness among fishes [40]. The second component includes the role of interconnected skin, tendons, and muscles around the skeletal elements and their effect on overall stiffness [42]. While whole body stiffness was also not measured, we know American eel has 103 – 111 vertebrae compared to only 28 – 33 found in bluegill [25,43] which likely contributes to the enhanced flexibility of American eel under most strike scenarios. Injury severity and mortality may also be related to proximity of blade strike to a species center of gravity. Blade strike impacts near the center of gravity may be especially traumatic because there would be less deflection and more force transmitted to the fish [22,44]. This relationship may not apply to American eel because the center of gravity is not located near the visceral mass, but mid-body strikes in this study did target the area with concentrated soft tissues. The center of gravity for bluegill is located roughly 40% of its total length [45] which also coincides with the location of most internal organs of the visceral mass. We observed more severe organ damage in American eel which could related to its lack of skeletal protection (i.e., ribs or intramuscular bones), whereas bluegill has an extensive protective

network that provides enhanced protection to soft tissues. Investigations into anatomical and biomechanical properties (e.g., flexibility or center of gravity) related to strike location are needed to better elucidate how fish may resist injury caused by blade strike.

Fish size was also compared between different size groups and across the entire range of fish tested suggesting size may affect mortality, but not necessarily in the same way described previously or under all conditions. EPRI (2008) was the first to demonstrate that fish survival was linked to the total length to blade width ratio (i.e., L/t ratio). Average American eel L/t ratio in our study (28.8) had no observed mortality and matched comparable trials (L/t = 31.8; velocity = 12.2 m/s) with no instantaneous mortality described in EPRI (2008). The average L/t ratios for small (2.25), medium (3.10), and large (3.36) bluegill all had observed mortality > 50%, though large fish had significantly higher observed mortality compared to medium fish. Combined mortality rates were higher for all bluegill L/t ratios (≥ 83%) and no obvious trend was detected. Our dose-response curves suggest that observed and functional mortality for 50% of small bluegill would occur at notably lower velocities than medium bluegill (Figure 13). Dose response analyses indicated that small fish are more susceptible to blade strike than larger individuals, which contrasts with lower mortality observed in small compared to larger rainbow trout [20]. No further comparisons can be made because of our limited number of L/t ratio groups and lack of direct comparison with our study species. Interestingly, logistic regression models suggested that size did not significantly impact mortality, which was influenced more by location, orientation, and velocity of blade strike impact. For eel, lack of significant effect on size may be related to the narrow range of sizes used (45 – 65 cm), whereas size is less important to bluegill provided that all sizes of fish tested experienced notably high mortality rates. Regardless, fish size is likely an important predictor of mortality, but other factors (e.g., species morphology or proximity of strike to center of gravity) should also be factored into estimates of mortality when accounting for size effects within or among species.

Many individuals of both species (39 American eel and 63 bluegill) survived at least one hour with one or more vertebral fractures which necessitated redefining mortality based on functional (ecological) death. While these animals were technically

considered survivors in our study, they would be less likely to escape predation and capturing food would also be challenging. More importantly, there were no obvious external signs of this severe injury that could be observed consistently. The logistic regression of injuries suggested many other internal injuries were significant predictors of mortality, but these injuries were always associated with high prevalence of fractured vertebrae in bluegill (Table 6). This is especially important to consider during turbine passage studies in the field because the assessor would be unable to detect functionally dead individuals without performing internal necropsies. To our knowledge, field studies do not perform internal necropsies suggesting that some apparent survivors may be functionally dead after the observation period ends. For example, American eel mortality increased to nearly 70% during a 96-hr observation period which was attributed to an unspecified internal injury [20]. Combined mortality rates >70% were detected in American eel when mortality estimates included functionally dead fish which suggests this endpoint is more indicative of long-term eel survival. To that end, we suggest internal exams should be a component of field and laboratory studies because it provides a more accurate estimate of injury and mortality rates. Inclusion of functionally dead fish should increase accuracy of mortality estimates, but we are uncertain that all vertebral fractures are lethal and unrecoverable provided some fish were observed with partial vertebral fractures. Additional trials that observe fishes for longer periods of time (i.e., ≥ 96 hours) would also help elucidate how functional death relates to changes in fish health, growth, or behavioral impairment following exposure to blade strike impact.

Conclusions

The data presented in this study will provide additional insights into how susceptible riverine fishes are to blade strike impact that may be experienced during passage through hydropower turbines or water pumping facilities. Our system is not meant to mimic complete turbine passage conditions like studies involving scale models and live fish. Instead, the blade strike apparatus used in this study was designed to expose fish to a blade with a similar shape, leading edge thickness, and strike velocity of a hydropower turbine blade during average turbine passage conditions [22]. Leading edge

width and velocity of our blade is also within the specifications of radial, mixed flow, and Hidrostal pumps used at water pumping stations worldwide [6,7,17]. The operation of both hydropower turbines and water pumping stations would also affect estimates of mortality as operators adjust flow rate or runner speed to maximize generation ability or water movement. Our methodology was also developed to cover as many exposure scenarios as possible with the given number of fish because strike conditions that occur to each fish passing through turbines or pumps is unknown. In addition, we designed our system to allow for precise, repeatable exposure of fishes to blade strike conditions to better account for variation and decrease uncertainty in our estimates of mortality. Fish struck by our stimulated turbine blade were not constricted in any way and were allowed to move freely after initial contact was made with the turbine blade. Prior studies used monofilament tethers to hold fish in place to better control where the blade impacted fish; as a result, this method also led to estimates of mortality that were confounded by a tether that restricted fish movement [20,21]. The apparatus and methodologies used here may be less realistic than in-situ passage studies, but our design maximizes the ability to control dose (e.g., blade width and strike velocity) to provide more accurate estimates of mortality.

Our system was well suited to quantify blade strike dose-responses that will parameterize the Biological Performance Assessment (BioPA) model and Hydropower Biological Evaluation Toolset (HBET) – both are being developed to inform safer turbine designs [46,47]. Development of safer turbine designs using biologically relevant data is not a new concept and has already led to design and implementation of more fish friendly systems [9]. Our data are of growing importance as dam operators are faced with the rigors of relicensing through the Federal Energy Regulatory Committee (FERC) which stipulates renewal of licenses every 30 – 50 years. Part of this renewal process includes detailed and costly environmental impact assessments which always includes a component of turbine passage and survival of fishes most likely to become entrained. The native ranges of American eel and bluegill put them in direct contact with nearly 50% of all hydropower projects in the USA, suggesting the risk of entrainment and turbine passage is high for both species [48]. While more detailed and holistic estimates of

mortality and dose-response models will be released in the future, we suggest the following to maximize utility of our data presented as is. To date, no exposure conditions tested with our system or others has been able to replicate the severe trauma (e.g., eels severed in half) observed at some dams. To that end, we suspect that grinding and tearing of eels via pinch points is the more likely cause of these kinds of injuries compared to the internal injuries we observed which were more likely to be caused by direct blade strike. Mortality of eels is more likely if passage through turbines or pumping stations includes blade characteristics that are moderately thin (< 26 mm) and moving at velocities ≥ 12.0 m/s. Bluegill, which is much less resistant to blade strike, will likely experience high mortality under most scenarios because strike velocities as low as 5.0 m/s were lethal. Furthermore, our data indicate that fish species is an important consideration in mortality estimates and suggests that size effects may be confounded by species anatomical and morphology disparities. Future research should include more blade widths for both species a wider range of strike velocities in eel specifically to better elucidate how blade strike effects mortality. We also recommend continued investigations into more morphologically distinct species and account for fish biomechanics to better understand how blade strike impact affects mortality or riverine fishes.

Acknowledgments

This research was funded by the US Department of Energy's Waterpower Program to Oak Ridge National Laboratory (ORNL)/UT-Battelle, LLC under Contract No. DE-AC05-00OR22725. Animal use approval was granted by the ORNL Animal Care and Use Committee [protocol #0444]. Fish used in this study were obtained from Southeastern Pond Management in Jackson, TN, and Delaware Valley Fish Company in, Norristown, PA. Special thanks to Rebecca Brink, Miles Mobley, and Clara Layzer for assistance in the lab and Gary Johnson (Pacific Northwest National Laboratory, PNNL) and Shelaine Curd (ORNL) for project management. Reviews from Brenda Pracheil (ORNL) and Brett Pflugrath (PNNL) strengthened the content of this manuscript.

References

1. Pracheil, B.M.; DeRolph, C.R.; Schramm, M.P.; Bevelhimer, M.S. A fish-eye view of riverine hydropower systems: The current understanding of the biological response to turbine passage. *Rev. Fish Biol. Fish.* **2016**, *26*, 153–167.

2. van Esch, B.P.M.; Spierts, I.L.Y.; Tierney, K. Validation of a model to predict fish passage mortality in pumping stations. *Can. J. Fish. Aquat. Sci.* **2014**, *71*, 1910–1923.

3. Hostetter, N.J.; Evans, a. F.; Roby, D.D.; Collis, K.; Hawbecker, M.; Sandford, B.P.; Thompson, D.E.; Loge, F.J. Relationship of external fish condition to pathogen prevalence and out-migration survival in juvenile steelhead. *Trans. Am. Fish. Soc.* **2011**, *140*, 1158–1171.

4. Mueller, M.; Pander, J.; Geist, J. Evaluation of external fish injury caused by hydropower plants based on a novel field-based protocol. *Fish. Manag. Ecol.* **2017**, *24*, 240–255.

5. Pracheil, B.M.; Mestl, G.E.; Pegg, M.A. Movement through dams facilitates population connectivity in a large river. *River Res. Appl.* **2015**, *31*, 517–525.

6. van Esch, B.P.M. Fish injury and mortality during passage through pumping stations. *J. Fluids Eng.* **2012**, *134*, 071302.

7. McNabb, C.D.; Liston, C.R.; Borthwick, S.M. Passage of juvenile chinook salmon and other fish species through Archimedes lifts and a hidrostal pump at Red Bluff, California. *Trans. Am. Fish. Soc.* **2003**, *132*, 326–334.

8. Baumgartner, L.J.; Reynoldson, N.K.; Cameron, L.; Stanger, J. Effects of irrigation pumps on riverine fish. *Fish. Manag. Ecol.* **2009**, *16*, 429–437.

9. Čada, G.F. The development of advanced hydroelectric turbines to improve fish passage survival. *Fisheries* **2001**, *26*, 14–23.

10. Binder, T.R.; Cooke, S.J.; Hinch, S.G. Physiological specializations of different

fish groups: Fish migrations. In *Encyclopedia of Fish Physiology: From Genome to Environment*; Farrell, A.P., Cech Jr., J.J., Richards, J.G., Stevens, E.D., Eds.; Elsevier Inc.: San Diego, California, **2011**; pp. 1921–1952 ISBN 9780123745538.

11. Grubbs, R.D.; Kraus, R.T. Fish Migration. In *Encyclopedia of Animal Behavior*; Breed, M.D., Moore, J., Eds.; Elsevier Academic Press: San Diego, California, **2010**; pp. 715–724.

12. McIntyre, P.B.; Liermann, C.R.; Childress, E.; Hamann, E.J.; Hogan, J.D.; Januchowski-Hartley, S.R.; Koning, A.A.; Neeson, T.M.; Oele, D.L.; Pracheil, B.M. Conservation of migratory fishes in freshwater ecosystems. In *Conservation of Freshwater Fishes*; Closs, G.P., Krkosek, M., Olden, J.D., Eds.; Cambridge University Press: Cambridge, United Kingdom, **2016**; pp. 324–360 ISBN 9781107040113.

13. Colotelo, A.H.; Goldman, A.E.; Wagner, K.A.; Brown, R.S.; Deng, Z.D.; Richmond, M.C. A comparison of metrics to evaluate the effects of hydro-facility passage stressors on fish. *Environ. Rev.* **2017**, *25*, 1–11.

14. Uria-Martinez, R.; Johnson, M.M.; O'Connor, P.W.; Samu, N.M.; Witt, A.M.; Battey, H.; Welch, T.; Bonnet, M.; Wagoner, S. *2017 Hydropower Market Report*; Oak Ridge, Tennessee, **2018**.

15. Fu, T.; Deng, Z.D.; Duncan, J.P.; Zhou, D.; Carlson, T.J.; Johnson, G.E.; Hou, H. Assessing hydraulic conditions through Francis turbines using an autonomous sensor device. *Renew. Energy* **2016**, *99*, 1244–1252.

16. Martinez, J.J.; Deng, Z.D.; Titzler, P.S.; Duncan, J.P.; Lu, J.; Mueller, R.P.; Tian, C.; Trumbo, B.A.; Ahmann, M.L.; Renholds, J.F. Hydraulic and biological characterization of a large Kaplan turbine. *Renew. Energy* **2019**, *131*, 240–249.

17. Helfrich, L.A.; Bark, R.; Liston, C.R.; Weigmann, D.L.; Mefford, B. Live transport of striped bass and rainbow trout using a hidrostal pump. *J. World Aquac. Soc.* **2004**, *35*, 268–273.

18. Pracheil, B.M.; McManamay, R.A.; Bevelhimer, M.S.; DeRolph, C.R.; Čada, G.F. A traits-based approach for prioritizing species for monitoring and surrogacy selection. *Endanger. Species Res.* **2016**, *31*, 243–258.

19. Turnpenny, A.W.H. Mechanisms of fish damage in low head turbines: An experimental appraisal. In *Fish Migration and Fish Bypasses*; Jungwirth, M., Schmutz, S., Weiss, S., Eds.; Blackwell Publishing Ltd: Malden, Massachusetts, **1998**; pp. 300–314 ISBN 0-85238-253-7.

20. EPRI, (Electric Power Research Institute) *Evaluation of the effects of turbine blade leading edge design on fish survival*; Palo Alto, CA, **2008**.

21. EPRI, (Electric Power Research Institute) *Tests examining survival of fish struck by turbine blades*; Palo Alto, CA, **2011**.

22. Bevelhimer, M.S.; Pracheil, B.M.; Fortner, A.M.; Saylor, R.; Deck, K.L. Mortality and injury assessment for three species of fish exposed to simulated turbine blade strike. *Can. J. Fish. Aquat. Sci.* **2019**, *76*, 2350–2363.

23. Coutant, C.C.; Whitney, R.R. Fish behavior in relation to passage through hydropower turbines: A review. *Trans. Am. Fish. Soc.* **2000**, *129*, 351–380.

24. Haro, A. Anguillidae: Freshwater Eels. In *Freshwater Fishes of North America: Petromyzontidae to Catostomidae*; Warren Jr., M.L., Burr, B.M., Eds.; Johns Hopkins University Press: Baltimore, Maryland, **2014**; pp. 313–331.

25. Froese, R.; Pauly, D. Fishbase. *Fishbase* **2020**.

26. Eyler, S.M.; Welsh, S.A.; Smith, D.R.; Rockey, M.M. Downstream passage and impact of rurbine ahutdowns on survival of ailver American eels at five hydroelectric dams on the Shenandoah River. *Trans. Am. Fish. Soc.* **2016**, *145*, 964–976.

27. Carr, J.W.; Whoriskey, F.G. Migration of silver American eels past a hydroelectric dam and through a coastal zone. *Fish. Manag. Ecol.* **2008**, *15*, 393–

400.

28. USACE, (United States Army Corp of Engineers) National Inventory of Dams Available online: http://nid.usace.army.mil/cm_apex/f?p=838:5:0::NO (accessed on Dec 23, 2020).

29. Jager, H.I.; Elrod, B.; Samu, N.; McManamay, R.A.; Smith, B.T. *ESA Protection for the American Eel: Implications for U.S. Hydropower*; Oak Ridge, Tennessee, **2013**; Vol. Ocotober.

30. Cooke, S.; Philipp, D. *Centrarchid Fishes: Diversity, Biology and Conservation*; Cooke, S., Philipp, D., Eds.; 1st ed.; Wiley-Blackwell Publishing, **2009**; ISBN 9781405133425.

31. Keefer, M.L.; Taylor, G.A.; Garletts, D.F.; Helms, C.K.; Gauthier, G.A.; Pierce, T.M.; Caudill, C.C. High-head dams affect downstream fish passage timing and survival in the Middlefork Williamette River. *River Res. Appl.* **2013**, *29*, 483–492.

32. Javahery, S.; Nekoubin, H.; Moradlu, A.H. Effect of anaesthesia with clove oil in fish (review). *Fish Physiol. Biochem.* **2012**, *38*, 1545–1552.

33. Sneddon, L.U. Clinical Anesthesia and Analgesia in. *J. Exot. Pet Med.* **2012**, *21*, 32–43.

34. Campbell, I. Chi-squared and Fisher-Irwin tests of two-by-two tables with small sample recommendations. *Stat. Med.* **2007**, *26*, 3661–3675.

35. Ritz, C.; Baty, F.; Streibig, J.C.; Gerhard, D. Dose-response analysis using R. *PLoS One* **2015**, *10*, 1–13.

36. R Core Team R: A language and environment for stastical computing. **2019**.

37. Hilbe, J.M. *Practical Guide to Logistic Regression*; 1st ed.; Chapman and Hall/CRC: Boca Raton, Florida, **2016**;

38. Helfman, G.S.; Collette, B.B.; Facey, D.E.; Bowen, B.W. *The Diversity of Fishes: Biology, Evolution, and Ecology*; 2nd ed.; Wiley-Blackwell Publishing: West

Sussex, UK, **2009**;

39. Collar, D.C.; Wainwright, P.C. Ecomorphology of centrarchid fishes. In *Centrachid Fishes: Diversity, Biology and Conservation*; Cooke, S., Philipp, D., Eds.; Blackwell Publishing Ltd: West Sussex, UK, **2009**; pp. 70–89.

40. Brainerd, E.L.; Patek, S.N. Vertebral column morphology, C-start curvature, and the evolution of mechanical defenses in tetraodontiform fishes. *Copeia* **1998**, 971–984.

41. Swain, D.P. The functional basis of natural selection for vertebral traits of larvae in the stickleback Gasterosteus aculeatus. *Evolution (N. Y).* **1992**, *46*, 987–997.

42. Long, J.H.; Nipper, K.S. The importance of body stiffness in undulatory propulsion. *Am. Zool.* **1996**, *36*, 678–694.

43. Nelson, J.S.; Grande, T.C.; Wilson, M.V.H. *Fishes of the World*; 5th ed.; John Wiley & Sons: Hoboken, New Jersey, **2016**.

44. Turnpenny, A.W.H.; Davis, M.H.; Fleming, J.M.; Davies, J.K. *Experimental studies relating to the passage of fish and shrimps through tidal power turbines*; Southampton, United Kingdom, **1992**.

45. Tytell, E.D.; Lauder, G. V. Hydrodynamics of the escape response in bluegill sunfish, Lepomis macrochirus. *J. Exp. Biol.* **2008**, *211*, 3359–3369.

46. Richmond, M.C.; Serkowski, J.A.; Radowski, C.; Strickler, B.; Weisbeck, M.; Dotson, C. Computational tools to assess turbine biological performance. *Hydroreview* **2014**, *33*, 1–6.

47. Hou, H.; Deng, Z.; Martinez, J.; Fu, T.; Duncan, J.; Johnson, G.; Lu, J.; Skalski, J.; Townsend, R.; Tan, L. A Hydropower Biological Evaluation Toolset (HBET) for characterizing hydraulic conditions and impacts of hydro-structures on fish. *Energies* **2018**, *11*, 990–1002.

48. Bevelhimer, M.S.; Derolph, C.R. *Market assessment for hydropower turbine*

design tools using integrated datasets of dams, turbines, owners, and fish; **2019**.

Appendix

Table 3. Experimental overview of the study including all 37 treatment groups and two control (C) groups for American eel and bluegill. Size classes are reported for bluegill only (Sma; small, Med; medium, and Lar; large). Blade strike characteristics including blade width (Wid; mm), velocity (Vel; m/s), impact angle (Ang), location (Loc, with M; mid-body or H; head), orientation (Ort, with L; lateral, D; dorsal, and V; ventral). The total number in each group (N) is reported along with counts of observed (OMort), functional (FMort), and combined mortalities (CMort). Rates were calculated for observed and combined mortalities only. Results of one-tailed Chi-square test with Yate's correction are presented as p-values for observed and combined mortality of each treatment group tested against the species' control group. We assumed $\alpha = 0.05$; significant comparisons are in bold.

#	Species	Size	Wid	Vel	Ang	Loc	Ort	N	Number of Deaths			Rates			
									OMort	FMort	CMort	OMort	p-value	CMort	p-value
C	American eel	--	--	--	--	--	--	20	0	0	0	0.0	--	0.0	--
1	American eel	--	19	12.0	90	M	L	11	0	3	3	0.0	1.000	27.3	**0.034**
2	American eel	--	19	12.0	90	M	D	10	0	9	9	0.0	1.000	90.0	**<0.001**
3	American eel	--	19	13.6	90	M	L	20	3	3	5	15.0	0.115	25.0	**0.028**
4	American eel	--	19	13.6	90	M	D	11	0	11	11	0.0	1.000	100.0	**<0.001**
5	American eel	--	19	13.6	90	M	V	13	1	0	1	7.7	0.413	7.7	0.413
6	American eel	--	19	13.6	90	H	L	19	3	1	4	15.8	0.106	21.1	0.051
7	American eel	--	19	13.6	90	H	D	11	5	9	10	45.5	**0.003**	90.9	**<0.001**
8	American eel	--	19	13.6	90	H	V	16	0	0	0	0.0	1.000	0.0	1.000
9	American eel	--	26	12.0	90	M	L	15	1	0	1	6.7	0.442	6.7	0.442
10	American eel	--	26	12.0	90	H	L	15	0	0	0	0.0	1.000	0.0	1.000
11	American eel	--	26	12.0	90	H	D	15	3	11	11	20.0	0.138	73.3	**<0.001**
C	Bluegill	--	--	--	--	--	--	48	0	0	0	0.0	--	0.0	--
12	Bluegill	Med	26	7.7	90	M	L	18	16	17	18	88.9	**<0.001**	100.0	**<0.001**
13	Bluegill	Med	26	8.6	90	M	L	36	35	35	35	97.2	**<0.001**	97.2	**<0.001**
14	Bluegill	Sma	52	4.7	90	M	L	14	1	8	8	7.1	0.254	57.1	**<0.001**

Table 3 continued…

15	Bluegill	Sma	52	5.3	90	M	L	15	5	13	13	33.3	**<0.001**	86.7	**<0.001**
16	Bluegill	Sma	52	6.1	90	M	L	14	10	13	14	71.4	**<0.001**	100.0	**<0.001**
17	Bluegill	Sma	52	7.3	90	M	L	14	12	14	14	85.7	**<0.001**	100.0	**<0.001**
18	Bluegill	Med	52	5.5	90	M	L	18	2	3	4	11.1	0.062	22.2	**0.003**
19	Bluegill	Med	52	6.4	90	M	L	18	9	15	15	50.0	**<0.001**	83.3	**<0.001**
20	Bluegill	Med	52	7.3	90	M	L	17	15	14	16	88.2	**<0.001**	94.1	**<0.001**
21	Bluegill	Med	52	9.1	90	M	L	17	16	14	16	94.1	**<0.001**	94.1	**<0.001**
22	Bluegill	Lar	52	6.4	90	M	L	18	18	18	18	100.0	**<0.001**	100.0	**<0.001**
23	Bluegill	Med	52	7.3	45	M	L	15	14	10	14	93.3	**<0.001**	93.3	**<0.001**
24	Bluegill	Med	52	8.0	45	M	L	15	13	14	14	86.7	**<0.001**	93.3	**<0.001**
25	Bluegill	Med	52	7.3	135	M	L	15	11	12	14	73.3	**<0.001**	93.3	**<0.001**
26	Bluegill	Med	52	8.0	135	M	L	15	12	9	13	80.0	**<0.001**	86.7	**<0.001**
27	Bluegill	Med	52	7.5	90	M	D	9	0	0	0	0.0	1.000	0.0	1.000
28	Bluegill	Med	52	8.7	90	M	D	17	10	11	13	58.8	**<0.001**	76.5	**<0.001**
29	Bluegill	Med	52	9.4	90	M	D	9	5	8	9	55.6	**<0.001**	100.0	**<0.001**
30	Bluegill	Med	52	7.5	90	M	V	9	0	0	0	0.0	1.000	0.0	1.000
31	Bluegill	Med	52	8.7	90	M	V	17	3	3	5	17.6	**0.011**	29.4	**<0.001**
32	Bluegill	Med	52	9.4	90	M	V	9	5	3	5	55.6	**<0.001**	55.6	**<0.001**
33	Bluegill	Med	52	7.1	90	H	L	14	0	0	0	0.0	1.000	0.0	1.000
34	Bluegill	Med	52	8.8	90	H	L	17	2	8	9	11.8	0.055	52.9	**<0.001**
35	Bluegill	Med	52	9.0	90	H	L	14	11	10	13	78.6	**<0.001**	92.9	**<0.001**
36	Bluegill	Med	52	8.0	45	H	L	15	1	8	9	6.7	0.268	60.0	**<0.001**
37	Bluegill	Med	52	8.3	45	H	L	13	0	0	0	0.0	1.000	0.0	1.000

Table 4. Results of two-tailed, pairwise comparisons using Chi-square test with Yate's correction for observed and combined mortality rates of American eel and bluegill. Trials (treatment groups separated by a comma) being compared are referenced from data in Table 1. The main variable to be tested (Var) is listed with blade strike characteristics including blade width (Wid; mm), velocity (Vel; m/s), impact angle (Ang), location (Loc, with M; mid-body or H; head), orientation (Ort, with L; lateral, D; dorsal, and V; ventral). Rates of observed (OMort) and combined mortalities (CMort) are provided with p-values (p) for each comparison. We assumed $\alpha = 0.05$; significant comparisons are in bold.

Species	**Var**	**Trials**	**Wid**	**Vel**	**Ang**	**Loc**	**Ort**	**OMort**		***p***	**CMort**		***p***
American eel	Wid	1, 9	19, 26	12.0	90	M	L	0 (0.0)	1 (6.7)	*0.873*	3 (27.3)	1 (6.7)	*0.374*
	Vel	1, 3	19	12.0, 13.6	90	M	L	0 (0.0)	3 (15.0)	*0.474*	3 (27.3)	5 (25.0)	*0.771*
		2, 4	19	12.0, 13.6	90	M	D	0 (0.0)	0 (0.0)	*1.000*	9 (90.0)	11 (100.0)	*0.961*
	Loc	3, 6	19	13.6	90	M, H	L	3 (15.8)	3 (15.8)	*0.707*	5 (21.1)	4 (21.1)	*0.930*
		4, 7	19	13.6	90	M, H	D	0 (0.0)	5 (45.4)	***0.021***	11 (100.0)	10 (90.9)	*0.500*
		5, 8	19	13.6	90	M, H	V	1 (7.1)	0 (0.0)	*0.473*	1 (7.1)	0 (0.0)	*0.203*
	Ort	1, 2	19	12.0	90	M	L, D	0 (0.0)	0 (0.0)	*1.000*	3 (27.3)	9 (90.0)	***0.014***
		3, 4	19	13.6	90	M	L, D	3 (15.0)	0 (0.0)	*0.474*	5 (25.0)	11 (100.0)	***<0.001***
		3, 5	19	13.6	90	M	L, V	3 (15.0)	1 (7.1)	*0.751*	5 (25.0)	1 (7.1)	*0.598*
		4, 5	19	13.6	90	M	D, V	0 (0.0)	1 (7.1)	*0.932*	11 (100.0)	1 (7.1)	***<0.001***
		10, 11	26	12.0	90	H	L, D	0 (0.0)	3 (20.0)	*0.224*	0 (0.0)	11 (73.3)	***<0.001***
Bluegill	BW	12, 20	26, 52	~7.5	90	M	L	16 (89.9)	15 (88.2)	*0.638*	18 (100.0)	16 (94.1)	*0.978*
		13, 21	26, 52	~8.8	90	M	L	35 (97.1)	16 (94.1)	*0.827*	35 (97.2)	16 (94.1)	*0.827*
	Vel	12, 13	26	7.7, 8.6	90	M	L	16 (89.9)	35 (97.1)	*0.529*	18 (100.0)	35 (97.2)	*0.721*
		18, 19	52	5.5, 6.4	90	M	L	2 (11.1)	9 (50.0)	***0.030***	4 (22.2)	15 (83.3)	***<0.001***
		18, 20	52	5.5, 7.3	90	M	L	2 (11.1)	15 (88.2)	***<0.001***	4 (22.2)	16 (94.1)	***<0.001***

Table 4 continued…

	18, 21	52	5.5, 9.1	90	M	L	2 (11.1)	16 (94.1)	***<0.001***	4 (22.2)	16 (94.1)	***<0.001***
	19, 20	52	6.4, 7.3	90	M	L	9 (50.0)	15 (88.2)	***0.038***	15 (83.3)	16 (94.1)	*0.638*
	19, 21	52	6.4, 9.1	90	M	L	9 (50.0)	16 (94.1)	***0.012***	15 (83.3)	16 (94.1)	*0.638*
	20, 21	52	7.3, 9.1	90	M	L	15 (88.2)	16 (94.1)	*1.000*	16 (94.1)	16 (94.1)	*0.466*
	27, 28	52	7.5, 8.7	90	M	D	0 (0.0)	10 (58.8)	***0.012***	0 (0.0)	13 (76.5)	***<0.001***
	28, 29	52	8.7, 9.4	90	M	D	10 (58.8)	5 (55.6)	*0.797*	13 (76.5)	9 (100.0)	*0.312*
	27, 29	52	7.5, 9.4	90	M	D	0 (0.0)	5 (55.6)	***0.035***	0 (0.0)	9 (100.0)	***<0.001***
	30, 31	52	7.5, 8.7	90	M	V	0 (0.0)	3 (17.6)	*0.487*	0 (0.0)	5 (29.4)	*0.198*
	31, 32	52	8.7, 9.4	90	M	V	3 (17.6)	5 (55.6)	*0.122*	5 (29.4)	5 (55.6)	*0.379*
	30, 32	52	7.5, 9.4	90	M	V	0 (0.0)	5 (55.6)	***0.035***	0 (0.0)	5 (55.6)	***0.035***
	23, 24	52	7.3, 8.0	45	M	L	14 (93.3)	13 (86.7)	*1.000*	14 (93.3)	14 (93.3)	*0.464*
	25, 26	52	7.3, 8.0	135	M	L	11 (73.3)	12 (80.0)	*1.000*	14 (93.3)	13 (86.7)	*1.000*
	33, 34	52	7.1, 8.8	90	H	L	0 (0.0)	2 (11.8)	*0.553*	0 (0.0)	9 (52.9)	***0.005***
	34, 35	52	8.8, 9.0	90	H	L	2 (11.8)	11 (78.6)	***<0.001***	9 (52.9)	13 (92.9)	***0.041***
	33, 35	52	7.1, 9.0	90	H	L	0 (0.0)	11 (78.6)	***<0.001***	0 (0.0)	13 (92.9)	***<0.001***
Ang	20, 23	52	7.3	90, 45	M	L	15 (88.2)	14 (93.3)	*0.909*	16 (94.1)	14 (93.3)	*0.522*
	20, 25	52	7.3	90, 135	M	L	15 (88.2)	11 (73.3)	*0.909*	16 (94.1)	14 (93.3)	*0.522*
	23, 25	52	7.3	45, 135	M	L	14 (93.3)	11 (73.3)	*0.464*	14 (93.3)	14 (93.3)	*0.464*
	24, 26	52	8.0	45, 135	M	L	13 (86.7)	12 (80.0)	*1.000*	14 (93.3)	13 (86.7)	*0.464*
	34, 37	52	~8.6	90, 45	H	L	2 (11.8)	0 (0.0)	*0.588*	9 (52.9)	0 (0.0)	***0.006***
Loc	20, 33	52	~7.2	90	M, H	L	15 (88.2)	0 (0.0)	***<0.001***	16 (94.1)	0 (0.0)	***<0.001***
	21, 35	52	~9.1	90	M, H	L	16 (94.1)	11 (78.6)	*0.455*	16 (94.1)	13 (92.9)	*0.554*
	24, 36	52	8.0	45	M, H	L	13 (86.7)	1 (6.7)	***<0.001***	14 (93.3)	9 (60.0)	*0.084*

Table 4 continued…

Ort	20, 27	52	~7.4	90	M	L, D	15 (88.2)	0 (0.0)	***<0.001***	16 (94.1)	0 (0.0)	***<0.001***
	20, 30	52	~7.4	90	M	L, V	15 (88.2)	0 (0.0)	***<0.001***	16 (94.1)	0 (0.0)	***<0.001***
	21, 29	52	~9.3	90	M	L, D	16 (94.1)	5 (55.6)	*0.064*	16 (94.1)	9 (100.0)	*0.742*
	21, 32	52	~9.3	90	M	L, V	16 (94.1)	5 (55.6)	*0.064*	16 (94.1)	5 (55.6)	*0.064*
	27, 30	52	7.5	90	M	D, V	0 (0.0)	0 (0.0)	*1.000*	0 (0.0)	0 (0.0)	*1.000*
	28, 31	52	8.7	90	M	D, V	10 (58.8)	3 (17.6)	***0.034***	13 (76.5)	5 (29.4)	***0.016***
	29, 32	52	9.4	90	M	D, V	5 (55.6)	5 (55.6)	*0.635*	9 (100.0)	5 (55.6)	*0.089*

Table 5. Observed mortality (OMort) among American eel and bluegill related to major injury categories for each species. One-tailed p-values were calculated from Chi-square test with Yate's correction between the observed mortality rates of each injury category against mortality rate of total injured & uninjured fish of both species. We assumed $\alpha = 0.05$. Significant comparisons are in bold. Notes provide additional injury or analysis details for observed mortalities.

Species	Category	Total	OMort	Rate	p-value	Notes
American eel	Injured & uninjured	176	16	0.091	--	--
	Integument	39	2	0.051	*0.312*	--
	Head	24	5	0.208	*0.080*	--
	Mouth cavity	40	8	0.200	***0.044***	7 of 8 had internal decapitation
	Pectoral fin	69	9	0.130	*0.247*	--
	Gill	4	0	0.000	--	Sample size too small to test
	Viscera	9	1	0.111	*0.349*	--
	Heart	4	0	0.000	--	Sample size too small to test
	Liver	51	3	0.059	*0.329*	--
	Gall bladder	2	0	0.000	--	Sample size too small to test
	Spleen	11	1	0.091	*0.294*	--
	Swim bladder	3	0	0.000	--	Sample size too small to test
	Stomach	1	0	0.000	--	Sample size too small to test
	Kidney	5	0	0.000	*0.463*	--
	Muscle	29	1	0.034	*0.255*	--
	Haemal spines	18	0	0.000	*0.188*	--
	Internal decapitation	21	7	0.333	***0.002***	--
	Caudal vertebrae	26	1	0.038	*0.301*	--
Bluegill	Injured & uninjured	450	226	0.502	--	--
	Integument	143	102	0.713	***<0.001***	94 of 102 had vertebral damage
	Head	1	0	0.000	--	Sample size too small to test
	Eye	34	17	0.500	*0.439*	--
	Operculum	11	7	0.636	*0.283*	--
	Fins (all)	13	6	0.462	*0.497*	--
	Gill	9	8	0.889	***0.025***	8 of 8 had vertebral damage
	Viscera	67	41	0.612	*0.061*	35 of 41 had vertebral damage
	Heart	18	8	0.444	*0.405*	--
	Liver	20	11	0.550	*0.425*	--

Table 5 continued…

Spleen	12	5	0.417	*0.385*	--
Intestine	1	1	1.000	--	Sample size too small to test
Swim bladder	224	184	0.821	***<0.001***	182 of 184 had vertebral damage
Gonads	53	38	0.717	***0.002***	36 of 38 had vertebral damage
Kidney	62	42	0.677	***0.007***	36 of 42 had vertebral damage
Muscle	74	41	0.554	*0.242*	--
Ribs	30	28	0.933	***<0.001***	28 of 28 had vertebral damage
Internal decapitation	36	15	0.583	*0.223*	--
Vertebrae	276	213	0.772	***<0.001***	--

Table 6. Results of a logistic regression of combined mortality and strike impact conditions and observed mortality and injury categories for bluegill and American eel. Coefficient estimates (Coeff; log odds), standard error (SE), odds ratio (OR) with 95% confidence interval (CI), p-value (p) assuming $\alpha = 0.05$, and Akaike Information Selection Criteria (AIC) are provided using stepwise model selection. Significant variables are in bold.

Model	Variable	Coeff	SE	OR	OR (95% CI)		p	AIC
					Lower	Upper		
Strike impact								
American eel	(Intercept)	3.01	0.775	--	--	--	**<0.001**	85.81
	Orientation [L]	-4.35	0.806	0.013	0.002	0.051	**<0.001**	
	Orientation [V]	-6.09	1.281	0.002	0.000	0.019	**<0.001**	
	Blade [26 mm]	-1.91	0.840	0.15	0.021	0.64	**0.023**	
Bluegill	(Intercept)	-13.89	2.114	--	--	--	**<0.001**	270.62
	Location [M]	4.37	0.578	79.3	27.3	266.7	**<0.001**	
	Orientation [L]	3.84	0.645	46.7	13.9	177.7	**<0.001**	
	Orientation [V]	-1.46	0.575	0.23	0.07	0.70	**0.011**	
	Velocity	1.16	0.189	3.2	2.2	4.7	**<0.001**	
Injury category								
Bluegill	(Intercept)	-3.57	0.446	--	--	--	**<0.001**	275.92
	Integument	1.33	0.392	3.80	1.81	8.50	**<0.001**	
	Operculum	1.72	1.138	5.57	0.75	65.5	0.131	
	Viscera	1.13	0.542	3.10	1.11	9.44	**0.037**	
	Liver	1.54	0.751	4.66	1.10	20.8	**0.040**	
	Swim bladder	0.88	0.503	2.43	0.88	6.49	0.078	
	Int. decapitation	2.93	0.603	18.7	5.94	64.3	**<0.001**	
	Vertebral fracture	3.68	0.601	39.5	12.7	140.6	**<0.001**	

Note: The logistic regression of American eel injury category against observed mortality was not significant and was omitted (see text for detail).

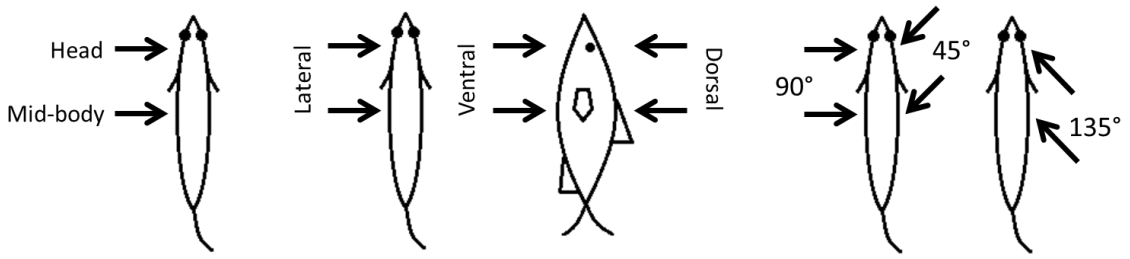

Figure 12. Diagram depicting major blade strike conditions related to the fish body and impact of the blade. Major variables included location (head or mid-body), orientation of fish (lateral, ventral, or dorsal), and impact angle (45, 90, or 135°). See Table 1 for more detailed information on exposure conditions of each treatment group.

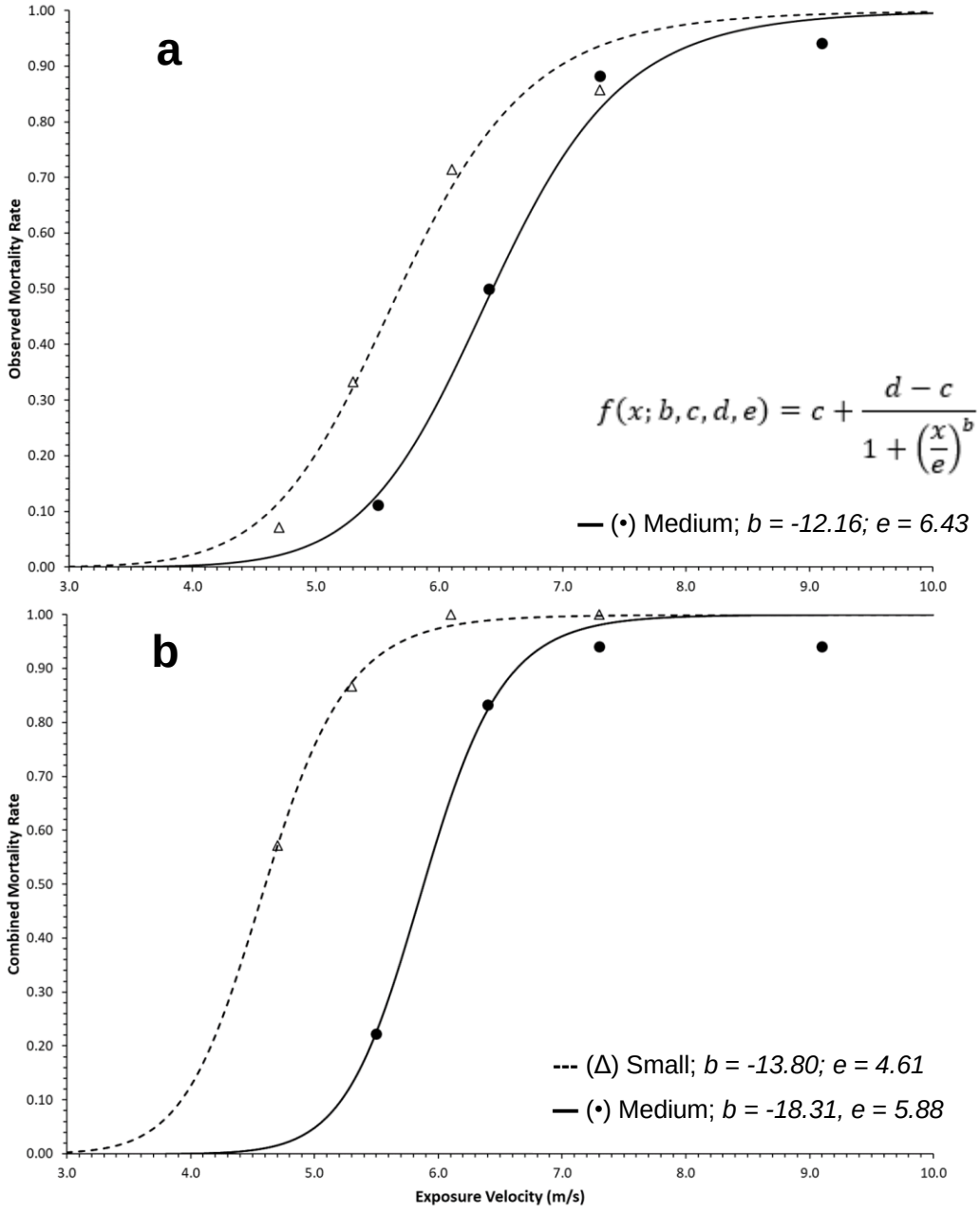

Figure 13. Dose-response relationships between blade strike velocity (m/s) and observed (a) and combined (b) mortality in small (dashed line) or medium sized (solid line) bluegill. Lines represent a four-parameter log-logistic regression (*c* and *d* fixed at 0.0 and 1.0, respectively) while points are group mortality rates according to blade strike velocity.

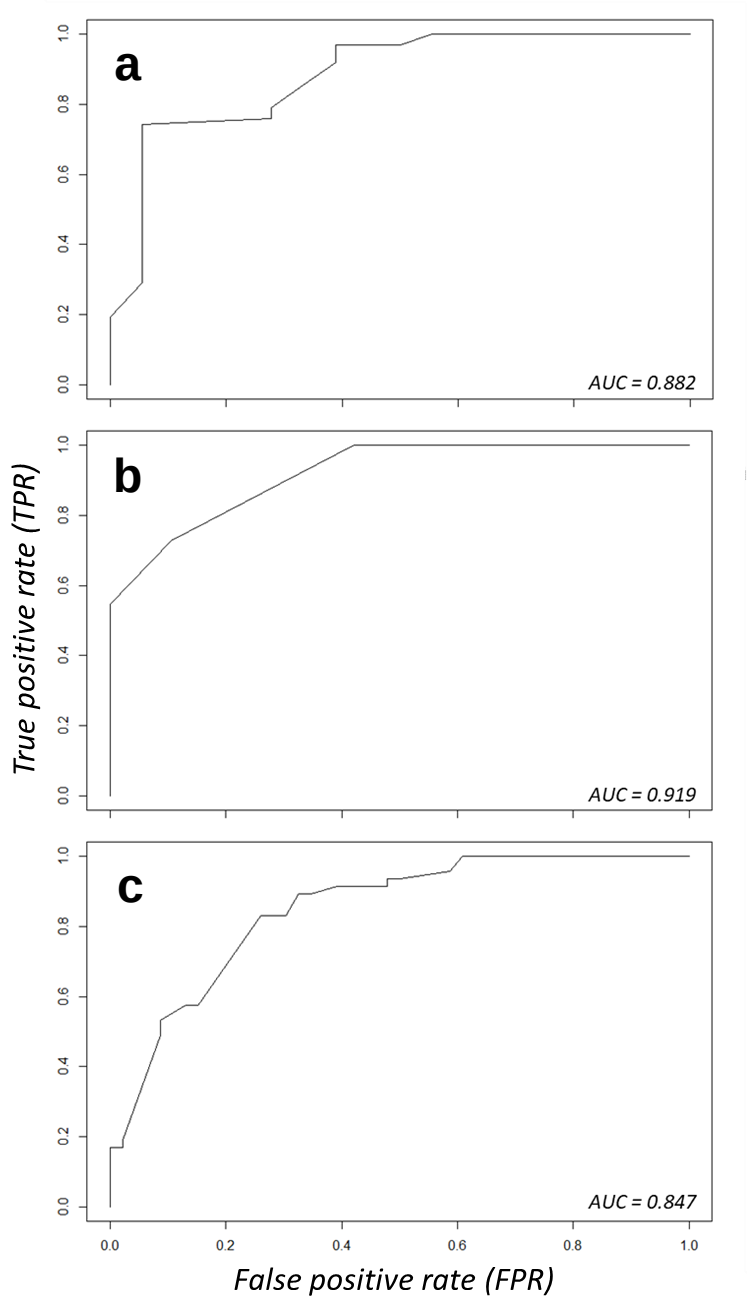

Figure 14. Receiver operating plots (ROC) of logistic regression models fitted to combined mortality and blade strike conditions for (**a**) bluegill and (**b**) American eel or (**c**) observed mortality and injury category among bluegill. Presented with area under the curve (AUC) values. Values of AUC closer to 1.0 are considered to have good predictive ability compared to values closer to 0.5.

CHAPTER III

WITHIN AND AMONG FISH SPECIES DIFFERENCES IN SIMULATED TURBINE BLADE STRIKE MORTALITY: LIMITS ON THE USE OF SURROGACY FOR UNTESTED SPECIES

A version of this chapter was originally published by Ryan Kurt Saylor, et al:

Ryan Saylor[*1,2], Dustin Sterling[2], Mark Bevelhimer[2], Brenda Pracheil[2]. "Within and among fish species differences in simulated turbine blade strike mortality: Limits on the use of surrogacy for untested species." *Water* 12(3), 2020, 1-27.

Affiliations:

[1] Bredesen Center for Interdisciplinary Research and Graduate Education, University of Tennessee, Knoxville, Tennessee 37996

[2] Environmental Science Division, Oak Ridge National Laboratory, Oak Ridge, Tennessee 37830

*Corresponding Author: Ryan Saylor

1 Bethel Valley Road

Oak Ridge National Laboratory

Oak Ridge, Tennessee 37830

Phone: 865-974-7709

E-mail: saylorr@ornl.gov

Author Contributions:

Conceived or designed experiments – RKS, with input from MB

Blade strike experimentation – RKS, with assistance from DS and MB

Fish necropsies – RKS, with assistance from DS

Analysis of data – RKS, with input from MB

Composition of paper – RKS, with input from DS, MB, and BP

Revisions and draft reviews – RKS, with input from MB and BP

Project management – MB and PB

Abstract

Use of surrogacy remains a useful method for prioritizing research on representatives of at-risk groups of fishes, yet quantifiable evidence in support of its use is generally not available. Blade strike impact represents one of the most traumatic stressors experienced by fish during non-volitional movements through hydropower turbines. Here, we use data generated from laboratory trials on blade strike impact experiments to directly test use of surrogacy for salmonid and clupeid fishes. Results of logistic regression indicated that a taxonomy (genus) variable was not a significant predictor of mortality among large rainbow trout and brook trout. Similar results were found for young of the year shad species, but genus-level taxonomy was a significant predictor of mortality while species was not. Multivariate analysis of morphometric data showed that shad clustered together based on similarities in fish shape which was also closely associated with genus. Logistic regression including size as a major covariate suggested total fish length was not a significant predictor of mortality, yet dose-response data suggest differential susceptibility to lower strike velocities. We suggest that use of surrogacy among species is justifiable but should be avoided within a species since the effects of size remain unclear.

Introduction

Downstream passage of fish through hydropower facilities represents a direct threat to migratory fishes worldwide. The threat is magnified globally because most of the largest rivers in the world are impounded which impedes natural movement of riverine fishes [1]. Fish passing through hydropower turbines are exposed to a suite of injurious or lethal stressors including, rapid decompression, cavitation, shear forces, and impact with structures such as turbine blades [2–5]. Field trials are often used to estimate morbidity and mortality rates of turbine-passed fish related to turbine characteristics or dam operation parameters; however, these trials are incapable of linking a specific stressor to risk of injury or death because exact exposure conditions are unknown. Physical impact of the turbine blade with fish (e.g., blade strike) is one of the most

injurious stressors fish must endure [6]. The risk and severity of injury is also dependent on turbine type, design, and operations which makes it difficult to apply inferences from one facility to another. Two of the most common turbine types are Francis and propeller type turbines (e.g., Kaplan) [7], with higher rates of mortality observed in Francis compared to propeller turbines [8,9]. Blade leading edge thickness and strike velocity are two important turbine blade characteristics; maximum runner velocity data are generally available but blade thickness descriptions are more difficult to obtain as they are often considered proprietary by turbine manufacturers [10,11]. In general, thicker blades are less injurious than thinner blades and faster velocities are more damaging than slower velocities [10–14]. Understanding how turbine type or associated characteristics impact survival of fishes is important, but rates of mortality are also affected by how the fish interacts with the turbine.

Other aspects of blade strike impact linked with interactions with the fish include the strike location (e.g., the head, mid-body, or tail), fish orientation (dorsal, lateral, or ventral surface), and angle of blade strike impact. Previous laboratory work suggests that mid-body, lateral strikes perpendicular to the body have the highest mortality rates and represent the worst-case scenario for blade strike [11,13,15]. Strikes of this nature are likely more fatal because the impact and forces acting on biological tissue occurs closer to the fish's center of gravity where major organs are found. Glancing strikes at shallow angles or impacts to the tail are much less traumatic and mortality rates are low even with thinner blades moving at higher velocities [10–12]. Regardless, estimates of overall mortality must also include how the fish interacts with the turbine blade as it passes through the turbine.

Traits of the fish itself (e.g., size and species) also impact overall susceptibility to turbine blade impact during non-volitional movements through turbines. Fish size has been linked with differential rates of mortality so that larger fish often experience higher rates of mortality given other factors such as blade leading edge thickness and velocity remain constant [10,12]. Size-based trends likely vary by species because other work found that rates of mortality in different species were high overall, regardless of size, because smaller individuals were as susceptible to blade strike as larger individuals [13].

Inherent differences in body shape, morphology, and the musculoskeletal system observed among riverine fishes may impact overall susceptibility to blade strike.

Estimating mortality as a function of turbine blade and fish characteristics is important as turbine manufacturers and dam operators strive to increase survival of turbine-passed fish. To better inform design of turbines, biological data must be gathered for as many blade strike conditions as possible and reported in mathematical terms. Biological response data is often conveyed in terms of dose-response relationships, i.e., predicted rate of mortality (the response) against blade leading edge thickness or strike velocity (the dose) [11,13]. Dose-response relationships can be applied to stressor exposure distributions for a particular turbine type or turbine operation. Stressor exposure distributions express the likelihood that a fish will encounter various magnitudes of a stressor while passing through the turbine and can be estimated from computational fluid dynamics (CFD) models of theoretical particles passing through hydropower turbines [16,17]. Comparing dose-response relationships to exposure distributions can better inform design of safer hydropower turbines. In practice, opportunities to improve passage survival may occur during mandatory relicensing of hydropower projects that occurs every 30 to 50 years through the Federal Energy Regulatory Committee (FERC). Relicensing often requires environmental assessments that include investigating solutions meant to mitigate impacts of fish passage for species at highest risk of entrainment. Dose-response data for stressors like blade strike (and others) are incredibly useful to meet that end but are limited by data availability for most species of concern.

The remarkable diversity of fish species makes it impossible to study all species, so methods have been developed to group and study fishes with shared functional traits. In this way, one can study an entire community of riverine fishes without the need to capture, hold, and experiment on every species found in that system. Taxonomic groupings form the basis of this understanding by placing species into hierarchical groups (i.e., genera, family, etc.) based on shared genetic and morphological traits [18]. Furthermore, shared traits among group members allow researchers to investigate fewer, representative or surrogate species instead of every member of the group. Species surrogacy, use of one species in place of another because the targeted species is rare,

difficult to collect, or protected by law, has been used in many fields including research on hydropower impacts [19]. For example, species prioritization via surrogacy and traits-based methods has been applied to assess which riverine fishes are at the greatest risk of entrainment [19,20]. This prioritization has also led to targeted, full-scale laboratory experimentation on representative species most likely to experience adverse effects during turbine passage. In fact, mortality data available on blade strike currently is the result of research on surrogate species that best represent at-risk taxonomic groups of fishes [11,13]. Another potential application of surrogacy is assessing whether data from one size group can realistically represent another within the same species. The beneficial aspects of surrogacy are obvious, but there is a paucity of data available to suggest using surrogacy for hydropower related studies is reliable.

Fishes in the salmonid and clupeid families are great test species for surrogacy because both groups contain predominantly anadromous species impacted by hydropower dams [21,22]. Representatives of both families are easy to collect, can be maintained in captivity, and are of conservation concern globally. Salmon, trout, and chars within Salmonidae are well known for their anadromous migrations and juvenile fish within this family are at high risk of turbine passage when smolts migrate downstream to the ocean [22]. Members of Clupeidae, including shad and herring, are also anadromous and many species are threatened throughout much of their native range globally [23]. Both families also contain multiple species and genera which present additional opportunities for testing application of surrogacy at different taxonomic levels.

The objectives of this study are to 1) determine if taxonomic variables (species, genus, or neither) for salmonid and clupeid fishes are important predictors of mortality, 2) analyze and compare morphometric data for juvenile shad species to test what taxonomic level best captures similarities in fish shape, 3) test if and how total length impacts predicted mortality within a species, and 4) use these analyses to directly test application of surrogacy via blade strike dose-response data. More specifically, we will use non-linear regression analyses to directly test surrogacy by including species or genus terms in one model compared to another which excludes taxonomic terms. Evidence in support of surrogacy may include selection of a parsimonious model that excludes a

species or genus term, thereby suggesting species dose-response data may adequately predict mortality of salmonid or clupeid fishes in general when exposed to simulated blade strike impact. Clupeid morphometric data will be used to estimate fish shape based on relative location of morphological landmarks (e.g., snout, head, fins, etc.). Fish shape is the best approximation of species available because detailed musculoskeletal and biomechanical data related to blade strike impact are unavailable. Further support of surrogacy would be achieved if shad morphology data are grouped together based on similarities in body shape at higher taxonomic levels (e.g., genus and above). To that end, shad species grouped together based on shared morphology may also be presumed to have similar dose-response relationships related to blade strike impact. Lastly, non-linear regression analysis will also be used to test if total length (e.g., fish size) is a significant predictor of mortality and therefore assess if dose-response data should always be separated by fish size within each species. Combined, these methods offer a quantifiable way to test if surrogacy can be used reliably for salmonid and clupeid blade strike dose-response data.

Materials and Methods

Fish Collection and Care

Most fishes used in blade strike impact trials were acquired locally and transported back to the Aquatic Ecology Laboratory (Oak Ridge National Laboratory, Oak Ridge, Tennessee, USA) to be used in experiments between June to November 2019. One hundred sixty large (mean total length [TL] = 25.8 ± 2.37 cm and mass = 152.0 ± 48.12 g) rainbow trout, *Oncorhynchus mykiss*, and 155 large (mean TL = 24.2 ± 2.39 cm and mass = 131.1 ± 39.14 g) brook trout, *Salvelinus fontinalis*, were obtained from United States Fisheries and Wildlife Service (USFWS) Dale Hollow National Fish Hatchery. An additional 67 large rainbow (n = 227 total) were obtained from a Tennessee Wildlife Resource Agency (TWRA) state hatchery (Tellico Trout Hatchery, Tellico Plains, Tennessee, USA). We also acquired 161 small (mean TL = 11.4 ± 1.02 cm and 13.6 ± 4.38 g) rainbow trout from another TWRA hatchery (Buffalo Springs Trout

Hatchery, Rutledge, Tennessee, USA). Lastly, 92 gizzard shad, *Dorosoma cepedanium*, with mean TL of 16.0 ± 0.65 cm and mass of 31.5 ± 3.80 g were purchased from a local bait shop (Big Fish Outfitters, Lenoir City, Tennessee, USA). All fish were distributed equally into separate 680 L, dual-hull fiberglass, circular tanks that received constant water supply and aeration. Fish were fed daily except 24 hours prior to experimentation to prevent fouling of the housing tank and blade strike apparatus.

Shad used in blade strike trials were obtained with the help of South Carolina Department of Natural Resource (SCDNR) fisheries biologists. More specifically, young-of-the-year (YOY) American shad, *Alosa sapidissima*, were targeted by boat electrofishing during nighttime field collections from Lake Moultrie and Lake Marion, South Carolina, USA on October 7 to 10, 2019. Fish were transported back to the SCDNR hatchery (Dennis Wildlife Center Fish Hatchery, Bonneau, South Carolina, USA) where they were housed until experimentation. While American shad were the target species, sympatric blueback herring, *Alosa aestivalis*, were inadvertently included in the American shad samples. YOY of both species have remarkably similar morphology at this life stage and are difficult to distinguish without additional handling. We initially waited to identify species until after experimentation to avoid handling stress but eventually were able to identify species through quick visual inspection immediately prior to immersion in anesthesia. A total of 43 American shad (mean TL = 8.5 cm and mass = 5.35 g) and 116 blueback herring (mean TL = 7.2 cm and mass = 3.70 g) were collected and used in the blade strike impact study. Transport and housing of both shad species required holding fish in 4 – 8 ‰ sodium chloride solution to minimize stress and increase survival. Back at the SCDNR hatchery where strike trials were conducted, groups of fish (50 – 100 individuals) were housed in 680 – 1420 L fiberglass tanks which received constant water supply and aeration. Fish were held ~12 hours prior to experimentation to confirm fish were healthy following capture and transportation stress.

Additional shad were collected from local reservoirs in Tennessee or South Carolina described previously for use in morphological analysis in October and November 2019. YOY fish (≤ 10.0 cm TL)—i.e., American shad, gizzard shad, and threadfin shad (*Dorosoma pretenense*) along with blueback herring, were targeted to limit

the effects of size in our analysis. Eight blueback herring and 11 American shad were collected by boat electrofisher during the collection of fish used in blade strike trials. Eight threadfin shad and 13 gizzard shad were collected via boat electrofisher from Melton Hill Lake near Oak Ridge, Tennessee, USA. Upon arrival at the hatchery facility or laboratory, fish were euthanized via overdose of 250 ppm clove oil by dissolving pure clove oil extract (NOW® 100% Pure Clove Oil, Item #051193, www.gnc.com) in 95% ethanol (1:10) followed by dilution to desired concentration using dechlorinated water. After euthanasia, fish were refrigerated at 4°C until individual fish were processed.

Blade Strike Experimentation and Analyses

Simulated blade strike trials were performed using a spring-powered blade strike apparatus that propelled a turbine blade through water to impact fish (Figure 15). Blades had a semicircular leading edge with leading edge widths of 26-, 52-, or 76-mm. Strike impact velocities ranged from 4.7 to 9.7 m/s which approximate typical turbine passage conditions according to Bevelhimer et al. [11]. Other major strike variables included location (mid-body [M] or head [H]), orientation (lateral [L], dorsal [D], or ventral [V]), and angle (45, 90, or 135°) of blade strike impact [13]. A high-speed camera (Model IL4, Fastec Imaging, San Diego, California, USA) and stroboscope (Nova-Pro 300, Monarch Instrument, Amherst, New Hampshire, USA) were synchronized, and recorded each blade strike impact at 1000 fps perpendicular to the blade path to confirm strike impact conditions. Impact velocity was estimated (± 0.1 m/s) by reviewing four high speed videos, i.e., one before and after each exposure group and two actual treatment fish within the exposure group, using Kinovea software (v0.8.15, www.kinovea.org). Each treatment group was a combination of one variable from each exposure category (e.g., blade width, impact velocity, location, etc.) and contained 15 – 20 treatment fish and 3 control fish. Control fish were pooled together by species or size group within species for analysis.

The blade strike protocol used in this study followed that described in Saylor et al. [13] though modifications were necessary to accommodate our test species. Fish were anesthetized in 14 L of clove oil solution until reaching deep anesthesia characterized by

loss of equilibrium, infrequent gill ventilation, and lack of movement [24]. Concentrations of clove oil were 25 – 30 ppm for rainbow trout, American shad, and blueback herring or 40 ppm for brook trout and gizzard shad [25,26]. Anesthetized fish were randomly assigned as treatment or control and placed into the blade strike apparatus. At this point, fish were placed on brackets containing rubber tubing to gently hold fish in place but allowed free movement following impact with the blade. Exact treatment groups and exposure conditions varied among species (Table 7). Controls were treated in the exact same way as treatment fish but did not receive simulated blade strike. Following blade strike, both trout species and gizzard shad were individually tagged in the mandible using labeled tag fasteners (PAG, 52 mm Fine Tagging Barb Fasteners, www.amazon.com). Because of their small size, American shad and blueback herring were not tagged to avoid additional handling stress, but were instead placed into individually labeled, plastic containers, containing 4 L of 4 – 8 ‰ sodium chloride solution and constant aeration. Individuals of all species were monitored every 15 minutes for 1-hour and were removed early if fish exhibited signs of severe distress, i.e., consistent inability to maintain upright position, labored and erratic swimming, excessive hemorrhaging, or obvious signs of spinal fracture. Individuals were categorized as (1) survivor with no signs of distress, (2) moribund and removed early, (3) moribund at 1-hour mark, or (4) direct death marked by cessation of gill ventilation. All fish were placed in 250 ppm euthanasia solution of clove oil and water until gill ventilations were not observed for at least 10 minutes, removed from the euthanasia bath, and placed on ice. Following euthanasia, external examinations and necropsies were performed and observed injuries were recorded following Saylor et al. [13]. Survivors observed with severe injuries, including internal decapitation or vertebral fractures were considered ecologically dead, i.e., incapable of avoiding predation or acquiring food. Here, mortality was considered any category 2, 3, or 4 fish and any survivor observed with severe injuries. Necropsies were performed by the assessor without knowledge of treatment category.

Mortality rates were calculated for each treatment group and used to generate dose-response relationships according to species or size-group. Dose-responses predicted

mortality as a function of impact velocity according to the following log-logistic equation [27]:

$$f(x; b, c, d, e) = c + \frac{d-c}{1+\left(\frac{x}{e}\right)^b}, \quad (1)$$

where *f(x; b, c, d, e)* is the predicted rate of mortality, *b* is the inclination point or slope of the curve, *c* is the lower bound fixed at 0.0, *d* is upper bound fixed at 1.0, and *e* is the effective dose (of velocity in m/s) at which 50% of the population would be predicted to experience mortality (i.e., E_{50} value). Dose-response curves were generated for fish that were struck with the same blade on the mid-body, lateral surface at 90°, and had at least four impact velocity treatments. Dose-response analyses were performed using the "*drc*" package [27] in *R v3.6.2* [28]. All statistical decisions were based on $\alpha = 0.05$. Curves were produced for large rainbow trout and brook trout, small rainbow trout, gizzard shad, and *Alosa* spp.; American shad and blueback hearing were combined (*Alosa* spp.) because samples sizes in each treatment group were low compared to other species.

We used logistic regression and model selection criteria to test species surrogacy using generalized linear models (glm) with a logit link function in *R v3.6.2* [28]. Logistic regression analyses were performed on mortality as the binary predictor variable against continuous variables (e.g., blade impact velocity [m/s] or fish size [cm]) and categorical variables including species or genus, blade width (26 or 52 mm), location (M or H), orientation (L or D), and angle (90 or 135°). Variables were considered significant predictors of mortality when $p < 0.05$. We used a train to test ratio of 80:20 to assess model performance using package "*ROCR*" to create receiver operating plots (ROC) and area under the curve (AUC) estimates to test the ability of our models to predict mortality. Akaike Information Criterion (AIC), Second order Akaike Information Criteria (AICc), and Informational and Complexity (ICOMP) criterion were calculated using package *"MuMin*" [29] to compare logistic models. We performed three analyses to help determine if species or fish size were necessary parameters of the most parsimonious models that predicted mortality. The first analysis compared two models associated with large rainbow trout and brook trout data struck with the 52-mm blade, where both models included velocity, location, orientation, angle of impact, and total length variables (n =

276). The two models differed in that one included a species (e.g., RBT and BKT) term in the predictive model of mortality while the other did not. The second analysis included small and large rainbow trout data only for fish struck on the mid-body, lateral surface at 90° (n = 197). Both models included blade width and velocity terms, but only one included total length in the final predictive model. The third analysis included blade strike data for gizzard shad, American shad, and blueback herring that were struck with the 52 mm blade on the mid-body, lateral surface at 90° (n = 158). Major variables in both models included strike velocity and total length, but one model included species (GZS, AMS, or BBH) while the other included a genus (*Dorosoma* or *Alosa*) term to test which taxonomic level would best predict mortality. If two competing models had similar criteria values (i.e., within 2 units), we selected the model containing the fewest parameters because it required the least complexity to account for comparable levels of variation [30]. These analyses provide an opportunity to directly test if species or size terms are necessary predictors of mortality and help objectively determine if dose-response data from one species or size group can be used as a surrogate for another.

Fish Morphology Measurements and Analyses

The sub-sample of shad (n = 40 across all species) were used to estimate fish shape via morphometric analysis of body landmarks. Initial measurements included total and standard length (± 0.1 cm) as well as mass (± 0.01 g). Three sets of measurements were taken including 1) lengths relative to snout tip, 2) body depths, and 3) body widths at each landmark. Major landmarks were identified to approximate body shape of each species including the anterior edge of the eye (e.g. snout) and posterior margin of operculum (e.g., head), as well as the leading edge of the dorsal, pectoral, pelvic, anal, and caudal fins (Figure 16). We used a fish measuring board (± 0.1 cm; Fish Measuring Board, Mini, Model #118-E40, Wildco, Yulee, Florida, USA) to estimate lengths and digital calipers (± 0.01 mm; iGaging Origin Cal Digital Calipers, Model #100-032-901WB, Brownells Inc., Grinnell, Iowa, USA) for body depth and width measurements. Condition factor (K) was calculated according to Cone [31] using the following equation:

$$K = \frac{100M}{TL^3} \qquad (2)$$

where *M* is mass in grams and *TL* is total length in centimeters. Individuals with a condition factor > 3 standard deviations above or below the species average were considered outliers and excluded from analysis – only one gizzard shad met these criteria and was removed from further analysis. Raw measurement data were not used so each landmark measurement was converted to a proportion of maximum body length, depth, or width.

Morphometric data were analyzed using multivariate analyses to assess similarities in body shape according to taxonomic level among clupeid fishes. A total of 39 fish (4 species) and 22 variables were used including a species term and 21 morphometric variables – seven landmark proportions each for body length, depth, and width. We used principal component analysis (PCA) to determine which of the 21 morphometric variables accounted for the most variation in our data set. A scree plot was created to visualize percentage of variation explained with each successive principal component to help prioritize which PCs would be used in the cluster analysis. Results of PCA were then used to perform a Hierarchical Clustering on Principal Components (HCPC) analysis to test how shad may cluster or group according to similarities (or dissimilarities) in body shape. Hierarchical clustering was performed using Ward's linkage method to measure dissimilarity between clusters because it produced the highest agglomerative coefficient. Gap statistics and silhouette method were used to determine optimal number of clusters while a factor map was created to visualize clusters. Both PCA and HCPC analyses were performed using packages "*FactoMineR*" and "*factoextra*" in *R v3.6.2* [28].

Results

Blade Strike Impact

Mortality varied by species, but our data suggests large brook and rainbow trout were most susceptible, followed by all clupeids, and small rainbow trout representing the most resistant group in this study. Brook trout mortality occurred at the lowest velocity of 4.9 m/s, while small rainbow trout were observed with a few survivors at velocities up to

8.7 m/s when struck on mid-body, lateral surface at 90°. Blades with thicker leading edges had lower estimated mortality in both small and large rainbow trout (26 > 52 mm) and *Alosa* (26 > 52 > 76 mm). Mortality associated with the thickest blade (e.g., 76 mm) remained below 25% at velocities up to 9.4 m/s in *Alosa*, while mortality with the thinnest blade (e.g., 26 mm) was nearly always fatal at velocities near 6.6 m/s in small and large rainbow trout. Mid-body strikes on the dorsal surface at 90° had higher mortality than strikes to the lateral surface, while lateral strikes at 135° had lower mortality compared to those at 90° in both large rainbow trout and brook trout. Smaller rainbow trout had a lower mortality rate of 15.8% at 6.7 m/s compared with 55% in larger individuals exposed to the same velocity. None of the control fishes of any species died during anesthesia, handling, or observation so that the mortality rate of control fish was 0.0 (Table 7).

We successfully tested 752 individuals and 34 blade strike impact treatments across all species included in this study. Trends in the number of survivors that contained major injuries varied by species and size with very few injured survivors in large trout (< 7% of all survivors) compared to nearly 70% observed in gizzard shad. We also observed 20 to 25% of all survivors among the smallest fish tested (*Alosa* and rainbow trout) with major injuries. Major injuries were most often observed as vertebral fractures (up to 5 separate fractures) near the point of impact regardless of species, size, or treatment group. In contrast, internal decapitation was most often associated with lateral strikes to the head at 90° or in combination with vertebral fractures when struck on the mid-body, lateral surface of trout but was mostly absent in shad. Among trout (both species and sizes), injuries to muscle and kidney tissue near the vertebral fractures were also observed along with multiple rib fractures. Noticeable hemorrhaging and formation of clots in the buccal and opercular chambers in trout were observed in the same fish with vertebrate factures, especially those closer the head. Noticeable damage to the eyes was observed in *Alosa* in the form of exophthalmia (n = 8) and in extreme cases complete amputation of one eye (n = 6) at the highest velocity (e.g., 9.7 m/s). All fish that experienced eye amputation were considered dead within the first 15 minutes of observation and were also observed with complete vertebral fractures during necropsy.

Dose-response Curves

Log-logistic regression of mortality against blade strike velocity produced dose-response curves for each species that covered a 2.0 m/s velocity range (Figure 17). The blade strike velocity range for gizzard shad was greater (e.g., 3.4 m/s) than other species but no mortalities were observed at the lowest velocity group of 4.7 m/s suggesting its range was also closer to 2.0 m/s. Overall shape of the curves (and inherent relationship therein) were similar for both species of large trout but small rainbow trout had much different curve structure (Figure 17A), while gizzard shad and *Alosa* spp. data produced curves of similar shape (Figure 17B). Gizzard shad and brook trout curves produced the lowest ED_{50} values of 5.7 and 6.0 m/s, respectively. The highest ED_{50} values were predicted for the small rainbow trout (7.1 m/s) and *Alosa* (7.9 m/s) regressions, while large rainbow trout fell in the middle with a value of 6.6 m/s. Values for the point of inclination or steepness of the curve (*b*), were the lowest in large rainbow trout and brook trout and steepness increased with average total length of fish regardless of species. The highest steepness values were observed with small rainbow trout (-29.33) and *Alosa* (-37.31) suggesting smaller changes in velocity are associated with comparatively higher probabilities of mortality than other species. All parameter estimates were considered significant for all species included in our dose-responses analyses (Table 8).

Logistic Regression Analyses

The logistic regression of large rainbow trout and brook trout suggested blade strike characteristics were significant predictors of mortality, and the species term was not included in the accepted model. Both models tested had AIC, AIC*c*, and ICOMP values that were less than one unit apart (Table 9) so the Trouts.m2 model that did not have a species term was accepted because it required less complexity to explain comparable levels of variance in our data. Interestingly, the model that contained the species term also indicated that species (rainbow trout or brook trout) was not a significant predictor of mortality (Table 9). Significant predictors of mortality in the accepted model included velocity, orientation, angle of impact, and total length while location was not significant. Variables with the greatest significant effect on mortality

were velocity and impact angle. For every 1.0 m/s increase in strike velocity, fish were ~6X more likely to die (at average total length, constant orientation and impact angle). While total length was a significant predictor of mortality for large rainbow trout and brook trout, the odds of survival was predicted to increase by 20% for every 1.0 cm increase in fish length at average velocity and constant location, orientation, and impact angle (Table 9). Our data suggests that species is not an important predictor of mortality for both rainbow and brook trout compared to velocity when exposed to similar blade strike conditions. The ROC curve and AUC value for *Trouts.m2* suggest this model has high specificity and properly classified mortality as a function of blade strike characteristics without including species (Figure 18A).

Analysis of rainbow trout data that included both small and large individuals found that blade velocity and leading-edge width significantly influenced mortality among trout, but the effect of total length was not as clear. One small rainbow trout was removed from the data set as an outlier because its standardized residual was greater than 3.00, i.e., making the final sample size equal to 197. Both models produced selection criteria values that were within 2.0 units of one another; however, AIC and AICc criteria suggested the model with total length was best (RBT.m1) while ICOMP values were lowest when excluding the total length term (RBT.m2; Table 9). The total length term in RBT.m1 was not considered significant, but the p-value (0.061) was just above the 95% confidence level used here. The odds of mortality would be slightly higher (~7%) for every 1.0 cm increase in total length of rainbow trout when blade width was held constant and at average velocity. The combination of non-significance, small change in odds of mortality, and lower ICOMP value suggests that the *RBT.m2* model excluding total length would be best. This model had an AUC value of 0.959 suggesting it adequately classified mortalities and the ROC indicates high specificity of the RBT.m2 model that did not include total length (Figure 18B).

The shad logistic regression suggested mortality was significantly influenced by velocity and the model with a genus (*Dorosoma* vs. *Alosa*) term accounted for variation slightly better than species (GZS vs. AMS vs. BBH). Importantly, fish total length was not considered significant for either model and was not included in the most

parsimonious model of our shad blade strike data. Like the analyses above, all selection criteria values were within 2.0 units of one another, but the *Shads.m8* model had slightly lower criteria values (Table 9). The genus term was considered a significant predictor of mortality ($p < 0.001$) and the model suggested the *Dorosoma* species were ~6000X more likely to experience mortality compared to *Alosa* species when struck on the mid-body, lateral surface at 90° and average velocity. While we chose the model containing the genus term, the alternative model that had a species term (Shads.m6) also predicted that gizzard shad was more susceptible than the other shad species. Interestingly, even though species was considered a significant predictor of mortality ($p < 0.001$), this was only true for gizzard shad compared to blueback herring. Blueback herring was significantly indistinguishable from American shad ($p = 0.622$), i.e., predicted mortality is the same for both species. The combination of lower selection criteria and observation of non-significance between American shad and blueback herring suggests that the model containing a genus-level taxonomic term will adequately predict mortality among shad. Furthermore, the ROC plot and an AUC value of 0.908 suggests that our accepted model (Shads.m8) has high specificity and properly classified mortality as a function of velocity and genus (Figure 18C).

Morphometric Multivariate Analyses

Initial analyses of morphometric data suggested that discrepancies in size affected our analysis of body proportions, but also predicts two clusters which align with genus level taxonomy instead of species. All gizzard shad used in this analysis were ~4.0 cm longer on average than the other species and at least one larger threadfin shad (12.2 cm) was used as well. The effect of size was evident in a biplot of these data where all gizzard shad are grouped separate and the largest threadfin (TFS17) was included within an ellipse that overlaps with American shad and blueback herring ellipses (Figure 19A). Similarly, the HCPC analysis suggested three clusters best represented these morphometric data – gizzard shad and threadfin shad each clustered separately, and the single large threadfin shad was included in the third cluster containing American shad and blueback herring (Figure 19B). To that end, we removed all gizzard shad and the

largest threadfin shad from further analysis because the effect of size may confound interpretations of our morphometric data since smaller gizzard shad were not available for our analysis. The result of excluding gizzard and threadfin data left proportional morphometric data for 26 fish across all species (TL < 10.0 cm) to be used in another set of PCA and HCPC analyses. The results of PCA suggest that 50% of the variation in these morphometric data was described by the first three dimensions while over 75% was explained by including up to six dimensions (Figure 20). Twelve of the 21 morphometric variables explained more variation than would be expected if all variables contributed equally, and no single variable appeared to be more important than the others. The HCPC analysis using six principal components produced two clusters, one representing the combination of American shad and blueback herring (i.e., *Alosa*) and the second representing threadfin shad (Figure 21). Both the average silhouette method (Figure 22A) and gap statistic (Figure 22B) indicate that two clusters are optimal for our shad data. Combined, these multivariate analyses suggest that use of *Alosa* is permissible for blade strike studies since YOY of both American shad and blueback herring have similar overall body shape at this life stage.

Discussion

Results of our analyses suggest use of surrogacy for blade strike data is acceptable, i.e., dose-response data for one species should sufficiently represent another, though the exact taxonomic application varies by family. Within Salmonidae, we tested large fish from two of the three most common genera in North America (i.e., *Oncorhynchus* and *Salvelinus*) and logistic regression indicated that inclusion of genus was not necessary to predict mortality. In terms of surrogacy using dose-response data, this suggests that combining response data for both species into a singular curve should adequately represent this family. The dose-response curves for each species are also quite similar and the confidence bands for both curves overlap across the entire velocity range (Figure 23A). Within Clupeidae, surrogacy seems equally applicable, but taxonomic level did significantly influence predicted mortality. The accepted logistic model for our shad data indicated species-level taxonomy within a genus was not important, but genus-level

taxonomy within a family was a significant predictor of mortality (Table 9). This is especially evident in the logistic regression that suggested gizzard shad were three orders of magnitude more likely to experience death when compared to *Alosa* spp. (Table 9). Similarly, morphometric data showed shad within *Alosa* had a proportionally similar shape that was distinctly separate from *Dorosoma* (Figure 21). While the shad dose-response curves have similar shapes, the ED_{50} value for gizzard shad occurred at velocities 2.2 m/s slower than *Alosa* spp. which also suggests gizzard shad is more susceptible to blade strike (Figure 20B). The discrepancy in mortality susceptibility could be related to size differences since gizzard shad were ~4.0 cm longer on average than other shad species. In this way, we suggest the dose-response curve for *Alosa* spp. data remains useful as is, but the dose-response curve for gizzard shad must be kept to represent *Dorosoma*.

Based on available data, use of surrogacy for larger salmonids or YOY *Alosa* spp. is justifiable with two caveats. First, while rainbow trout and brook trout should represent the salmonid family well, it is unclear if inclusion of data from other diverse genera (i.e., *Salmo*) would show similar responses to blade strike. This study also did not include comparison between species within the same genus, though results of the logistic regression suggest species is likely not an important predictor of mortality. Differences in species may become apparent if more treatment conditions other than mid-body, lateral strikes at 90° were included in regression models. For example, mortality for rainbow and brook trout hit on the mid-body, dorsal surface at 90° both experienced high, but unequal rates of mortality (Table 7). Inclusion of multiple blade leading widths or strike velocities for mid-body, dorsal or 135° strikes could also help further separate a species effect. To date, mid-body, lateral strikes at 90° prioritized in this study have consistently been associated with higher overall mortality regardless of species [10–13]. Blade strike laboratory data for threadfin shad was also not available which could help elucidate if species within *Dorosoma* have similar responses to blade strike velocity. Second, surrogacy in this case is supported for trout with total length from 16.5 to 31.5 cm (i.e., size range for both species of large trout tested in this study), and shad dose-response data may only be applicable to YOY American shad and blueback herring because smaller

gizzard shad were unavailable. Sizes of both trout and shad data are, however, broadly representative of the size ranges that pass through hydropower turbines as they migrate downstream to their native coastal habitat. Regardless, application of our dose-response curves to markedly smaller or larger size groups of trout or shad is not advisable pending the collection and analysis of more varied size data.

Application of surrogacy within rainbow trout as a function of body size may also be possible but the evidence is less conclusive. Both rainbow trout models suggested that total length was not a significant predictor of mortality, even if values were close to significant (e.g., RBT.m1; Table 8) because the odds of mortality were nearly the same across all sizes of rainbow trout. In addition, a logistic regression of only mortality and total length suggested that fish size remained a non-significant predictor of mortality. This simplistic model also did not properly account for variation in our data considering the AIC value was much higher (184.06) compared to our accepted model (Table 9). A similar trend was detected in Saylor et al. [13] who found that size was not a significant contributor of mortality in bluegill compared to blade leading edge width or velocity. The lack of significance in bluegill was attributed to the marked susceptibility of the species overall, but smaller fish experienced mortality at lower velocities than larger fish [13]. In contrast, the shapes of small and large dose-response curves appear to be different and the confidence intervals of both do not overlap at lower velocities (Figure 23B). Other researchers studying similarly sized rainbow trout (i.e., 10.0 to 25.0 cm fork length) found that larger fish had markedly higher rates of mortality compared to smaller trout [10,12]. We found similar trends when large (~25.0 cm) trout struck by a 52-mm blade had noticeably higher mortality compared to small (~10.0 cm) trout (Groups 2 & 11; Table 7); however, the thinnest 26-mm blade caused ~100% mortality regardless of trout size in this study (Groups 6 & 15; Table 7). Work by EPRI et al. [10,12] did not make statistical comparisons between treatment groups or model responses simultaneously over their entire data set which limits more direct comparisons with this study. In the absence of more conclusive agreement between this analysis and previous studies, dose-response relationships within the same species should be treated separately, i.e., surrogacy according to size is not advisable for rainbow trout. To that end, understanding how size

effects mortality within a species remains unclear and suggests trends in size are also linked closely with fish species.

Conclusions

Our use of surrogacy in this study should help turbine manufacturers and researchers better understand the effects of turbine passage stressors by increasing inference space of blade strike data. Brook trout data should be a suitable representative to species like bull trout, *Salvelinus confluentus*, which is threatened throughout much of its' native range in North America [32,33]. Additional dose-response data for *Salmo* spp. or multiple, similarly sized *Dorosoma* spp. would better inform application of surrogacy but is unwarranted because there is currently no evidence to suggest other species within either genus would respond markedly different from species tested here, though fish length has a confounding effect on mortality. Our use of morphometric analyses and fish shape is the best approximation of species available for blade strike analyses currently, but future work should investigate the biomechanical properties of the fish musculoskeletal system including how scales, skeletal complexity, and center of gravity affect whole-fish flexibility. For example, early work by Turnpenny [15] measured each species' center of gravity and found that injury and mortality rates were higher when the blade struck the fish's center gravity, i.e., a direct strike. Biomechanical data may account for fish species better than body shape alone in models used to predict mortality caused by blade strike impact. Understanding the effects of size remains a challenge; however, use of dose-response data from one size class as a surrogate for that species may be the only option in absence of desired data. Otherwise, size and species can be easily accounted for by adjusting model parameters (both b and e) based on changes in mortality linked with other treatment conditions. Our methods prefer inclusion of fewer fish in more treatment groups to extend our inference space of blade strike data. Smaller sample sizes increase total variation in our regression models, but we also cover more possible blade strike scenarios which can better inform a species' total passage risk. In certain scenarios it may be beneficial to use actual species' dose-response models (when available) if that species is of great concern. Alternatively, enough insight may be gained

by use of surrogate data that represents average genus- or family-level responses, or for circumstances where data do not exist. Regardless, our data will help populate and broaden the application of the Biological Performance Assessment (BioPA) model [34] and the Hydropower Biological Evaluation Toolset (HBET) [35] which are available to turbine manufacturers and/or project managers attempting to design safer hydropower turbines that can ameliorate impacts of turbine passage without stark losses in electricity production.

Acknowledgments

Fish use approval was granted by the ORNL Institutional Animal Care and Use Committee [protocol #0461]. The authors would like to thank Bill Post, Jarrett Gibbons, and all the fisheries biologists, hatchery technicians, and field crews from the South Carolina Department of Natural Resources Dennis Wildlife Center and Fish Hatchery for research space, onsite housing, and collection of American shad and blueback herring. We thank Andrew Currie and Steven Arms (United States Fish and Wildlife Service Dale Hollow National Fish Hatchery) for rainbow and brook trout. We also must thank John Ellis and Roger Bitz (Tellico and Buffalo Springs State Hatcheries, respectively, Tennessee Wildlife Resource Agency) for additional rainbow trout. Special thanks to Rebecca Brink (ORNL) for assistance with laboratory trials and Evin Carter (ORNL), Brett Pflugrath (Pacific Northwest National Laboratory, PNNL), Ryan Harnish (PNNL), and Robert Mueller (PNNL) for reviewing this article. We also thank Lara Aston and Alison Colotelo (PNNL) and Shelaine Curd (ORNL) for project management.

References

1. Silva, A.T.; Lucas, M.C.; Castro-Santos, T.; Katopodis, C.; Baumgartner, L.J.; Thiem, J.D.; Aarestrup, K.; Pompeu, P.S.; O'Brien, G.C.; Braun, D.C.; et al. The future of fish passage science, engineering, and practice. *Fish Fish.* **2018**, *19*, 340–362.

2. Neitzel, D. a; Dauble, D.D.; Cada, G.F.; Richmond, M.C.; Guensch, G.R.; Mueller, R.R.; Abernethy, C.S.; Amidan, B. Survival estimates for juvenile fish subjected to a laboratory-generated shear environment. *Trans. Am. Fish. Soc.* **2004**, *133*, 447–454.

3. Čada, G.; Loar, J.; Garrison, L.; Fisher, R.; Neitzel, D. Efforts to reduce mortality to hydroelectric turbine-passed fish: Locating and quantifying damaging shear stresses. *Environ. Manag.* **2006**, *37*, 898–906.

4. George, S.D.; Baldigo, B.P.; Smith, M.J.; McKeown, D.M.; Faulring, J.W. Variations in water temperature and implications for trout populations in the Upper Schoharie Creek and West Kill, New York, USA. *J. Freshw. Ecol.* **2015**, *31*, 93–108.

5. Colotelo, A.H.; Goldman, A.E.; Wagner, K.A.; Brown, R.S.; Deng, Z.D.; Richmond, M.C. A comparison of metrics to evaluate the effects of hydro-facility passage stressors on fish. *Environ. Rev.* **2017**, *25*, 1–11.

6. Čada, G.F. The development of advanced hydroelectric turbines to improve fish passage survival. *Fisheries* **2001**, *26*, 14–23.

7. Uria-Martinez, R.; Johnson, M.M.; O'Connor, P.W.; Samu, N.M.; Witt, A.M.; Battey, H.; Welch, T.; Bonnet, M.; Wagoner, S. *2017 Hydropower Market Report*; Oak Ridge, Tennessee, **2018**.

8. Fu, T.; Deng, Z.D.; Duncan, J.P.; Zhou, D.; Carlson, T.J.; Johnson, G.E.; Hou, H.

Assessing hydraulic conditions through Francis turbines using an autonomous sensor device. *Renew. Energy* **2016**, *99*, 1244–1252.

9. Martinez, J.J.; Deng, Z.D.; Titzler, P.S.; Duncan, J.P.; Lu, J.; Mueller, R.P.; Tian, C.; Trumbo, B.A.; Ahmann, M.L.; Renholds, J.F. Hydraulic and biological characterization of a large Kaplan turbine. *Renew. Energy* **2019**, *131*, 240–249.

10. EPRI, (Electric Power Research Institute) *Evaluation of the effects of turbine blade leading edge design on fish survival*; Palo Alto, CA, **2008**.

11. Bevelhimer, M.S.; Pracheil, B.M.; Fortner, A.M.; Saylor, R.; Deck, K.L. Mortality and injury assessment for three species of fish exposed to simulated turbine blade strike. *Can. J. Fish. Aquat. Sci.* **2019**, *76*, 2350–2363.

12. EPRI, (Electric Power Research Institute) *Tests examining survival of fish struck by turbine blades*; Palo Alto, CA, **2011**.

13. Saylor, R.; Fortner, A.; Bevelhimer, M. Quantifying mortality and injury susceptibility for two morphologically disparate fishes exposed to simulated turbine blade strike. *Hydrobiologia* **2019**, *842*, 55–75.

14. Turnpenny, A.W.H. Mechanisms of fish damage in low head turbines: An experimental appraisal. In *Fish Migration and Fish Bypasses*; Jungwirth, M., Schmutz, S., Weiss, S., Eds.; Blackwell Publishing Ltd: Malden, Massachusetts, **1998**; pp. 300–314 ISBN 0-85238-253-7.

15. Turnpenny, A.W.H.; Davis, M.H.; Fleming, J.M.; Davies, J.K. *Experimental studies relating to the passage of fish and shrimps through tidal power turbines*; Southampton, United Kingdom, **1992**.

16. Romero-Gomez, P.; Richmond, M.C. Movement and collision of Lagrangian particles in hydro-turbine intakes: a case study. *J. Hydraul. Res.* **2017**, *1686*, 1–15.

17. Harding, S.F.; Richmond, M.C.; Mueller, R.P. Experimental observation of inertial particles through idealized hydroturbine distributor geometry. *Water (Switzerland)* **2019**, *11*, 471.

18. Nelson, J.S.; Grande, T.C.; Wilson, M.V.H. *Fishes of the World*; 5th ed.; John Wiley & Sons: Hoboken, New Jersey, **2016**.

19. Pracheil, B.M.; McManamay, R.A.; Bevelhimer, M.S.; DeRolph, C.R.; Čada, G.F. A traits-based approach for prioritizing species for monitoring and surrogacy selection. *Endanger. Species Res.* **2016**, *31*, 243–258.

20. Čada, G.F.; Schweizer, P.E. *The application of traits-based assessment approaches to estimate the effects of hydroelectric turbine passage on fish populations*; Oak Ridge, Tennessee, **2012**; Vol. April.

21. Grubbs, R.D.; Kraus, R.T. Fish Migration. In *Encyclopedia of Animal Behavior*; Breed, M.D., Moore, J., Eds.; Elsevier Academic Press: San Diego, California, **2010**; pp. 715–724.

22. Binder, T.R.; Cooke, S.J.; Hinch, S.G. Physiological specializations of different fish groups: Fish migrations. In *Encyclopedia of Fish Physiology: From Genome to Environment*; Farrell, A.P., Cech Jr., J.J., Richards, J.G., Stevens, E.D., Eds.; Elsevier Inc.: San Diego, California, **2011**; pp. 1921–1952 ISBN 9780123745538.

23. Waldman, J.R.; Limburg, K.E. The world's shads: summary of their status, conservation, and research needs. In Proceedings of the Biodiversity, status, and conservation of the world's shads; Limburg, K.E., Waldman, J.R., Eds.; American Fisheries Society Symposium 35: Bethesda, Maryland, **2003**; pp. 363–369.

24. Sneddon, L.U. Clinical Anesthesia and Analgesia in. *J. Exot. Pet Med.* **2012**, *21*, 32–43.

25. Javahery, S.; Nekoubin, H.; Moradlu, A.H. Effect of anaesthesia with clove oil in

fish (review). *Fish Physiol. Biochem.* **2012**, *38*, 1545–1552.

26. Priborsky, J.; Velisek, J. A Review of Three Commonly Used Fish Anesthetics. *Rev. Fish. Sci. Aquac.* **2018**, *26*, 417–442.

27. Ritz, C.; Baty, F.; Streibig, J.C.; Gerhard, D. Dose-response analysis using R. *PLoS One* **2015**, *10*, 1–13.

28. R Core Team R: A language and environment for stastical computing. **2020**.

29. Barton, K. MuMIn: Multi-Model Interfernce **2020**, Available online: https://cran.r-project.org/package=MuMIn.

30. Sakamoto, Y.; Ishiguro, M.; Kitagawa, G. *Akaike information criterion statistics*; 1st ed.; KTK Scientific Publishers: Tokyo, Japan, **1986**.

31. Cone, R.S. The Need to Reconsider the Use of Condition Indices in Fishery Science. *Trans. Am. Fish. Soc.* **1989**, *118*, 510–514.

32. U.S. Fish and Wildlife Service Recovery Plan for the Coterminous United States Population of Bull Trout (Salvelinus confluentus). **2015**, 179.

33. Dunham, J.B.; Rieman, B.E. Metapopulation structure of bull trout: Influences of physical, biotic, and geometrical landscape characteristics. *Ecol. Appl.* **1999**, *9*, 642–655.

34. Richmond, M.C.; Serkowski, J.A.; Radowski, C.; Strickler, B.; Weisbeck, M.; Dotson, C. Computational tools to assess turbine biological performance. *Hydroreview* **2014**, *33*, 1–6.

35. Hou, H.; Deng, Z.; Martinez, J.; Fu, T.; Duncan, J.; Johnson, G.; Lu, J.; Skalski, J.; Townsend, R.; Tan, L. A Hydropower Biological Evaluation Toolset (HBET) for characterizing hydraulic conditions and impacts of hydro-structures on fish. *Energies* **2018**, *11*, 990–1002.

Appendix

Table 7. Experimental overview of the study including 34 treatment groups and five control (C) groups for rainbow trout (large and small), brook trout, gizzard shad, and *Alosa* spp. (species data combined because sample sizes of American shad and blueback herring were small. Mean total length (TL) is reported with standard deviation (SD) with units of centimeter (cm). Blade strike characteristics included blade width (BW; mm), velocity (Vel; m/s), location (Loc, with M; mid-body or H; head), orientation (Ort, with L; lateral, D; dorsal, and V; ventral), impact angle (Ang). The total number in each group (N) is reported with counts (Mort) and rates (MR) of mortalities. Analyses include dose-response (DR) and logistic regression (LR) used in this study. P-values are calculated for Chi-square tests with Yate's correction using the following equation [1]:

$$\chi^2_{Yates} = \frac{(|ad - bc| - 0.5N)^2 N}{mnrs}$$

and compared each treatment to the species' control group. We assumed α = 0.05; significant comparisons are in bold.

No.	Spp	TL ± SD (cm)	BW	Vel	Loc	Ort	Ang	N	Mort	MR	Analyses	p-value
C	Rainbow trout	25.8 ± 2.37	--	--	--	--	--	26	0	0.0	--	--
1			52	5.5	M	L	90	20	1	5.0	DR; LR	0.447
2			52	6.6	M	L	90	20	11	55.0	DR; LR	< **0.001**
3			52	7.4	M	L	90	20	15	75.0	DR; LR	< **0.001**
4			52	8.0	M	L	90	20	19	95.0	DR; LR	< **0.001**
5			52	6.6	M	L	135	21	9	42.9	LR	< **0.001**
6			26	6.6	M	L	90	20	20	100.0	LR	< **0.001**
7			52	6.6	M	D	90	20	16	80.0	LR	< **0.001**
8			52	6.6	M	V	90	20	6	30.0	LR	**0.005**
9			52	6.6	H	L	90	20	4	20.0	LR	**0.032**
10			52	7.4	H	L	90	20	16	80.0	LR	< **0.001**
C	Rainbow trout	11.4 ± 1.02	C	C	C	C	C	21	0	0.0	--	--
11			52	6.7	M	L	90	19	3	15.8	DR; LR	0.098
12			52	7.2	M	L	90	19	14	73.7	DR; LR	< **0.001**

Table 7 continued…

13			52	8.0	M	L	90	20	19	95.0	DR; LR	**< 0.001**
14			52	8.7	M	L	90	20	19	95.0	DR; LR	**< 0.001**
15			26	6.6	M	L	90	20	18	90.0	LR	**0.002**
C	Brook trout	24.2 ± 2.39	--	--	--	--	--	20	0	0.0	--	--
16			52	4.9	M	L	90	20	2	10.0	DR; LR	0.234
17			52	5.7	M	L	90	20	9	45.0	DR; LR	**0.001**
18			52	6.8	M	L	90	21	13	61.9	DR; LR	**< 0.001**
19			52	7.3	M	L	90	20	20	100.0	DR; LR	**< 0.001**
20			52	6.8	M	D	90	19	17	89.5	LR	**< 0.001**
21			52	6.8	H	L	90	20	13	65.0	LR	**< 0.001**
22			52	6.8	M	L	135	15	5	33.3	LR	**0.011**
C	Gizzard shad	16.0 ± 0.65	--	--	--	--	--	12	0	0.0	--	--
23			52	4.7	M	L	90	20	0	0.0	DR; LR	1.000
24			52	6.1	M	L	90	20	17	85.0	DR; LR	**< 0.001**
25			52	6.7	M	L	90	20	19	95.0	DR; LR	**< 0.001**
26			52	8.1	M	L	90	20	20	100.0	DR; LR	**< 0.001**
C	*Alosa* spp.	7.5 ± 0.71	--	--	--	--	--	29	0	0.0	--	--
27			52	7.1	M	L	90	2	0	0.0	LR	--
28			52	7.6	M	L	90	14	3	21.4	DR; LR	1.000
29			52	8.3	M	L	90	25	22	88.0	DR; LR	**0.026**
30			52	9.2	M	L	90	17	17	100.0	DR; LR	**< 0.001**
31			52	9.7	M	L	90	20	19	95.0	DR; LR	**< 0.001**
32			26	8.2	M	L	90	17	17	100.0	--	**< 0.001**

Table 7 continued…

33	76	8.1	M	L	90	19	2	10.5	--	0.148
34	76	9.4	M	L	90	16	3	18.8	--	**0.037**

Note: Data containing (--) indicate this column was not applicable to this treatment group. Control fish for all species were not used in dose-response or logistic regression analyses and p-values were not reported because treatment groups are compared to control groups to generate statistical inferences.

Table 8. Results of log-logistic regression of mortality against blade strike impact velocity for each species, size class within a species, or combination of species.

Species	TL ± SD (cm)	n	Parameter	Estimate	Standard Error	p-value
Rainbow trout	25.8 ± 2.37	80	b	-12.60	2.925	< ***0.001***
			e	6.59	0.142	< ***0.001***
Rainbow trout	11.4 ± 1.02	78	b	-29.33	9.158	***0.002***
			e	7.08	0.069	< ***0.001***
Brook trout	24.2 ± 2.39	81	b	-9.19	1.926	< ***0.001***
			e	5.99	0.172	< ***0.001***
Gizzard shad	16.0 ± 0.65	80	b	-22.56	9.141	***0.016***
			e	5.66	0.179	< ***0.001***
Alosa spp.	7.5 ± 0.71	76	b	-37.31	7.998	< ***0.001***
			e	7.87	0.073	< ***0.001***

Note: Mean total length (TL) is reported with standard deviation (SD) in centimeters (cm), sample size (N), parameters (inclination point *b*; effective dose for 50% of the population *e*), parameter estimates, standard error, and p-values are reported for each model. All statistical decisions were based on $\alpha = 0.05$; significant comparisons are in bold.

Table 9. Results of a logistic regression of mortality and strike impact conditions including adult rainbow trout and brook trout data (Trouts), small and large rainbow trout (RBT), and data for gizzard shad, American shad, and blueback herring (Shads).

Model	N	Variable	Coeff	SE	OR	CI_{lower}	CI_{upper}	p	AIC	AICc	ICOMP
Trouts.m1	276	(Intercept)	-7.16	2.515	--	--	--	**0.004**	226.95	227.47	231.12
		Species [RBT]	-0.49	0.366	0.61	0.296	1.248	0.178			
		Velocity	1.86	0.281	6.44	3.842	11.644	< **0.001**			
		Location [M]	0.74	0.467	2.11	0.846	5.342	0.111			
		Orientation [L]	-1.31	0.567	0.27	0.080	0.768	**0.021**			
		Angle [90°]	1.19	0.502	3.28	1.249	9.048	**0.018**			
		Total length	-0.20	0.074	0.82	0.703	0.943	**0.007**			
Trouts.m2	276	(Intercept)	-6.70	2.504	--	--	--	**0.007**	226.78	227.12	231.69
		Velocity	1.83	0.285	6.23	3.704	11.396	< **0.001**			
		Location [M]	0.82	0.461	2.28	0.928	5.711	0.074			
		Orientation [L]	-1.21	0.557	0.30	0.091	0.836	**0.030**			
		Angle [90°]	1.31	0.492	3.72	1.450	10.113	**0.008**			
		Total length	-0.23	0.071	0.79	0.686	0.909	**0.001**			
RBT.m1	197	(Intercept)	-13.48	3.123	--	--	--	< **0.001**	122.17	122.44	130.01
		Blade [52]	-3.18	0.801	0.04	0.006	0.164	< **0.001**			
		Velocity	2.29	0.425	9.86	4.676	25.298	< **0.001**			
		Total length	0.07	0.035	1.07	0.999	1.147	0.061			
RBT.m2	197	(Intercept)	-10.93	-10.93	--	--	--	< **0.001**	123.95	124.10	126.27
		Blade [52]	-3.03	-3.03	0.05	0.007	0.186	< **0.001**			

Table 9 continued…

		Velocity	2.07	2.07	7.93	3.941	19.280	< **0.001**		
Shads.m6	158	Intercept	-29.56	6.001	--	--	--	< **0.001**	61.93	62.25	66.63
		Species [BBH]	-0.45	0.918	0.64	0.097	3.743	0.622		
		Species [GZS]	8.50	1.817	4906.57	209.565	3.006×10^5	< **0.001**		
		Velocity	3.76	0.748	42.90	12.542	260.179	< **0.001**		
Shads.m8	158	Intercept	-29.57	5.960	--	--	--	< **0.001**	60.17	60.37	65.16
		Genus [Dor]	8.71	1.776	6052.05	284.503	3.467×10^5	< **0.001**		
		Velocity	3.72	0.736	41.44	12.310	241.992	< **0.001**		

Note: Total sample size (N), coefficient estimates (Coeff; log odds), standard error (SE), odds ratio (OR) with 95% confidence interval (CI), p-value (p) assuming $\alpha = 0.05$, Akaike Information Criteria (AIC), Second order Akaike Information Criteria (AIC*c*), and Informational and Complexity (ICOMP) criterion are provided for each model and aided with model selection.

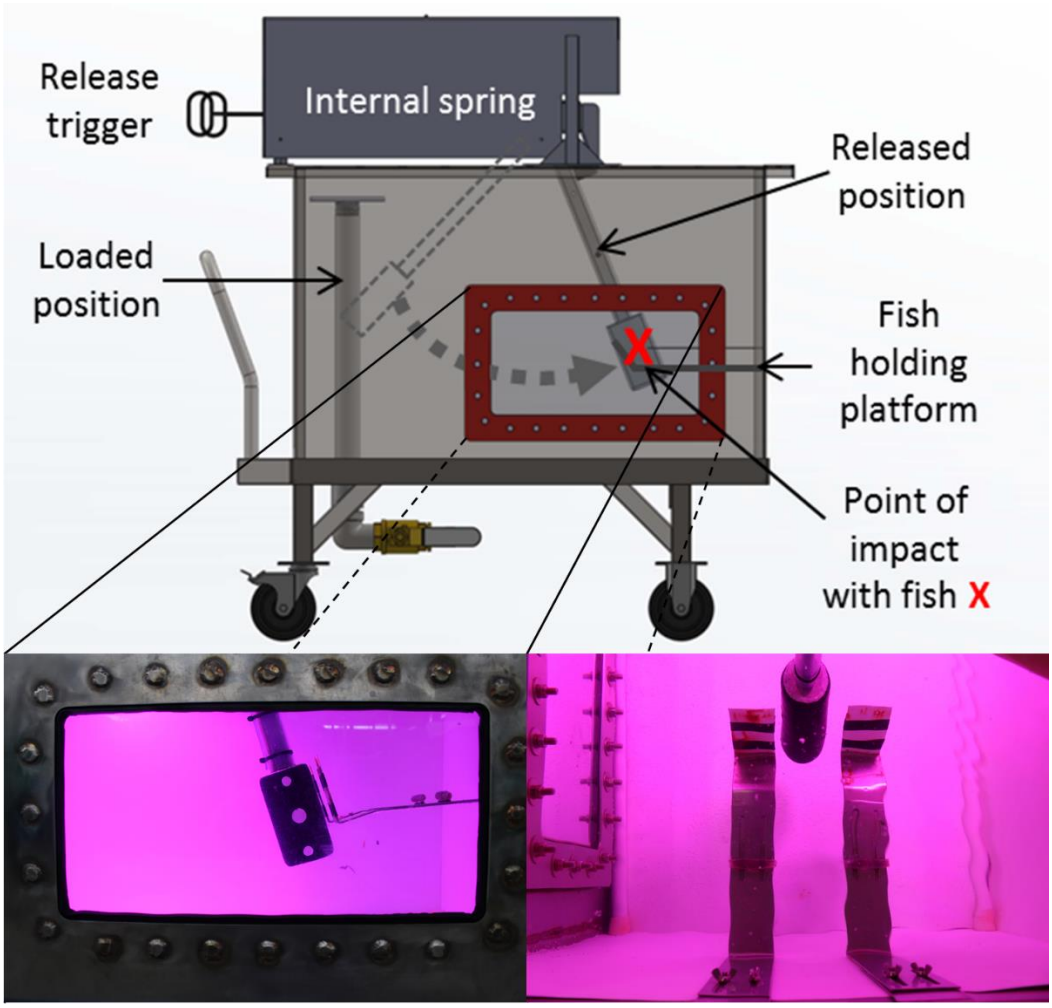

Figure 15. A diagram of the apparatus used to simulate turbine blade strike. The top panel shows the entire apparatus and approximate path and impact point of the blade with anesthetized fish. The bottom left panel is a side view through the viewing window and the bottom right panel is a top view through the lid – both show the simulated turbine blade and holding platform where fish were positioned during trials.

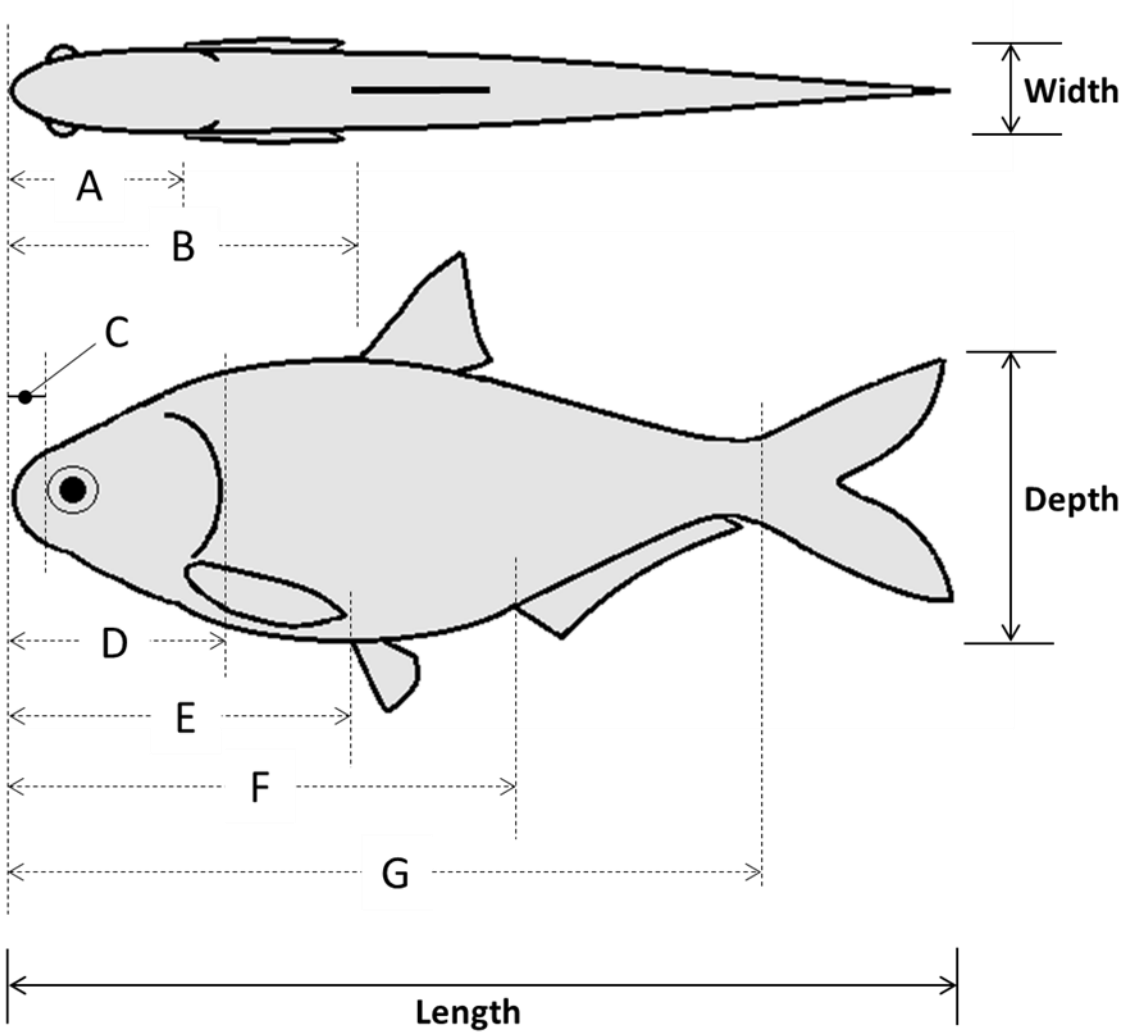

Figure 16. Diagram of major body landmarks from which morphometric measurements were taken related to body length, depth, and width (solid lines). Dashed vertical lines correspond to landmarks including pectoral fin (A), dorsal fin (B), snout (C), head (D), pelvic fin (E), anal fin (F), and caudal fin (G). Horizontal dashed lines represent length measurements between the snout tip and each landmark, while body depth and width measurements were taken on the body at each landmark (i.e., near vertical lines).

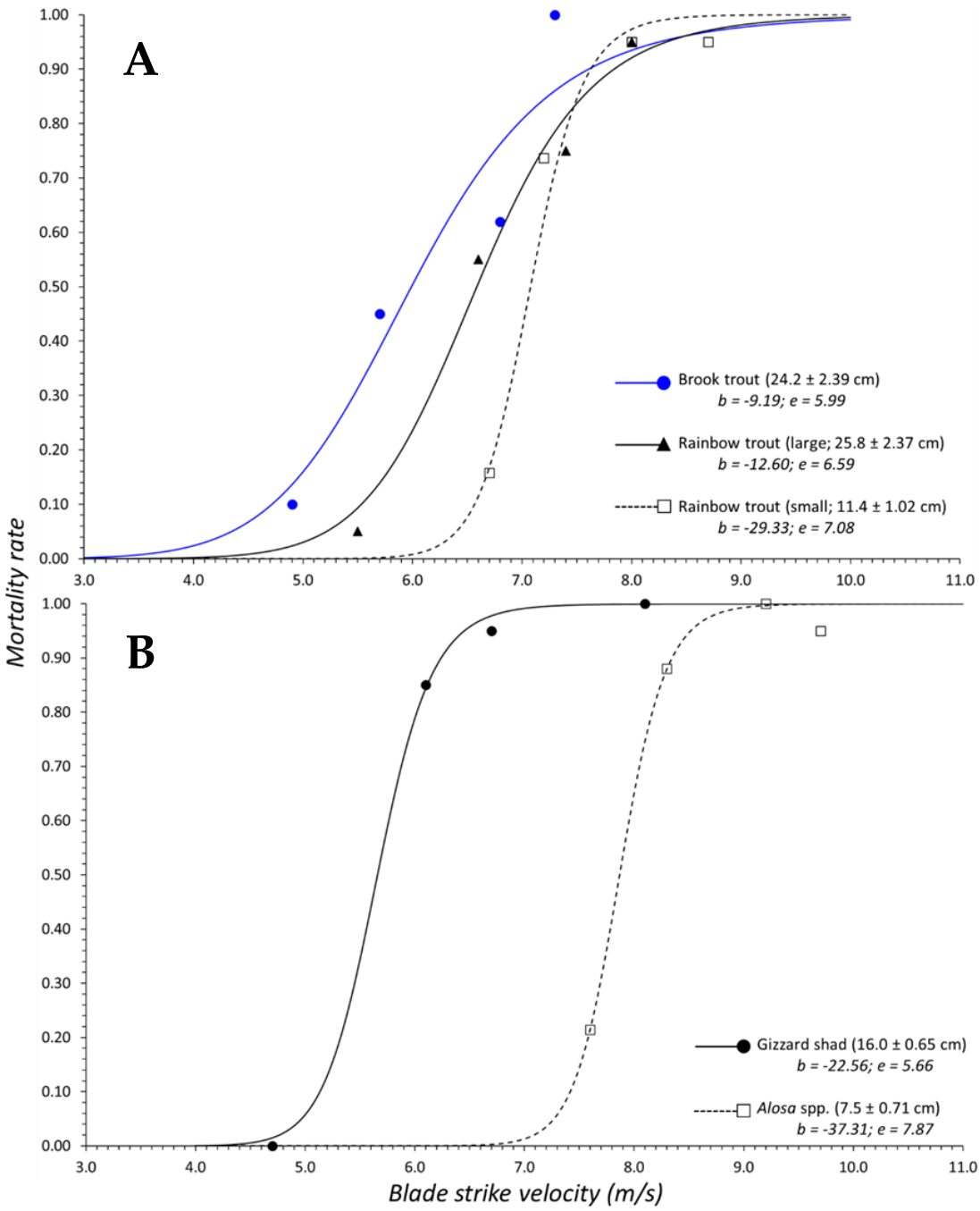

Figure 17. Graphs of dose-response curves using log-logistic regression to predict mortality according to blade strike velocity (m/s). Curves were produced for, (A) small (black; dashed line; open squares) and large rainbow trout (black; solid line; closed triangles) and brook trout (blue; solid line; closed circles) or (B) gizzard shad (black; solid line; closed circles) and *Alosa* spp. (black; dashed line; open squares).

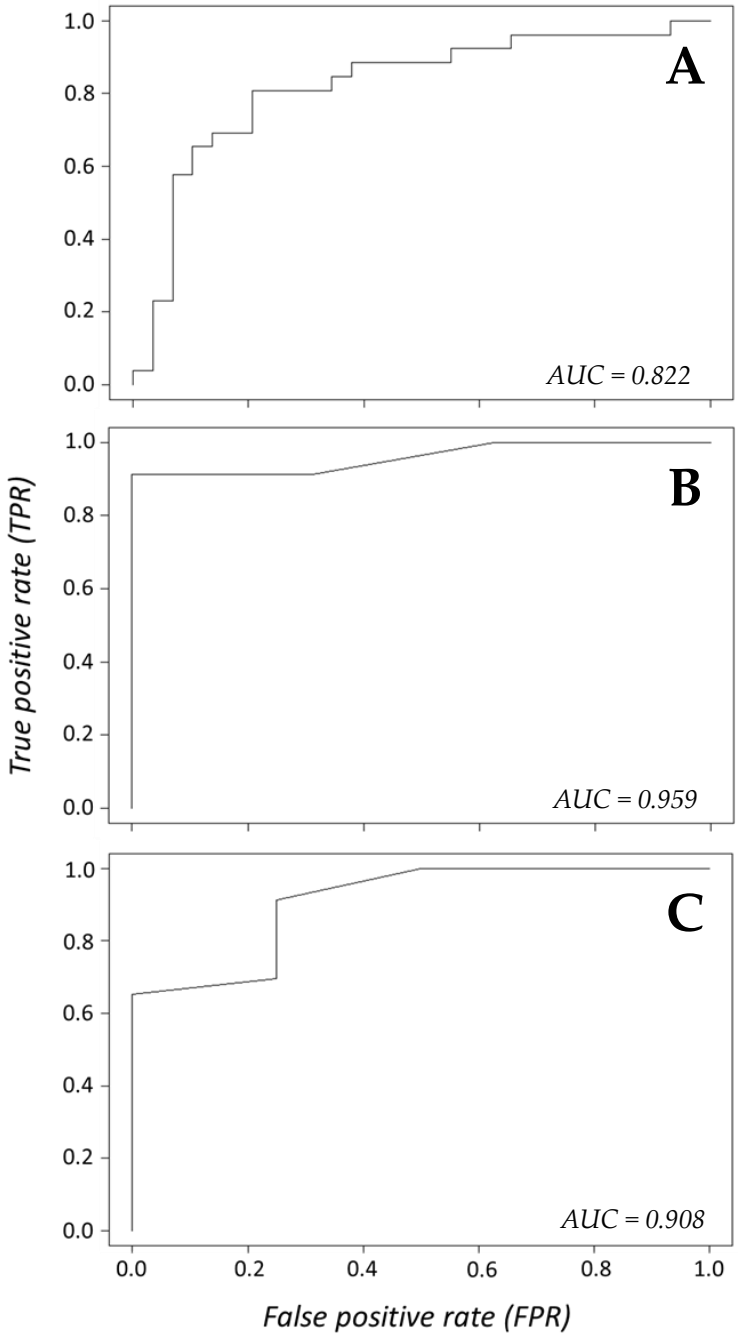

Figure 18. Receiver operating (ROC) plots with area under the curve (AUC) values depicting specificity of logistic regression models used to predict mortality as a result of blade strike conditions. Logistic models were produced for large rainbow trout and brook trout (A), small and large rainbow trout (B), or gizzard shad, American shad, and blueback herring (C).

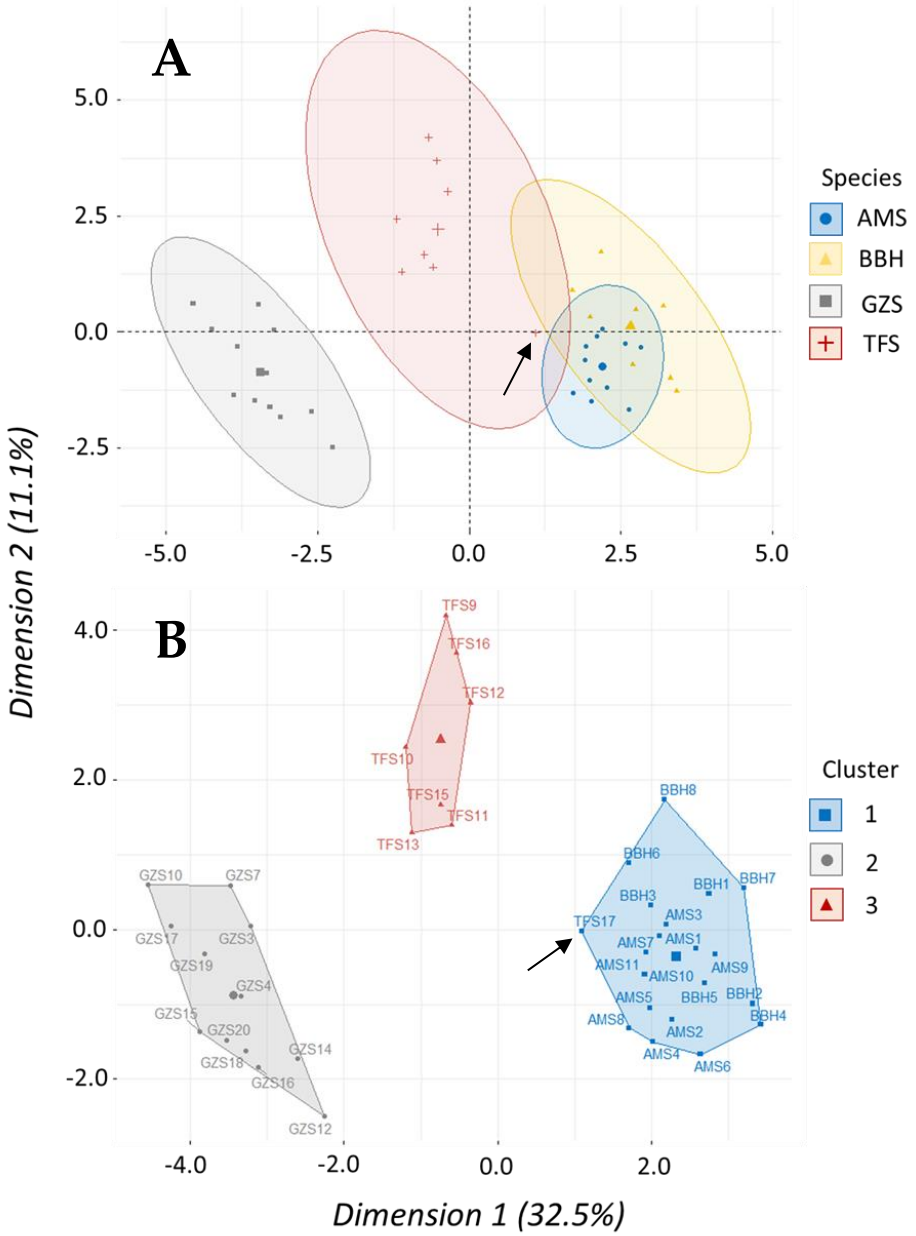

Figure 19. Initial results of principal component analysis and hierarchical clustering on principal components using morphometric data collected from American (AMS), blueback (BBH), gizzard (GZS), and threadfin (TFS) shad. (A) Biplot showing ellipses encircling individual fish considered part of that group according to PCA. (B) Cluster factor map showing results of HCPC analysis that produced three clusters. Gizzard shad and threadfin shad #17 (black arrow) were all ~4.0 cm larger on average than other shad species so all gizzard shad and TFS17 data were removed from the final analysis to preclude the confounding effects of fish size.

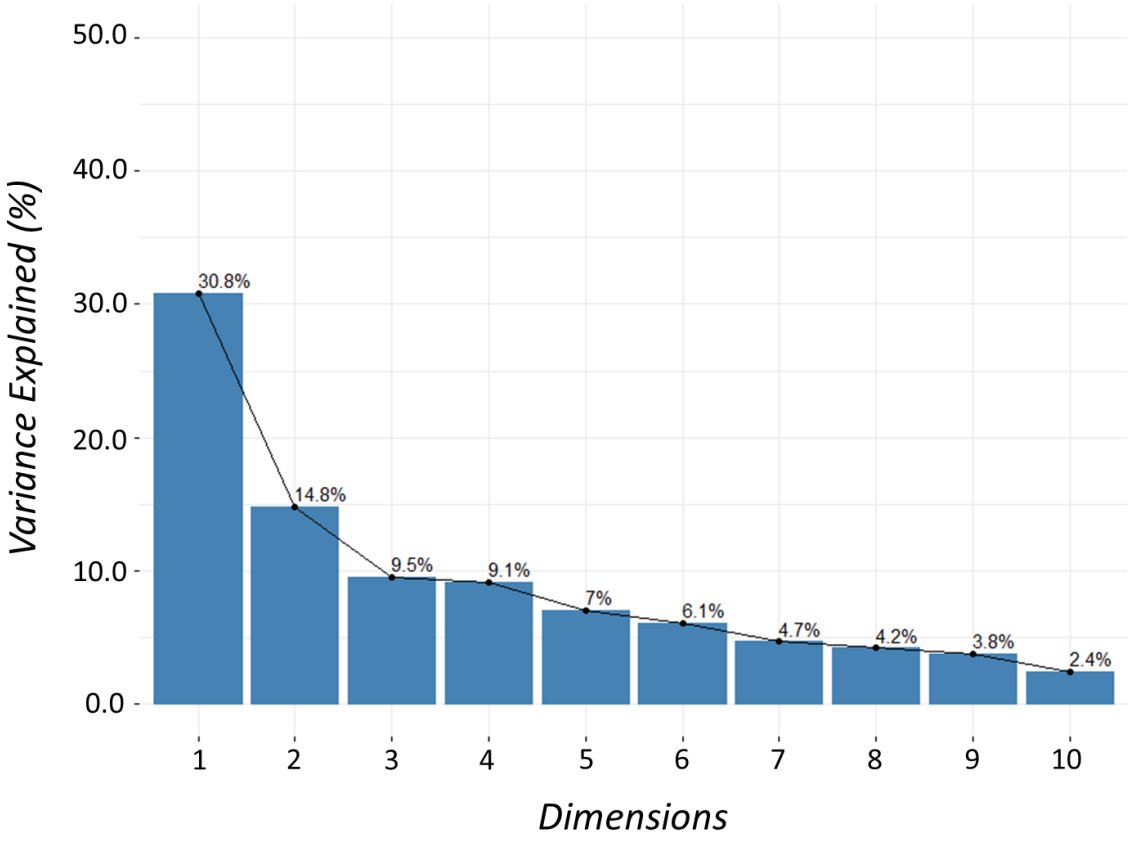

Figure 20. Scree plot produced from principal component analysis of shad morphometric data containing one species term and 21 morphometric variables.

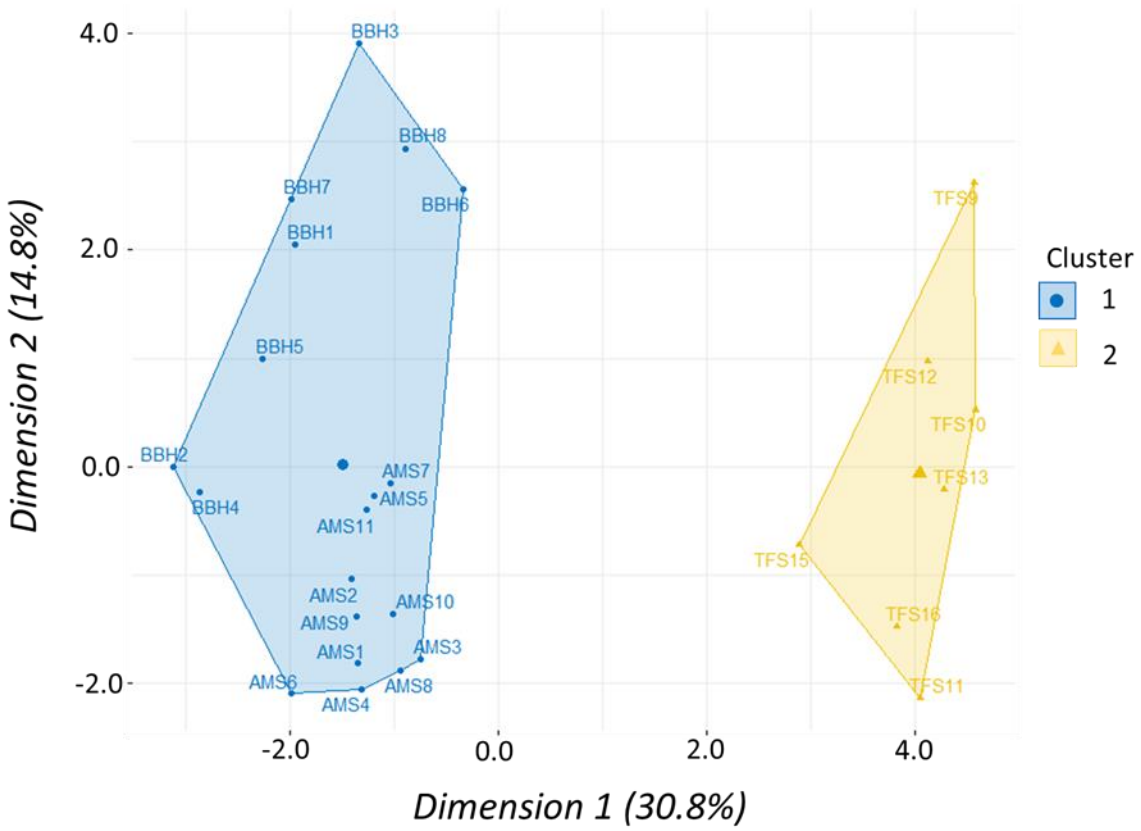

Figure 21. Cluster factor map produced from hierarchical clustering on six principal components for American shad (AMS), blueback herring (BBH), and threadfin shad (TFS) morphometric data.

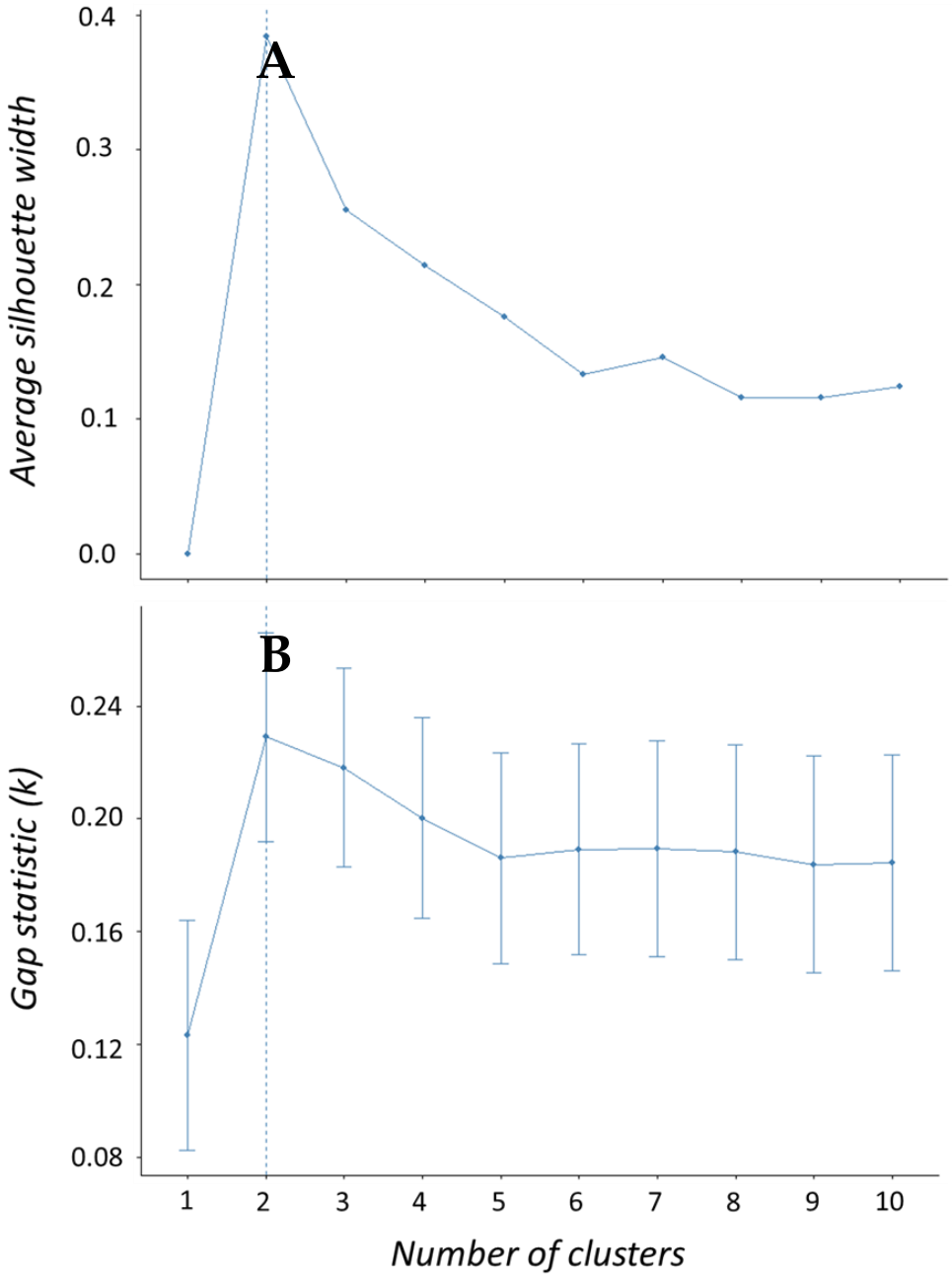

Figure 22. Graph depicting two common methods to determine optimal number of clusters to be used in a hierarchical cluster analysis. Methods include (A) average silhouette which measures how well data lies within each cluster so that higher values indicate better fit, and (B) the gap statistic which compares intracluster variation to a null reference and clusters with highest values representing the greatest distance from uniform.

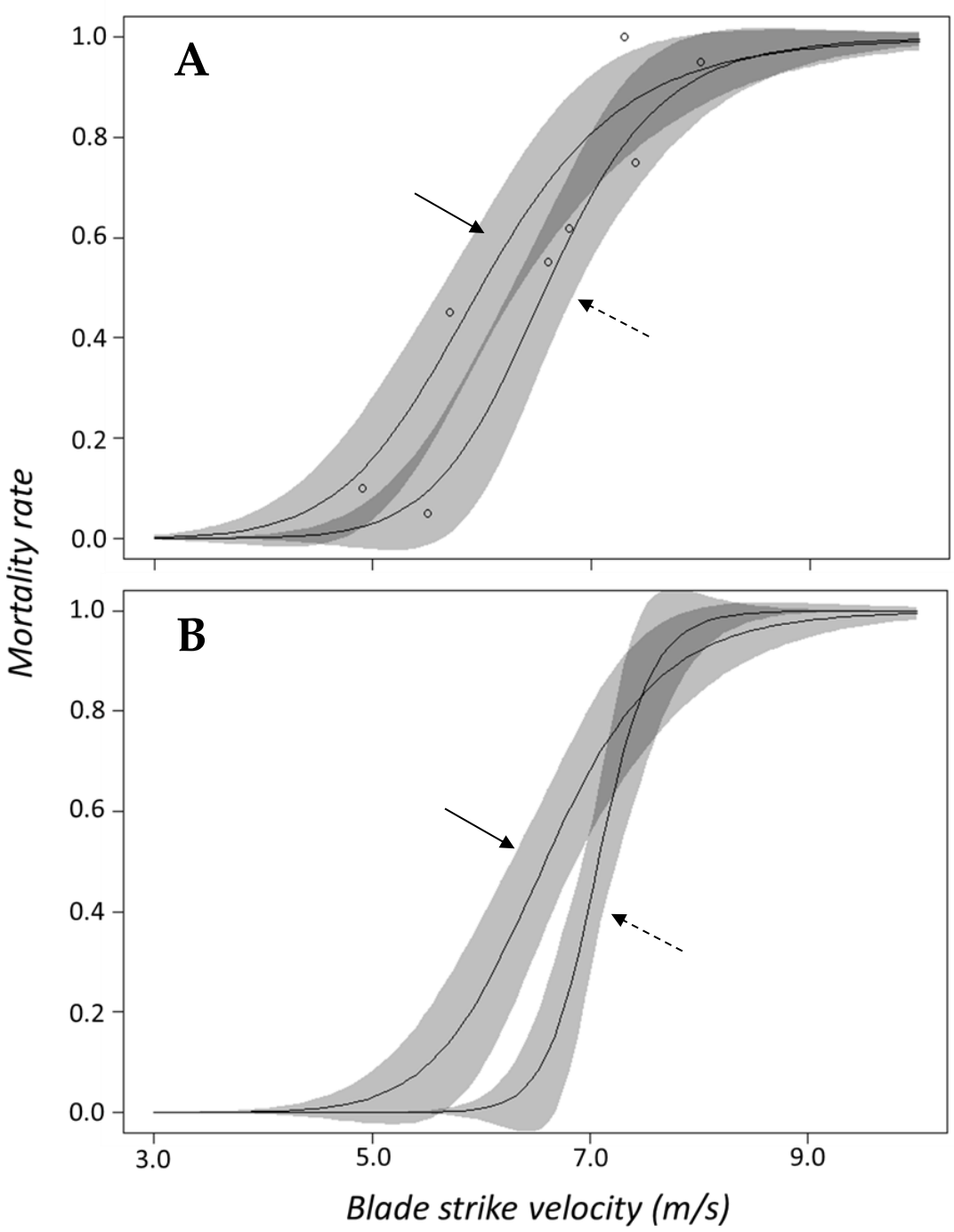

Figure 23. Plot of dose-response curves for (A) large rainbow (solid arrow) and brook (dashed arrow) trout and (B) small (dashed arrow) and large (solid arrow) rainbow trout which highlights the 95% confidence bands for each curve.

CHAPTER IV

CREATION OF A PROTOTYPE BIOMIMETIC FISH TO BETTER UNDERSTAND IMPACT TRAUMA CAUSED BY HYDROPOWER TURBINE BLADE STRIKES

A version of this chapter has undergone peer-review and is being revised for resubmission as Ryan Kurt Saylor, et al:

Ryan Saylor[1,2*], Peter Wang[3], Mark Bevelhimer[1], Peter Lloyd[3], Jesse Goodwin[3], Robert Laughter[3], David Young[3], Dustin Sterling[1], Paritosh Mhatre[3], Celeste Atkins[3], Brian Post[3]. "Creation of a prototype biomimetic fish to better understand impact trauma caused by hydropower turbine blade strikes." *PeerJ* (*in revision*).

Affiliations:

[1] Bredesen Center for Interdisciplinary Research and Graduate Education, University of Tennessee, Knoxville, Tennessee 37996

[2] Environmental Science Division, Oak Ridge National Laboratory, Oak Ridge, Tennessee 37830

[3] Manufacturing Demonstration Facility, Oak Ridge National Laboratory, Oak Ridge, Tennessee, USA

*Corresponding Author: Ryan K. Saylor

1 Bethel Valley Road

Oak Ridge National Laboratory

Oak Ridge, Tennessee 37830

Phone: 865-974-7709

E-mail: saylorr@ornl.gov

Author Contributions:

Ballistic gelatin experimentation – RKS and DS with input from MB

3D Scanning & Printing – PW, JG, and CA with input from BP

Sensor design/development – PL, RL, DY, PM with input from BP

Gelfish model testing – RKS, DS, RL, and DY with input from PL & BP

Data analysis – RKS, PW, JG, RL, and DY with input from MB

Composition of paper – RKS with input from PW

Article review and revisions – ALL

Abstract

Biomimetic model organisms could be a useful surrogate for live animals in many applications if of sufficient biofidelity. One such application is for use in field and laboratory tests of fish mortality associated with passage through hydropower turbines. Laboratory trials suggest that blade strikes are especially injurious and often causes mortality when fish are struck by thinner blades moving at higher velocities. Dose-response relationships have been created from these data, but the exact relationship between fish mortality and the actual forces enacted on fish during simulated blade strike testing remains unknown. Here, we describe the methods used to create a prototype biomimetic model fish composed of ballistic gelatin and covered with a surrogate skin to better approximate the natural properties of a fish body. Frozen fish were scanned with high-fidelity laser scanners, and a 3D-printed, reusable mold was created from which to cast our gelatin model. Computed tomography scan data, imaged directly or taken from online data repositories, were also successfully used to create CAD models for use in additive manufacturing of molds. One 3-axis accelerometer was embedded into the gelatin to compare accelerometer data to data from previous laboratory research on live fish. The resulting model (hereto after, Gelfish) had a statistically similar tissue durometer to that of real fish tissue and its flexibility was comparable to that of a live fish during simulated blade strike impact testing. Gelfish was fundamentally designed with biofidelity as its guiding principle and our results suggest initial experimentation was successful. Future research will include replication of initial Gelfish test results, quantitative measurement of model flexibility relative to real fish, and surrogate skeletal structures to enhance biofidelity. Use of more sophisticated sensors would also provide better quantification of the physical forces of blade strike impact and determine how said forces correlate with rates of mortality observed during tests on live fish.

Introduction

The field of biomimetics often produces revolutionary inventions and innovations that overcome persistent engineering challenges—many such breakthroughs are the result of studying aquatic organisms. Fishes and marine mammals are at the center of many

studies because of their unique adaptations to sense the environment and move efficiently to obtain resources while evading potential threats [1–3]. For example, the lateral line of fish and sensory structures of marine mammals have inspired instrumentation that allows for enhanced navigation in water [4,5]. Similarly, fish shape and body movement have been replicated to better overcome hydrodynamic drag and allow ships and submersible vehicles to move more efficiently in the water [6]. In addition, detailed study of the integumental complex and fins have led to innovations that allow for enhanced movement efficiency and maneuverability of marine vessels [7,8]. Many of these innovations are used to design aquatic robots with onboard sensors, fin-like structures, and body shapes that provide more efficient movement through the water [2,9–11]. Fish scales are also well-studied because the imbrication patterns and material properties provide flexibility for movement and puncture resistance against predatory attacks, which has been applied to body armor development [12–15]. Production of biomimetics continues and has helped overcome many engineering obstacles, but innovations are also needed to help protect the organisms that serve as inspiration.

Laboratory research using live organisms is obligatory in certain studies, but biomimetic models may serve as a useful substitute for live organisms in others. Vertebrate animals specifically are used in a multitude of laboratory and field studies [16–19], but fishes form the basis of much laboratory research [20,21]. Legal use of fishes in federally funded scientific research must meet rigorous animal welfare standards monitored by the Institutional Animal Care and Use Committee (IACUC) in the USA [16,21]. In addition to the cost of acquiring or producing live animal subjects, research costs also include care and maintenance which is expensive and time consuming. High standards of animal care ensure regulatory compliance and is also essential for scientific purposes because laboratory animals must be healthy, accurate representatives of the population. Studies involving fish often require dozens if not hundreds of individuals to properly account for natural variability, which further increases the financial burden of animal husbandry. In certain circumstances, the desired fish species may not be available because it is rare, difficult to capture or keep alive in captivity, or protected by state and federal laws. To successfully receive authorization to use live animals, researchers are

usually required to explain why use of an animal model (or computer simulation) is not possible and many fields are beginning to substitute animal models where possible [18]. In most cases, it is difficult to mimic or recreate an organism without studying it first, but the loop could be closed by creating a biomimetic model for future use in place of live animals. All these facts suggest that if a biomimetic model existed, with sufficiently high biofidelity, the need for live animals would be less necessary in certain fields.

One application for a biomimetic model fish would include field and laboratory tests related to concerns of fish passage through hydropower turbines. There are nearly 2500 hydroelectric dams in the USA [22] and many riverine fishes are at a particularly high risk of turbine passage due to their migratory behavior [23,24]. Live fish are often used during passage survival testing that is a part of the relicensing process for conventional hydropower dams. Hydropower facilities must undergo relicensing every 30–50 years and hundreds of dams are projected to submit relicensing applications within the next decade [25]. Exact passage conditions of fish are generally unknown and have relied on insights from computational fluid dynamic (CFD) models to estimate probability of exposure to turbine passage stressors. Impacts from turbine blade runners are one of the most injurious stressors and laboratory tests on live fish suggest it may cause organ damage, skeletal fractures, amputation, and death [26–28]. Rates of injury and death are highest with thinner blades, higher impact velocities, and when struck on the lateral surface near the center of gravity of a fish [26,27,29–31]. Dose-response relationships generated from these laboratory trials are an important resource for designing more fish-friendly turbines; however, these data are limited in scope to just a few fish species exposed to what is presumed to be the worst-case impact scenarios. Furthermore, technology like the hard-bodied autonomous Sensor Fish™, that records actual hydraulic conditions from within a functioning turbine [32–35], is available but incapable of sufficiently mimicking responses of live fish impacted by turbine blades. To that end, a biomimetic fish would be a useful surrogate for live animal tests because it could be used more than once and be validated using previously generated dose-response data.

Herein we detail the methods used to create a prototype biomimetic model fish (hereafter referred to as Gelfish) composed of ballistic gelatin and containing an embedded sensor. We used 3D scanning and imaging technologies to successfully replicate the general shape and surface features of multiple fish species. Scanned images were used to additively manufacture a reusable mold from which to cast the ballistic gelatin model. Ballistic gelatin was chosen for our initial model because of its extensive use as a tissue simulant in ballistic testing. Tissue durometer (firmness) of the Gelfish was compared to real fish tissue to assess biofidelity of our model. Durometer was chosen because it is easy to measure and is well-established in medicine to assess changes in tissue [36–38] and organ [39] hardness caused by disease, or to confirm biofidelity of cosmetic surgery [40,41], which suggests it is a viable option for fish tissue as well. In addition, preliminary observations of model flexibility were also compared to live fish to better assess Gelfish biofidelity following a simulated turbine blade strike. To our knowledge, 3D printing molds instead of the animal model directly, has not been applied to the production of a whole-organism biomimetic model before. More specifically, the objectives of this study were to 1) test the ability of ballistic gelatin to match whole-body firmness of fish tissues, 2) quantify how preparation temperature and warming time affect gelatin durometer, 3) determine efficacy of Plasti Dip® as a surrogate fish skin, 4) additively manufacture molds and cast gelatin models for at least five species of fish, 5) embed a 3-axis accelerometer into Gelfish to record characteristics of blade strike impact, and 6) compare Gelfish responses to available data from live fish when exposed to simulated blade strike impacts to help assess model biofidelity.

Materials and Methods

Ballistic Gelatin Experiments

To our knowledge, there are no published accounts of ballistic gelatin being used as a surrogate for fish tissue, so we designed several experiments to establish its baseline material properties. Ballistic gelatin was chosen because of its established use as a human and animal tissue simulant in ballistics research [42,43]. Furthermore, there are well

established protocols and recipes for ballistic gelatin that were easy to modify to meet our needs. We used ballistic gelatin powder specifically formulated to simulate human body density (Vyse® Professional Grade Ballistic Gelatin; Lot #12953; Custom Collagen, Inc., Addison, Illinois, USA) for all trials and final model preparation. Our main metric to measure the material properties of gelatin was tissue durometer (i.e., material hardness or resistance to indentation) for all ballistic gelatin trials. More specifically, we measured durometer with a Shore Type-OO durometer (Model DD-4 Digital Durometer; Precision = ± 0.1 units; Rex Instruments, Buffalo Grove, Illinois, USA) which is best suited to measure soft gels and animal tissue. An automated stand (Model OS-1 Operating Stand, Rex Instruments, Buffalo Grove, Illinois, USA) lowered the meter to the sample at precisely the same rate under a consistent load pressure for all samples, thereby decreasing measurement error.

In preliminary trials, we tested two methods of ballistic gelatin preparation that were modified from other sources to accommodate our smaller sample volumes [42–44]. Method one (referred to as cooling hydration) included heating deionized water to a desired temperature using a water bath (Thermo Scientific Precision Microprocessor Controlled 280 Series Water Bath; thermofisher.com), followed by adding the heated water into a large (~900 mL) polypropylene container containing gelatin powder. The water and gelatin were then mixed with a metal spatula until completely homogenized so that no clumps remained. At this point, up to 150 µL of de-foaming agent (Custom Collagen, Inc., Addison, Illinois, USA) was added to remove foam and excess bubbles. The mixture then cooled to room temperature (~22°C) which allowed the gelatin to hydrate. After this cooling hydration period, the container was covered with a lid and refrigerated for 12 hours at 4°C to allow the gelatin to completely set. Finally, the block of ballistic gelatin could be removed, cut into pieces, re-melted, and distributed as needed into other containers for testing. The second method (referred to as heated hydration) was similar to the previous except the heated water and gelatin mixture was covered with parafilm wax, placed back into the same temperature water-bath, and allowed to hydrate at this temperature for at least 10 minutes. Following the heated hydration period, the gelatin mixture could be distributed into test containers, allowed to cool to room

temperature, and refrigerated for 12 hours at 4°C. We preferred the heated hydration method because it allowed the gelatin mixture to hydrate without cooling, avoided evaporative water loss during re-melting, and samples could be poured immediately into test containers. Both methods produced comparable estimates of durometer in our ballistic gelatin samples, but heated hydration was preferred because of more consistent heating and avoided unnecessary re-melting. Lastly, we used cinnamon oil to increase the shelf-life of our ballistic gelatin samples well beyond the normal 7 to 11-day limitation [42,45]. We used cinnamon oil (NOW® Cinnamon Cassia oil; Item #051210; gnc.com) dissolved in 95% ethanol (1:10) at a concentration of 515 ppm as a microbial growth inhibitor. Cinnamon oil was dissolved in 95% ethanol to make it more miscible in water because pure cinnamon oil extract will separate from the gelatin [42]. Use of the heated hydration method and cinnamon oil ensured more consistent durometer measurements during experimental trials.

Most published accounts of ballistic gelatin include use of 10 or 20% solutions (mass to volume) of gelatin powder dissolved in deionized water [42,46]; however, we were unsure which concentration best mimicked fish tissue. We tested a total of five concentrations including 10, 15, 20, 25, and 30% to determine which concentration best approximated the durometer of actual fish tissue (see last experiment). Each ballistic gelatin concentration was prepared in triplicate. A heated hydration protocol with a preparation temperature of 65°C was used to create each gel mixture. Following hydration, ~60 mL of each replicate was added to a 100-mL, polystyrene weigh boat and allowed to cool at room temperature. When the gelatin reached room temperature (denoted by solidification of the gelatin) all samples were labelled, placed into a large, 33 × 38 cm, 6-Mil plastic storage bag, and refrigerated over-night. Following refrigeration, three randomly selected weigh boats were removed and allowed to warm to room temperature for 30 minutes. Ten durometer measurements were recorded for each sample by removing it from the weigh boat, flipping it over, and taking measurements across the gelatin's bottom surface. The durometer measurements for each replicate were averaged and the arithmetic mean of all three represented the average durometer of each concentration.

There are conflicting accounts of which water temperature is best for preparation of ballistic gelatin with respect to maintaining optimal material properties of gelatin. Preparation temperatures may range from 40 to 90°C or higher; however, manufacturers recommend temperatures near 40°C to maintain its tissue-simulating properties [46,47]. We also experimented with preparation temperature to determine how it affected the durometer of our ballistic gelatin samples. All ballistic gelatin samples in these experiments were made using a 25% gelatin concentration. Three temperature treatments – 45, 55, and 65°C – were prepared in triplicate and durometer was measured for each sample. In addition, we also tested how warming time following refrigeration affects durometer measurements. This experiment included preparation of three replicate gelatin samples using a concentration of 25% and a water temperature of 45°C. Following refrigeration, five durometer measurements were made immediately (time 0), every 10 min up to 1 hour, then 15 min up to 2 hours, and finally every 30 minutes for up to 4 hours. Durometer was measured and reported in the same manner as the concentration experiment for each temperature and warming time treatment.

The final set of experiments compared the material properties of ballistic gelatin to that of an actual fish to determine how closely we could mimic natural tissue. In addition to gelatin, we tested the use of an artificial skin surrogate that covered our ballistic gelatin samples. We used commercially available Plasti Dip® as a skin surrogate and found that spraying was preferable over dipping to sufficiently cover the gelatin samples. The first set of experiments was used to determine if the surrogate skin covering would significantly increase durometer compared to uncovered samples. We prepared an additional three replicates of 25% ballistic gelatin at 45°C for use in these tests. After refrigeration, we allowed samples to warm for 30 minutes and took 10 durometer measurements. One layer of surrogate skin was then applied to the gelatin sample and allowed to cure for 30 minutes under a fume hood. The samples were then refrigerated for an additional 12 hours, after which they were removed, allowed to warm for 30 minutes, and durometer measurements were taken. The same protocol was repeated for two, three, and four additional layers of surrogate skin for comparison. Next, we collected durometer data from three bluegill sunfish, *Lepomis macrochirus*, with a total

length of ~16 cm and mass of ~90 grams. All three fish were euthanized via overdose of 250 ppm clove oil in 95% ethanol (1:10) immediately prior to durometer measurements. Durometer was taken for each bluegill at 27 different locations along the entire body surface except the head which was mostly bone and the fins which were too thin to measure (Figure 24). In addition, the shapes of the Gelfish models and bluegill specimens required us to take durometer measurements by hand because both surfaces were curved which precluded use of the automated stand used for other ballistic gelatin experiments. Another set of 27 durometer measurements were taken on the same three fish after removing scales from the entire lateral surface. In this way, we created data sets for bluegill whole-fish durometer with and without scales for comparison of ballistic gelatin with and without a skin surrogate. Durometer was measured and reported in the same manner as the concentration experiment for each surrogate skin layer sample and bluegill tested.

All statistical tests were performed using R *v.4.0.2* statistical programing language and Sigma Plot v12. One-way analyses of variance (ANOVA) were used to compare the average durometer of 1) different ballistic gelatin concentrations prepared at 45 °C and 2) preparation temperature groups composed of 25% ballistic gelatin. A one-way repeated measures ANOVA was used to analyze the difference in average durometer between warming time and skin-layer treatment groups. Paired t-tests were used to compare average durometer between 1) Gelfish with and without Plasti Dip skin and 2) bluegill sunfish with and without scales, whereas an unpaired t-test was used to compare average durometer between Gelfish with skin and bluegill sunfish with scales. In the event a significant difference was detected by ANOVA, we used Benjamini-Hochberg post-hoc multiple comparison tests to determine the statistical relationship between treatment groups. Finally, linear regression was used to test the relationship between ballistic gelatin concentration and average durometer. All statistical decisions were based on $\alpha = 0.05$.

Fish Scanning and Image Collection

Most biometric image data used to create our Gelfish model originated from 3D scans of freshly caught fish. We scanned four species of fish including bluegill sunfish, rainbow trout (*Oncorhynchus mykiss*), gizzard shad (*Dorosoma cepedianum*), and white bass (*Morone chrysops*) which varied in size (Table 10). These species were chosen because they represent the range of fish body shapes that may pass through hydropower turbines and because blade strike laboratory data are available for each species [26–28,48,49]. To prepare for scanning, live fish were euthanized in an overdose of 250 ppm clove oil in 95% ethanol (1:10) for at least 15 minutes. Each fish was secured in an upright position with paired fins placed against the body and with the mouth and operculum closed. Individuals were frozen in this position at –20°C for 12 hours prior to scanning. Freezing was necessary to prevent movement of appendages during scanning which helped minimize image processing time. Additionally, the frozen fish was secured to a platform in an upright position that prevented movement but allowed for complete access to scan the entire fish. Finally, each fish was completely covered with a white, matte-finish spray paint to reduce surface reflections caused by fish scales. Two different scanners were used to capture fish images: a Leica Laser Tracker and Scanner (accuracy ± 0.060 mm; lieca-geosystems.com) and a FARO® SCANARM blue light laser scanner (accuracy ± 0.075 mm; www.faro.com). During scanning, Verisurf software (verisurf.com/software) was used to convert images into a point cloud file.

All laser-scanned point cloud data were processed and converted into a computer-aided design (CAD) model to be used for 3D printing. The point cloud data were converted to ASCII files and imported into Geomagic Design X (3dsystems.com) software. Some noise and unneeded areas (i.e., scanning platform or fish restraint device) of the point cloud file were manually removed. The dorsal, pelvic, and anal fins were removed from the model to simplify preparation of the mold. We used internal software features like “reduce noise” with a smoothing level of 1 and default levels of “sampling” to smooth the point cloud data. After smoothing, we used the “wrap” command to transform the point cloud into a mesh. If the mesh contained more holes the images went through additional smoothing using the “fill holes” or “repair” features to close minor or

larger gaps in the mesh, respectively. The final mesh was created by using “remesh”, “smooth”, and “remove spikes” features. Lastly, the final mesh was converted into a SolidWorks surface image, using the “auto surface” feature with the specifications of an organic geometry type, target patch count of 500, and default adaptive tolerance. The SolidWorks surface model was exported as a .STL file to be used in 3D printing of the fish mold.

We also investigated two additional forms of image acquisition including use of computed tomography scans of preserved specimens or from online databases. Our fifth and final species, American eel, *Anguilla rostrata*, was created by scanning a preserved specimen. The eel we used was much smaller than most sizes known to pass through hydropower turbines (Table 10); however, it was used to test our ability to account for and change fish size during image processing. The eel was scanned using a computed tomography scanner through the Diagnostic Imaging Service available at the University of Tennessee College of Veterinary Medicine (UTCVM). The computed tomography scan of the eel was saved as digital imaging and communications in medicine (DICOM) file. An online digital repository called Morphospace (morphospace.org) was also used to find additional x-ray, computed tomography (also computed axial tomography; CAT), or laser-scanned images for white bass, *Morone americana*. While we generated our own 3D scan data, we were also interested in how readily available online data might also be used to create fish molds. Computed tomography images (either directly imaged or taken from repositories) are not available in point cloud form, so these images were first converted into .STL files using open source InVesalius 3 (invesalius.github.io) software. A contrast range with a lower bound between 42 and 65 and an upper bound of 255 best captured skin traits and underlying skeletal structures while simultaneously filtering out noise. Next, CloudCompare (daniel.gm.net/cc/) and MeshLab (meshlab.net) or Geomagic Design X were used to convert the .STL file into a point cloud by sampling one million points, which ensured sufficient detail for the CAD model while minimizing computational resources. The conversion of point cloud to a surface model (i.e., an .STL file) followed the same procedure as that described above for laser-scanned images.

Mold Printing and Construction

Each CAD model was further reviewed, and final modifications were made to ensure clean demolding and purging of air during casting. The thickness of the caudal fin and peduncle was increased so that the final cast model made of ballistic gelatin would not rip when removed from the mold. The bluegill and gizzard shad CAD models only included the caudal fin, whereas the rainbow trout and white bass CAD models also included slightly raised areas on the dorsal and ventral surfaces to represent dorsal and anal fins, respectively. Additional features found in all the species CAD models were raised areas that represented the eyes and operculum on the head which were also important landmarks for positioning sensors. The eel CAD model also went through additional processing to remove its notably longer dorsal, anal, and caudal fins. Other modifications to the eel model included scaling-up body proportions to account for different sizes of eel because the original fish was smaller than most eels known to pass through turbines. A fill hole was added to each CAD model on the anterior (head region) through the mouth to avoid disrupting the shape of the body and allow easy access for filling the mold with ballistic gelatin. The final CAD model was split in half and an extruded box was placed around the fish to allow sufficient room for alignment holes, pry points, and mounting hardware that ensured the mold was properly sealed and aligned during casting. Molds were printed using a Stratasys Fortus 400mc printing system and were composed of spares infill acrylonitrile butadiene styrene (ABS). The inside of each half of the final molds were polished with acetone to completely seal each surface prior to casting [50,51].

Sensor Design and Specification

A 3-axis digital accelerometer (ADXL375, www.analog.com) with a capable measurement range of ± 200 g was used for data acquisition in the ballistic gelatin model during simulated blade strike impact trials. Output data was accessed through the I2C interface at the rate of 800Hz. The I2C protocol was configured with supply voltage V_S = 3.3V, interface voltage range V_(DD/IO) = 3.3V and external pull-up resistors R_P = 1020Ω (Figure 25). The maximum pull-up resistor value (R_{Pmax}) was limited to 1180Ω by

the rise time (t_r) for SCL and SDA and the capacitive load on each bus line (C_b), which is given by the following equation:

$$R_{Pmax} = \frac{t_r}{0.8437 \times C_b} \quad [1]$$

Data acquisition consisted of NI cRIO 9067 (sine.ni.com), utilized as a target device and NI 9402 (sine.ni.com) module to provide the digital lines for SDA and SCL wires of I2C protocol. All hardware was programmed in LabVIEW (sine.ni.com) using the SPI and I2C Driver API, which served as the I2C master, and used the NI 9402 digital I/O to interface with the accelerometer. The LabVIEW Host code included in the API, in addition to the FPGA code, was used for initializing the accelerometer, configuring the I2C protocol parameters, data read/write, and data logging operations. Data logging frequency was set via a timed loop in the host code and stored in a .tdms file with a local time stamp associated with each reading. Calibration of the sensor was achieved by following the single point calibration scheme specified by the original equipment manufacturer. The 0g measurements represent a potential bias in acceleration that can result in incorrect output from the sensor, so 0g measurements were specified for all three axes. This calibration scheme aligned the x- and y- axes to the 0g field, while the z-axis was oriented to the 1g field. Alignment with the 1g field also required additional sensitivity compensation of the z-axis to ensure 0g was registered correctly. All 0g offset values were then stored in the LabVIEW code and written to the dedicated offset registers during sensor initialization. The wired accelerometer was potted with black epoxy potting compound (3M-DP270, www.3m.com) using a custom mold. This provided the accelerometer, and the connections with the data acquisition system, necessary mechanical rigidity and watertight seal. The potted accelerometer was embedded into the ballistic gelatin model and could be used multiple times, i.e., used in multiple ballistic models without deterioration.

Gelfish Model Preparation and Testing

For our initial complete Gelfish model, we chose to use rainbow trout because the body depth and width of this species could better accommodate an accelerometer. During Gelfish production, the accelerometer was held in place within the rainbow trout mold

using a monofilament line that stretched from head to tail. We positioned the accelerometer posterior to where the operculum would be on a real fish. This location represents the mid-body area, which is associated with the highest rates of injury and mortality when fish are struck by hydropower turbine blades, including rainbow trout [26,28,30,31]. The mold was then securely closed and kept in an upright position to cast the mold. A 25% ballistic gelatin solution was prepared at 45°C and injected into the mold using a 60-mL syringe with an extended tip. The syringe tip was inserted completely into the mold and gelatin was injected from the bottom upwards to avoid formation of bubbles. After it was filled, the ballistic gelatin was cooled for 10 minutes at room temperature, followed by refrigeration at 4°C for 90 minutes. Refrigeration was used to accelerate cooling and decrease the time required for the gelatin to completely set. Following refrigeration, the ballistic gelatin model was removed from the mold, placed into a sealed plastic baggie, and refrigerated again at 4°C overnight. A surrogate skin (i.e., Plasti Dip®) was applied after overnight refrigeration such that four separate layers were added with at least 45 minutes of curing time between each layer. The final Gelfish model was then placed back into the baggie and refrigerated prior to its use in blade strike impact trials.

We used the same simulated blade strike apparatus and procedure described in Saylor et al. 2020, to strike the rainbow trout Gelfish model. We struck the Gelfish 12 times, with each strike accounting for a different velocity and leading-edge blade width, as well as a different impact location and orientation on the model itself, while all blade strikes with the model occurred at 90° (Table 11). These strike conditions were chosen based on previous laboratory tests which found that mid-body, lateral strikes caused the highest rates of injury and death among rainbow trout [26,28], and also based on relative proximity to the embedded accelerometer. We considered impacts a “direct” sensor strike when the blade made contact with the model at the approximate center of the accelerometer. Alternatively, an indirect impact was considered any strike where the blade made contact with the model posterior (towards caudal fin) and away from the accelerometer (Figure 26). All of these conditions were used to assess the ability of the accelerometer to detect differences in strike impact location on our model, which is

impossible to determine on live fishes that pass through hydropower turbines. All strikes were recorded at 1000 fps with a high-speed video camera (Model IL4, Fastec Imaging, San Diego, California) and integrated stroboscope LED lighting system (Monarch Nova-Pro 300, www.monarchinstrument.com) for later review and to confirm blade strike impact velocity.

Data acquisition from the 3-axis accelerometer was initiated immediately prior to engaging the simulated blade strike apparatus. Estimated blade impact velocity with Gelfish was calculated using the running average of the previous 10 frames (e.g., 10 msec) prior to and including impact. Following blade strike, acceleration data were averaged over 10 ms and 30 ms intervals. Maximum acceleration (α_{MAX}) was determined using the following equation:

$$a_{MAX} = MAX\left[\frac{1}{t_2 - t_1}\int_{t_1}^{t_2} a(t)dt\right] \qquad [2]$$

according to time t and the desired time interval t_1 to t_2 during the acceleration pulse, which is reported as acceleration of gravity (g). We estimated maximum acceleration using 10 and 30 ms running average intervals to test which interval best captured trends in acceleration. Maximum acceleration is a running average derived from National Highway Traffic Safety Administration (NHTSA) specifications for head injury criteria when using one accelerometer [52]. Observed acceleration (α_{obs}) was converted overall magnitude (across all three axes) according to the following equation:

$$\alpha_{obs} = \sqrt{\alpha_x^2 + \alpha_y^2 + \alpha_z^2} \qquad [3]$$

with observed values of gravitation acceleration for the x-axis (α_x), y-axis (α_y), and z-axis (α_z) at each time point, which was plotted as 10 ms and 30 ms running averages of observed acceleration against time (ms). Plots of acceleration were used to determine the relative difference in magnitude between strike impact scenarios (Table 11). In addition, we attempted to link changes in acceleration to rates of injury and mortality reported from previous blade strike impact experiments performed on live rainbow trout [28].

Results

Ballistic Gelatin Experiments

The ballistic gelatin concentration could be easily modified to account for different tissue durometers when prepared at 45°C and a standardized durometer measurement protocol was used. In fact, average durometer at 45°C significantly increased with every 5% increase in ballistic gelatin across the entire range tested (one-way ANOVA, $F_{4,10} = 162.40$, $p < 0.001$). We also detected a significant (one-way ANOVA, $F_{1,13} = 532.22$, $p < 0.0001$) relationship between ballistic gelatin concentration and average durometer given by the following linear model:

$$D_{30} = 1.48 \times BG + 0.33 \quad [4]$$

where D30 is the durometer following 30 minutes of warming and BG is the percentage of ballistic gelatin. Ballistic gelatin (prepared at 45°C) concentration explained ~97% of the variation in average durometer of the linear model ($R2 = 0.974$; Figure 27). Preparation temperatures of 45, 55, and 65°C did not significantly impact the durometer of our 25% ballistic gelation samples and all three temperatures produced an average durometer of ~35 units. Warming time significantly (one-way repeated measures ANOVA; $F_{14,28} = 378.96$, $p < 0.001$) impacted average durometer for 25% ballistic gelatin prepared at 45°C after 10 minutes of warming at room temperature (22.1°C) according to Benjamini-Hochberg multiple comparison tests. Average durometer continued to decrease significantly in a linear fashion after every 10 minutes for the first hour of warming except between the 20 to 30-min time period. The average durometer continued to decrease after each warming period but was not significant again until it warmed for 90 minutes. Eventually, average durometer reached its nadir near 44 units after 150 minutes of warming where it plateaued for the remainder of the warming experiment (Figure 28). Ballistic gelatin temperature increased quickly to 19°C within the first 60 minutes of warming and did not increase above 20°C for the remainder of this experiment (Figure 28).

The use of a surrogate skin increased average durometer of ballistic gelatin blanks (Table 12) and initial Gelfish models (Table 13). Addition of just one layer of surrogate

skin significantly (one-way repeated measures ANOVA; $F_{4,8} = 323.96$, $p < 0.001$) increased average durometer by ~10 units, according to a Benjamini-Hochberg pairwise comparison with samples without surrogate skin. Each additional layer applied to the ballistic gelatin samples also significantly increased durometer, except between two and three layers, which were both near 57 units (Table 12). Up to four layers of surrogate skin caused average durometer to increase by nearly 20 units, to 60.2 ± 0.9 units, compared to samples without surrogate skin (average durometer = 42.3 ± 0.5). Gelfish without surrogate skin (36.2 ± 0.6) had a significantly (two-tailed, dependent t-test; $t = -22.209$, $p = 0.002$) lower average durometer than the Gelfish model with surrogate skin (61.6 ± 1.4; Table 13). Similarly, bluegill sunfish with scales removed (54.0 ± 3.2) had significantly (two-tailed, dependent t-test, $t = 4.9391$, $p = 0.039$) lower average durometer than bluegill with scales intact (66.8 ± 1.8; Table 13). Lastly, average durometer of the Gelfish model with a surrogate skin was statistically indistinguishable from bluegill samples with scales according to a two-tailed, independent t-test (Figure 29).

3D Scanning and Printing Fish Molds

We successfully laser-scanned and printed molds for four species while a fifth was successfully printed from CT scan data. Scanning frozen fish in an upright position and use of Geomagic Design X software decreased image post-processing time from nearly 40 hours (manual processing) down to only 2 to 3 hours (with Geomagic software). The resulting SolidWorks models contained more surface features for the rainbow trout versus the bluegill, which required markedly more processing time (Figure 30). The SolidWorks surface models produced using this method were also easier to upload and it was easier to modify features such as fin thickness prior to printing, to ensure the resulting ballistic gelatin model did not tear (Figure 31). The time required to complete 3D printing of each mold varied by species (i.e., smaller species took less time) but was between 8 to 12 hours. Printing molds upright (versus lying flat) was necessary to limit warping of the mold halves from thermal stresses and ensured the mold halves sealed completely during casing. Acetone sealing successfully prevented ballistic gelatin infiltration through the mold, which reduced cleaning and ensured consistent casting for

each model. Additional mounting brackets were included on both the dorsal and ventral surface of the final mold, which allowed the accelerometer to be suspended within the ballistic gelatin using a monofilament line (Figure 32). Multiple Gelfish were cast from the same mold and there is no indication that casting multiple models deteriorated any of the molds. Total preparation time was ~12 hours, including casting (1.5 hours), model refrigeration at 4°C (8 hours), and application of four layers of surrogate skin (2.5 hours) to the model prior to testing. Many Gelfish models could be created during this time if multiple molds were available.

Gelfish Model Testing

The Gelfish model was capable of withstanding multiple blade strike impacts at comparably high velocities (i.e., up to 11.5 m/s) without deteriorating. The rainbow trout model was successfully exposed to nine different impact scenarios before the skin separated from gelatin model; however, the accelerometer remained functional for all 12 strike tests. While the surrogate skin did separate from the gelatin during testing, the gelatin did not deteriorate and could be reused after reapplying skin layers. Similarly, the accelerometer maintained its functionality and could also be cast into another model fish. The flexibility of the model also mimicked actual rainbow trout struck under the same conditions (i.e., mid-body, lateral strikes with 52-mm blade at ~6.8 m/s); though overall body curvature appeared to be slightly more pronounced with the Gelfish model (Figure 33). For example, body curvature of Gelfish was noticeably more pronounced during (+0.014s) and after (+0.024s) blade strike impact. The model also followed a similar trajectory out of the holding brackets following blade strike impact, which mimicked trials on live rainbow trout. The surrogate skin also allowed the model to maintain its integrity throughout the impact process, allowing the entire model (head to tail) to react similarly to real fish.

Changes in acceleration were detected in all three axes, including just prior to impact, during impact, and as the model moved away following contact with the blade (Figure 34). Peak magnitude generally occurred 10 ms after the bow wave produced by the blade pushed the model prior to impact. The entire impact sequence took less than 30

ms to complete. The highest peak magnitude and maximum acceleration were detected from a mid-body lateral strike with a 52-mm blade moving at 11.5 m/s (Table 11; Figure 34). All indirect strikes had noticeably lower peak magnitudes and maximum accelerations, regardless of other strike impact scenarios. Direct impacts to the mid-body ventral surface produced comparable levels of acceleration as mid-body lateral strikes and only differed in the main axis of movement caused by the strike, i.e., x-axis versus z-axis, respectively. Strikes with the same blade moving slower also had noticeably lower magnitudes—158.73 and 107.38 for the 52-mm blade moving 6.8 m/s and 76-mm blade moving at 5.0 m/s, respectively (Figure 25). Maximum acceleration detected with a 10 ms time interval was always higher than acceleration averaged across 30 ms, regardless of group. Gelfish trials completed without a surrogate skin (Trials 7 to 9) had lower values than the same trial performed on the Gelfish model with an intact surrogate skin (Trials 10 to 12; Table 11). Trends in magnitude and maximum acceleration suggest that the Gelfish model is also capable of detecting differences in impact scenarios, i.e., indirect strikes versus strikes at slower velocities or with thicker blades. A more detailed analysis of correlation with injury risk and mortality was not possible given that only one Gelfish model was tested.

Discussion

Ballistic gelatin (25% prepared at 45°C) was used successfully to mimic whole-body tissue firmness of real fish, i.e., bluegill sunfish (Figure 29). Furthermore, gelatin concentration can be easily modified to account for differences in durometer (15 to 45 units; Figure 27) among species, associated with anatomical disparities in scales and/or muscle tissue. Durometer also appears to be a reproduceable means of estimating the material properties and biofidelity of ballistic gelatin compared to real fish tissue. Durometer varied significantly as a result of warming, so experimental protocols must be standardized to ensure measured values can be compared, i.e., we used a 30-minute warming time at room temperature. The exact warming time does not matter provided it is used consistently during experimentation; however, warming in excess of 60 minutes may cause evaporative water loss and shrinkage of the gelatin. No change in average

durometer was detected based on preparation temperatures up to 65°C for 25% ballistic gelatin, but we suggest a 45°C (or lower) preparation temperature is ideal because additional heating is unnecessary. Temperatures greater than 65°C may cause detrimental changes to the material properties of ballistic gelatin prepared at lower concentrations of 10 or 20% [43,46]. Use of cinnamon oil increased the usable shelf-life of the Gelfish samples, but refrigeration was still required to avoid evaporative water loss associated with prolonged warming or air exposure. Plasti Dip applied over the ballistic gelatin created models that more closely mimicked the durometer of our whole-fish samples, and the number of layers could be used to further refine durometer as necessary (Table 12). The addition of simulated skin also maintained body shape integrity during blade strikes. Overall, ballistic gelatin appears to mimic tissue properties well, is non-toxic and easy to handle, and produces transparent models that are well-suited for implantation of additional sensors.

Our scanning techniques successfully created realistic 3D models and molds of multiple species that captured species-specific differences in external morphology. To our knowledge, this is first use of high-fidelity laser and computed tomography scans to design and produce a mold of an entire organism from which to cast a biomimetic model. To date, use of additive manufacturing for creation of high biofidelic models has mostly centered around 3D printing the desired animal model directly from scanned data [53–55]. The cost of printing multiple fish models directly is far greater than multiple models cast from just one mold; consequently, the additive manufacturing industry has focused on printing molds which are less labor intensive, cheaper to produce, and of comparable durability to traditional sand-cast molds [56–58]. Freezing fish worked well for scanning purposes to minimize movement of the specimen during scanning. The FARO scanning system was the easiest to use and produced a high-fidelity rendered model in about 10 minutes. In contrast, the Leica laser tracker and scanning system was very sensitive to slight deviations in fish positioning (caused by thawing) which made image rendering more difficult and increased post-processing time. Mounting the frozen fish on a turntable and securing the laser scanner may help decrease scanning time without compromising the quality of the 3D rendered images. Use of the software Geomagic

Design X decreased post-processing time and produced a final CAD model with more realistic landmarks (Figure 30B) compared to a model that required 40 hours of manual image processing (Figure 30A). Computed tomography scans of a small American eel (scanned at UTCVM) were also used to create a small and large eel mold. Similar CT scan data from online repositories were not always useful because many images only captured skeletal features and excluded soft tissues (e.g., muscle and skin) which are necessary to model body shape. The success of our 3D scanning and printing techniques suggests these methods can accurately recreate the desired features of any organism scanned directly or rendered from scans available via online databases.

Gelfish responses were similar to real fish with respect to overall flexibility during simulated impact trials. The model began to bend immediately prior to impact, followed by whole-body curvature during impact, and free movement after the impact sequence (Figure 33) which is similar to responses observed in rainbow trout laboratory trials [26,28,30,59]. Body curvature was observed as a spike in acceleration in the z-axis (e.g., lateral, side-to-side movement) and tumbling of the model after impact was observed as noticeable changes in acceleration across all three axes (Figure 34). The surrogate skin (Plasti Dip) enhanced overall Gelfish performance by adding stiffness to the model. Analysis of high-speed videos suggested that the amount of curvature in the Gelfish model may have exceeded that of real rainbow trout in its current form (Figure 33A4 & B4). Additional flexibility in our model is likely because it lacks an endoskeleton, overlapping myomeres, and imbricated scales of an actual fish which impose limits on natural flexibility. The number and size of vertebral centra, specifically, has a profound effect on flexibility (or stiffness) among fish [60–62] and inclusion of a simulated vertebral column could better mimic natural flexibility. In addition, the lack of a vertebral column and/or other support elements caused a delayed response in the movement of the tail compared to the body of the model, following contact with the blade. The Gelfish model was successfully struck 12 times without disintegrating, but the surrogate skin eventually separated from the gelatin and was removed after the ninth strike trial. The latter suggests that our model could be used more than once without losing its structural integrity and while maintaining consistent responses to multiple

impact scenarios. More detailed insights into model behavior or flexibility are not warranted because only one model was tested; however, the overall performance and response of Gelfish compared to actual fish supports the biofidelity of this basal model.

The single 3-axis accelerometer worked well to capture changes in acceleration that a fish may experience during impacts from turbine blades. We detected changes in acceleration during all aspects of the blade impact sequence, including a rise in acceleration as the blade approached, a peak during impact with the model, and random changes in all axes as the model tumbled after impact (Figure 34). The greatest changes in acceleration co-occur with lateral bending of the model along the z-axis, observed during review of high-speed videography (Figure 33). While we only tested one complete model, there were notable changes in absolute magnitude and time-averaged acceleration associated with blade leading-edge width, impact velocity, and orientation of the model (Table 11). More specifically, faster velocities and the thinnest blade had the highest observed changes in peak and time-averaged acceleration—these conditions are also thought to be the most injurious and lethal to rainbow trout struck by turbine blades [26,28,30,59]. Trends in time-averaged acceleration (both 10 and 30 ms) also detected higher changes in peak magnitude as a result of mid-body lateral strikes, compared to both tail lateral and mid-body ventral strikes, which is consistent with estimated mortality rates for this species [26,28]. The exact relationship between acceleration and probability of injury or mortality has yet to be determined; however, development of injury criteria and/or probability of fracture models, similar to automobile safety tests [52,63–65], may help connect accelerometer data to laboratory dose-response relationships. Our sensor detected similar estimates of peak acceleration as the Sensor Fish package (i.e., 213 and 223 g, respectively) struck under the same conditions, and at a higher velocity of 7.5 m/s [26]. The latter suggests our sampling rate of 800 Hz was capable of detecting comparable levels of peak acceleration, given that the Sensor Fish sampling frequency is 2.5 times higher [33,34]. More impact trials are needed on multiple Gelfish models to establish repeatability and estimate the variation in peak magnitude before making more detailed comparisons between Gelfish and Sensor Fish.

Conclusions

Use of ballistic gelatin and 3D scanning to produce reusable molds worked well to recreate the overall shape and basic biomechanical properties of a real fish. Ballistic gelatin was easy to work with and could be modified to account for small changes in tissue firmness related to different species. Ballistic gelatin does have a limited shelf life (even with preservatives) and the need for refrigeration was important to minimize evaporative water loss. The Plasti Dip surrogate skin also appeared to bond well with ballistic gelatin and its inclusion better captured the natural flexibility of a real fish following impact from a simulated turbine blade. Laser and CT scan image data were successfully used to capture the overall shape and identifying surface details of each fish species. Scanning frozen fish was necessary to limit unwanted movement of the fish, which would significantly increase post-processing time. We successfully used these scanned images to create and print molds using additive manufacturing, which enabled casting of multiple models with no indication of mold deterioration.

The response of the Gelfish model from simulated impact conditions suggests it may be slightly more flexible than real fish, but more tests are required to quantitively confirm its biomechanical properties. Results of blade strike impact tests suggest that the embedded accelerometer detected changes in acceleration associated with impacts at different velocities, leading edge widths, and locations along the body. These changes were consistent with the responses of actual fish exposed to the same scenarios, i.e., differential rates of injury and mortality as strike conditions change. Changes in time-averaged and peak acceleration will likely be most useful if linked to novel injury criteria or mortality thresholds like those used during impact safety tests in the automobile industry. Initial production of prototype Gelfish was successful, but more development is needed to assess its biomechanical accuracy and determine how sensor output may be linked to rates of injury or mortality detected during dose-response testing.

The basic Gelfish model and the process used to create it needs further development to augment its biofidelity and make it more versatile for use in other applications. At the least, additional impact trials on multiple models are needed to establish variation in model responses and assess the replicability of sensor output. While

our method can produce any desired species, the same model would be more useful if it accurately represented groups of similar fishes (taxonomically or functionally) defined by the intended application. For example, surrogate species are used to represent taxonomic groups of fishes for blade strike trials, yet the functional or biomechanical relevance of these groups has yet to be addressed [28].

Ballistic gelatin worked well to mimic fish tissue but refrigeration was necessary to prevent water loss and warming time affected firmness of the model. Newer versions of this model may seek to create a model using synthetic polymers which can be modified to enhance model biofidelity without the need for refrigeration or preservatives. Further development of a simulated skin, and dedicated inclusion of structures that mimic the materials properties of bone and organs, may also better approximate the natural flexibility and responses of the fish body. All new model developments should be replicated and the biomechanics of impact observed in the model should be compared to that of real fish to maximize biofidelity. Inclusion of more than one accelerometer or the use of new sensors, including strain or fracture gauges, would provide additional information to better link sensor output with biological response data. The next model should also prioritize smaller sensors with higher sampling rates that increase the precision of sensor output while minimizing unnecessary gains in mass to the model. Finally, newer versions of Gelfish would benefit from onboard storage and/or wireless communication technologies to allow it to move more freely and make it recoverable during field tests.

While we developed this model with hydropower applications in mind, our techniques described here may have other applications well. Similar applications might include 1) testing blade strikes associated with irrigation and water pumping stations, 2) strikes from marine hydrokinetic turbines, 3) impacts from boat impellors on large fishes (e.g., sturgeon or paddlefish) and coastal marine mammals (manatees and whales), 4) mortality of birds and bats caused by impacts from wind turbine blades, and 5) mortality among fish, sea turtles, and other marine life caused by unintended interactions with commercial fishing gear. Regardless, biofidelity remains paramount for future Gelfish

development and application, which further distinguishes it from lower-biofidelity technologies, like Sensor Fish, currently used in a similar application.

Acknowledgements

We must first and foremost thank Mark Peterson, Brennan Smith, Eric Pierce, and Stan Wullschleger (Energy and Environment Sciences Directorate Energy Efficiency and Renewable Energy Program, Oak Ridge National Laboratory) for their fervent and continued support of this project from the beginning. We also thank summer intern Clara Layzer for her work and insights during initial development of the Gelfish project. Much thanks are given to the members of the Laboratory Directed Research and Development (LDRD) Seed Money Fund Committee and the anonymous reviewers of our proposal for their feedback and support. Lastly, we thank Teresa Mathews (Group Leader, Biodiversity and Ecosystem Health Group, ORNL) for her technical review and comments on this article.

References

1. Fish, F.E. Limits of nature and advances of technology: What does biomimetics have to offer to aquatic robots? *Appl. Bionics Biomech.* **2006**, *3*, 49–60.

2. Salazar, R.; Fuentes, V.; Abdelkefi, A. Classification of biological and bioinspired aquatic systems: A review. *Ocean Eng.* **2018**, *148*, 75–114.

3. Triantafyllou, M.S.; Weymouth, G.D.; Miao, J. Biomimetic survival hydrodynamics and flow sensing. *Annu. Rev. Fluid Mech.* **2016**, *48*, 1–24.

4. Kottapalli, A.G.P.; Asadnia, M.; Miao, J.; Triantafyllou, M.S. Biomimetic microsensors inspired by marine life. *Biomim. Microsens. Inspired by Mar. Life* **2016**, 1–112.

5. Yang, Y.; Nguyen, N.; Chen, N.; Lockwood, M.; Tucker, C.; Hu, H.; Bleckmann, H.; Liu, C.; Jones, D.L. Artificial lateral line with biomimetic neuromasts to emulate fish sensing. *Bioinspiration and Biomimetics* **2010**, *5*.

6. Fish, F.E.; Kocak, D.M. Biomimetics and marine technology: An introduction. *Mar. Technol. Soc. J.* **2011**, *45*, 8–13.

7. Lauder, G. V.; Wainwright, D.K.; Domel, A.G.; Weaver, J.C.; Wen, L.; Bertoldi, K. Structure, biomimetics, and fluid dynamics of fish skin surfaces. *Phys. Rev. Fluids* **2016**, *1*.

8. Wainwright, D.K.; Lauder, G. V. Mucus matters: The slippery and complex surfaces of fish. In *Function Surfaces in Biology III*; Gorb, S.N., Gorb, E. V., Eds.; Springer International Publishing: Gewerbestrasse, Switzerland, **2017**; pp. 223–246 ISBN 9783319741437.

9. Hosseini, S.; Tabrizi, K.D.; Meghdari, A. Design and fabrication and hydrodynamic analysis of a fish robot for underwater surveillance. *Int. J. Mod. Stud. Mech. Eng.* **2019**, *5*.

10. Zhang, L.; Zhao, W.; Hu, Y.; Zhang, D.; Wang, L. Development and depth control of biomimetic robotic fish. *IEEE Int. Conf. Intell. Robot. Syst.* **2007**, 3560–3565.

11. Serchi, F.G.; Arienti, A.; Laschi, C. Biomimetic vortex propulsion: Toward the new paradigm of soft unmanned underwater vehicles. *IEEE/ASME Trans. Mechatronics* **2013**, *18*, 484–493.

12. Browning, A.; Ortiz, C.; Boyce, M.C. Mechanics of composite elasmoid fish scale assemblies and their bioinspired analogues. *J. Mech. Behav. Biomed. Mater.* **2013**, *19*, 75–86.

13. Sherman, V.R.; Quan, H.; Yang, W.; Ritchie, R.O.; Meyers, M.A. A comparative study of piscine defense: The scales of Arapaima gigas, Latimeria chalumnae and Atractosteus spatula. *J. Mech. Behav. Biomed. Mater.* **2017**, *73*, 1–16.

14. Zhu, D.; Szewciw, L.; Vernerey, F.; Barthelat, F. Puncture resistance of the scaled skin from striped bass: Collective mechanisms and inspiration for new flexible armor designs. *J. Mech. Behav. Biomed. Mater.* **2013**, *24*, 30–40.

15. Yang, W.; Chen, I.H.; Gludovatz, B.; Zimmermann, E.A.; Ritchie, R.O.; Meyers, M.A. Natural flexible dermal armor. *Adv. Mater.* **2013**, *25*, 31–48.

16. Bennett, R.H.; Ellender, B.R.; Mäkinen, T.; Miya, T.; Pattrick, P.; Wasserman, R.J.; Woodford, D.J.; Weyl, O.L.F. Ethical considerations for field research on fishes. *Koedoe* **2016**, *58*, 1–15.

17. Cooke, S.J.; Wilson, A.D.M.; Elvidge, C.K.; Lennox, R.J.; Jepsen, N.; Colotelo, A.H.; Brown, R.S. Ten practical realities for institutional animal care and use committees when evaluating protocols dealing with fish in the field. *Rev. Fish Biol. Fish.* **2016**, *26*, 123–133.

18. Sloman, K.A.; Bouyoucos, I.A.; Brooks, E.J.; Sneddon, L.U. Ethical

considerations in fish research. *J. Fish Biol.* **2019**, *94*, 556–577.

19. Couto, M.; Cates, C. Laboratory guidelines for animal care. In *Vertebrate Embryogenesis*; Pelegri, F., Ed.; Spring Science+Business media, LLC: Humana, New York, NY, **2019**; pp. 407–430.

20. Borski, R.J.; Hodson, R.G. Fish research and the institutional animal care and use committee. *ILAR J.* **2003**, *44*, 286–294.

21. Lawrence, C.; Sanders, G.E.; Varga, Z.M.; Baumann, D.P.; Freeman, A.; Baur, B.; Francis, M. Regulatory compliance and the zebrafish. *Zebrafish* **2009**, *6*, 453–456.

22. EIA, (Energy Information Administration) Hydropower Explained Available online: https://www.eia.gov/energyexplained/index.php?page=hydropower_home (accessed on Dec 23, 2020).

23. Pracheil, B.M.; McManamay, R.A.; Bevelhimer, M.S.; DeRolph, C.R.; Čada, G.F. A traits-based approach for prioritizing species for monitoring and surrogacy selection. *Endanger. Species Res.* **2016**, *31*, 243–258.

24. Silva, A.T.; Lucas, M.C.; Castro-Santos, T.; Katopodis, C.; Baumgartner, L.J.; Thiem, J.D.; Aarestrup, K.; Pompeu, P.S.; O'Brien, G.C.; Braun, D.C.; et al. The future of fish passage science, engineering, and practice. *Fish Fish.* **2018**, *19*, 340–362.

25. Uria-Martinez, R.; Johnson, M.M.; O'Connor, P.W.; Samu, N.M.; Witt, A.M.; Battey, H.; Welch, T.; Bonnet, M.; Wagoner, S. *2017 Hydropower Market Report*; Oak Ridge, Tennessee, **2018**.

26. Bevelhimer, M.S.; Pracheil, B.M.; Fortner, A.M.; Saylor, R.; Deck, K.L. Mortality and injury assessment for three species of fish exposed to simulated turbine blade strike. *Can. J. Fish. Aquat. Sci.* **2019**, *76*, 2350–2363.

27. Saylor, R.; Fortner, A.; Bevelhimer, M. Quantifying mortality and injury susceptibility for two morphologically disparate fishes exposed to simulated turbine blade strike. *Hydrobiologia* **2019**, *842*, 55–75.

28. Saylor, R.; Sterling, D.; Bevelhimer, M.; Pracheil, B. Within and among fish species differences in simulated turbine blade strike mortality: Limits on the use of surrogacy for untested species. *Water* **2020**, *12*, 1–27.

29. Turnpenny, A.W.H.; Davis, M.H.; Fleming, J.M.; Davies, J.K. *Experimental studies relating to the passage of fish and shrimps through tidal power turbines*; Southampton, United Kingdom, **1992**.

30. EPRI, (Electric Power Research Institute) *Evaluation of the effects of turbine blade leading edge design on fish survival*; Palo Alto, CA, **2008**.

31. Amaral, S. V; Watson, S.M.; Schneider, A.D.; Rackovan, J.; Baumgartner, A. Improving survival: Injury and mortality of fish struck by blades with slanted, blunt leading edges. *J. Ecohydraulics* **2020**.

32. Deng, Z.; Carlson, T.; Duncan, J.; Richmond, M. Applications of the sensor fish technology. *Hydro Rev.* **2007**, *26*, 10–14.

33. Deng, Z.; Carlson, T.J.; Duncan, J.P.; Richmond, M.C. Six-degree-of-freedom sensor fish design and instrumentation. *Sensors* **2007**, *7*, 3399–3415.

34. Deng, Z.D.; Lu, J.; Myjak, M.J.; Martinez, J.J.; Tian, C.; Morris, S.J.; Carlson, T.J.; Zhou, D.; Hou, H. Design and implementation of a new autonomous sensor fish to support advanced hydropower development. *Rev. Sci. Instrum.* **2014**, *85*.

35. Carlson, T.J.; Duncan, J.P.; Gilbride, T.L. The Sensor Fish: Measuring fish passage in severe hydraulic conditions. *Hydro Rev.* **2003**, *22*, 62–69.

36. Falanga, V.; Bucalo, B. Use of a durometer to assess skin hardness. *J. Am. Acad. Dermatol.* **1993**, *29*, 47–51.

37. Moon, K.W.; Song, R.; Kim, J.H.; Lee, E.Y.; Lee, E.B.; Song, Y.W. The correlation between durometer score and modified Rodnan skin score in systemic sclerosis. *Rheumatol. Int.* **2012**, *32*, 2465–2470.

38. Cuaderes, E.; Khan, M.M.; Azzarello, J.; Lamb, L.W. Reliability and limitations of the durometer and PressureStat to measure plantar foot characteristics in Native Americans with diabetes. *J. Nurs. Meas.* **2009**, *17*, 3–18.

39. Belyaev, O.; Herden, H.; Meier, J.J.; Muller, C.A.; Seelig, M.H.; Herzog, T.; Tannapfel, A.; Schmidt, W.E.; Uhl, W. Assessment of pancreatic hardness — Surgeon versus durometer. *J. Surg. Res.* **2010**, *158*, 53–60.

40. Brown, T.; Brown, S.; Murphy, T. Breast durometer (mammometer): A novel device for measuring soft-tissue firmness and its application in cosmetic breast surgery. *Aesthetic Plast. Surg.* **2017**, *41*, 265–274.

41. Murphy, T.; Brown, S.; Brown, T.; Plast, F.; Plast, F. A durometer (mammometer) for objective measurement capsular contraction following breast implant surgery. *Am. J. Cosmet. Surg.* **2020**, 1–6.

42. Jussila, J. Preparing ballistic gelatine - Review and proposal for a standard method. *Forensic Sci. Int.* **2004**, *141*, 91–98.

43. Maiden, N.R.; Fisk, W.; Wachsberger, C.; Byard, R.W. Ballistics ordnance gelatine - How different concentrations, temperatures and curing times affect calibration results. *J. Forensic Leg. Med.* **2015**, *34*, 145–150.

44. Cronin, D.S. Ballistic gelatin characterization and constitutive modeling. In Proceedings of the Proceedings of the 2011 Annual Conference on Experimental and Applied Mechanics; Proulx, T., Ed.; Spring Science+Business media, LLC: New York city, NY, **2011**; Vol. 1, pp. 51–55.

45. Staymates, J.L.; Gillen, G. Fabrication and characterization of gelatin-based test

materials for verification of trace contraband vapor detectors. *Analyst* **2010**, *135*, 2573–2578.

46. Cronin, D.S.; Falzon, C. Characterization of 10% ballistic gelatin to evaluate temperature, aging and strain rate effects. *Exp. Mech.* **2011**, *51*, 1197–1206.

47. Fackler, M.L.; Malinowski, J.A. *Ordnance gelatin for ballistic studies: Detrimental effect of excess heat used in gelatin preparation*; San Francisco, California, **1987**.

48. Bevelhimer, M.S.; Derolph, C.R. *Market assessment for hydropower turbine design tools using integrated datasets of dams, turbines, owners, and fish*; **2019**.

49. Pracheil, B.M.; DeRolph, C.R.; Schramm, M.P.; Bevelhimer, M.S. A fish-eye view of riverine hydropower systems: The current understanding of the biological response to turbine passage. *Rev. Fish Biol. Fish.* **2016**, *26*, 153–167.

50. Lalehpour, A.; Barari, A. Post processing for fused deposition modeling parts with acetone vapour bath. *IFAC-PapersOnLine* **2016**, *49*, 42–48.

51. Sikder, S.; Barari, A.; Kaji, F.; Kishawy, H. Using acetone vapour treatment to improve secondary finishing operations in additive manufacturing. *Proc. - ASPE 2014 Spring Top. Meet. Dimens. Accuracy Surf. Finish Addit. Manuf.* **2014**, *3898*, 223–224.

52. Eppinger, R.; Sun, E.; Bandak, F.; Haffner, M.; Khaewpong, N.; Maltese, M.; Kuppa, S.; Nguyen, T.; Takhounts, E.; Tannous, R.; et al. *Development of improvied injury criteria for the assessment of advanced automotive restraint systems - II*; Washington, D.C., **1999**.

53. Walker, M.; Humphries, S.; Walker, M.; Banks, J. 3D printing: Applications in evolution and ecology. *Ecol. Evol.* **2019**, *9*, 4289–4301.

54. Rhyne, B.J.; Post, B.K.; Chesser, P.; Roschli, A.; Love, L.J. Reverse engineering

a transhumeral prosthetic design for additive manufacturing. In Proceedings of the Proceedings of the 28th Annual International Solid Freeform Fabrication Symposium – An Additive Manufacturing Conference; University of Texas, Austin: Austin, Texas, **2017**; pp. 2419–2429.

55. Tetzla, S.J.; Estrada, A.; Degregorio, B.A.; Sperry, J.H. Identification of factors affecting predation risk for juvenile turtles using 3D printed models. *Animals* **2020**, *10*, 1–16.

56. Hassen, A.A.; Springfield, R.; Lindahl, J.; Post, B.; Love, L.; Duty, C.; Vaidya, U.; Pipes, R.B.; Kunc, V. The durability of large-scale additive manufacturing composite molds. In Proceedings of the The Composites and Advanced Materials Expo. Conference Proceedings; Beckwith, S.W., Brusso, J., Busel, J., Fullwood, D., Hyden, M., Howell, D., Eds.; American Composites Manufacturers Association: Anaheim, California, **2016**; pp. 1–10.

57. Hassen, A.A.; Noakes, M.; Nandwana, P.; Kim, S.; Kunc, V.; Vaidya, U.; Love, L.; Nycz, A. Scaling up metal additive manufacturing process to fabricate molds for composite manufacturing. *Addit. Manuf.* **2020**, *32*, 101093.

58. Hawaldar, N.; Zhang, J. A comparative study of fabrication of sand casting mold using additive manufacturing and conventional process. *Int. J. Adv. Manuf. Technol.* **2018**, *97*, 1037–1045.

59. EPRI, (Electric Power Research Institute) *Tests examining survival of fish struck by turbine blades*; Palo Alto, CA, **2011**.

60. Long, J.H.; Nipper, K.S. The importance of body stiffness in undulatory propulsion. *Am. Zool.* **1996**, *36*, 678–694.

61. Brainerd, E.L.; Patek, S.N. Vertebral column morphology, C-start curvature, and the evolution of mechanical defenses in tetraodontiform fishes. *Copeia* **1998**, 971–984.

62. Lindsey, C.C. Form, fuction, and locomotory habits in fish. In *Fish Physiology Volume 7 Locomotion*; Hoar, W.S., Randall, D.J., Eds.; Academic Press, Inc, **1978**; pp. 1–100 ISBN 0123504074.

63. Digges, K.H. Injury measurements and criteria. In Proceedings of the RTO Meeting Proceedings 20: Models for Aircrew Safety Assessment: Uses, Limitations and Requirements; Quebec, Canada, 1998; p. K2.1-K2.5.

64. McHenry, B. Head injury criterion and the ATB. In Proceedings of the ATB Users' Group; Salt Lake City, Utah, **2004**; pp. 1–8.

65. Faerber, E.; Kramer, F. On the application of the HIC as head protection criterion. In Proceedings of the Proceedings of the International Research Council on the Biomechanics of Injury; I: Goteberg, Germany, **1985**; pp. 235–252.

Appendix

Table 10. Size dimensions and scanning techniques used to create 3D images of each fish species.

Common name	TL (cm)	M (g)	Scanning Method
Bluegill	16.4	85.9	FARO® SCANARM
Rainbow trout	25.5	157.9	Leica Laser Tracker & Scanner
Gizzard shad	18.4	50.0	Leica Laser Tracker & Scanner
White bass	28.0	297.8	FARO® SCANARM
American eel	27.5	24.4	Computed-tomography

NOTE: The total length (TL) and wet mass (M) is included with each species scanned in this study.

Table 11. Blade strike impact conditions and changes in acceleration from trials performed on the rainbow trout Gelfish model.

Trial No.	Blade width (mm)	Blade velocity (m/s)	Location (H, M, T)	Orientation (D, L, V)	Alignment axis (x, y, z)	Impact relative to sensor	A_{MAX} (g)		Peak magnitude (g)
							10 ms	30 ms	
1	52	11.5	M	L	x	Direct	102.52	64.72	213.90
2	52	11.5	T	L	x	Indirect	98.32	51.95	145.23
3	52	11.5	M	V	y	Direct	102.12	56.17	197.47
4	52	6.8	M	L	x	Direct	69.59	37.69	158.73
5	52	6.8	M	L	x	Indirect	53.48	26.13	81.32
6	52	6.8	M	V	y	Direct	65.39	35.42	175.01
7	76	5.0	M	L	x	Direct	43.99	25.50	107.38
8	76	5.0	T	L	x	Indirect	33.12	16.19	39.27
9	76	5.0	M	V	y	Direct	45.98	25.20	132.60
10*	76	5.0	M	L	x	Direct	42.89	25.25	77.03
11*	76	5.0	T	L	x	Indirect	34.76	19.68	44.07
12*	76	5.0	M	V	y	Direct	38.31	24.85	103.46

NOTE: Location of strike was mid-body (M) or tail (T) while orientation was lateral (L) or ventral (V). Alignment axis refers to which of three axes the Gelfish model aligned when held in place prior to blade strike testing. Impacts relative to the sensor were considered "Direct" if the blade contacted the model fish at the center of the accelerometer whereas "Indirect" strikes occurred when the blade made contact with the model posterior (towards the caudal fin) to the accelerometer. *The Gelfish model used in trials 10 to 12 was the same as trials 7 to 9 except the surrogate skin was removed from the model prior to strike.

Table 12. Results of a one-way repeated measures ANOVA ($F_{4,8} = 323.96$, $p < 0.001$) on average durometer versus number of surrogate skin layers applied to ballistic gelatin samples.

No. of Surrogate Skin Layers	Durometer (± SE)	Significance
None	42.3 ± 0.5	a
1-layer	53.8 ± 0.4	b
2-layers	57.0 ± 0.1	c
3-layers	57.3 ± 0.4	c
4-layers	60.2 ± 0.4	d

Note: Durometer is presented as average ± standard error (SE) for each skin-layer group (n = 3 replicates per group). Skin layer groups with different letters indicate a significant difference according to Benjamini-Hochberg multiple comparison tests. All statistical decisions were based on $\alpha = 0.05$.

Table 13. Results of statistical tests on durometer for Gelfish models and intact bluegill samples.

No.	Group of Interest	Durometer (± SE)	Paired-t	Unpaired-t
1	Gelfish no skin	36.2 ± 0.6	a	--
2	Gelfish with surrogate skin	61.6 ± 1.4	b	c
3	Bluegill intact	66.8 ± 1.8	x	d
4	Bluegill without scales	54.0 ± 3.2	y	--

Note: Durometer is presented as average ± standard error (SE) for each group (n = 3 replicates per group). Significance tests included paired (dependent) or unpaired (independent) t-tests—groups with different letters were considered statistically significant based on $\alpha = 0.05$. Paired t-tests were only performed between Gelfish (skin versus no skin) or bluegill (intact versus without scales) groups, while one unpaired t-test was used to compare average durometer of Gelfish with skin to intact bluegill.

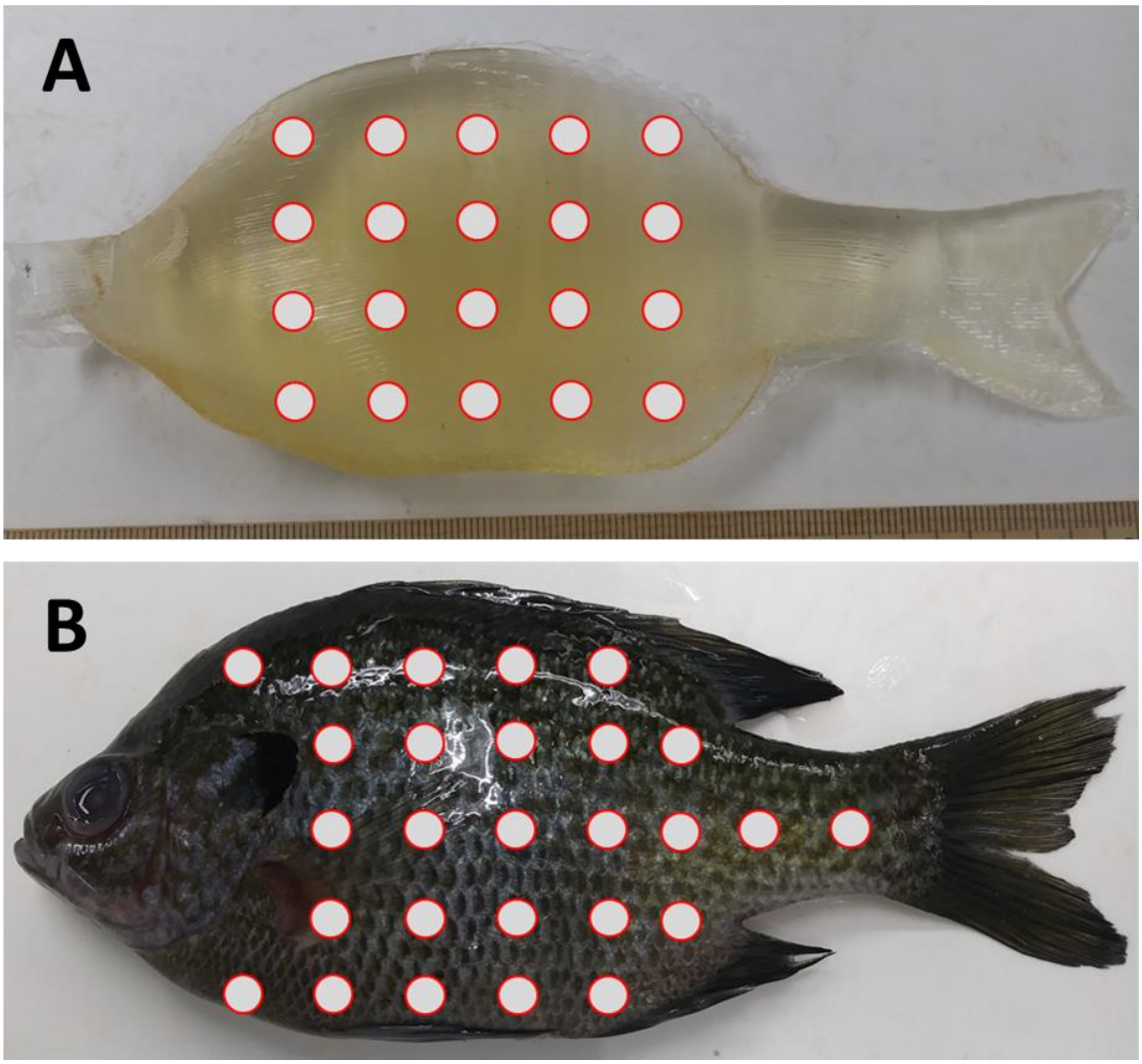

Figure 24. Relative durometer measurement locations (circles) were taken on the left side of (A) Gelfish cast without skin and (B) bluegill with scales. Durometer measurements were replicated for both Gelfish and actual bluegill, i.e., n = 3 for each. The Gelfish models and bluegill were ~16 cm total length and ~90 g mass. We also measured Gelfish with surrogate skin and bluegill without scales at the same approximate locations (not pictured).

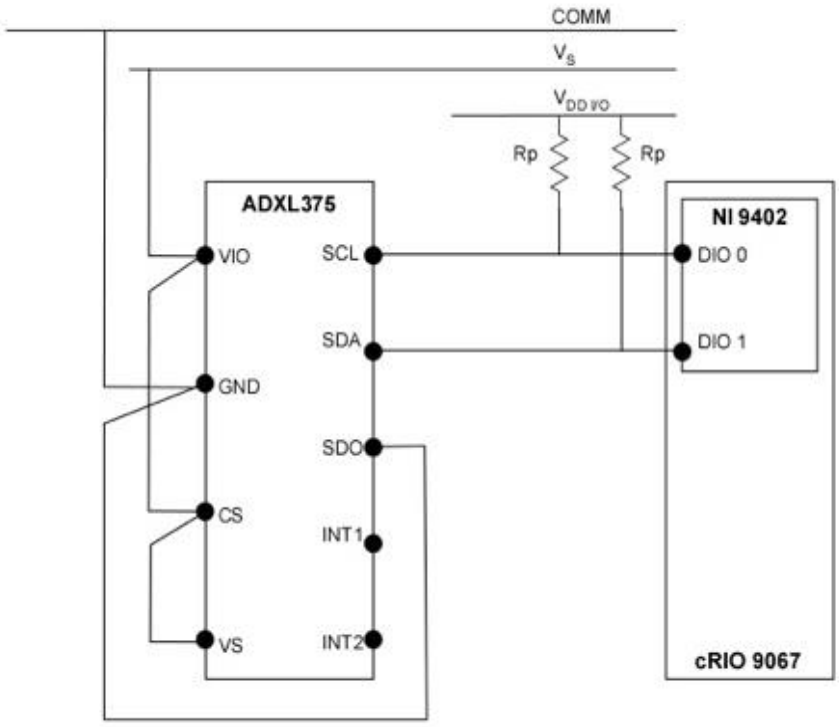

Figure 25. Wiring schematic of the single 3-axis accelerometer (ADXL375), data acquisition (cRIO 9067), and interface system (NI 9402) used in the Gelfish model.

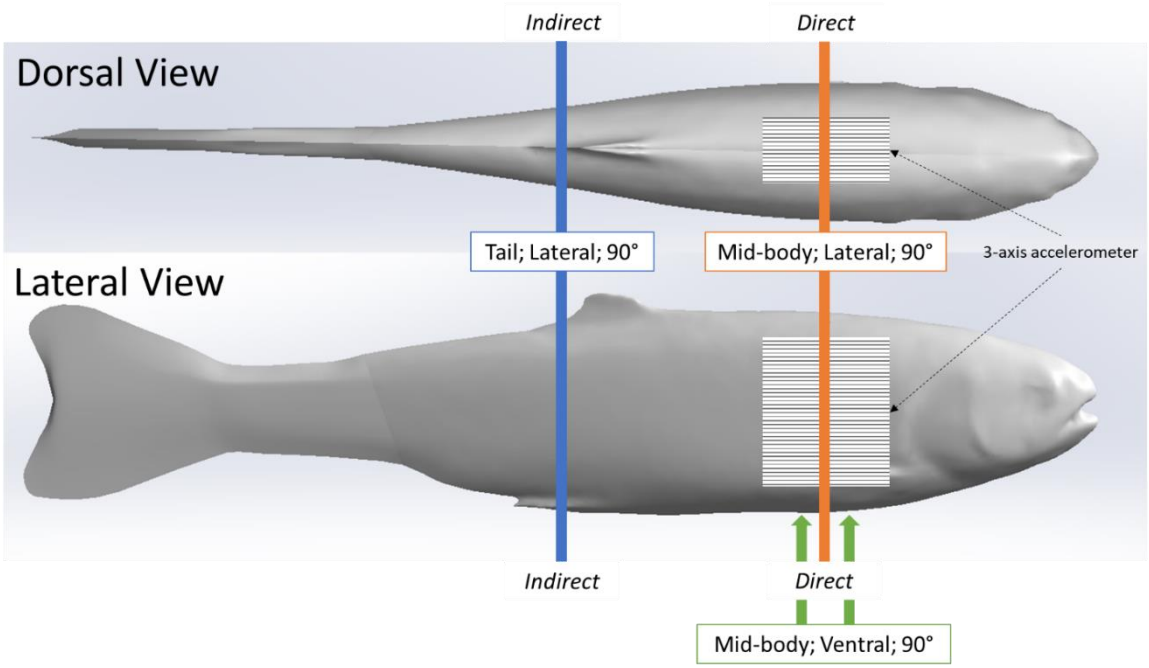

Figure 26. Relative location of 12 blade strike impact trials performed on our rainbow trout Gelfish model. Direct impacts were associated with mid-center strikes to the 3-axis accelerometer embedded posterior to the operculum. Indirect strikes occurred near the caudal fin so that any acceleration was the result of movement following strike. Vertical lines indicate the relative location and orientation combinations we tested including mid-body lateral strikes (orange), tail lateral strikes (blue), and mid-body ventral strikes (green) – all strikes occurred at a 90° angle relative to the longitudinal axis of the model.

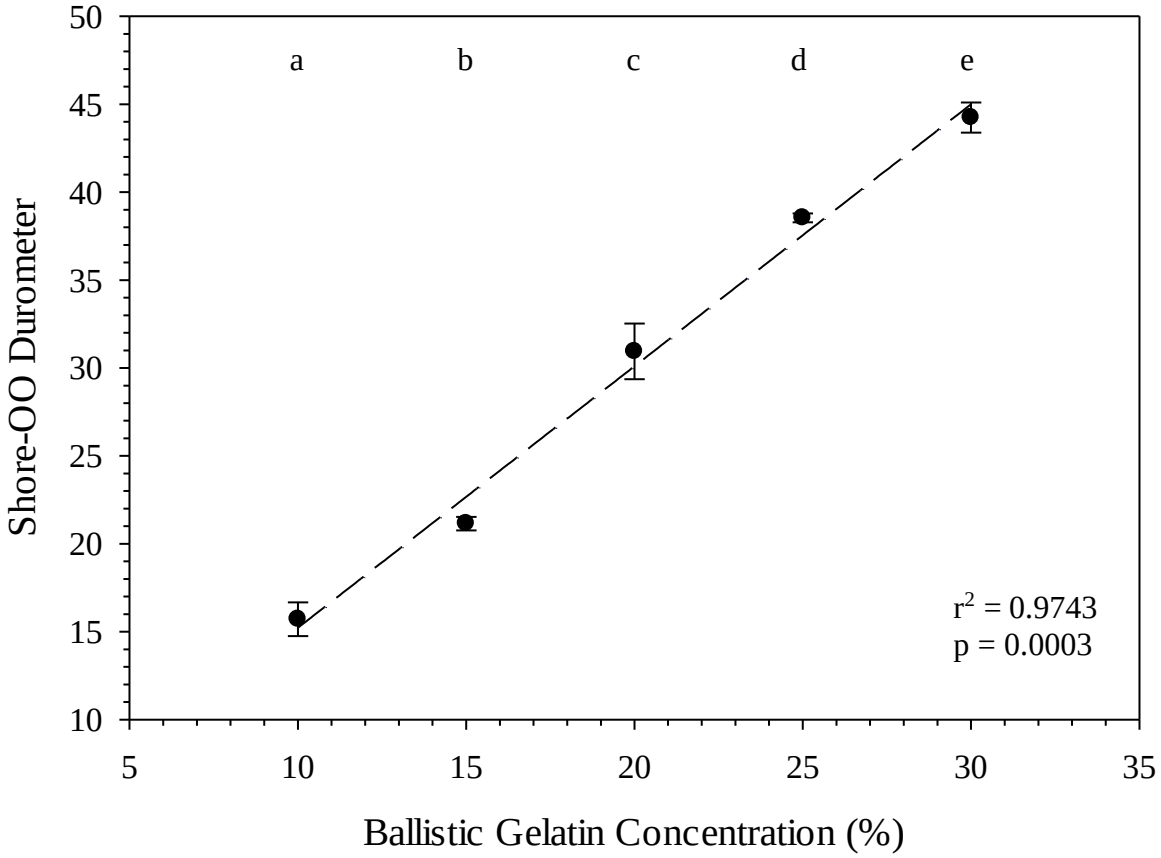

Figure 27. Average Shore-OO durometer versus ballistic gelatin concentration. The dashed line (— —) represents a significant linear regression model ($F_{1,14} = 532.22$, $p < 0.0001$, $r^2 = 0.9743$) fit to these data. Concentration groups with different letters indicate a significant difference according to Benjamini-Hochberg pairwise comparisons which assumed $\alpha = 0.05$.

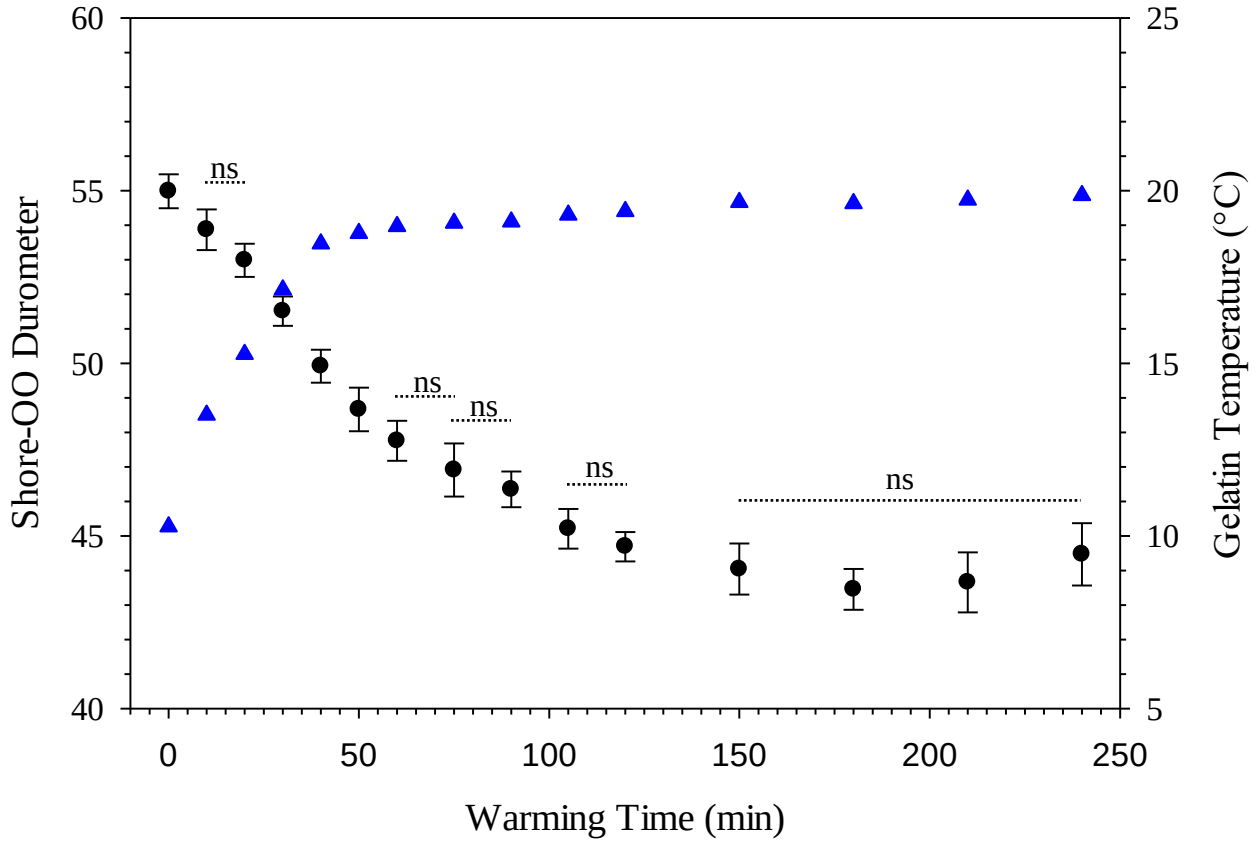

Figure 28. Changes in average Shore-OO durometer (●) and gelatin temperature (▲) as a function of warming time (min). Bars for average durometer represent standard error of the mean. Average durometer decreased significantly (except between time periods indicated with dotted lines which were not significant; ns) as gelatin samples warmed according to one-way repeated measures ANOVA ($F_{14,28} = 378.96$, $p < 0.001$) and Benjamini-Hochberg multiple comparison tests assuming $\alpha = 0.05$. Ambient temperature was 22.1°C during experimentation.

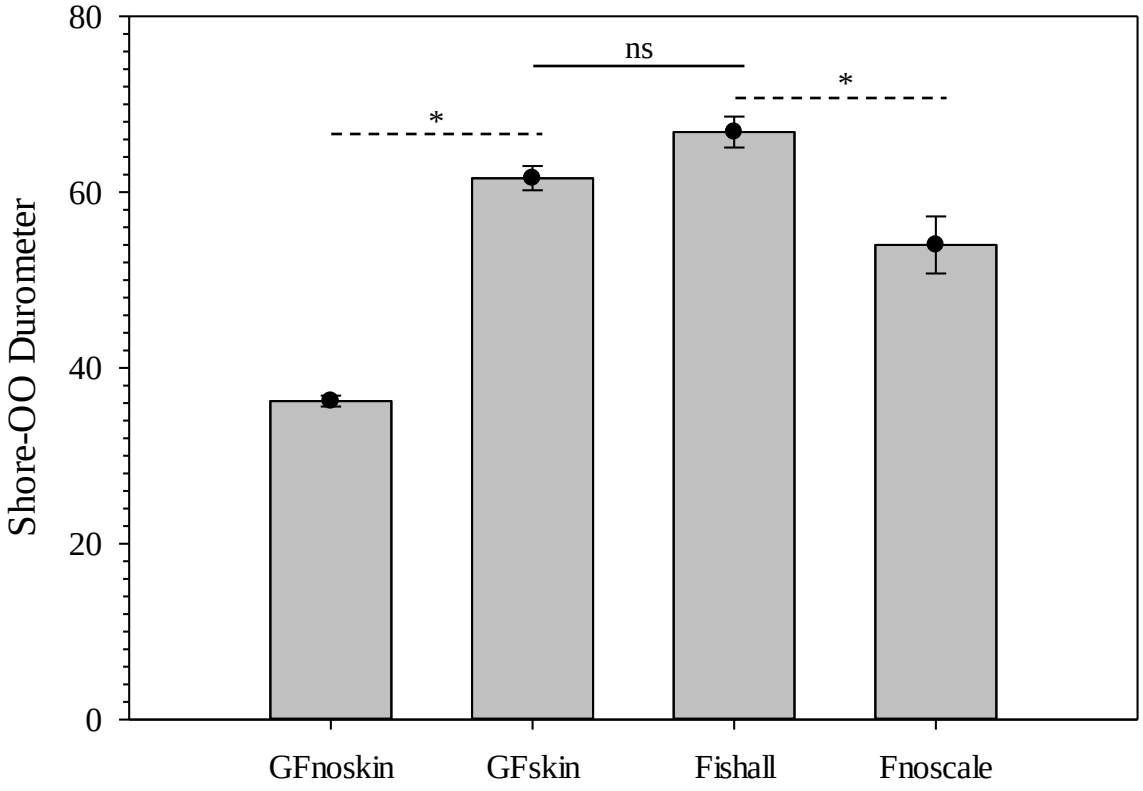

Figure 29. Average Shore-OO durometer for one of four groups including Gelfish with no surrogate skin (GFnoskin) or with surrogate skin (Plasti Dip; GFskin) versus actual bluegill sunfish, *Lepomis macrochirus*, that were intact (Fishall) or with scales removed (Fnoscale). Average durometer is reported with standard error of the mean for each group (n = 3 samples per group). Dashed lines (– – –) represent comparisons between average durometer using two-tailed, dependent t-tests while the solid line (—) refers to a two-tailed, independent t-test between treatment groups. Note: Results of statistic tests were considered significant (*) or not (ns) assuming $\alpha = 0.05$.

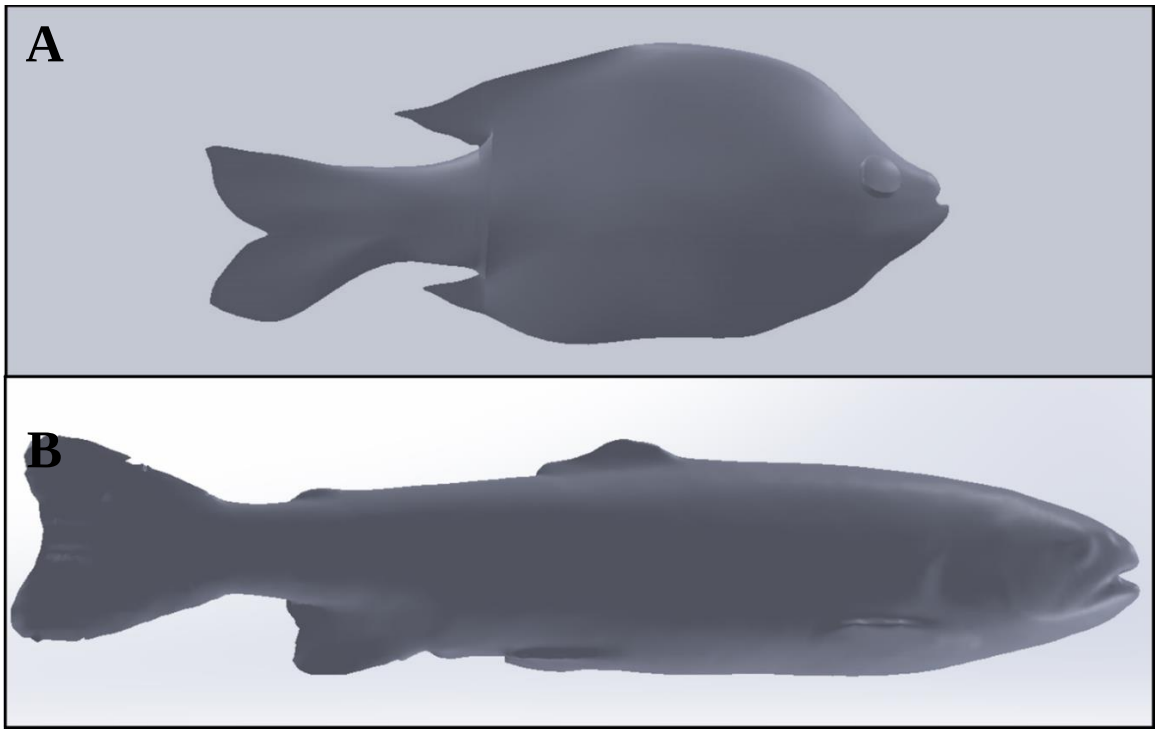

Figure 30. SolidWorks surface models of bluegill sunfish (A) created after nearly 40 hours of manual user manipulation compared to rainbow trout (B) created in less than 3 hours by using Geomagic Design X software to automatically render images and remove unwanted background features from point cloud files. Major landmarks on the bluegill were restricted to the eye, mouth, and the dorsal, caudal, and anal fins. Additional landmarks are visible on the rainbow trout model including eye, mouth, and operculum as well as dorsal, adipose, caudal, anal, pelvic and pectoral fins which are useful for properly embedding each sensor.

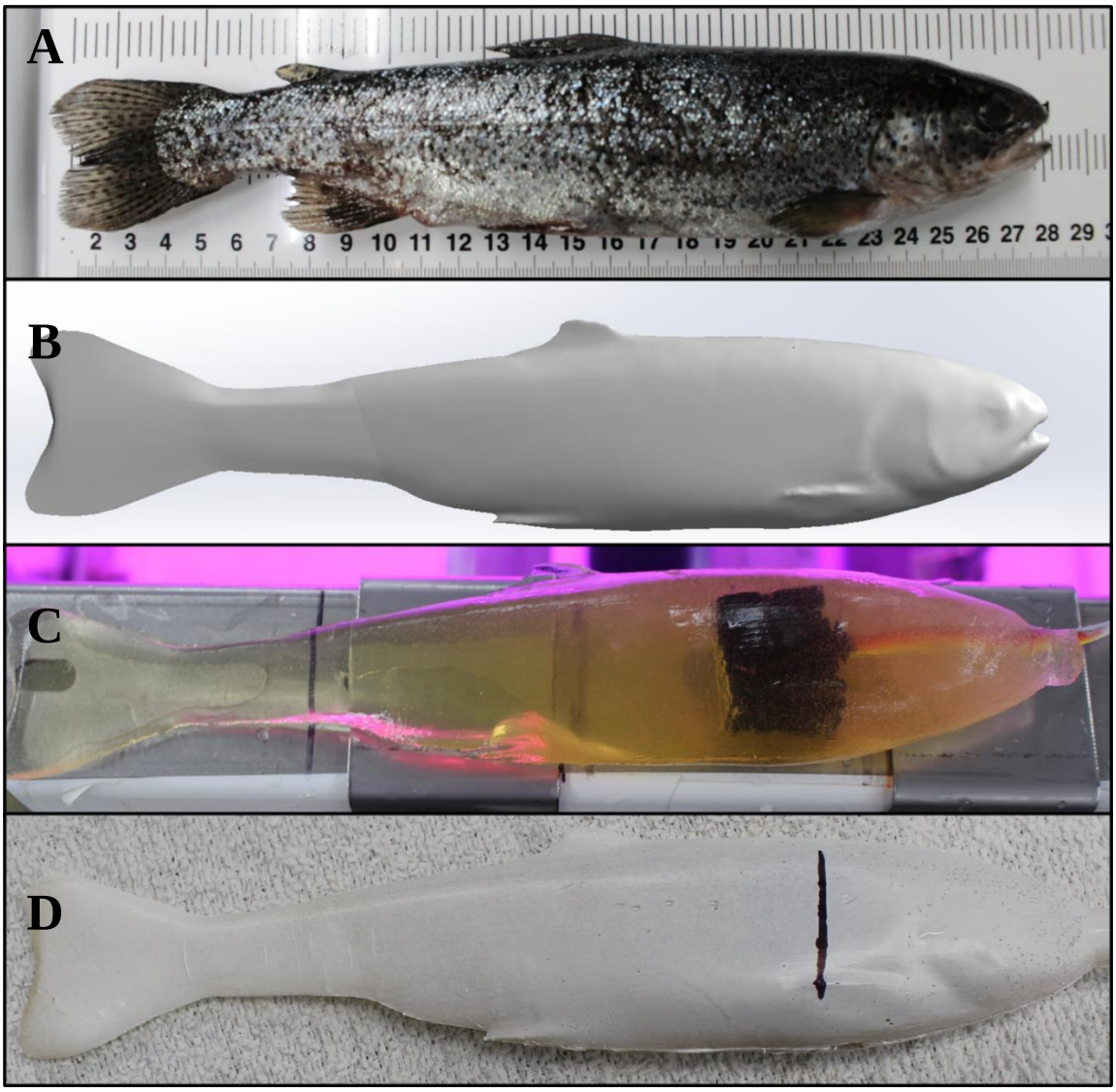

Figure 31. Series of photographs showing the transition from (A) real rainbow trout, (B) to the final Solidworks surface model (i.e., removing most fins and thickening the caudal fin and peduncle), (C) *Gelfish* model containing one three-axis accelerometer, and (D) the final *Gelfish* model with four layers of simulated (e.g., Plasti Dip) skin. Images C also shows the wire connecting the accelerometer to the external data acquisition system. The vertical black line in image D is the approximate center point of the embedded accelerometer used to choose target areas during model testing.

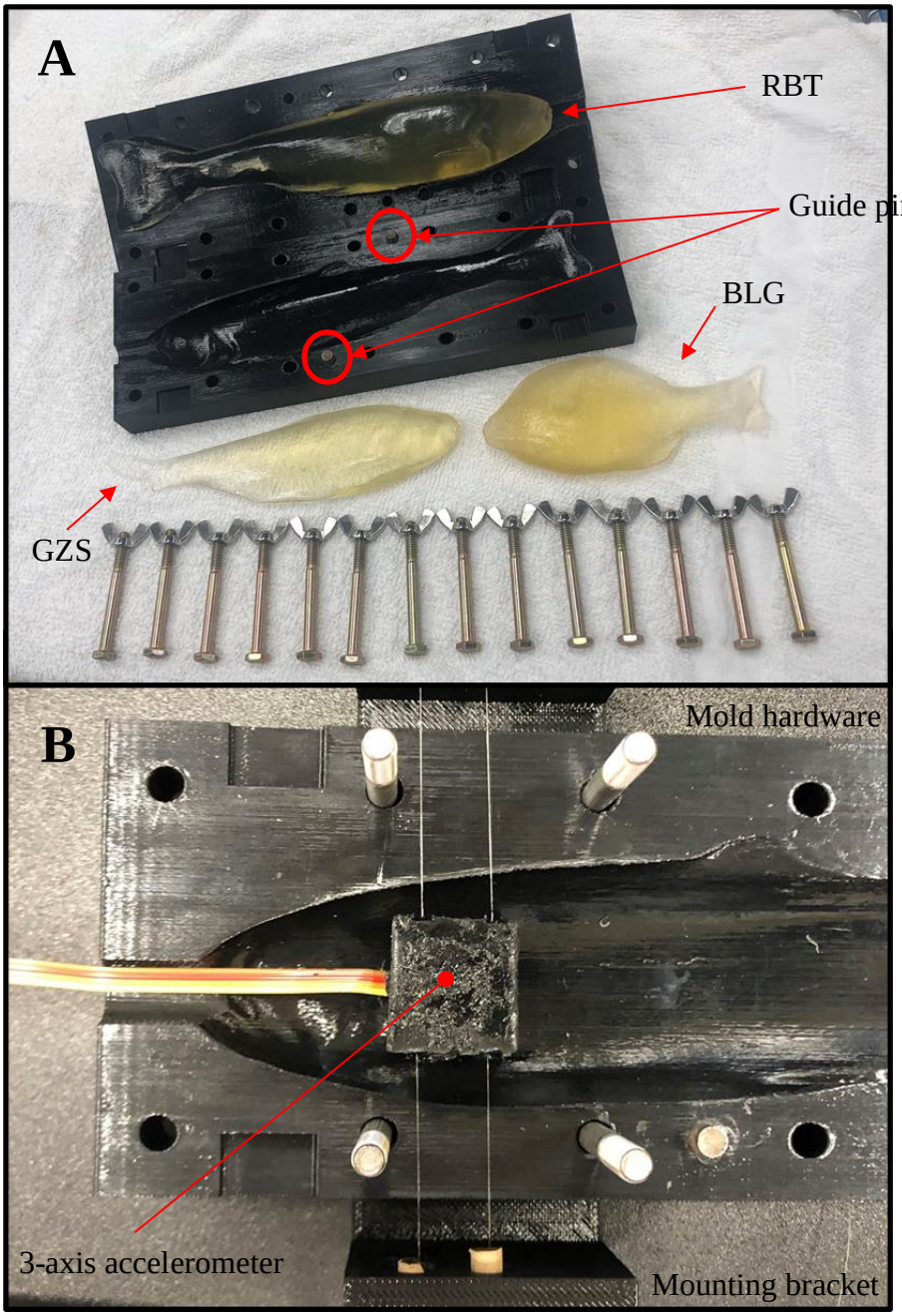

Figure 32. Image (A) represents the completed rainbow trout mold including hardware and guide pins (red circles) used to completely close and seal each half of the mold. Image (B) shows the anterior region of the rainbow trout mold including a mounting bracket (also 3D printed) used to guide monofilament tethers that held the potted accelerometer in place during casting. Note: completed *Gelfish* models (ballistic gelatin only) of rainbow trout (RBT), gizzard shad (GZS), and bluegill (BLG) are also shown in image A.

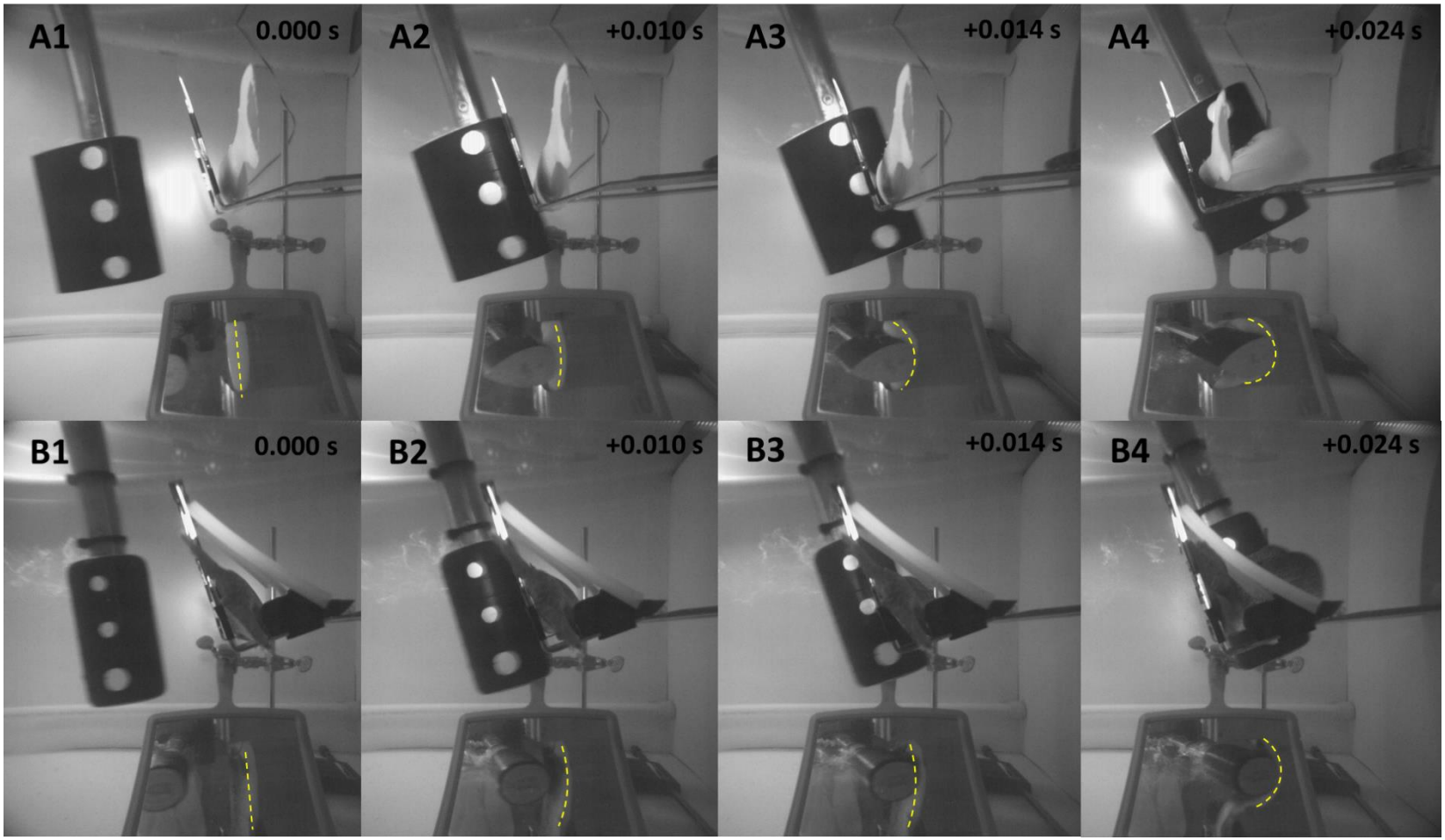

Figure 33. Highspeed video (1000 fps) images of the A) *Gelfish* model and B) sub-adult rainbow trout being struck with a 52-mm blade at ~6.8 m/s at approximately the same location on the mid-body lateral surface at 90°. Dashed lines were included to show body curvature of the ventral surface of both the model and trout in each frame including blade approach (0.000 s; reference), just before contact (+0.010 s), at impact (+0.014 s), and through maximum curvature following impact (+0.024 s).

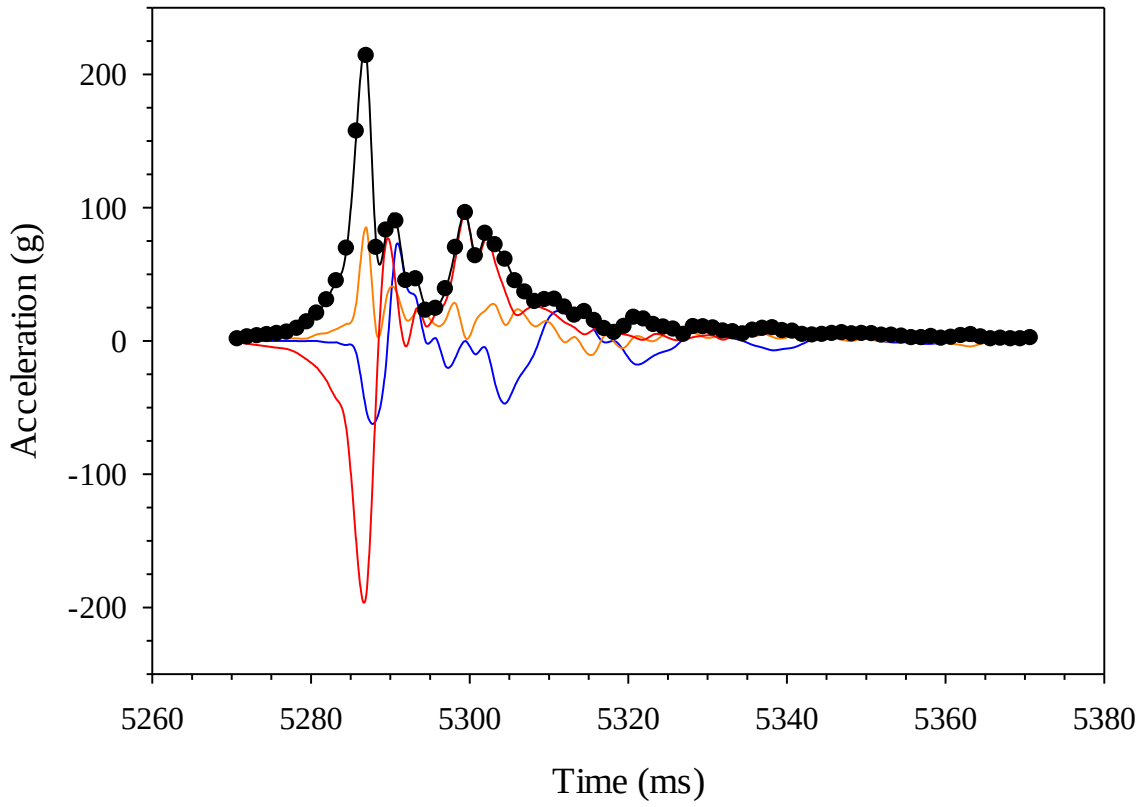

Figure 34. Example plot of acceleration (g) for the *Gelfish* model struck with the 52-mm blade on the mid-body, lateral surface at 11.5 m/s. Magnitude was calculated across all three axes for each time step and reached a peak of nearly 220 g in this trial (#1; Table 2).

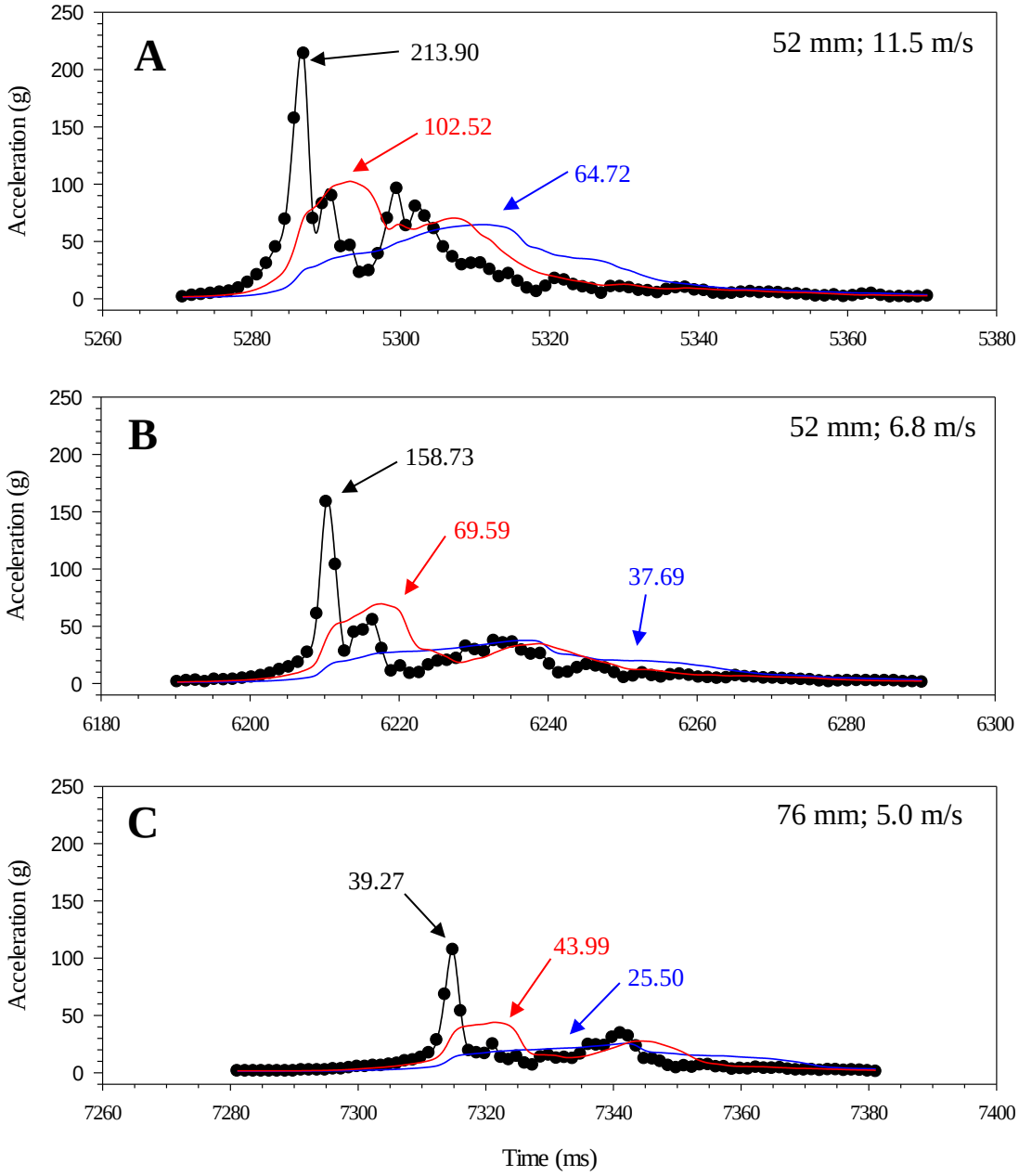

Figure 35. Three plots of overall magnitude (black lines) and 10 ms (red) or 30 ms (blue) running average of acceleration versus time (ms). Results from three impact scenarios are shown including mid-body lateral strikes at 90° and A) the 52-mm blade moving at 11.5 m/s, B) 52-mm blade moving at 6.8 m/s, or C) 76-mm blade moving at 5.0 m/s. Numbers reported with each curve include peak magnitude or maximum acceleration.

CHAPTER V

A TRAITS-BASED APPROACH TO ASSESS SUSCEPTIBILITY OF RIVERINE FISHES TO HYDROPOWER TURBINE BLADE STRIKE

A version of this chapter is being submitted for publication by Ryan Kurt Saylor:

Ryan Saylor[1,2*], "A traits-based approach to assess susceptibility of riverine fishes to hydropower turbine blade strike." *PLOS One* (*in preparation*).

Affiliations:

[1] Bredesen Center for Interdisciplinary Research and Graduate Education, University of Tennessee, Knoxville, Tennessee 37996

[2] Biodiversity and Ecosystem Health Group, Oak Ridge National Laboratory, Oak Ridge, Tennessee 37830

*Corresponding Author: Ryan K. Saylor

1 Bethel Valley Road

Oak Ridge National Laboratory

Oak Ridge, Tennessee 37830

Phone: 865-974-7709

E-mail: saylorr@ornl.gov

Author Contributions:

Conceptualization – RKS

Experimentation – RKS

Data curation – RKS

Analysis of data – RKS

Composition of paper – RKS

Review and Editing – RKS

Abstract

Traits-based approaches often focus on life history to study fish functional ecology, but applications based on biochemistry, bioengineering, or biomechanical data are less common. Data of this nature would serve as useful metrics to describe the differential susceptibility of riverine fishes to turbine passage stressors like blade strike impact. Furthermore, traits-based approaches would be an ideal way to study riverine species at greatest risk of turbine passage because many are difficult to collect, rare, protected by state or federal law, or a combination of them all. Anatomical, morphological, and biomechanical data were directly measured or estimated from recently collected fish samples broadly representative of an impounded fish community in the USA. Principal component and hierarchical clustering techniques were used successfully to identify seven functionally relevant anatomorphic functional guilds (AFGs). While many AFGs were also closely related to family or order-level taxonomy, the cypriniform and perciform fishes were separated into two groups based on functionally significant differences in anatomorphic traits. Multiple linear regression using anatomorphic functional traits and guilds produced a significant linear relationship with relative flexibility. Model select criteria also indicated that AFG categorical variables were better predictors of relative flexibility than strictly taxonomic groups (i.e., species, genus, family, or order). Predicted susceptibility to blade strike impact of each guild was similar to those predicted by laboratory trials on blade strike impact. However, some unexpected trends were observed and likely linked to assumptions used to create many biomechanical variables or omission of yet-to-be identified anatomorphic variables. Regardless, the traits-based method worked well on anatomorphic functional data which suggests applying similar methods on other riverine systems would better assess effects of anthropogenic stressors on fish communities worldwide.

Introduction

The incredible diversity of fishes has led to the development of traits-based approaches that combine species into groups with shared, functionally relevant traits to better study fish communities [1–4]. Initial identification of taxonomic level (i.e., genera,

family, etc.) confers information about member species which have shared genetic, behavioral, physiological, or ecological traits [5]. Traits-based approaches also group fishes according to shared behavioral, physiological, or ecological traits that can transcend phylogenetic relationships [6]. Comparisons between traits-based and taxonomic groupings has shown traits-based approaches may offer more useful insights at smaller geographical scales compared to strict taxonomic conventions [7,8]. Taxonomically unrelated species have also been placed into groups based on reproductive, life history, or environmental traits to study fish communities [4,9–14]. Traits-based approaches are also useful for studying how anatomical similarities may be linked to predator guilds [15] or using morphometric traits to describe and characterize diversity of fish communities [16]. Use of both taxonomic and traits-based grouping methods relies on readily availability and comprehensive fish community data or requires identification of fewer, broadly representative "umbrella" species for more thorough study [2]. This aspect of a traits-based approach is especially useful because data on certain species is more available than others because they are abundant, economically valuable, or have a longer publication history. Identification of surrogate species—any species used in place of another because the targeted species is rare, difficult to collect, or protected by law—is also a hallmark of traits-based or taxonomic groupings [2]. Surrogates allow every group to be represented in the analysis and is especially useful for fish communities that are not well studied and/or are data deficient. More importantly, surrogate data were found to capture the same overall trends as the analysis that included all species, suggesting surrogacy is a viable option using traits-based data [12]. Use of a traits-based approaches have expanded into many fields because of the utility of umbrella or surrogate species to represent groups in community analyses.

Most applications of traits-based approaches are found within the field of functional ecology and there are fewer examples of using similar methods to study how anthropogenic stressors affect fish communities. One such application includes studying the impacts of hydropower dams on diverse riverine fish communities that contain migratory species. Beyond disruption of riverine connectivity from the physical dam, riverine fishes may also become entrained and pass through turbines at hydroelectric

facilities [17–19]. Turbine passage can lead to severe injury and death as fishes are exposed to suite of stressors including rapid decompression, hydraulic shear, cavitation, and physical impact with turbine blades or stationary structures [20–23]. Fish mortality may have community-level affects and diversity of riverine species in these impounded systems make it impossible to study all at-risk species. To overcome this limitation, a traits-based system was developed based on riverine species occurrence and life history traits data to better predict entrainment risk [1,24]. Risk was often linked to relationships among fishes within family or order-level taxonomy and individual species were identified as surrogates for each group to help prioritize laboratory experimentation into turbine passage stressors like blade strike impacts. Blade strike laboratory trials have shown this stressor is particularly injurious and also indicates that susceptibility (rates of severe injury or death) was linked to size and species [21,25,26]. The diversity of responses to blade strike suggests that data from one species may not be used to predict susceptibility of another, especially for taxonomically disparate species. Blade strike studies also require using hundreds of live fish to accurately quantify susceptibility, which is logistically unfeasible for most at-risk riverine species. To that end, a traits-based approach could also be used to better understand how turbine passage stressors like blade strike affect an entire community of impounded riverine fishes.

Susceptibility to blade strike may be linked to many anatomical, morphological, and biomechanical traits that could also be used as functionally relevant traits. Impacts from turbines cause severe bending of the fish body as the blade makes contact with the body [27] such that limitations in whole-body flexibility could be linked to susceptibility among species. Blade strike trials also suggest that strikes closer to the center of gravity also cause the fish body to wrap almost completely around the blade, which lead to more significant injuries and higher rates of mortality [21,25]. Creation of a new biomechanically relevant index of flexibility would be a useful metric from which to compare susceptibility between functional guilds containing unrelated species. In general, fishes are inherently flexible organisms, and examples of remarkable body curvature have been observed during C-start predator avoidance behavior in many species [28–32]. In contrast, disparities in body shape and swimming performance have shown that natural

differences in flexibility also exist. For example, filiform anguillids are highly flexible compared to the more rigid body movements observed in subcarangiform salmonids [33,34]. Changes in body shape (i.e., length relative to body depth or width), scale morphology, and vertebral morphometrics (vertebrae number, size, and complexity) have also been linked with changes in body flexibility among fishes [35–41]. Body flexibility of fish can also be approximated using beam theory which can model the fish body as a cantilever beam (elliptical cylinder) in order to approximate mechanical properties like flexural stiffness [38,42–45]. All of these potential traits are easy to measure or approximate which suggests use of traits-based methods, functional guilds, and a new metric for flexibility would allow susceptibility to blade strike to be assessed for an entire community of fishes.

The purpose of this study is to use a trait-based approach to group species into novel anatomorphic (anatomical + morphological) functional guilds (AFGs) with respect to relative flexibility. Here, relative flexibility was used as a surrogate metric of susceptibility to blade strike impact (i.e., less flexibility means higher susceptibility) in all regression analyses. Identifying guilds will rely on traits associated with morphometrics of body shape, anatomorphic measurements related to scales and the vertebral column, as well as biomechanical measurements linked to whole-body flexibility. The AFGs created using traits-based approaches will be compared directly to strict taxonomic groupings to determine which is better at predicting relative flexibility among riverine fishes. Taxonomic groupings are usually the default functional unit based on shared selective pressures over time; however, biogeographical processes have also shaped current fish communities in North America [46], suggesting that adaptive convergence of shared functional traits occurs separately from phylogenetic influences [6,8,12]. Additionally, susceptibility to turbine blade strike is an anthropogenic (artificial) selective force from which fishes have no comparable natural process to adapt, which also suggests that shared traits among guilds are likely not taxonomic [2]. To that end, I predict that AFGs will correspond closely to the mixed taxonomic groupings used to prioritize species for laboratory research but with two exceptions (Table 14). First, the centrarchid family of fishes contain genera with markedly different eco-morphological

traits [47] linked to accelerated speciation [48], which indicates this family will likely form at least two guilds. Similarly, the disparate body shapes of the catostomid and cyprinid families suggests the rotund catostomids will need to be separated from the more compressed cyprinids. The main research hypothesis is that AFGS will predict relative flexibility as well or better than strictly taxonomic groups of riverine fishes. The specific study objectives were to 1) compile an anatomorphic traits dataset from a locally representative riverine fish community, 2) identify and delineate AFGs using multivariate statistical analyses, 3) determine the relationship between fish relative flexibility and anatomorphic traits, AFGs, or taxonomic groups, and 4) compare trends in relative flexibility with published biological response data to assess susceptibility (or risk) of injury and mortality due to blade strike impact.

Materials and Methods

Fish Collection and Care

All fish were collected from local water bodies in Eastern Tennessee near the Aquatic Ecology Laboratory (Oak Ridge National Laboratory, Oak Ridge, Tennessee, USA). Eastern Tennessee hosts ~221 species that represent 26 families and 18 orders of fishes found within the Cumberland and Tennessee River drainages [49] according to taxonomic classification schemes presented in Etnier [49] and Page et al. [50]. All encountered species were collected, but only individuals between 100 to 400 mm in total length were retained for analysis. This size range was chosen because it is comparable to the size of fish used in simulated blade strike testing to date [21,25,26]. Many species within the cyprinid (minnows), catostomid (suckers), ictalurid (North American catfish), and percid (perch-like fishes) families were not targeted because of small adult size (< 100 mm), are considered locally endemic, or are state and/or federally protected in the USA. At least three, but up ten individuals for every unique species were collected using backpack and boat electrofishing from September 2019 to January 2020. Sub-adult rainbow trout, *Oncorhynchus mykiss*, were donated by Tellico Trout Hatchery (Tennessee Wildlife Resource Agency, Tellico Plains, Tennessee). A total of 133 individuals that

represented 27 species, 17 genera, 9 families and 5 orders were successfully acquired (Table 15). Fish were transported back to the Aquatic Ecology Laboratory and up to 20 fish were placed into separate 785-liter, 1.28 m diameter, round fiberglass holding tanks. Each holding tank received a constant flow of dechlorinated, UV-sterilized freshwater, rigorous aeration, and food was offered daily. Fish disposition was checked multiple times per day, and all fish were euthanized for data collection within one week of capture. Individuals were euthanized in a water bath containing 450 ppm clove oil extract (NOW® 100% Pure Clove Oil, Item #051193, www.gnc.com) dissolved in 95% ethanol (1:10) and diluted to final volume using dechlorinated freshwater. Following euthanasia, anatomorphic and biomechanical data were collected immediately, but some data necessitated freezing fish at -20°C overnight prior to data collection.

Fish Shape Characterization

Shape was measured in three body dimensions including length, depth, and width at each of seven landmarks for all species. Measurements for body length were made using a fish measuring board (± 0.1 cm; Fish Measuring Board, Mini, Model #118-E40, Wildco, Yulee, Florida, USA) while digital calipers (± 0.01 mm; iGaging Origin Cal Digital Calipers, Model #100-032-901WB, Brownells Inc., Grinnell, Iowa, USA) were used to measure body depth and width. Major landmarks included the head (snout tip to posterior edge of operculum), pectoral, dorsal, pelvic, and anal fins (snout tip to anterior edge of each fin). All body depth and width measurements were taken at the anterior edge of each defined landmark (Figure 36). In addition to body landmarks, standard length, total length (*TL*) and wet mass (*M*; ± 0.1 g) were measured. Condition factor (*K*) was calculated according to Cone [51]:

$$K = \frac{100M}{TL^3} \quad (1)$$

and was used to remove individuals from analysis that had anomalously low or high values relative to all other individuals within the same species. To characterize fish shape for analysis, all raw landmark data were converted to proportion of total length, maximum body depth, and maximum body width. The length between the posterior edge of operculum and anterior edge of the anal fin was divided by the standard length to

represent the "mid-body" proportion of each fish. Mid-body was defined because strikes to this region are often considered the most injurious to fishes during blade strike testing [21,25,26], most body curvature during strike occurs between these landmarks, and to provide an additional estimate of body shape among species. Ellipticity (e) was used to estimate cross-sectional body shape (depth relative to width) at each landmark and was calculated according to the following equations [52]:

$$IF\ d > w; e = \sqrt{\frac{d^2 - w^2}{d^2}} \quad (2a)$$

$$IF\ d < w; e = \sqrt{\frac{w^2 - d^2}{w^2}} \quad (2b)$$

where d is one-half body depth and w is one-half body width. Values of ellipticity range between 0.0 to 1.0 where values closer to zero indicate a circular cross-section and values closer to unity indicate an elliptical profile. Average ellipticity was calculated for the mid-body area only which included depth and width measurements taken for the head, pectoral fin, dorsal fin, pelvic fin, and anal fin. The assumption of ellipticity was also important when estimating 2nd moment of area and flexural stiffness of the fish body described below. Lastly, fineness ratio (standard length divided by maximum depth) and body aspect ratio (standard length divided by maximum body width) were calculated according to Porter et al. [38], and cross-sectional ratio (maximum depth divided by maximum width) was also calculated to approximate fish shape. A total of 25 variables including body proportions, ellipticity, and body ratios were used to represent fish shape and size in multivariate analyses (Table 16).

Scale Morphometrics

Scale data was collected from a sub-sample of three scales removed from the left mid-body surface, but omitted lateral line scales. Each scale was removed, type was visually confirmed, and photographed through a dissection microscope at 10 X normal magnification. In addition to scale type (cycloid or ctenoid), the presence or absence of inter-radial grooves was noted for both the anterior (embedded) and posterior (exposed) scale margins. Six margin types (similar to tree leaf margins) were also identified along the anterior margin of scales including 1) entire, 2) undulate, 3) lobate, 4) crenate, 5)

crenulate, and 6) sinuate (Figure 37; Table 16). Inter-radials and margin type were included to test if these disparities in scale shape or morphology were also linked with changes in relative flexibility. Scale measurements were taken using the line and analyze features of ImageJ (National Institute of Health, https://imagej.nih.gov/ij/) software. Specific measurements included length (± 0.01 mm), depth (± 0.01 mm), perimeter (± 0.01 mm), area (± 0.01 mm^2), and area of scale exposed (± 0.01 mm^2). Initial measurements were used to calculate scale aspect ratio (length divided by depth), proportion of the scale embedded in the scale pocket (hereafter imbrication) according to the following equation:

$$ED = 1 - \frac{A_{EX}}{A_{TOT}} \quad (3)$$

where *ED* is a proportion estimating imbrication, A_{EX} is the area of scale surface exposed (i.e., part of the scale with pigmentation), and A_{TOT} is total scale area. The average value of aspect ratio, total area, and imbrication was calculated for each individual using all three sub-samples. Number of mid-body scales (mid-body scale coverage) was estimated by multiplying scale density (unity divided by average scale area scales/cm^2) by the surface area of the left, mid-body lateral surface (cm^2). Mid-body scale coverage was estimated because scale density correlated strongly with fish length. Use of scale coverage helped distinguish species with many smaller scales compared to those with fewer, large scales during relative flexibility analyses. Inclusion of scale morphometrics created an additional 14 variables used in multivariate analyses (Table 16).

Vertebral Column Morphometrics

The final set of anatomorphic data was derived from vertebral centra and the vertebral column as a whole. Bone type was identified as either cellular or acellular where the latter is considered a derived trait found predominantly in Neoteleosts [53]. Frozen fish were X-rayed in a cranio-caudal and dorso-ventral orientation at the Radiology and Diagnostic Imaging Department of University of Tennessee College of Veterinary Medicine. X-ray images were uploaded into ImageJ software and used to identify, enumerate, and measure individual vertebrae. Pre-caudal vertebrae included the atlas and all rib-bearing centra, whereas caudal vertebrae included all centra with haemal

arches and spines but omitted the urostyle of the caudal fin (Figure 38) [54]. Vertebrae between the posterior edge of the operculum and anterior edge of anal fin were considered mid-body vertebrae similar to the mid-body lateral surface described above. Total vertebrae were calculated by adding pre-caudal and caudal vertebrae, but was also visually enumerated as well. The curved length (± 0.01 mm) of the entire vertebral column was measured using the line function of ImageJ by tracing the vertebral column from the anterior edge of the atlas to the posterior edge of the last caudal vertebrae. Centra length (± 0.01 mm) of each vertebra was also measured and the average centrum length was calculated for each individual. The average intervertebral joint length (IVJ_{len}: ± 0.01 mm) was estimated according to:

$$IVJ_{len} = \frac{CL - \sum L_{cen}}{V_{tot} - 1} \quad (4)$$

where CL is the curved length, L_{cen} is the length of each vertebra, and V_{tot} is the total number of vertebrae. Additional measurements on individual vertebra were also made by removing one of each type which was then photographed under a dissection microscope at 10 X normal magnification. Vertebrae images were uploaded to ImageJ and the length, depth, and width (± 0.01 mm) were measured as described previously. Several calculations for pre-caudal and caudal vertebrae were made from these measurements including length to depth, length to width, and depth to width aspect ratios. Volume (± 0.01 mm^3) was also calculated for each type by assuming vertebrae were elliptical cylinders. Average values for all aspect ratios and volume were calculated using the pre-caudal and caudal data to represent the entire vertebral column. A total of 19 variables were included to represent the vertebral column in multivariate analyses (Table 16).

Biomechanical Variables

The next few variables were directly measured as biomechanical estimates of the fish body. Center of gravity was estimated as a proportion of standard length by placing frozen fish on a fulcrum and identifying the point along the body length it was balanced following Turnpenny [25]. Durometer, a measure of tissue firmness, was measured from intact freshly-deceased, whole-fish samples using a Shore Type-OO durometer (Model DD-4 Digital Durometer; Precision = ± 0.1 units; Rex Instruments, Buffalo Grove,

Illinois, USA). Immediately following euthanasia, 20 durometer measurements were taken in a grid-like pattern along the left lateral body surface except the head. The average value of these 20 measurements was calculated to represent durometer for each individual. Relative whole-body flexibility of each fish was directly measured on fresh fish samples immediately following euthanasia. Each fish was secured in an upright position using a clamp tightened around the operculum so that the snout pointed directly downward. In this position, a natural pivot point between the cranium and vertebral column was created, which allowed the fish body to bend as a result of gravity (Figure 39). Each fish was held in this position for a few minutes until it settled and photographed in front of a background containing 2.0 × 2.0 cm grid for size reference. Pictures were uploaded into ImageJ to measure the deflection length (distance from the tip of snout to the posterior edge of the caudal fin; ± 0.01 cm) and the maximum bending angle (degrees) formed between the tip of the snout, anterior edge of the dorsal fin, and posterior edge of the caudal fin similar to methods described in Porter et al. [38]. Relative flexibility (Bod_{cur}) was calculated according to the following equation [38]:

$$Bod_{cur} = 1 - \frac{DL}{SL} \quad (5)$$

where *DL* is the deflection length and *SL* were the standard length of each fish. The values of body curvature ranged between 0 to 1, with values closer to zero indicating little flexibility while values near unity suggesting high flexibility. That is, the smaller the deflection length (i.e., the closer the caudal peduncle is to the snout) the more inherently flexible the individual was assumed to be for analyses used herein. Body curvature measured here represents an index of relative flexibility because excess force was not placed on the body (i.e., dynamic three-point bending tests) to the point of failure, i.e., maximum flexibility was not estimated. Rather, the goal of this study was to regress anatomorphic variables against relative flexibility (a surrogate for susceptibility to blade strike) to test if functionally relevant groups were significant predictors of relative body curvature.

The remaining variables were approximated by modelling the fish mid-body and vertebral column as elliptical cylinders for which principles of engineering beam theory

may be used to estimate the biomechanical properties of the fish body [42,45]. More specifically, beam theory was applied by assuming the fish body was a cantilever beam secured at one end (the head), while a force (gravity) was applied to the free end (the caudal fin) of the body to cause a known deflection distance (Figure 39) [44]. Approximations were only considered for medio-lateral flexibility, with body width and depth forming the major and minor axes, respectively, of an elliptical cylinder in cross section. All approximations also assumed that the material composition of an elliptical cylinder is homogenous and that body depth and width did not change across the mid-body section—both assumptions are false since the body of fish is a complex mixture of many tissues and shape dimensions changed at each landmark [38,42,45]. Thus, all calculations discussed herein are used to approximate mechanical properties of a complex biological system to compare species and test how well these variables may predict body curvature. Second moment of area of the body (I_b; m^4) was estimated for elliptical cross section following Porter et al. [38] given the following equation:

$$I_b = \frac{\pi(0.5d)(0.5w)^3}{4} \quad (6)$$

which includes body depth (d) and body width (w) in meters calculated at each landmark within the mid-body region (i.e., head, pectoral, dorsal, pelvic, and anal fin). The average value for second moment of area of the body was calculated across all mid-body landmarks to represent each individual in this analysis. Second moment of area estimates the resistance of a beam to change shape or bend when force is applied so that higher values equal higher resistance to bending [42,44]. Flexural stiffness (EI; $N \cdot m^2$) was also estimated for the fish body according to the following equation [44,45]:

$$EI_b = \frac{FSL^3}{3DL} \quad (7)$$

with force (F) approximated as 9.81 Newtons (i.e., force applied to one kilogram due to gravity), standard length (SL) converted to meters, and deflection length (DL) also converted to meters. As estimated flexural stiffness of the body increases the relative flexibility would be expected to decrease. Maximum range of motion (MRM; degrees) was calculated for the pre-caudal and caudal vertebrae following the equation given by Nowroozi et al. [39]:

$$MRM = acos\left(\frac{Cen_d^2+Cen_w^2+IVJ_{len}^2}{2Cen_dCen_w}\right) \quad (8)$$

where Cen_d was vertebra depth (mm), Cen_w was vertebra width (mm), and IVJ_{len} was the average intervertebral joint length (mm). An average value that represented the maximum range of motion for the entire vertebral column was also calculated using pre-caudal and caudal vertebrae numbers. Wider or deeper vertebrae with shorter intervertebral joint lengths would be expected to have less range of motion, which may vary significantly between pre-caudal and caudal vertebrae [39]. The second moment of inertia (I_v; cm^4;) was calculated by assuming the vertebral column formed an elliptical rod which could rotate around the center of mass using the equation in Baliga and Mehta [55]:

$$I_v = \frac{1}{12}\rho\pi(0.5Cen_d)(0.5Cen_w)SL^3 \quad (9)$$

where density (ρ) varied by bone type and centra length and width were converted to centimeters. Here, cellular bone density was 786 mg/cm^3 while acellular bone density was 993 mg/cm^3, which was approximated from opercula and rib bones for each bone type following Cohen et al. [56]. Finally, to represent the 2nd moment of inertia for entire vertebral column, the weighted average was calculated using the following equation:

$$\overline{I_v} = \frac{(N_{PC})(I_{PC})+(N_C)(I_C)}{N_T} \quad (10)$$

where *NPC*, *NC*, and *NT* are the number of pre-caudal, caudal, and total vertebrae, respectively [55]. Finally, to reduce the influence of size on estimates of average 2nd moment of inertia, each value was normalized by dividing by the vertebrae width to the fourth power [45]. This created an additional seven variables to characterize biomechanical nature of fish body and vertebral column in the multivariate analyses (Table 16).

Data Analyses

Principal component and hierarchical clustering (HCPC) analyses were performed using the "*FactoMineR*" and "*factoextra*" packages [57,58] in R Statistical Software *v4.0.2* [59]. A total of 40 variables (Table 16) were used to identify functional guilds from anatomorphic data representing shape (m = 24), scale morphometrics (m = 4), vertebral column morphometrics (m = 9), and biomechanical traits (m = 3) for n = 105

fish. Principal components were used instead of raw data to better account for variation and reduce dimensionality prior to clustering. All data were scaled (relative to the variable mean and standard deviation) prior to principal component analysis. The minimal number of principal components that described at least 75% of the variation were used in hierarchical clustering of the anatomorphic data. Hierarchical clustering was performed using Euclidean distance to calculate dissimilarity and Ward's linkage to create clusters because it minimizes within cluster variance [60]. Factor maps and dendrograms were used to visualize results and help identify functionally related guilds (clusters) of fish. The most functionally useful clusters would include all individuals of the same species while also containing multiple non-taxonomically related species (i.e., different family or order) with similar anatomorphic traits. The actual number of clusters depends on where the dendrogram is "cut" along the tree which the user may specify. Since the latter is mostly subjective, multiple cluster arrangements were tested in multiple regression analyses to determine which cluster scheme explained variation in relative flexibility better.

Multiple linear regression analyses were performed using the linear model [*lm*] function in the base statistical package available in R Statistical Software *v4.0.2* [59] as well as the "*leaps*" [61], "*MASS*" [62], and "*MuMIn*" [63] packages to assist with model selection. Relative flexibility was used as the main predictive variable in all analyses because preliminary testing suggested it accounted for variation better than maximum bending angle [38]. All categorical data were converted to dummy variables (e.g., scale type, bone type, anterior/posterior inter-radials, and anterior scale margin type) and included as independent variables. The "*car*" [64] and "*corrplot*" [65] packages were used to confirm normality, homoscedasticity, absence of outliers, and minimal multicollinearity among independent variables. Preliminary regression analyses indicated many independent variables were highly correlated with standard length and also showed scale type correlated perfectly with bone type (i.e., all fish with cycloid scales also had cellular bone) so all three variables were removed from further analyses. A similar problem was identified with the anterior scale margin category which correlated too strongly with guild and taxonomic groups tested so it was omitted from further analysis.

Stepwise (both forward and backward) and best subset model selection analyses were used to determine optimal number of variables in the final predictive model of relative flexibility. Adjusted R^2 and model selection criteria including AIC, corrected AIC (AICc), and ICOMP were used to select the most parsimonious predictive model. All statistical decisions were made assuming $\alpha = 0.05$.

Up to 28 variables were identified as candidates for the first regression, but the number included in the analysis was reduced based on predicted influence on relative flexibility. Fineness ratio, body aspect ratio, cross-sectional aspect ratio, average ellipticity, and proportion of mid-body were included to test if changes in body shape significantly predicted relative flexibility. For example, as body width increased relative to depth, flexibility was predicted to significantly decrease. Higher imbrication of scales was predicted to decrease flexibility, i.e., scales that are embedded deeper restricted flexibility more. Mid-body scale coverage was predicted to increase relative flexibility when smaller, more dense scales were present compared to species with fewer, large scales. Scale aspect ratio (length to depth) was predicted to decrease relative flexibility for individuals with more rectangular scales (i.e., length > depth) which would resist bending more than circular-shaped scales. Categorical variables related to presence or absence of inter-radial grooves on the anterior or posterior edge of scales were analyzed because overlapping grooves may create additional friction that could also limit relative flexibility. Aspects of the vertebral column focused on variables that approximate the entire vertebral column because of the low sample size of each vertebrae type. Variables included total number of vertebrae as well as average ratios (length to depth, length to width, and depth to width), centra volume, intervertebral joint length, and maximum range of motion. Relative flexibility was predicted to increase as the number of vertebrae and average intervertebral length increased, while it would decrease as average volume increased (i.e., overall size of vertebrae increased and total number of vertebrae decreased). Biomechanical variables including average durometer, adjusted 2^{nd} moment of inertia for the vertebral column, adjusted 2^{nd} moment of area, and flexural stiffness were also included. In all cases, as these biomechanical variables increased, relative flexibility would be predicted to significantly decrease as a result. A total of 21 predictor

variables were included in the initial multiple linear regression of relative flexibility (Table 16).

The second regression analysis incorporated all significant predictors of body curvature in the first regression and added anatomorphic functional guild or taxonomic group categorical predictor variables. Both anatomorphic functional guilds and taxonomic groups were converted to dummy variables and whenever possible, the group that contained bluegill sunfish was used as a reference group. Bluegill sunfish are the most susceptible to injury and death during blade strike impact compared to other species tested to date [66]. Two potential relationships between relative flexibility and grouping method were hypothesized: 1) AFGs would account for variation in relative flexibility as well or better than taxonomic group and 2) if taxonomic groupings were better predictors of relative flexibility, genus-level taxonomy would account for variation better and produce the most parsimonious model. Model selection criteria and adjusted R^2 were used to identify the most parsimonious model by comparing grouping methods (AFGs or taxonomic) to the fully parametrized (individual-based) model analyzed in the first multiple linear regression.

Results

Anatomorphic Functional Guilds

Functional guilds were successfully identified using anatomorphic data from 105 fish that represented 21 species, 14 genera, 9 families, and 5 orders. Of fish initially collected, 28 individuals were omitted from analyses for the following reasons: a species was only represented by one individual (n = 5), one species was represented by two individuals and its genus was already well represented (n = 2), fish with incomplete data (n = 2), individuals outside the 14.0 to 36.0 cm size range (n = 11), data for relative flexibility was impacted by rigor mortis (n = 4), and X-ray images were difficult to discern or indicated vertebral deformities (n = 4). In addition, three species were included in the analysis (Golden Redhorse, Skipjack Herring, and Smallmouth Bass) that only contained two individuals to better represent the genus in the analyses (Table 15). The

first six principal components explained 79.4% of the variation among these data and were used to cluster functionally related species (Figure 40). For most principal components, variable loadings suggest that ellipticity of body landmarks contributed more to each PC compared to direct landmark proportion, though all variables were retained to properly account for variation during clustering (Table 17; Figure 41). In addition, the number of vertebrae (pre-caudal, mid-body, and total), fineness ratio, relative flexibility, and mid-body proportion also contributed most of the variation to principal component axes one and two.

Results of hierarchical clustering identified as few as three or up to eight clusters could be used as representative AFGs. Three clusters divided fish based mostly on scale type (or lack of scales in the case of catfish) and was the default selection by the HCPC algorithm (Figure 42A); however, this was considered too inclusive because of the overall variation in these anatomorphic data. Selecting a higher number of clusters produced at least three unique groups that were always observed among these data. For example, catfish (e.g., Elongate–rotund siluriforms) was always a separate cluster even when scale data were excluded from analysis. Catostomids also formed a cluster (e.g., Elongate–compressed cypriniforms) and a separate cyprinid cluster (e.g., Moderate–slender cypriniforms) was also always observed. An interesting exception was observed when the central stoneroller (a cyprinid) was also included among the catostomid cluster. A fourth cluster contained both species of *Pomoxis* and was always separated from other perciforms; however, this separation was not used in further analysis. The 6-cluster scheme combined salmonids and clupeids into a single cluster while all other perciform (moronids, centrarchids, percids, and sciaenids) fishes represented by the last most populous cluster (Figure 42B). Seven clusters were identified when salmonids (e.g., Elongate–compressed salmoniforms) were separated from clupeids (e.g., Moderate–compact clupeiforms) to form two distinct guilds, while all perciform fishes formed into the last cluster (Figure 42C). Finally, the 8-cluster scheme was associated with the separation of Moderate–compressed perciforms from Stout–compact perciform species. More specifically, Moderate–compressed perciforms included *Micropterus* spp. within the centrarchid family, and all species within the percid, moronid, and sciaenid families

examined in this analysis, whereas Stout–compact perciform group was composed of all *Lepomis* spp. (Figure 42D). However, review of a factor map showed that the *Lepomis* and *Pomoxis* spp. cluster polygons overlapped which suggested these fishes should be combined to form the seventh (and final) cluster instead of separating them both (Figure 43). To that end, I used a slightly different 7-cluster scheme (Figure 42C) that may be more a functionally relevant representation of these anatomorphic data (Figure 44; Table 18). All cluster groups (e.g, three, six, seven, and eight) were included in the multiple linear regression to determine which clustering scheme was the best predictor of relative flexibility.

Relative Flexibility

The baseline model containing all variables (m = 21) produced a significant linear regression model of relative flexibility, but regression diagnostics indicated some assumptions might be violated. Plots of regression diagnostics suggested issues with homoscedasticity and normality may be present but absence of outliers was confirmed (Figure 45A–C). A plot of the correlation matrix also indicated high multicollinearity with cross-sectional aspect ratio, average ellipticity, and mid-body proportion variables so all three were removed from further analysis (Figure 45D). A log10 transformation was performed on relative flexibility and the resulting regression diagnostics confirmed normality and homoscedasticity among residuals (Figure 46). Results of stepwise model selection on the remaining 18 variables suggested a 10-parameter model, while best subset model selection indicated that a 7-parameter model was the most parsimonious (Table 19). The 7-parameter model was chosen but the scale imbrication variable was substituted for body aspect ratio while all other variables remained the same. This model produced a significant linear relationship ($F_{7,97} = 149.2$, $p < 0.001$, adj-$R^2 = 0.9089$) that accounted for ~91% of the variation in predicted log10-relative flexibility. This model included fineness ratio, scale imbrication, total vertebral number, average intervertebral length, average maximum range of motion, adjusted 2nd moment of inertia of the vertebral column, and flexural stiffness of the body, which were all significant predictors of log-relative flexibility. The 7-parameter model was used as the baseline from which to

add categorical variables (anatomorphic functional guilds or taxonomic groups) to the log-linear regression of relative flexibility.

The multiple linear regression that included seven anatomorphic functional guilds produced a significant linear model with the lowest model selection criteria compared to other AFG and taxonomic groups. The new model (AFG7a) included 13 variables and model selection criteria suggested the additional variables accounted for variation in body curvature better than the baseline (7-parameter) model (Table 19). Models representing six and eight AFGs were also significant and model selection criteria for the six, seven, and eight AFG models were all within two units of one another (Table 19). The model containing genus level predictors was the most parsimonious and explained variation in relative flexibility better compared to all other taxonomic groups (Table 19). All variables remained significant predictors of relative flexibility except fineness ratio which was also removed to produce the final model from which to describe predicted trends (Table 20). For every one percent increase in scale imbrication, relative flexibility was predicted to decrease by 43% when holding all other variables constant. Unit increases in the total vertebrae number and average intervertebral joint length (all other variables held constant) were predicted to increase body curvature by ~1% and 75%, respectively. Similarly, a one $N \bullet m^2$ increase in flexural stiffness was predicted to cause a 98% decrease in relative flexibility when all other variables were held constant. In contrast, a one degree increase in maximum range of motion was predicted to significantly decrease body curvature (~3%), while unit increases in 2nd moment of inertia (increased resistance of vertebral column to bending) would also lead to a small (<< 0.01%), yet significant increase in relative flexibility (Table 20). Trends in both variables indicate a relationship with relative flexibility that was opposite of initial predictions. Elongate-compressed cypriniforms and moderate-compressed perciforms had statistically higher relative flexibility (~20%) compared to stout-compact perciforms (the reference guild). In contrast, all other guilds were predicted to have significantly less relative flexibility when compared to stout-compact perciforms (Table 20). Furthermore, the elongate-rotund siluriform guild was predicted to have 62% lower relative flexibility (the lowest value) compared to the stout-compact perciforms. Model predictions of decreased relative

flexibility for most guilds relative to the reference was unexpected and contrary to original predictions.

Discussion

The creation of anatomorphic functional guilds in this study were a combination of functional relevance and taxonomic relatedness in traits among guild members. Three of the seven guilds can be linked to family- and order-level taxonomic group including clupeids, salmonids, and ictalurids. Formation of three unique groups was expected because these families do not have the same species richness compared to cypriniforms or perciforms found in the southeastern USA. Interestingly, clupeids and salmonids did form a unique cluster within a more inclusive 6-cluster scheme (Figure 7B), which was likely due to similarities in scale type and imbrication; however, separation seems advisable considering that number of vertebrae and maximum range of motion were quite disparate between both groups (Table 5). The moderate-sized, slender cypriniform group (e.g., golden shiner) was also observed within a unique cluster at higher clustering schemes (Figure 7B–D) though no singular trait beyond a slender cypriniform profile was especially distinctive for this group (Table 5). All four guilds, however, were represented by fewer than 10 individuals and only one species such that more species are needed to help support the functional relevance of these AFGs. For example, the esocids may form a separate cluster given their sagittiform body shape [67], distinctive scales [68], and different S-start body movements [69,70] may separate this family from other salmoniforms in terms of relative flexibility. In contrast, other morphological distinct fishes (i.e., petromyzontiform, acipenseriform, or anguilliform) would likely form separate guilds and only need to be confirmed by one representative species because of their distinctive anatomorphic traits. Catfish were always considered a separate guild in every cluster scheme (Figure 7) because relative body shape was opposite of other groups (i.e., is much wider than deep; Figure 9), they are scaleless, and had the lowest observed values of tissue firmness and whole-body flexural stiffness (Table 5).

The remaining three clusters included more functionally interesting member species that belonged to separate families of fishes. Elongate, compressed cypriniforms

also identified and included all catostomids which shared similarities in body shape and vertebral morphometrics with central stoneroller. Inclusion of large-bodies cyprinids like carp or buffalo and more characteristic “minnow” species in anatomorphic analysis would be especially useful to further refine and confirm this AFG. Separation of the perciforms into two separate guilds was also expected given the noticeable disparities in fineness and cross-sectional ratios among these fishes (Table 5). Many traits are shared between the moderate-sized and stout perciform groups including scale type, imbrication, and number of vertebrae. In contrast, the maximum range of motion, 2nd moment of inertia, and average vertebra length were noticeably higher in the more elongate perciforms like largemouth bass (Table 5). The moderate-sized, compressed perciforms actually contained members of four families which was unexpected because clustering also suggested freshwater drum fit best within this guild. Ideally, a multivariate analysis of variance or discriminant analysis could be used to test for significant differences between anatomorphic data and AFGs, but samples sizes and species representation in some guilds were too low to compare directly. Alternatively, cluster delineation and overall fit was visually assessed by allowing R to predict the location of unused individuals (six different species total; Table 2) on a plot containing the original 105 individuals and clusters. Points representing common carp, longear sunfish, warmouth (123 & 128), and hybrid sunfish all fit well within their predicted cluster (Figure 12). Similarly, white sucker and blue catfish were also found very near, but not inside, their respective clusters which suggest clusters fit these anatomorphic data well (Figure 12). To that end, inclusion of supplementary individuals suggests that AFGs are well defined and have properly included similar, yet taxonomically disparate fishes into functionally relevant groups that can be used to predict relative flexibility.

Anatomorphic functional variables used in this study were significant predictors of body curvature, though some unexpected trends were observed. At an individual level (i.e., no species identity was assigned), fineness ratio was considered highly significant, but represented the only non-significant variable when guilds were included in the model. The latter suggests fineness ratio (an approximation of body shape and overall length) was an important predictor of body curvature at an individual level but not at guild level

relative to all other variables. In fact, removing this variable produced a model with a higher adjusted R2 and smaller model selection criteria, which suggests inclusion of guilds (and a functional-group effect) is more important than size when predicting relative flexibility. Scale imbrication was always significant, such that a 1% increase was also predicted to significantly increase relative flexibility by ~18% at an individual level, while a ~42% decrease was predicted when guilds were included (Table 7). Perciform guilds had the highest observed values of imbrication (>75%) and some of lowest observed values of relative flexibility (Table 5) which suggests deeply embedded scales may also limit maximum flexibility. However, scale imbrication may not completely capture the variation in scale penetration or resistance to movement within the scale pockets of the integument. Shad imbrication was ~68% yet the scales of these fishes are known to be deciduous and are readily removed because they are held less securely [68]. Interestingly, shad scales also did not contain inter-radials and the anterior margin had a smooth profile compared to all other AFGs except the salmoniform guild. The presence or absence of inter-radial grooves and category of anterior margin profile was not predicted to significantly impact relative flexibility; however, this may be the result of not estimating maximal flexibility. Forceful bending of the body during blade strike could loosen scales and cause them to dislodge from the scale pockets, which would also likely inhibit overall flexibility. Under this scenario, highly imbricated (deeply embedded) scales interacting with one another via the inter-radial grooves, or between the scale pocket and scale margins, would also further limit maximum flexibility. While unexpected in some respects, all of the above trends suggest that the guild model more accurately predicts relative flexibility compared to the individual-based model. Vertebral morphometrics were also significant predictors of body curvature, and opposing trends detected here may be linked to unrealistic vertebral column assumptions used in this study. Increasing the number of vertebrae and intervertebral joint length were both predicted to increase relative flexibility which has also been documented in other species [35,39]. In contrast, as average maximum range of motion increased, all models tested in this study predicted that relative flexibility would decrease as a result which was not expected. In general, higher flexibility of the vertebral column has also been

associated with higher maximum range of motion, especially in caudal vertebrae [39]. The opposite trend detected in this study may be the result of modeling vertebrae as elliptical cylinders, because vertebral elements of bony fishes are more structurally complex. For example, many species contain zygapophyses (bony protrusions) on both the anterior-posterior and dorsal-ventral surfaces, which may also interlock with one another between vertebrae [54,71]. Both gizzard shad and rainbow trout contain these bony protrusions, but the overall size and amount of overlap between gizzard shad vertebrae is more profound and changes with position in the vertebral column (Figure 13). In addition, ribs attached to the pre-caudal vertebrae and the presence of up to three different types of intramuscular bones found among the myosepta and pre-caudal vertebrae [54,71] would also likely decrease the actual range of motion among species. To that end, the unexpected trend in maximum range of motion is likely the result of not including sufficient structural complexity into the multiple regression of relative flexibility. The apparent lack of vertebral structural complexity in the regression may also help explain why 2nd moment of inertia was expected to significantly increase body curvature instead of a decreasing trend (Table 7). Assuming the vertebral column is a simple elliptical cylinder is also too simplistic because precaudal vertebrae are mostly oblate (width > depth) versus the prolate (depth > width) elliptical shape caudal vertebrae provides evidence against this assumption. Furthermore, additional measurements from multiple pre-caudal and caudal vertebrae are needed to better account for variation between these vertebra types when attempting to model the entire vertebral column.

Relative flexibility was also significantly influenced by anatomorphic functional guild, but the relationship between stout-compact perciforms (the reference) and other guilds was exactly opposite initial predictions. Observed trends in relative flexibility suggested that stout-compact perciforms had the lowest overall flexibility compared to all other guilds, yet this guild was predicted to have the highest predicted relative flexibility. Evidence in support of this contrary trend may be found in the fact that vertebral zygapophyses in this guild are particularly small and do not overlap, i.e., flexibility would be higher. Similarly, the guilds predicted to have higher relative flexibility (elongate-compressed cypriniforms and moderate-compressed perciforms) either do not

have zygapophyseal projections, or if present, they are reduced in size and do not overlap. In contrast, moderate-compact cypriniforms, elongate-compressed salmoniforms, and elongate-rotund siluriforms also have these projections which suggests relative flexibility was also impacted as a result. An equally surprising trend that catfish would have the lowest body curvature relative to the stout perciforms, yet observed values indicated the opposite (Table 7). The catfish mid-body has an oblate (width > depth) cross-sectional profile so that beam theory would predict that an oblate elliptical cylinder would also have the highest flexural stiffness (lowest relative flexibility). Again, the opposite was observed with catfish measured in this study having the highest relative flexibility of all species tested (Table 7; Figure 14). However, further review of relative flexibility images suggests that catfish may not be as flexible as initially believed. Compared to other species, the catfish does not bend or pivot at the same point as other species because its dorsal fin is positioned directly above its snout, while the dorsal fin of other species bends away from the head (Figure 14). This is likely due to the wider cross-sectional profile of the mid-body compared to the caudal area of catfish, which causes the body to pivot near the anal fin (intersection of pre-caudal and caudal vertebrae) instead of the head. All of these observations suggest the method used to estimate relative flexibility may not be accurate for catfish which resulted in an overestimate of flexibility in this species. While all of the above may explain unexpected model predictions, it also suggests model accuracy is low, more pertinent variables should be included within the regression analysis, and maximal flexibility should be directly measured.

The main purpose of this study was to create functionally relevant guilds of fishes and use these groups to predict trends in relative flexibility as surrogate for susceptibility to blade strike impact. Of the seven guilds, rates of injury and mortality data are available for gizzard shad (moderate-compact clupeiforms), rainbow trout (elongate-compressed salmoniforms), hybrid striped bass (moderate-compress perciforms), and bluegill (stout-compact perciforms). Laboratory trials conducted at ORNL on blade strike suggest that gizzard shad and bluegill are the most susceptible, followed by rainbow trout, and hybrid striped bass are the most resistant to blade strike impacts [21,66]. Using relative flexibility (or lack thereof) as a surrogate for susceptibility suggests that gizzard shad and

trout would be the most susceptible, followed by bluegill, and hybrid striped bass would still be the most resistant. Higher relative flexibility predicted for the elongate-compressed cypriniform and perciform guilds also suggests these fishes may be more resistant to blade strike impact compared to the stout-compact perciforms. Increased susceptibility could be true for rainbow trout because larger trout are more susceptible to blade strike compared to smaller fish and the fish used in this study were 10.0 cm longer on average than those used in laboratory tests [21,72]. Gizzard shad measured here were also larger on average than those used in laboratory studies and size effects have not been directly tested on this species, which precludes further comparisons. The mismatch could also be caused by a lack of sufficient vertebral or scale morphometric variables needed to more accurately model relative flexibility in the regression analyses. Relative flexibility measured in this study is also only a relative estimate of flexibility and may need to be tested directly using quasi-static or dynamic impact tests to establish maximal flexibility. Flexibility may also simply not be the most important factor needed to predict mortality from impact testing because fish including bluegill have been observed with a high degree of body curvature during C-start predator avoidance behavior [28]. Impact from a blade causes non-volitional bending of the fish body as a result of physical contact, which is unnatural compared to the well-studied series of body movements and bending observed during the C-start escape response [32,73]. In addition, blade impact transfers a tremendous amount of energy into the fish as it wraps around the blade and quickly (< 10 ms) returns to its original position as the result of elastic recoil, i.e., a comparable version of whiplash in fish. Quick, high energy transfers of this nature suggest that changes in loading rates or mechanical deformation of the fish body must also be considered when estimating susceptibility to blade strike. Moving forward, a more accurate regression model may include additional morphometric variables and use maximal flexibility as the predictor variable so that links to susceptibility are also linked to quantifiable biomechanical limitations as well.

Conclusions

Anatomorphic functional guilds were successfully created by combining taxonomically diverse fishes into groups based on shared, functionally relevant traits and should have many other applications. The seven AFGs identified also mirrored the list of prioritized species used to direct species laboratory experiments of turbine passage stressors (Table 1); however, members of cypriniform and perciform groups were noticeably different and acipenseriform and anguillid fishes were not represented in this study (Table 7). In addition, most AFGs can be used to represent more than one species and identification of a surrogate species to represent the entire guild is also possible. Other untested families of fishes may also be represented by the guilds presented here including the mooneyes (Hiodontidae) which are similar in shape to clupeids and are not as well studied. More species that are likely members of the moderate-slender cypriniforms, elongate-compressed salmoniforms, and elongate-rotund siluriforms need to be studied to help confirm the validity of these guilds. Support of guild validity was provided when unused species were predicted to fit within or very close to each ellipse that represented these guilds (Figure 12). The method used to create AFGs would also be useful to help research the remarkably diverse fish assemblages found in the Amazon, Congo, and Mekong Rivers where hydropower development is accelerating at a remarkable pace [74]. Similar applications with different anatomorphic variables could also be used to better study the efficacy, and optimize the design of, fishway passage structures which are generally designed to benefit fewer, well-studied species [75]. Finally, functionally relevant guilds linked to fish thermal physiology, respirometry, and bioenergetics data would also be especially useful to better model the effects of a warming climate on diverse riverine fish communities worldwide.

While the AFGs appear to be well supported by the data, the predication accuracy and applicability of the multiple regression model of relative flexibility is more difficult to assess. A significant regression model that predicted relative flexibility according to multiple anatomorphic functional guilds was successfully identified. The inclusion of AFGs into the model was also significant and described the variation in the anatomorphic data better than the individual-based or taxonomic guild models; however, trends in

relative flexibility were often the opposite of what was originally predicted. Some of these unexpected outcomes may be linked to omission of as yet to be identified, yet important, anatomorphic variables into the regression model. More variables linked to scale morphometrics or the diverse vertebral morphology observed in fishes would likely lead to more accurate predictions of relative flexibility. An estimate of maximal flexibility would also help delineate effects between AFGs because it would be based on actual biological limits instead of a relative measurement of body curvature. Alternatively, the observed trends may be biologically relevant because susceptibility to blade strike has yet to be studied in most fishes, and the data that are available may not be applied to all sizes within the same species. In this way, contrary trends may be more indicative of fish responses than originally thought because predicted trends in susceptibility to blade strike based on relative flexibility described here were quite similar. Regardless, the AFG model accounted for variation in relative flexibility better than a strictly taxonomic model, which suggests using traits-based approaches to study biomechanical phenomena among fishes is useful technique to study highly diverse fish communities.

Acknowledgements

This manuscript has been authored by UT-Battelle, LLC under Contract No. DE-AC05-00OR22725 with the US Department of Energy. Fish use approval was granted by the ORNL Institutional Animal Care and Use Committee [protocol #0468]. First and foremost, I must thank Trent Jett, Michael Jones, and Nikki Jones (Oak Ridge National Laboratory) for their help finding and collecting most of the fish used in this study. Many thanks are also extended to Dustin Sterling (ORNL) who collected most of the anatomorphic data and for assisting with fish care in the Aquatic Ecology Laboratory. I thank John Ellis (Tennessee Wildlife and Resource Agency) from the Tellico Fish Hatchery for donating the Rainbow Trout used in this study. Finally, I thank Bart Carter (TWRA) for his assistance with finding and collecting study specimens as well.

References

1. Čada, G.F.; Schweizer, P.E. *The application of traits-based assessment approaches to estimate the effects of hydroelectric turbine passage on fish populations*; Oak Ridge, Tennessee, **2012**; Vol. April.

2. Pracheil, B.M.; McManamay, R.A.; Bevelhimer, M.S.; DeRolph, C.R.; Čada, G.F. A traits-based approach for prioritizing species for monitoring and surrogacy selection. *Endanger. Species Res.* **2016**, *31*, 243–258.

3. Benoit, D.M.; Jackson, D.A.; Chu, C. Partitioning fish communities into guilds for ecological analyses: an overview of current approaches and future directions. *Can. Jouranl Fish. Aquat. Sci.* **2021**.

4. Frimpong, E.A.; Angermeier, P.L. Fish traits: A database of ecological and life-history traits of freshwater fishes of the United States. *Fisheries* **2009**, *34*, 487–495.

5. Nelson, J.S.; Grande, T.C.; Wilson, M.V.H. *Fishes of the World*; 5th ed.; John Wiley & Sons: Hoboken, New Jersey, **2016**.

6. Balon, E.K. Reproductive guilds of fishes: A proposal and definition. *J. Fish. Res. Board Canada* **1975**, *32*, 821–864.

7. Pyron, M.; Williams, L.; Beugly, J.; Jacquemin, S.J. The role of trait-based approaches in understanding stream fish assemblages. *Freshw. Biol.* **2011**, *56*, 1579–1592.

8. Mims, M.C.; Olden, J.D.; Shattuck, Z.R.; Poff, N.L. Life history trait diversity of native freshwater fishes in North America. *Ecol. Freshw. Fish* **2010**, *19*, 390–400.

9. Balon, E.K.; Momot, W.T.; Regier, H.A. Reproductive guilds of percids: Results of the paleogeographical history and ecological succession. *J. Fish. Res. Board Canada* **1977**, *34*, 1910–1921.

10. Córdova-Tapia, F.; Zambrano, L. Fish functional groups in a tropical wetland of the Yucatan Peninsula, Mexico. *Neotrop. Ichthyol.* **2016**, *14*.

11. Frimpong, E.A.; Angermeier, P.L. Trait-based approaches in the analysis of stream fish communities. *Am. Fish. Soc. Symp.* **2010**, *73*, 109–136.

12. Winemiller, K.O.; Rose, K.A.; Rose, K.A. Patterns of life-history diversification in North American fishes: Implications for population regulation. *Can. J. Fish. Aquat.* **1992**, *49*, 2196–2218.

13. Schwartz, J.S.; Simon, A.; Klimetz, L. Use of fish functional traits to associate in-stream suspended sediment transport metrics with biological impairment. *Environ. Monit. Assess.* **2011**, *179*, 347–369.

14. Pease, A.A.; Gonzalez-Diaz, A.A.; Rodiles-Hernandez, R.; Winemiller, K.O. Functional diversity and trait-environment relationships of stream fish assemblages in a large tropical catchment. *Freshw. Biol.* **2012**, *57*, 1060–1075.

15. Maxwell, E.E.; Wilson, L.A.B. Regionalization of the axial skeleton in the "ambush predator" guild - Are there developmental rules underlying body shape evolution in ray-finned fishes? *BMC Evol. Biol.* **2013**, *13*, 1–17.

16. Caillon, F.; Bonhomme, V.; Möllmann, C.; Frelat, R. A morphometric dive into fish diversity. *Ecosphere* **2018**, *9*.

17. Hostetter, N.J.; Evans, a. F.; Roby, D.D.; Collis, K.; Hawbecker, M.; Sandford, B.P.; Thompson, D.E.; Loge, F.J. Relationship of external fish condition to pathogen prevalence and out-migration survival in juvenile steelhead. *Trans. Am. Fish. Soc.* **2011**, *140*, 1158–1171.

18. Čada, G.F. The development of advanced hydroelectric turbines to improve fish passage survival. *Fisheries* **2001**, *26*, 14–23.

19. Mueller, M.; Pander, J.; Geist, J. Evaluation of external fish injury caused by

hydropower plants based on a novel field-based protocol. *Fish. Manag. Ecol.* **2017**, *24*, 240–255.

20. Neitzel, D. a; Dauble, D.D.; Cada, G.F.; Richmond, M.C.; Guensch, G.R.; Mueller, R.R.; Abernethy, C.S.; Amidan, B. Survival estimates for juvenile fish subjected to a laboratory-generated shear environment. *Trans. Am. Fish. Soc.* **2004**, *133*, 447–454.

21. Bevelhimer, M.S.; Pracheil, B.M.; Fortner, A.M.; Saylor, R.; Deck, K.L. Mortality and injury assessment for three species of fish exposed to simulated turbine blade strike. *Can. J. Fish. Aquat. Sci.* **2019**, *76*, 2350–2363.

22. Colotelo, A.H.; Goldman, A.E.; Wagner, K.A.; Brown, R.S.; Deng, Z.D.; Richmond, M.C. A comparison of metrics to evaluate the effects of hydro-facility passage stressors on fish. *Environ. Rev.* **2017**, *25*, 1–11.

23. Čada, G.; Loar, J.; Garrison, L.; Fisher, R.; Neitzel, D. Efforts to reduce mortality to hydroelectric turbine-passed fish: Locating and quantifying damaging shear stresses. *Environ. Manag.* **2006**, *37*, 898–906.

24. Pracheil, B.M.; Pegg, M.A.; Powell, L.A.; Mestl, G.E. Swimways: Protecting Paddlefish through Movement-centered Management. *Fisheries* **2012**, *37*, 449–457.

25. Turnpenny, A.W.H.; Davis, M.H.; Fleming, J.M.; Davies, J.K. *Experimental studies relating to the passage of fish and shrimps through tidal power turbines*; Southampton, United Kingdom, **1992**.

26. EPRI, (Electric Power Research Institute) *Evaluation of the effects of turbine blade leading edge design on fish survival*; Palo Alto, CA, **2008**.

27. Amaral, S. V; Watson, S.M.; Schneider, A.D.; Rackovan, J.; Baumgartner, A. Improving survival: Injury and mortality of fish struck by blades with slanted,

blunt leading edges. *J. Ecohydraulics* **2020**.

28. Borazjani, I. The functional role of caudal and anal/dorsal fins during the C-start of a bluegill sunfish. *J. Exp. Biol.* **2013**, *216*, 1658–1669.

29. Cada, G.F.; Ryon, M.G.; Wolf, D.A.; Smith, B.T. *Development of a new technique to assess susceptibility to predation resulting from sublethal stresses (indirect mortality)*; Oak Ridge, Tennessee, **2003**; Vol. August;

30. Goldbogen, J.A. Fast-start muscle dynamics in the rainbow trout Oncorhynchus mykiss: phase relationship of white muscle shortening and body curvature. *J. Exp. Biol.* **2005**, *208*, 929–938.

31. Hale, M.E. The Development of Fast-Start Performance in Fishes: Escape Kinematics of the Chinook Salmon (Oncorhynchus tshawytscha). *Am. Zool.* **1996**, *36*, 695–709.

32. Wakeling, J.M. Fast-start Mechanics. In *Fish Physiology: Fish Biomechanics*; Randall, D.J., Farrell, Eds.; Elsevier Academic Press: San Diego, California, **2006**; Vol. 23, pp. 333–368 ISBN 0022-0949.

33. Webb, P.W. Body form, locomotion and foraging in aquatic vertebrates. *Integr. Comp. Biol.* **1984**, *24*, 107–120.

34. Blake, R.W. Review Paper: Fish functional design and swimming performance. *J. Fish Biol.* **2004**, *65*, 1193.

35. Brainerd, E.L.; Patek, S.N. Vertebral column morphology, C-start curvature, and the evolution of mechanical defenses in tetraodontiform fishes. *Copeia* **1998**, 971–984.

36. Long, J.H.; Koob-Emunds, M.; Koob, T.J. The mechanical consequences of vertebral centra. *Bull Mt Desert Isl. Biol Lab* **2004**, *43*, 99–101.

37. Ward, A.B.; Azizi, E. Convergent evolution of the head retraction escape response in elongate fishes and amphibians. *Zoology* **2004**, *107*, 205–217.

38. Porter, M.E.; Roque, C.M.; Long, J.H. Turning maneuvers in sharks: Predicting body curvature from axial morphology. *J. Morphol.* **2009**, *270*, 954–965.

39. Nowroozi, B.N.; Harper, C.J.; De Kegel, B.; Adriaens, D.; Brainerd, E.L. Regional variation in morphology of vertebral centra and intervertebral joints in striped bass, Morone saxatilis. *J. Morphol.* **2012**, *273*, 441–452.

40. Gemballa, S.; Bartsch, P. Architecture of the integument in lower teleostomes: Functional morphology and evolutionary implications. *J. Morphol.* **2002**, *253*, 290–309.

41. Bruet, B.J.F.; Song, J.; Boyce, M.C.; Ortiz, C. Materials design principles of ancient fish armour. *Nat. Mater.* **2008**, *7*, 748–756.

42. Wainwright, S.A. *Axis and Circumference*; 1st ed.; Harvard University Press: Cambridge, Massachusetts, **1988**; ISBN 0674057007.

43. Wainwright, S.A. The Animal Axis. *Am. Zool.* **2000**, *40*, 19–27.

44. Summers, A.P.; Long, J.H. Skin and bones, sinew and gristle: The mechanical behavior of fish skeletal tissues. In *Fish Physiology: Fish Biomechanics*; Randall, D.J., Farrell, Eds.; Elsevier Academic Press: San Diego, California, **2006**; Vol. 23, pp. 141–177 ISBN 9780123504470.

45. Etnier, S.A. Twisting and bending of biological beams: Distribution of biological beams in a stiffness mechanospace. *Biol. Bull.* **2003**, *205*, 36–46.

46. Ross, S.T.; Matthews, W.J. Evolution and ecology of North American freshwater fish assemblages. In *Freshwater Fishes of North America Volume 1: Petromyzontidae to Catostomidae*; Warren Jr., M.L., Burr, B.M., Eds.; Johns Hopkins University Press: Baltimore, Maryland, **2014**; pp. 1–49.

47. Collar, D.C.; Wainwright, P.C. Ecomorphology of centrarchid fishes. In *Centrachid Fishes: Diversity, Biology and Conservation*; Cooke, S., Philipp, D., Eds.; Blackwell Publishing Ltd: West Sussex, UK, **2009**; pp. 70–89.

48. Smith, A.J.; Nelson-Maney, N.; Parsons, K.J.; James Cooper, W.; Craig Albertson, R. Body shape evolution in sunfishes: Divergent paths to accelerated rates of speciation in the Centrarchidae. *Evol. Biol.* **2015**, *42*, 283–295.

49. Etnier, D.A.; Starnes, W.C. *The Fishes of Tennessee*; 1st ed.; The University of Tennessee Press: Knoxville, Tennessee, **1993**.

50. Page, L.M.; Espinosa-Perez, H.; Findley, L.T.; Gilbert, C.R.; Lea, R.N.; Mandrak, N.E.; Mayden, R.L.; Nelson, J.S. Scientific name, occurrence, and accepted common name. In *Common and Scientific Names of Fishes from the United States, Canada, and Mexico*; American Fisheries Society: Bethesda, Maryland, **2013**; Vol. Special Pu, p. 243 ISBN 978-1-934874-31-8.

51. Cone, R.S. The need to reconsider the use of condition indices in fishery science. *Trans. Am. Fish. Soc.* **1989**, *118*, 510–514.

52. Weisstein, E.W. Ellipticity Available online: https://mathworld.wolfram.com/Ellipticity.html (accessed on Feb 2, 2021).

53. Davesne, D.; Meunier, F.J.; Schmitt, A.D.; Friedman, M.; Otero, O.; Benson, R.B.J. The phylogenetic origin and evolution of acellular bone in teleost fishes: Insights into osteocyte function in bone metabolism. *Biol. Rev.* **2019**, *94*, 1338–1363.

54. Rojo, A.L. *Dictionary of evolutionary fish osteology*; 1st ed.; CRC Press, Inc.: Boca Raton, Florida, **1991**; ISBN 1138507024.

55. Baliga, V.B.; Mehta, R.S. Ontogenetic allometry in shape and flexibility underlies life history patterns of labrid cleaning behavior. *Integr. Comp. Biol.* **2016**, *56*,

416–427.

56. Cohen, L.; Dean, M.; Shipov, A.; Atkins, A.; Monsonego-Ornan, E.; Shahar, R. Comparison of structural, architectural and mechanical aspects of cellular and acellular bone in two teleost fish. *J. Exp. Biol.* **2012**, *215*, 1983–1993.

57. Lê, S.; Josse, J.; Husson, F. FactoMineR: An R package for multivariate analysis. *J. Stat. Softw.* **2008**, *25*, 1–18.

58. Kassambara, A.; Mundt, F. factoextra: Extract and visualize the results of multivariate data analyeses Available online: https://cran.r-project.org/package=factoextra (accessed on Feb 6, 2021).

59. R Core Team R: A language and environment for stastical computing. **2020**.

60. Kassambara, A. *Practical guide to principal compoenent methods in R*; 1st ed.; STHDA, **2017**; ISBN 1975721136.

61. Lumley, T. leaps: Regression subset selection. Available online: https://CRAN.R-project.org/package=leaps (accessed on Feb 6, 2021).

62. Venables, W.N.; Ripley, B.D. *Modern applied statistics with S.*; Chambers, J., Eddy, W., Hardle, W., Sheather, S., Tierney, L., Eds.; 4th ed.; Springer Science+Business Media, LLC: New York City, NY, **2002**; ISBN 0387954570.

63. Barton, K. MuMIn: Multi-model interface Available online: https://cran.r-project.org/package=MuMIn (accessed on Feb 6, 2021).

64. Fox, J.; Weisberg, S. *An R companion to applied regression*; 3rd ed.; SAGE Publications, Inc.: Thousand Oaks, California, **2019**; ISBN 1544336470.

65. Wei, T.; Simko, V. R package “corrplot”: Visualization of a correlation matrix Available online: https://github.com/taiyun/corrplot (accessed on Feb 7, 2021).

66. Saylor, R.; Fortner, A.; Bevelhimer, M. Quantifying mortality and injury susceptibility for two morphologically disparate fishes exposed to simulated turbine blade strike. *Hydrobiologia* **2019**, *842*, 55–75.

67. Senay, C.; Harvey-Lavoie, S.; Macnaughton, C.J.; Bourque, G.; Boisclair, D. Morphological differentiation in northern pike (Esox lucius): The influence of environmental conditions and sex on body shape. *Can. J. Zool.* **2017**, *95*, 383–391.

68. Lagler, K.F. Lepidological Studies 1. Scale Characters of the Families of Great Lakes Fishes. *Trans. Am. Fish. Soc.* **1947**, *66*, 149–171.

69. Schriefer, J.E.; Hale, M.E. Strikes and startles of northern pike (Esox lucius): A comparison of muscle activity and kinematics between S-start behaviors. *J. Exp. Biol.* **2004**, *207*, 535–544.

70. Liu, Y.C.; Hale, M.E. Alternative forms of axial startle behaviors in fishes. *Zoology* **2014**, *117*, 36–47.

71. Mettler, F.A.; Guiberteau, M.J. Skeletal System. *Lab. Fish* **2000**, 271–314.

72. Saylor, R.; Sterling, D.; Bevelhimer, M.; Pracheil, B. Within and among fish species differences in simulated turbine blade strike mortality: Limits on the use of surrogacy for untested species. *Water* **2020**, *12*, 1–27.

73. Wakeling, J.M. Biomechanics of fast-start swimming in fish. *Comp. Biochem. Physiol. - A Mol. Integr. Physiol.* **2001**, *131*, 31–40.

74. Winemiller, K.O.; McIntyre, P.B.; Castello, L.; Fluet-Chouinard, E.; Giarrizzo, T.; Nam, S.; Baird, I.G.; Darwall, W.; Lujan, N.K.; Harrison, I.; et al. Balancing hydropower and biodiversity in the Amazon, Congo, and Mekong. *Science (80-.).* **2016**, *351*, 128–129.

75. Silva, A.T.; Lucas, M.C.; Castro-Santos, T.; Katopodis, C.; Baumgartner, L.J.;

Thiem, J.D.; Aarestrup, K.; Pompeu, P.S.; O'Brien, G.C.; Braun, D.C.; et al. The future of fish passage science, engineering, and practice. *Fish Fish.* **2018**, *19*, 340–362.

Appendix

Table 14. List of fish taxonomic groups in the USA used to prioritize species for laboratory research on turbine passage stressors.

Taxa	Species of Interest	Region	Justification	Surrogate species	AFG
Anguillidae	American Eel	SE; NE	Conservation concern; Catadromous	None	One
Acipenseriformes	Paddlefish	MW; SW; SE	Listed under ESA; Potamodromous	None	One
	Sturgeons (all)	ALL	Listed under ESA; Catadromous	None	
Clupeidae	American Shad	SE; NE	Listed under ESA; Anadromous	Gizzard shad	One
	Blueback Herring	SE; NE	Listed under ESA; Anadromous	Gizzard Shad; American shad	
	Alewife	SE; NE	Species of concern NOAA; Anadromous	Gizzard Shad; American Shad	
Cypriniformes	River Redhorse	MW; SW; SE	State listed species; Potamodromous	White Sucker; Spotted Sucker	Two
Salmonidae	Steelhead	W	Listed under ESA; Anadromous	Rainbow Trout	One
	Bull Trout	W	Listed under ESA; Potamodromous	Brook Trout	
	Atlantic Salmon	NE	Listed under ESA; Anadromous	Brown Trout	
Centrarchidae	Largemouth Bass	ALL	Common reservoir gamefish	Bluegill Sunfish	Two
	Bluegill Sunfish	ALL	Common reservoir gamefish	*Lepomis* spp.	
Perciformes	Striped Bass	NE; SE	Common gamefish; Anadromous	Hybrid Striped Bass; White Bass	One
	Sauger	ALL	Common gamefish; Potamodromous	Yellow Perch; Walleye	

NOTE: Regions are West (W), Southwest (SW), Midwest (MW), Southeast (SE), Northeast (NE), or relevant to ALL regions. Some species are listed under the Endangered Species Act (ESA) or the purview of the National Oceanic and Atmospheric Administration (NOAA) in the USA. Surrogate species can be used in place of the desired species to represent each group. The last column is the predicted number of anatomorphic functional guilds (AFG) that will be needed to represent each taxonomic in this study.

Table 15. Comprehensive list of all fishes collected from eastern Tennessee and used to develop anatomorphic functional guilds.

Super Order	Order	Family	Common Name	Scientific name	ABV	N_T	N_S	TL	Mass
Clupeomorpha	Clupeiformes	Clupeidae	Skipjack Herring	*Alosa chrysochloris*	SJH	2	2	18.0 – 24.5	38.5 – 100.3
			Gizzard Shad	*Dorosoma cepedianum*	GZS	13	7	16.1 – 27.4	33.1 – 167.9
Ostariophysi	Cypriniformes	Cyprinidae	Golden Shiner	*Notemigonus crysolecusas*	GDS	10	8	17.4 – 20.3	48.4 – 98.4
			Central Stoneroller	*Campostoma anomalum*	CSR	6	5	14.1 – 18.6	26.1 – 55.9
			White sucker	*Catostomus commersonii*	WHS	1	0	21.5	76.4
			Common Carp	*Cyprinus carpio*	CC	1	0	46.7	1060.1
		Catostomidae	Spotted Sucker	*Minytrema melanops*	SPS	7	7	21.1 – 28.8	78.2 – 227.0
			Black Redhorse	*Moxostoma duquesni*	BRH	8	5	19.0 – 32.0	52.3 – 288.2
			Golden Redhorse	*Moxostoma erythrurum*	GRH	2	2	30.3 – 32.7	277.3 – 351.3
	Siluriformes	Ictaluridae	Yellow Bullhead	*Ameiurus natlalis*	YBH	6	6	21.2 – 28.8	106.7 – 284.3
			Blue catfish	*Ictalurus punctatus*	BCH	1	0	34.1	231.4
Protacanthopterygii	Salmoniformes	Salmonidae	Rainbow Trout	*Oncorhynchus mykiss*	RBT	5	5	26.3 – 34.0	187.8 – 380.9
Acanthopterygii	Perciformes	Moronidae	White Bass	*Morone chrysops*	WHB	7	5	28.8 – 36.1	250.0 – 457.7
			Yellow Bass	*Morone mississippiensis*	YLB	5	4	20.1 – 21.9	82.7 – 108.9
		Centrarchidae	Redbreast Sunfish	*Lepomis auritus*	RBS	4	4	15.0 – 21.4	51.8 – 166.4
			Green Sunfish	*Lepomis cyanellus*	GSF	5	5	14.5 – 16.6	46.9 – 83.1
			Warmouth	*Lepomis gulosus*	WM	2	0	14.7 – 21.6	60.0 – 209.0

Table 15 continued…

		Hybrid Sunfish	*Leposis gulosus × cyanellus*	HYB	1	0	13.0	35.5
		Bluegill Sunfish	*Lepomis macrochirus*	BLG	7	5	14.8 – 19.2	52.5 – 161.3
		Longear Sunfish	*Lepomis megalotis*	LES	1	0	13.2	44.7
		Redear Sunfish	*Lepomis microlophus*	RES	8	8	14.7 – 25.7	38.2 – 264.9
		Smallmouth Bass	*Micropterus dolomieu*	SMB	2	2	32.7 – 35.5	326.4 – 502.4
		Largemouth Bass	*Micropterus salmoides*	LMB	8	7	24.4 – 32.6	196.1 – 447.3
		White Crappie	*Pomoxsis annularis*	WCR	8	8	19.7 – 31.9	76.2 – 426.6
		Black Crappie	*Pomoxsis nigromaculatus*	BCR	3	3	20.4 – 28.1	108.0 – 298.8
	Percidae	Yellow Perch	*Perca flavescens*	YP	8	5	16.2 – 30.6	38.1 – 290.2
	Sciaenidae	Freshwater Drum	*Aplodinotus grunniens*	FWD	2	2	35.6 – 38.9	479.9 – 480.2
				Total	133	105		

NOTE: Each species is present with its own unique two or three letter abbreviation (ABV), total number collected (N_T), total number used (N_S), range in total length (TL; ± 0.1 cm), and wet mass (± 0.1 g). See text for description of how the total number used was determined.

Table 16. Detailed definitions for variables used in the hierarchical clustering of principal components (HCPC) and multiple linear regression (MLR) analyses.

Var	Description	A	B	C
Hed_len	Proportion of head length relative to total length	X		
Hed_dep	Proportion of head depth relative to maximum depth	X		
Hed_wid	Proportion of head width relative to maximum width	X		
Pec_len	Proportion of pectoral fin length relative to total length	X		
Pec_dep	Proportion of pectoral fin width relative to maximum body width	X		
Pec_wid	Proportion of pectoral fin depth relative to maximum body depth	X		
Dor_len	Proportion of dorsal length relative to total body length	X		
Dor_dep	Proportion of dorsal depth relative to maximum depth	X		
Dor_wid	Proportion of dorsal width relative to maximum width	X		
Pel_len	Proportion of pelvic fin length relative to total length	X		
Pel_dep	Proportion of pelvic fin depth relative to maximum depth	X		
Pel_wid	Proportion of pelvic fin width relative to maximum width	X		
Ana_len	Proportion of anal fin length relative to total length	X		
Ana_dep	Proportion of anal fin depth relative to maximum depth	X		
Ana_wid	Proportion of anal fin width relative to maximum width	X		
Hed_elp	Ellipticity near the posterior edge of operculum; traverse cross section	X		
Pec_elp	Ellipticity near the anterior edge of the pectoral fin; traverse cross section	X		
Dor_elp	Ellipticity near the anterior edge of the dorsal fin; traverse cross section	X		
Pel_elp	Ellipticity near the anterior edge of the pelvic fin; travers cross section	X		
Ana_elp	Ellipticity near the anterior edge of the anal fin; traverse cross section	X		
Elp_avg	Average mid-body ellipticity; head to anal fin	X	X	
MB_prp	Proportion of mid-body (head to anal fin) length relative to total length	X	X	
Fine_rat	Fineness ratio; standard length divided by maximum body depth	X	X	X
BAsp_rat	Body aspect ratio; standard length divided by maximum body width	X	X	
CSec_rat	Cross-sectional aspect ratio; maximum depth divided by maximum width		X	
Sca_type	Cycloid, Ctenoid, or None			
Sca_Ard	Scale has anterior inter-radial grooves		X	
Sca_PRd	Scale has posterior inter-radial grooves		X	
ENT	ENTIRE; no distinct profile, mostly semi-circular margin			
UND	UNDULATE; few shallow curves along margin profile			
LOB	LOBATE; usually 5 obvious high amplitude ridges/valleys			
CRE	CRENATE; ≤ 10 alternating ridges/valleys with mid-margin protrusion			
CUT	CRENULATE; ~10 small alternating ridges/valleys & flat margin profile			
SIN	SINUATE; ≥ 20 smaller ridges/valleys and flat margin profile			

Table 16 continued…

Sca_are	Average scale area from scales removed from the mid-body; mm^2	X		
Sca_ED	Average proportion of scale embedded within scale pocket	X	X	X
Sca_AR	Average aspect ratio from scales removed	X	X	
Sca_den	Average scale density (1 divided by average scale area)			
Sca_MBC	Estimated number of scales covering the left mid-body lateral surface	X	X	
Bon_type	Cellular (0) or Acellular (1)			
PC_vert	Number of pre-caudal vertebrate	X		
C_vert	Number of caudal vertebrae	X		
MB_vert	Number of mid-body vertebrae (between the head and anal fin)	X		
Tot_vert	Total number of vertebrae	X	X	X
Cen_len	Average length of all vertebrae (pre-caudal and caudal)			
Ivj_len	Average intervertebral joint length; mm	X	X	X
PC_lw	Pre-caudal vertebrae length to width aspect ratio	X		
PC_dw	Pre-caudal vertebrae depth to width aspect ratio	X		
PC_ld	Pre-caudal vertebrae length to depth aspect ratio			
PC_vol	Pre-caudal vertebrae volume assuming elliptical cylinder			
PC_mrm	Pre-caudal vertebrae maximum range of motion; degrees			
C_lw	Caudal vertebrae length to width aspect ratio	X		
C_dw	Caudal vertebrae depth to width aspect ratio	X		
C_ld	Caudal vertebrae length to depth aspect ratio			
C_vol	Caudal vertebrae volume assuming elliptical cylinder			
C_mrm	Caudal vertebrae maximum range of motion; degrees			
Tot_lw	Average vertebrae length to width aspect ratio		X	
Tot_dw	Average vertebrae length to width aspect ratio		X	
Tot_ld	Average vertebrae length to depth aspect ratio		X	
Tot_vol	Average vertebrae volume; mm^3		X	
Tot_mrm	Average maximum range of motion for the vertebral column; degree		X	X
Iv_adj	Weighted 2^{nd} moment of inertia for vertebral column and size adjusted		X	X
CoG	Center of gravity; proportion of standard length	X		
Duro	Average whole-body durometer (firmness)	X	X	
Bod_cur	Body curvature; relative flexibility of the body from gravity	X	X	X
I_adj	Average 2nd moment of area of the mid-body adjusted for size; m^4		X	
EI_body	Flexural stiffness of the mid-body; $N \cdot m^2$		X	X

NOTE: Analyses are indicated by (A) Hiearchical clustering on principal components, (B) Multiple linear regression of body flexibility against anatomorphic variables, and (C) Multiple linear regression including anatomorphic functional guilds or taxonomic groups. An "X" indicates this variable was included in the identified analysis.

Table 17. Variable loadings for the six principal components that accounted for 79.4% of total variation in the anatomorphic data.

Variable	PC1	PC2	PC3	PC4	PC5	PC6
Hed_len	0.2144	-0.1705	-0.0651	0.0124	-0.1322	0.1506
Hed_dep	0.1586	-0.1694	-0.2705	-0.1141	-0.0856	0.1965
Hed_wid	0.0160	0.0116	-0.3835	-0.1403	0.0081	0.2012
Hed_elp	0.2292	0.1165	-0.0718	0.1218	-0.0182	-0.0076
Pec_len	0.2020	-0.1797	-0.0744	-0.0644	-0.1237	0.1241
Pec_dep	0.1633	-0.1353	-0.2630	-0.1898	-0.0723	0.1932
Pec_wid	0.0300	-0.1285	-0.3868	-0.0267	0.0803	-0.0072
Pec_elp	0.2364	0.0696	-0.0718	0.1719	-0.0029	-0.0306
Dor_len	-0.1011	0.1909	0.1761	0.2368	-0.1396	-0.0200
Dor_dep	-0.0516	0.0414	-0.1371	-0.1412	-0.0050	0.0791
Dor_wid	0.0818	0.0594	0.2451	-0.2288	-0.1565	0.3151
Dor_elp	0.1836	0.2566	-0.0797	0.0795	-0.0034	-0.0723
Pel_len	-0.2434	0.0705	0.0126	0.0612	-0.0016	0.0541
Pel_dep	0.1185	-0.0304	-0.0343	-0.0178	0.3444	-0.0655
Pel_wid	0.1162	0.2058	0.1608	-0.1995	0.0478	0.0331
Pel_elp	0.1814	0.2449	-0.0886	0.0757	0.0028	-0.0557
Ana_len	-0.1813	0.1440	-0.1290	-0.2394	0.1012	0.0868
Ana_dep	0.1804	-0.1960	0.1086	0.2059	-0.0869	0.0347
Ana_wid	0.1931	0.0841	0.1781	0.1296	-0.1098	0.1675
Ana_elp	0.1945	0.0748	-0.1330	0.2018	0.0002	-0.1951
Elp_avg	0.2228	0.1818	-0.0914	0.1287	-0.0057	-0.0635
MB_prp	-0.2122	0.1781	-0.0387	-0.1613	0.1225	-0.0412
Fine_rat	-0.2374	-0.0829	-0.0220	-0.1031	0.0740	0.0421
BAsp_rat	0.0120	0.2726	-0.1591	0.1557	0.0892	-0.1389
Sca_are	-0.0058	0.0853	-0.0480	-0.2174	-0.2358	-0.4635
Sca_ED	0.1542	0.2460	-0.0756	-0.1988	-0.1064	0.0217
Sca_MBC	-0.0619	0.1603	-0.1977	0.1868	-0.0991	0.3166
Sca_AR	0.0097	0.3244	-0.0830	-0.2245	-0.0882	0.1150
PC_vert	-0.1245	0.2965	-0.0282	-0.0065	-0.0929	0.1965
C_vert	-0.1648	-0.0413	-0.1901	0.3016	0.0567	0.0363

Table 17 continued…

MB_vert	-0.2160	0.2000	-0.1118	0.0431	0.0435	0.0662
Tot_vert	-0.1954	0.1338	-0.1611	0.2269	-0.0085	0.1373
PC_lw	0.1712	0.0988	0.0885	-0.0743	0.3585	0.0585
PC_dw	0.1588	0.0452	-0.1155	0.1638	0.3319	0.0338
C_lw	0.1171	-0.0146	0.0828	-0.1712	0.4081	-0.0485
C_dw	0.0305	0.0375	0.1221	-0.1499	0.2596	0.0530
Ivj_len	0.0185	-0.0569	-0.2020	-0.1916	-0.2763	-0.3298
CoG	0.0811	0.1226	0.2215	0.0286	-0.2608	0.1437
Duro	0.1453	0.1889	-0.0226	-0.1357	-0.0659	-0.2302
Bod_cur	-0.1864	-0.0971	-0.1157	0.0801	-0.0702	-0.1899
Eigenvalues	13.5667	6.6182	3.7748	3.5032	2.6621	1.6511
Cum_Var	33.9	50.5	59.9	68.7	75.3	79.4

Note: Eigenvalues and cumulative variance (Cum_var) are also provided for each principal component. Variable identity and definitions can be found in Table 16.

Table 18. Detailed breakdown of the seven anatomorphic functional guilds identified from hierarchical clustering including member species, total number of individuals per guild, and average values for select anatomorphic traits.

Variable	**1**	**2**	**3**	**4**	**5**	**6**	**7**
Species	SPS; BRH; GRH; CSR	GDS	GZS; SJH	RBT	YBH	WHB; YLB; LMB; SMB; YP; FWD	BLG; RES; GSF; RBS; WCR; BCR
Number	19	8	9	5	6	25	33
Fine_rat	4.54	3.19	3.26	3.99	5.27	3.45	2.45
BAsp_rat	6.93	7.11	8.99	7.80	4.35	6.88	6.68
Csec_rat	1.53	2.23	2.79	1.96	0.83	2.01	2.74
Elp_avg	0.733	0.870	0.932	0.856	0.569	0.872	0.932
MB_prp	0.531	0.474	0.401	0.552	0.329	0.366	0.227
Sca_type	Cycloid	Cycloid	Cycloid	Cycloid	Scaleless	Ctenoid	Ctenoid
Sca_Ard	Yes (all)	Yes	No (all)	No	---	No (all)	No (all)
Sca_Prd	Y; Y; Y; N	No	No (all)	No	---	Yes (all)	Yes (all)
Sca_AM	CRE; CRE; CRE; ENT	UND	ENT	ENT	---	CUT; CUT; SIN; SIN; LOB; CRE	SIN; SIN; SIN; SIN; SIN; SIN
Sca_ED	0.696	0.587	0.682	0.630	---	0.795	0.763
Sca_MBC	105.2	147.5	194.5	1887.6	---	204.7	146.1
Bon_type	Cellular	Cellular	Cellular	Cellular	Cellular	Acellular	Acellular
PC_vert	19	17	13	30	5	12	12
PC_lw	0.931	1.262	0.971	0.898	0.699	1.156	1.176
PC_dw	0.754	0.949	0.980	0.936	0.798	0.951	0.944
PC_mrm	15.76	12.97	17.08	12.26	11.27	12.20	14.82

Table 18 continued…

C_vert	22	19	37	32	33	18	17
C_lw	1.05	1.22	1.04	0.90	1.02	1.26	1.13
C_dw	0.99	1.00	0.93	0.93	0.93	0.98	0.97
C_mrm	17.89	12.98	17.51	12.45	16.07	14.87	17.39
MB_vert	27	23	27	39	16	14	11
Tot_vert	40	36	50	62	38	30	29
Ivj_len	0.787	0.537	0.704	0.756	0.811	0.964	0.772
Cen_len	2.64	2.47	1.93	2.80	2.50	4.70	2.79
Tot_mrm	16.83	12.98	17.29	12.36	13.67	13.54	16.11
Iv_adj	4345.3	2950.7	12047.9	10485.7	13001.8	3974.7	1864.8
Bod_cur	0.371	0.238	0.343	0.438	0.562	0.294	0.185
MBA	75.9	87.5	72.1	61.7	50.8	81.9	98.1
COG	0.445	0.479	0.436	0.463	0.419	0.460	0.464
Duro	62.1	62.2	63.6	52.7	38.7	65.4	67.7
EI_body	0.363	0.310	0.323	0.497	0.245	0.577	0.465

NOTE: Species included Spotted sucker (SPS), Black Redhorse (BRH), Golden Redhorse (GRH), Central Stoneroller (CSR), Golden Shiner (GDS), Gizzard Shad (GZS), Skipjack Herring (SJH), Rainbow Trout (RBT), Yellow Bullhead (YBH), White Bass (WHB), Yellow Bass (YLB), Largemouth Bass (LMB), Smallmouth Bass (SMB), Yellow Perch (YP), Freshwater Drum (FWD), Bluegill Sunfish (BLG), Readear Sunfish (RES), Green Sunfish (GSF), Redbreast Sunfish (RBS), White Crappie (WCR), and Black Crappie (BCR). Each variable is defined in Table 16.

Table 19. Combined results of all multiple linear regressions of relative flexibility including anatomorphic functional guilds (AFG) and taxonomic groups.

Model	m	F-stat	Adj-R^2	AIC	AICc	ICOMP
{Full}	18	60.94	0.9121	-256.49	-246.49	-149.85
{Stepwise}	10	113.30	0.9152	-266.95	-263.56	-222.94
{Best subset}	7	154.10	0.9116	-265.22	-263.33	-242.58
{Base}	7	149.20	0.9089	-262.10	-260.21	-241.35
{AFG3}	9	138.20	0.9223	-277.01	-274.17	-250.60
{AFG6}	12	114.80	0.9292	-284.15	-279.48	-259.51
{AFG7}	13	104.80	0.9284	-282.16	-276.77	-257.08
{AFG7a}	13	108.20	0.9306	-285.36	-279.97	-260.72
{AFG8}	14	100.80	0.9307	-284.75	-278.57	-259.40
{Super Order}	10	101.80	0.9064	-256.61	-253.21	-231.25
{Order}	11	114.90	0.9233	-276.63	-272.63	-249.54
{Family}	15	82.94	0.9220	-271.42	-264.39	-239.11
{Genus}	20	81.27	0.9392	-293.61	-281.27	-253.27
{Species}	27	62.32	0.9409	-291.78	-268.58	-240.27

NOTE: The number of variables (m), F-stat from the analysis of variance, adjusted R^2, and model selection criteria are presented for each model. All models presented here were considered significant (p-values << 0.001). The AFG7a model was considered the most parsimonious and described variation in relative flexibility better than all other models tested.

Table 20. Detailed summary of the log-linear multiple linear regression of relative flexibility, anatomorphic trait data, and seven anatomorphic functional guilds (AFG).

Variables	Coefficient	Standard Error	p-value
Intercept	–0.3657	0.1024	< ***0.001***
Sca_ED	–0.430	0.1130	< ***0.001***
Tot_vert	0.009	0.0021	< ***0.001***
Ivj_len	0.755	0.0452	< ***0.001***
Tot_mrm	–0.032	0.0019	< ***0.001***
Iv_adj	2.02×10^{-5}	3.74×10^{-6}	< ***0.001***
EI_body	–0.979	0.0427	< ***0.001***
AFG–1	0.069	0.0302	***0.0248***
AFG–2	–0.089	0.0344	***0.0114***
AFG–3	–0.174	0.0518	***0.0012***
AFG–4	–0.174	0.0744	***0.0211***
AFG–5	–0.422	0.1009	< ***0.001***
AFG–6	0.081	0.0193	< ***0.001***
AFG–7	---	---	---

NOTE: Variables included scale imbrication (Sca_ED), total number of vertebra (Tot_vert), average intervertebral joint length (Ivj_len), average maximum range of motion (Tot_mrm), adjusted 2nd moment of inertia (Iv_adj), and flexural stiffness of the body (EI_body). Coefficients are presented as original log10 transformed numbers. The final regression produced a significant log-linear model ($F_{12,92} = 118.2$, $p < 0.001$, adj-$R^2 = 0.9311$) and had the lowest model selection criteria including AIC (-287.01), AICc (-282.35), and ICOMP (-262.72) among models tested. The seventh AFG is blank because the intercept applies to this group and it served as a reference from which the other AFGs were compared.

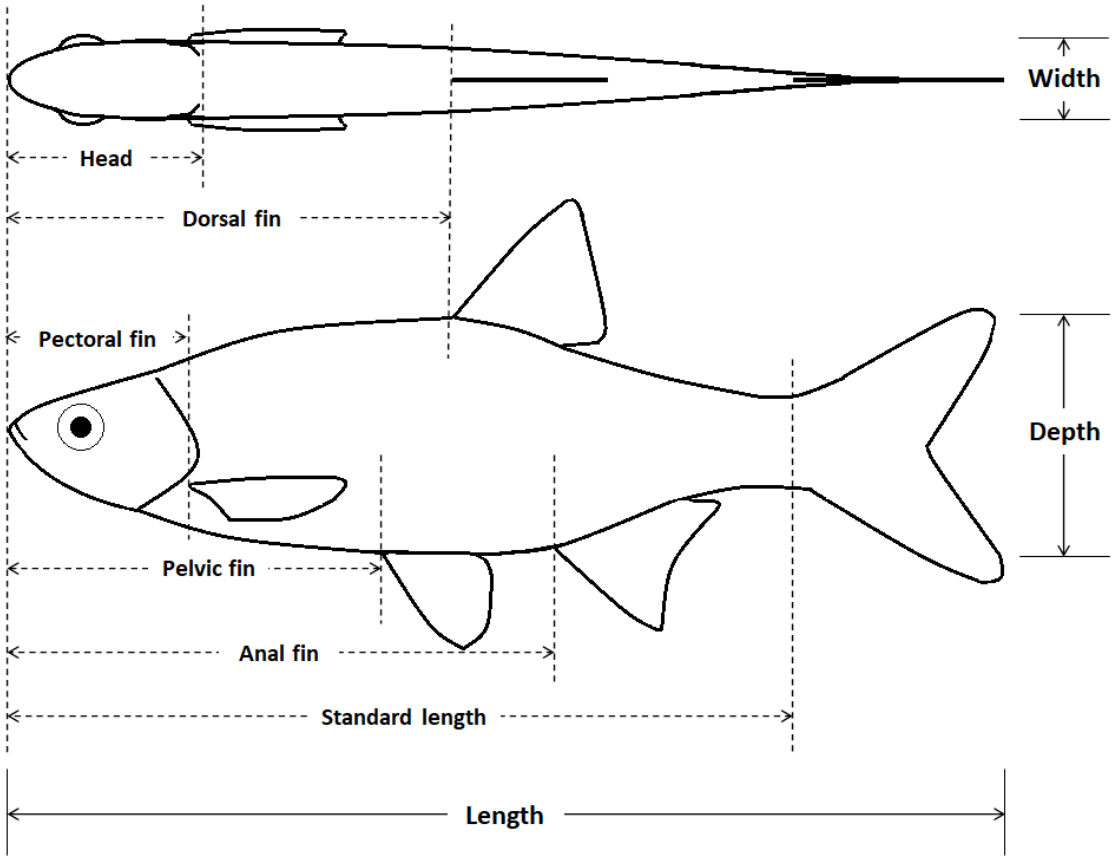

Figure 36. Diagram showing the major body landmarks and size dimensions (body length, depth, and width) that were measured for all fish. Length measurements were made within the indicated horizontal dashed arrows. Body depth and width measurements were taken at each landmark near the vertical dashed lines that mark each body landmark.

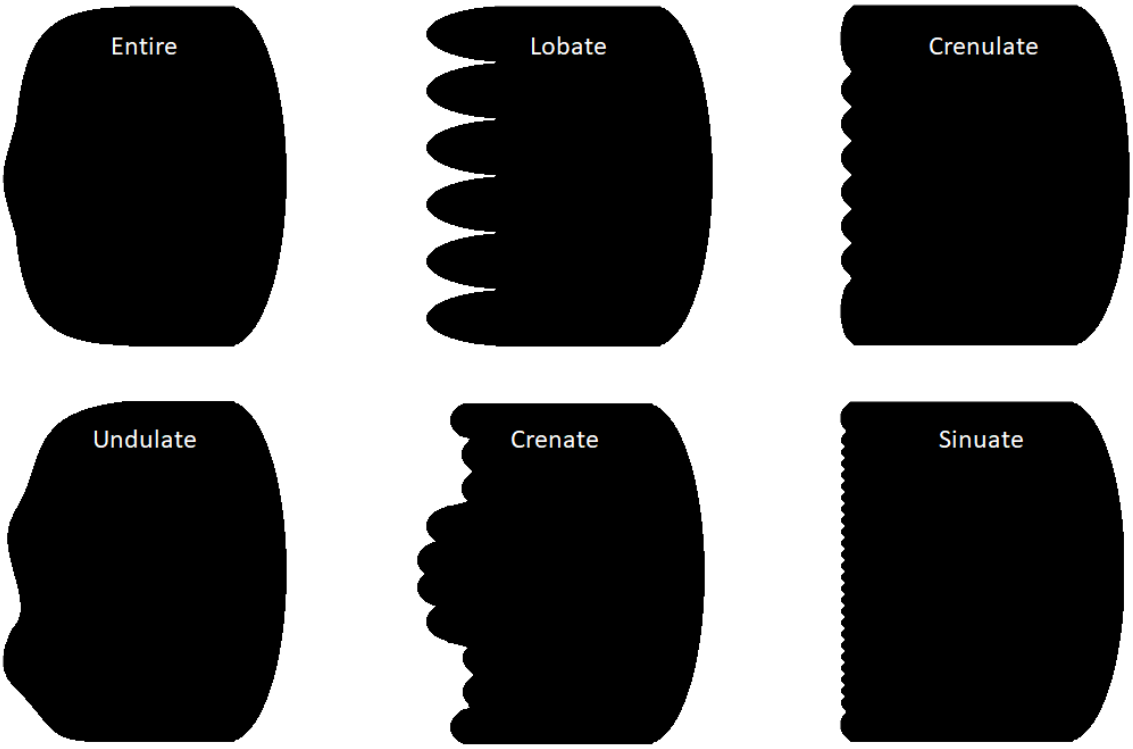

Figure 37. Examples of anterior scale margin morphology from scales taken on the left lateral surface between the posterior edge of the operculum and anterior edge of the caudal fin. Each scale image is drawn in the cranio-caudal (left → right) direction such that the left side is the anterior (embedded) margin while the right side is the posterior (exposed) margin.

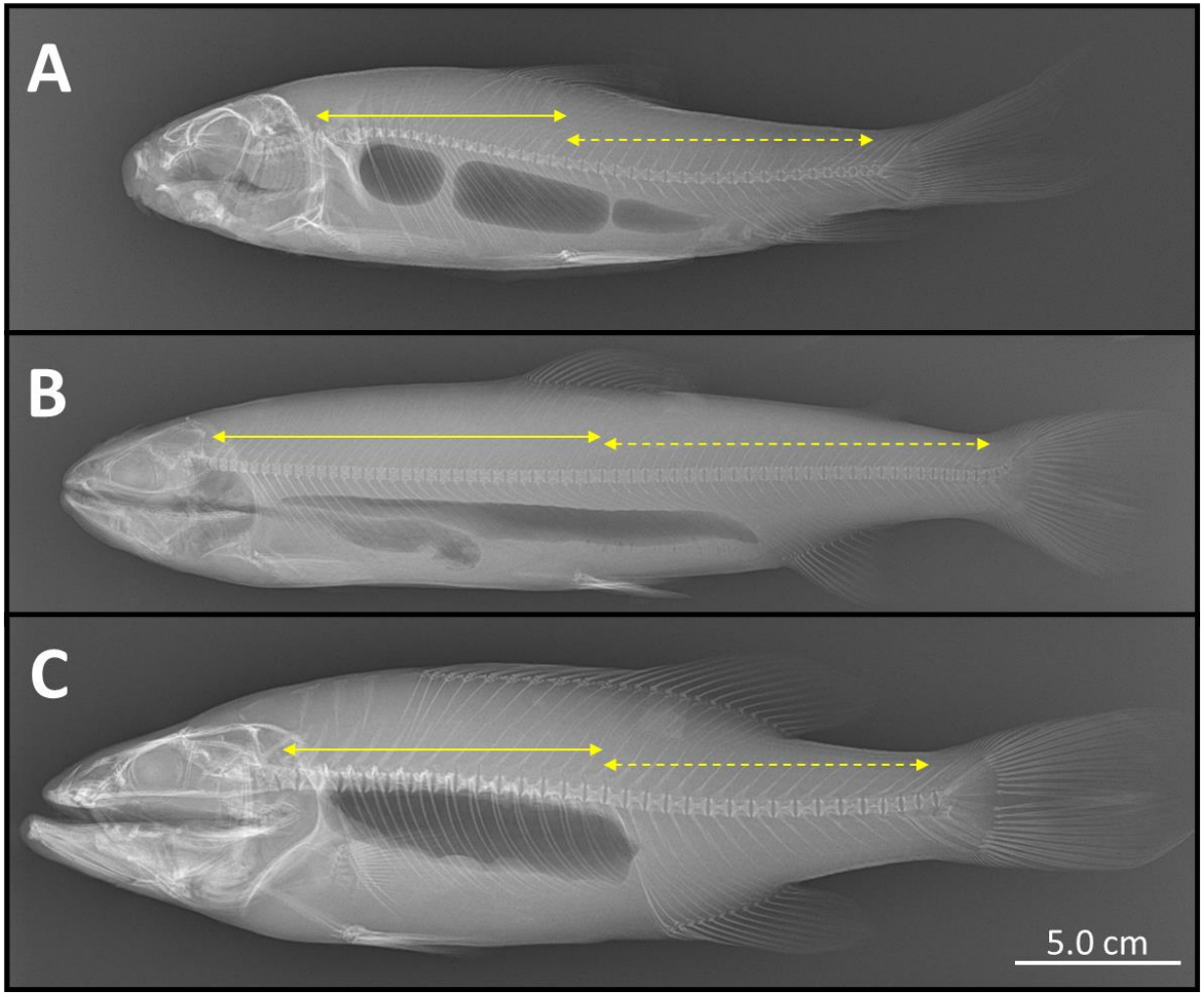

Figure 38. X-ray images of Golden redhorse (A), Rainbow trout (B), and Smallmouth bass (C) showing the relative location of precaudal (rib-bearing; solid yellow line) and caudal (haemal arch-bearing; dashed yellow line) vertebrae for these species.

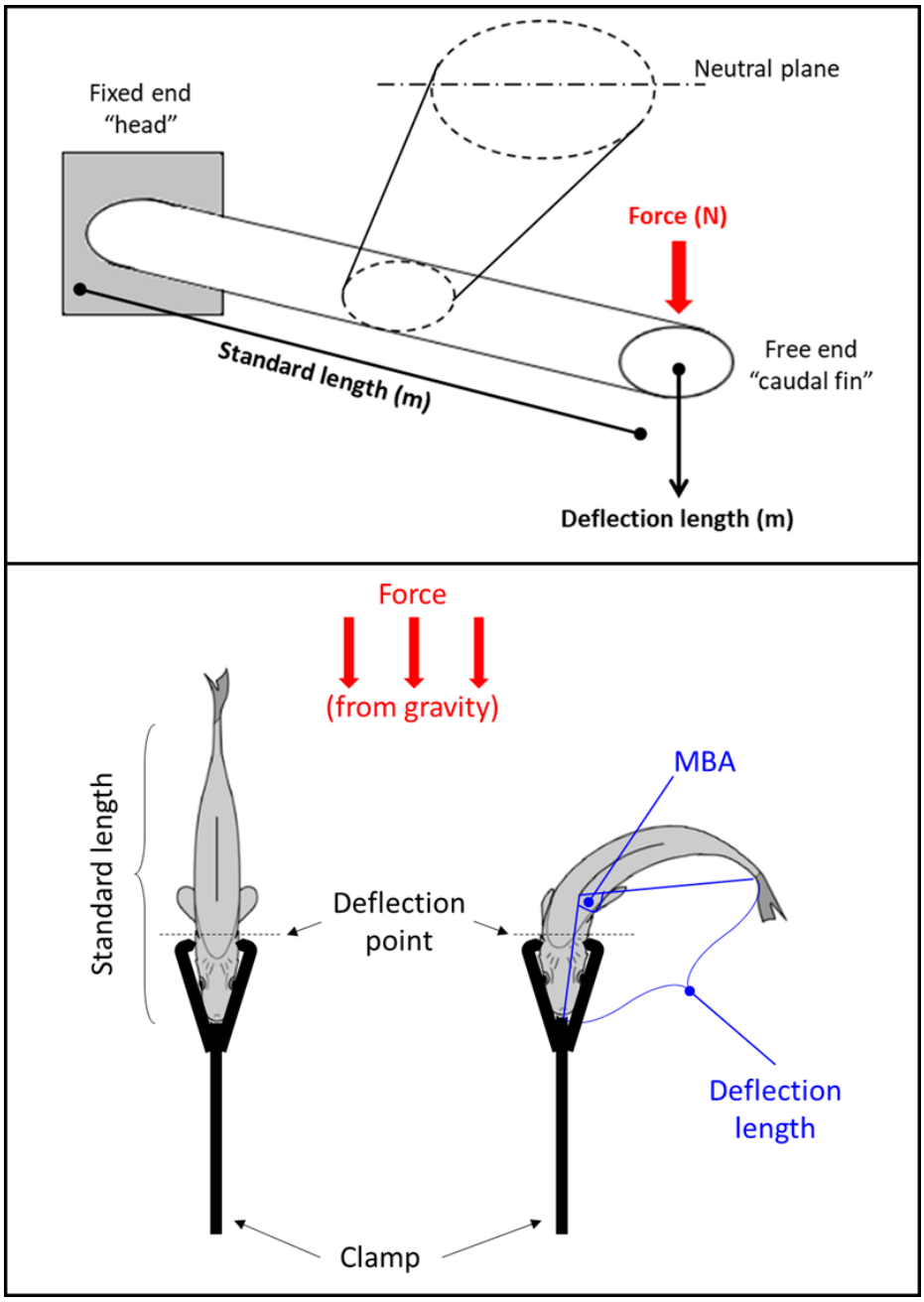

Figure 39. Basic principles of engineering beam theory (top panel) applied to the fish body which was modelled as an elliptical cylinder. Body curvature or relative flexibility (bottom panel) of each fish was estimated by securing the head of the fish and allowing the body to bend near the nape (i.e., the deflection point) to measure deflection length caused by gravity. Maximum bending angle (MBA) was the angle formed between the head, dorsal fin, and anterior edge of the caudal fin as the body bended about the deflection point.

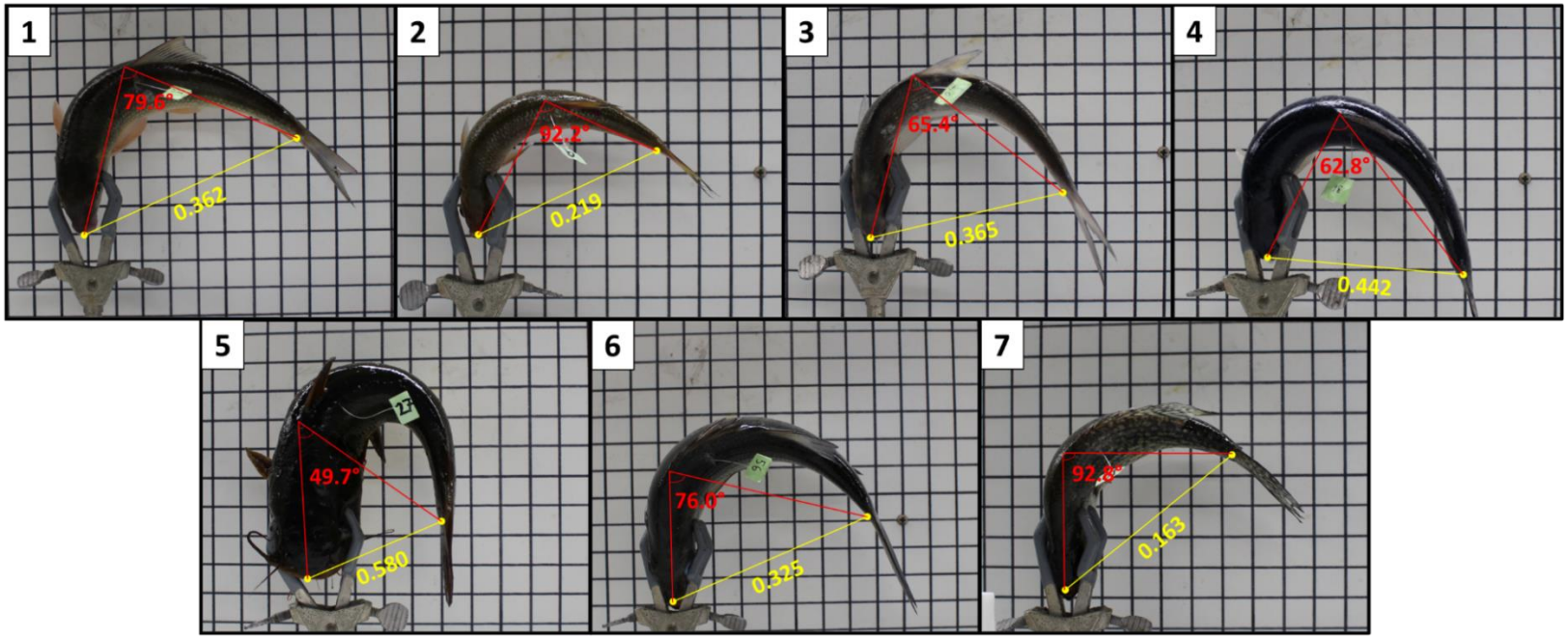

Figure 40. Images depicting how body curvature (an index of relative flexibility) was measured on a member of each anatomorphic function guild (1 – 7 identified from HCPC analysis; See text for more detail). The yellow lines and numbers represent estimated body curvature (ranges between 0 and 1), while the red lines and numbers represent the maximum bending angle formed between the snout tip, anterior edge of the dorsal fin, and caudal peduncle. A representative species of each guild is identified by each numbered image including [1] Black Redhorse, [2] Golden shiner, [3] Gizzard Shad, [4] Rainbow Trout, [5] Yellow Bullhead, [6] White Bass, and [7] White Crappie. Each square is 2.0 cm.

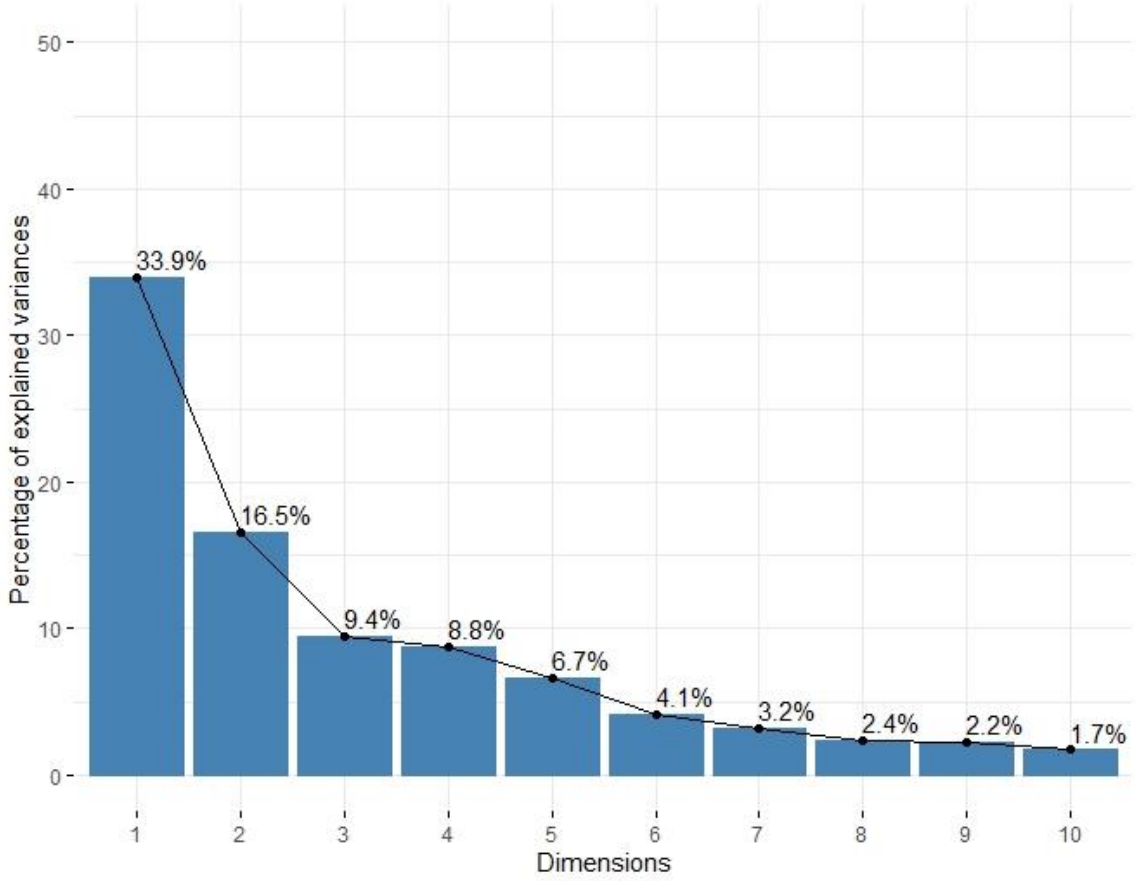

Figure 41. A scree plot of anatomorphic function data showing the first 10 principal components and percentage of variance explained by each.

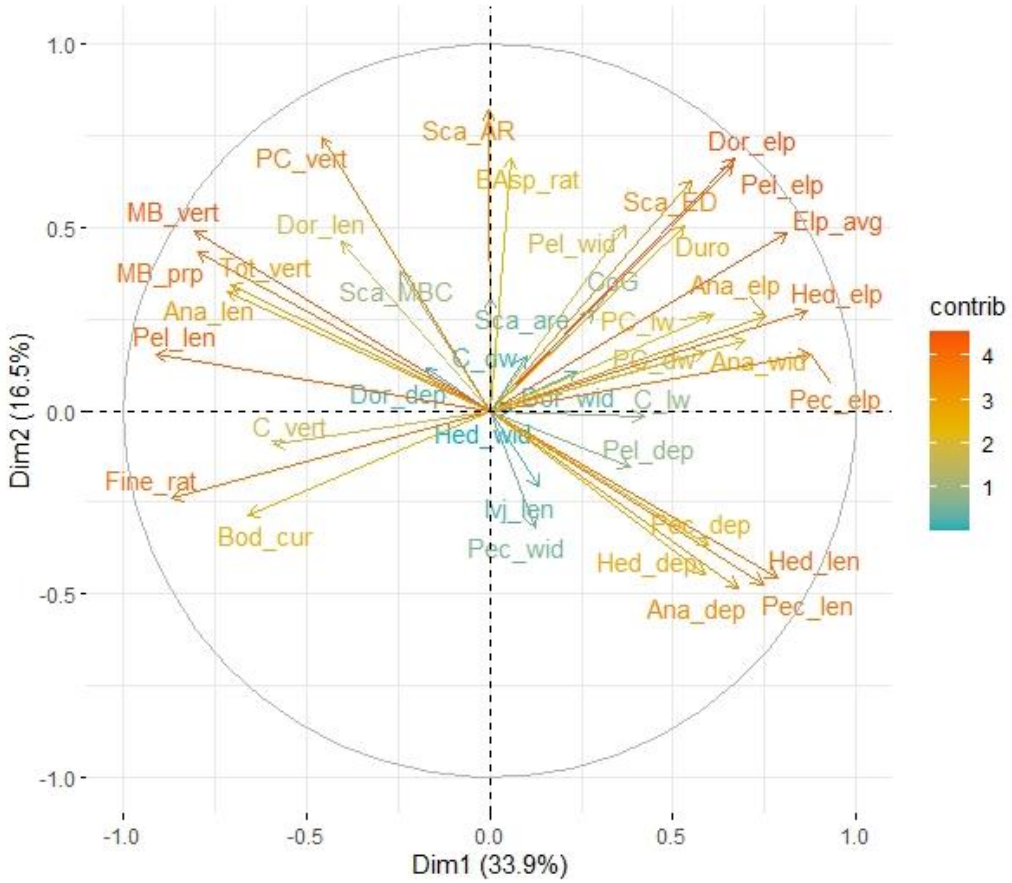

Figure 42. Contribution of each anatomorphic functional variable according to the first two principal component axes. Red colors indicate higher contribution to variation compared to blue colors.

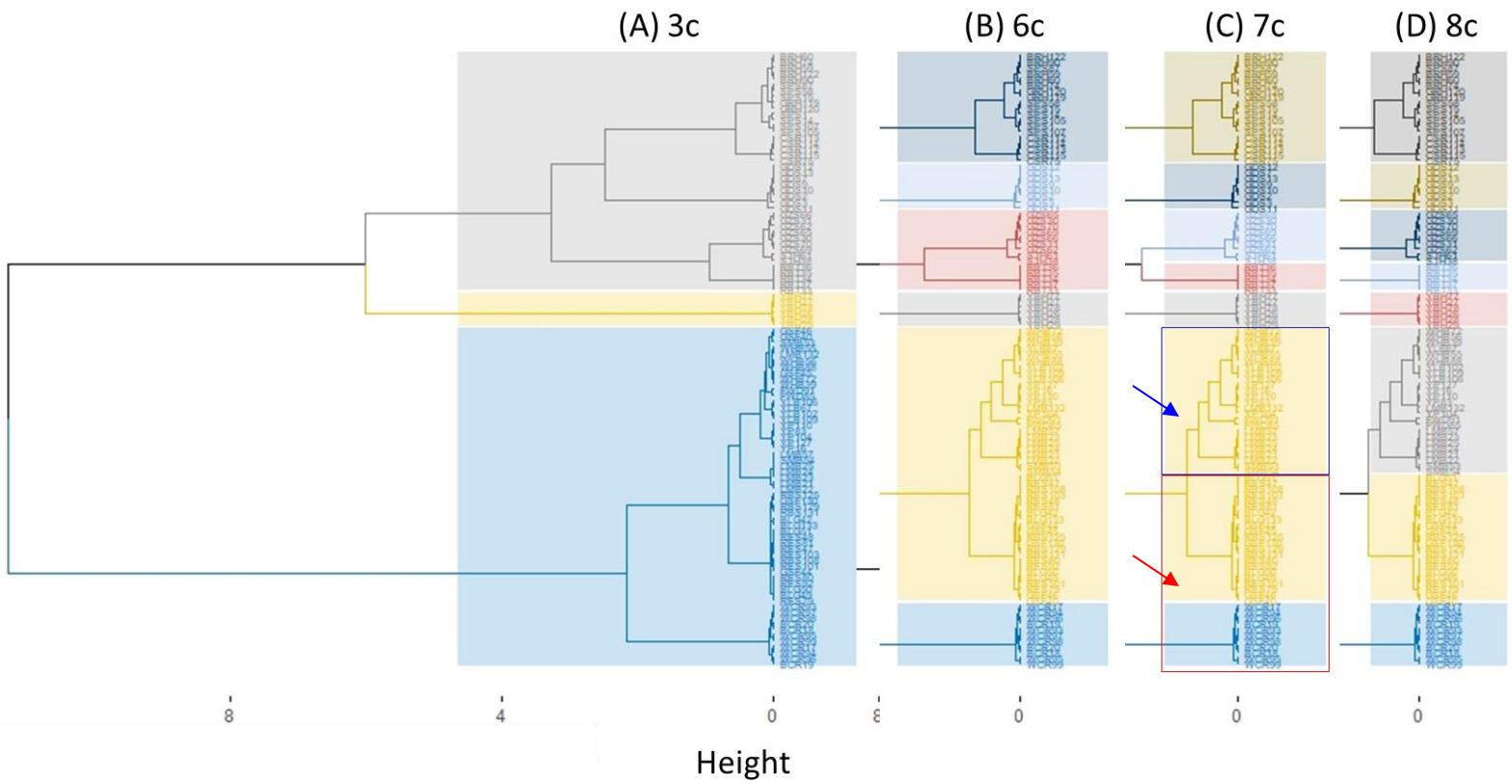

Figure 43. Proposed clusters (anatomorphic functional guilds) produced by hierarchical clustering of principal components (HCPC). The HCPC algorithm always selected (A) three clusters, compared to (B) six, (C) seven, or (D) eight clusters produced by cutting the tree different heights. The red and blue boxes (arrows) on (C) shows the modified 7-cluster scheme that was used for the remainder of the analyses in this study. See Table 3 for a list of member species and average traits associated with each AFG.

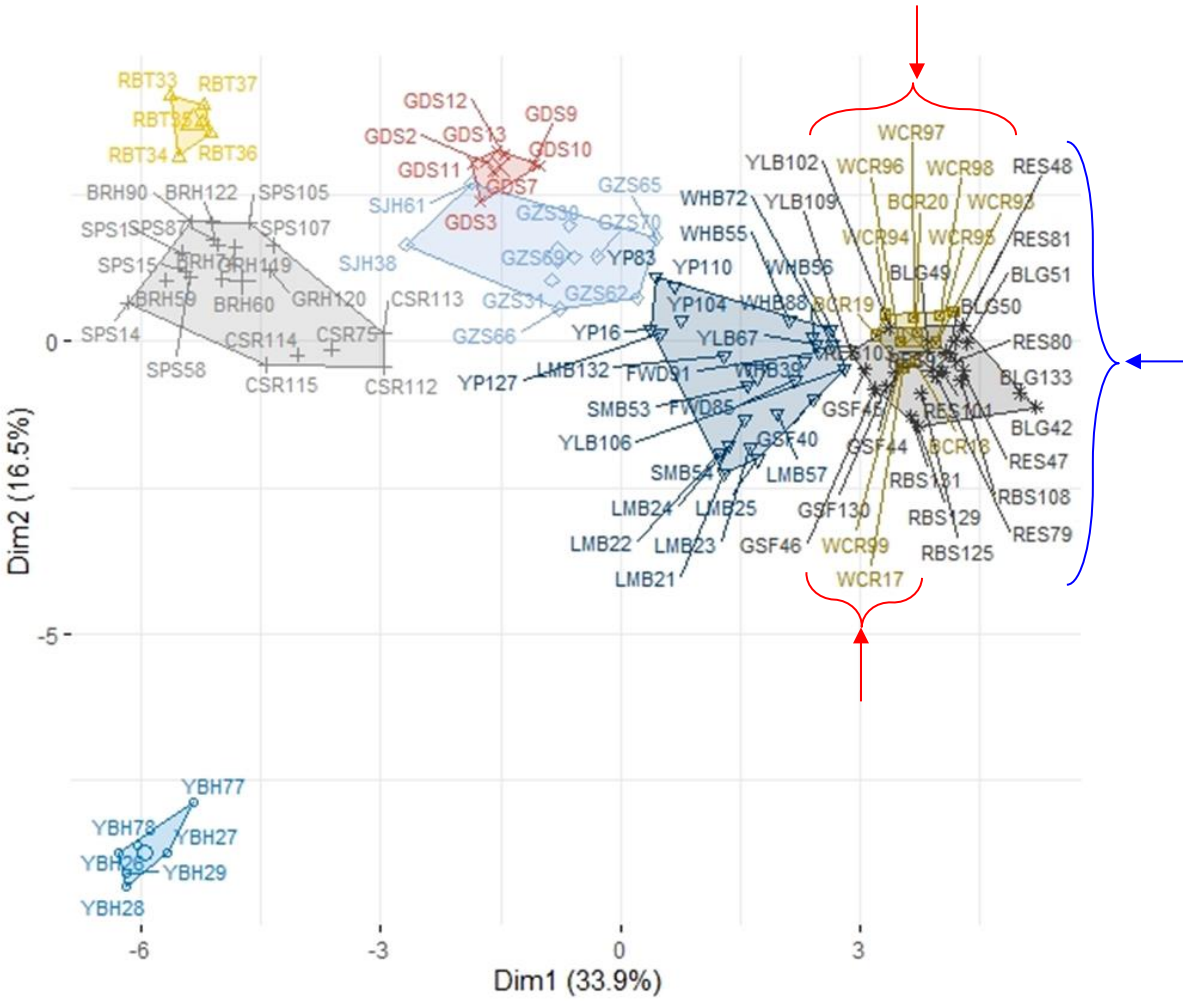

Figure 44. Factor map showing the proposed 8-cluster scheme using hierarchical clustering on principal component (HCPC) analysis. The red brackets show the *Pomoxis* cluster compared to the blue bracket highlighting the *Lepomis* cluster. These two clusters were combined into one cluster used in the modified 7-cluster scheme.

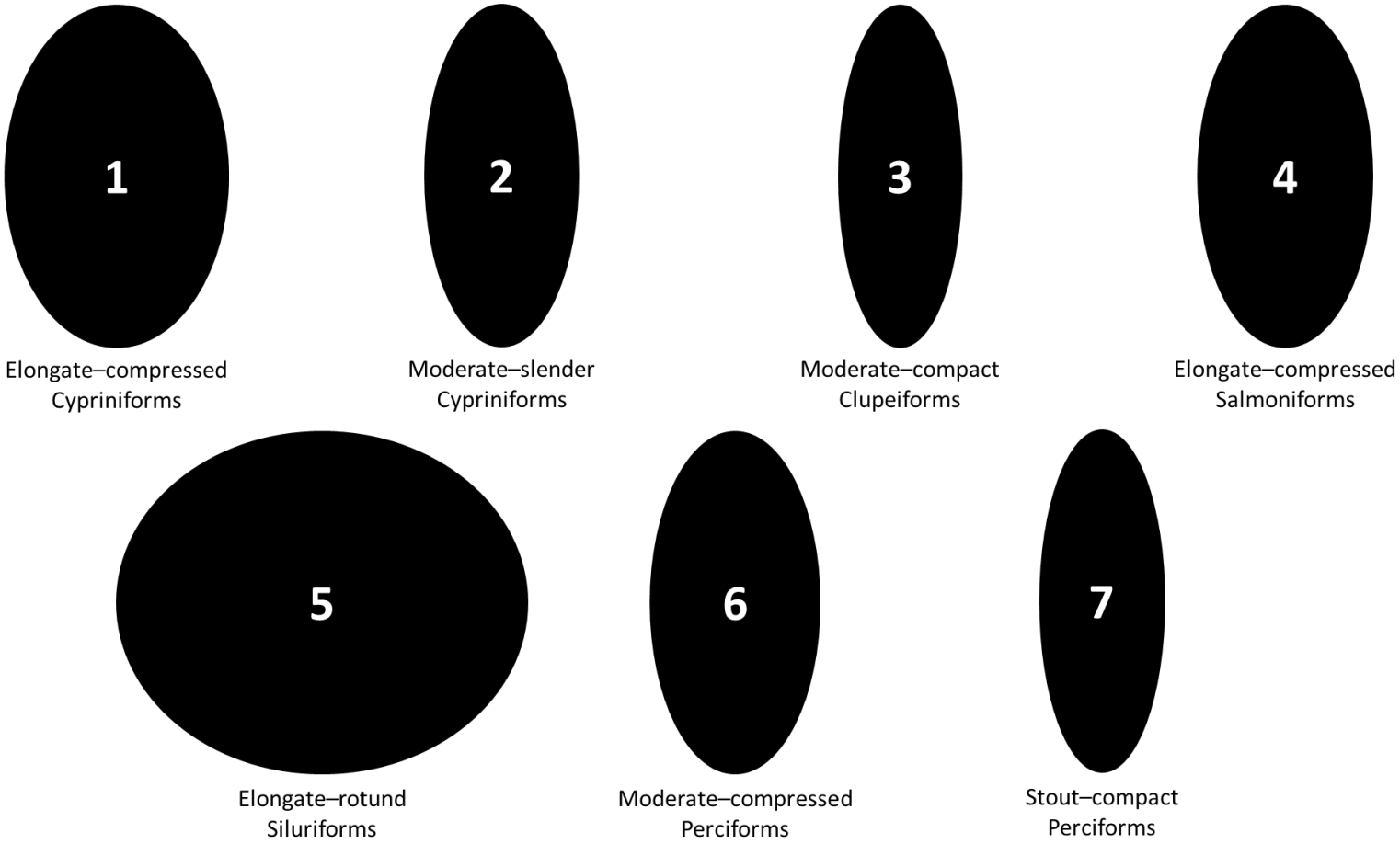

Figure 45. Cross-sectional body profiles for each of the seven anatomorphic functional guilds used in this study. The first describes the relative length while the second describes the relative girth (depth relative to width). The final term was used to represent the most relevant inclusive taxonomic level; however, most guilds were linked to a specific family because species representation was low.

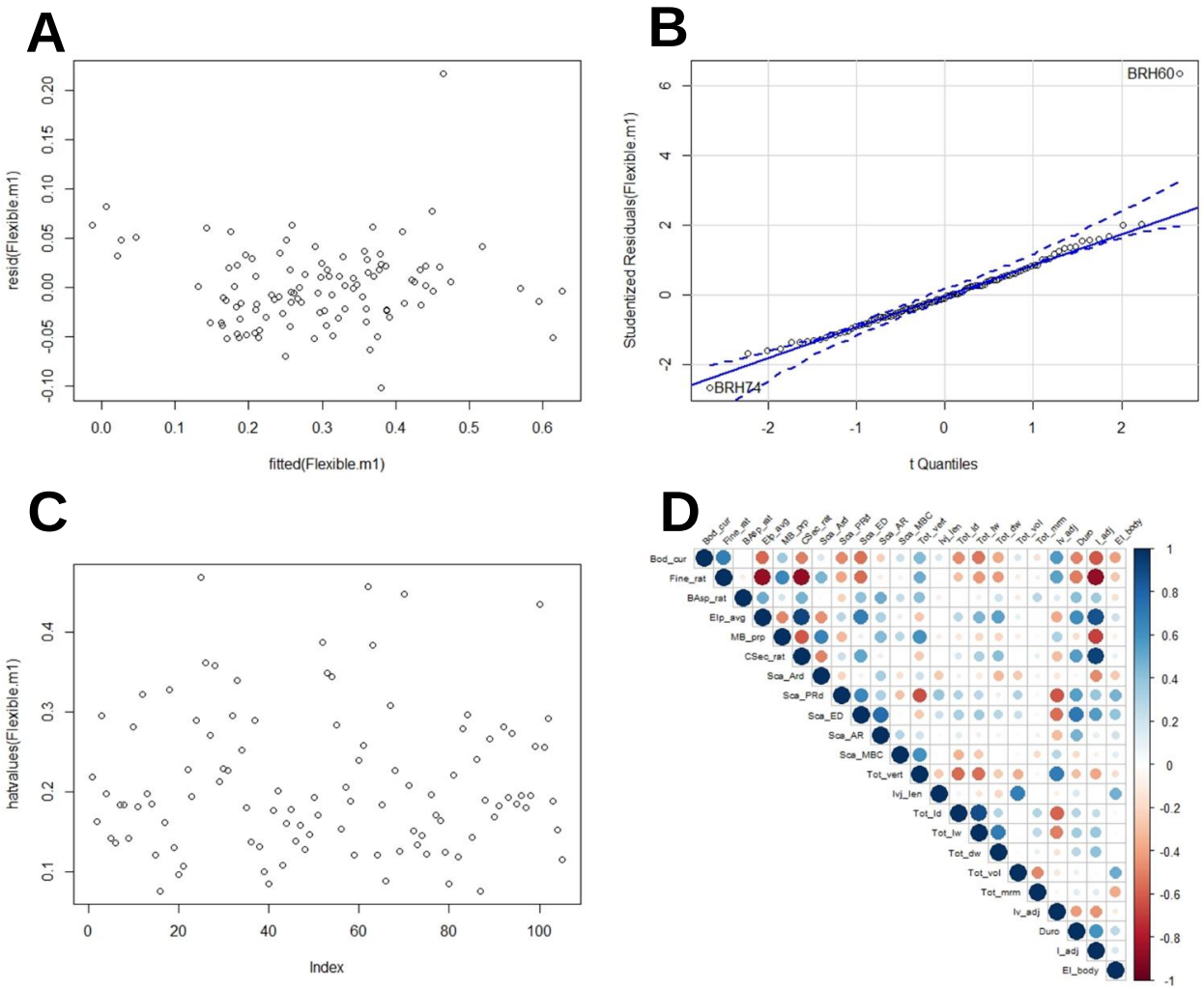

Figure 46. Diagnostic plots for the fully parameterized multiple linear regression model. Includes (A) model fitted values versus residual plot for homoscedasticity, (B) standardized residual plot for normality, (C) hat values plot to detect outliers, and (D) correlation plot for independent variables.

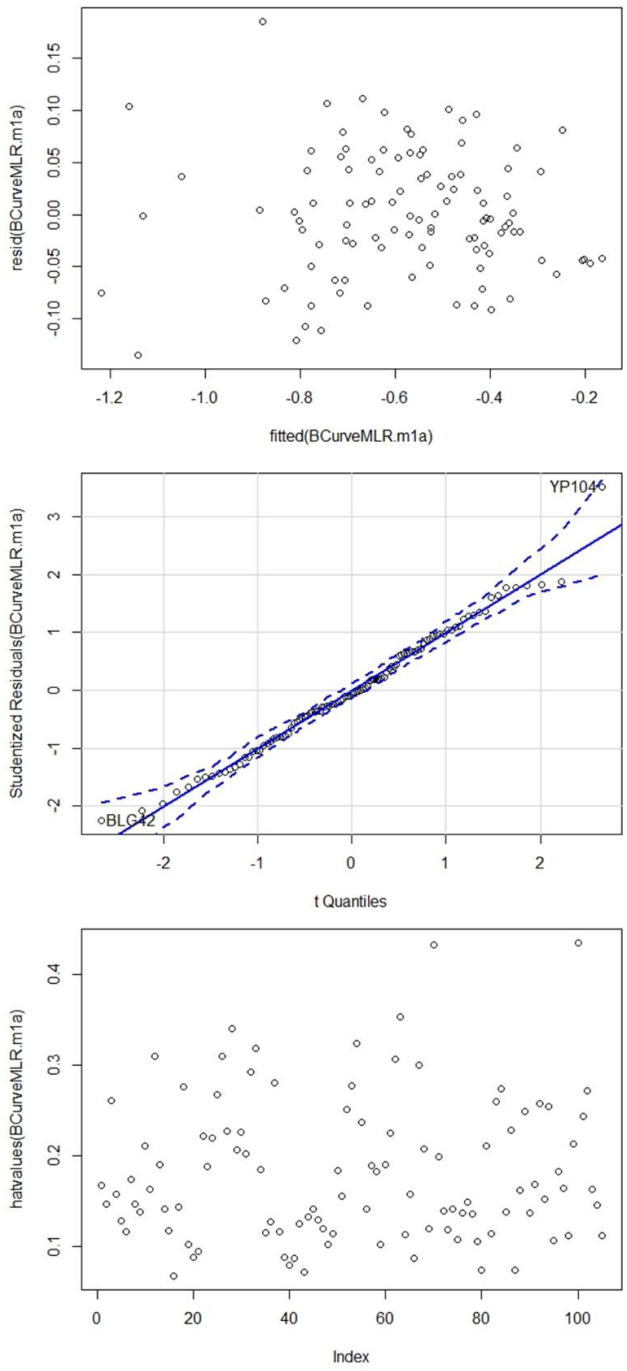

Figure 47. Diagnostic plots for the new model with highly collinear variables removed and log10 transformation of relative flexibility (the predictor variable). The top pane is model fitted values versus residual plot for homoscedasticity, middle panel is standardized residual plot for normality and the bottom panel is hat values plot to detect outliers.

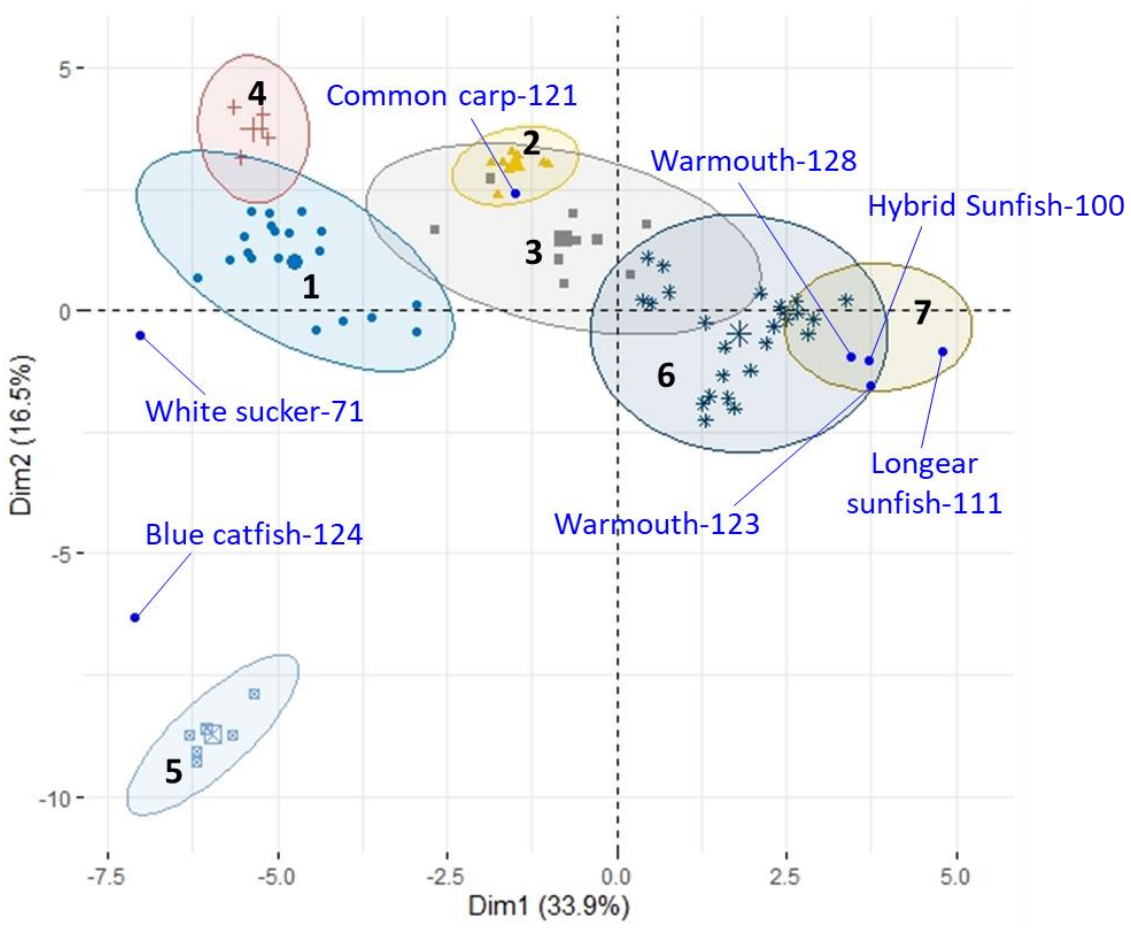

Figure 48. Plot of individuals on the first two principal component axes with ellipses representing each guild. Guild numbers are identified as [1] Elongate-compressed cypriniforms, [2] Moderate-slender cypriniforms, [3] Moderate-compact clupeiforms, [4] Elongate-compressed salmoniforms, [5] Elongate-rotund siluriforms, [6] Moderate-compressed perciforms, and [7] Stout-compact perciforms. The blue dots represent species that were only represented by one individual and were not included in the original analysis, but were projected onto these principal component axes based on their own anatomorphic data.

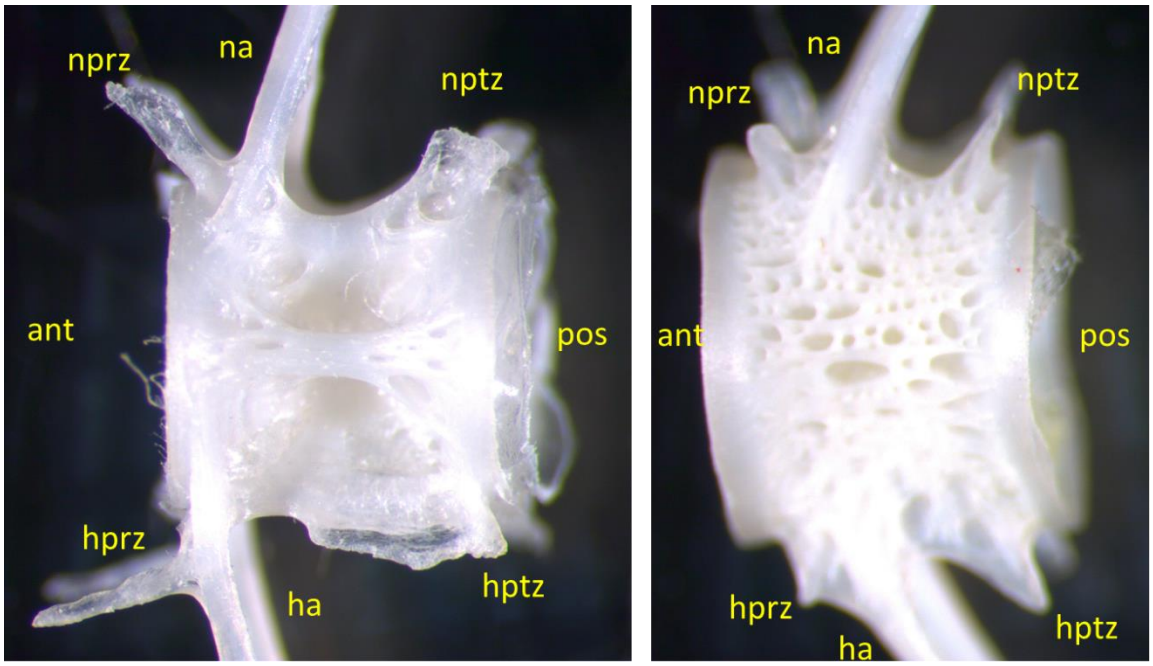

Figure 49. Anatomical disparities found in the caudal vertebrae of Gizzard Shad and Rainbow Trout. Caudal vertebrae are oriented in an anterior (ant) to posterior (post) direction. Specific features include neural prezygapophyses (nprz), neural arch (na), neural postzygapophyses (nptz), haemal prezygapophyses (hprz), haemal arch (ha), and haemal postzygapophyses (hptz).

CONCLUSION

Fish are exposed to many stressors during turbine passage events, but the main focus here was the investigation of blade strike impact specifically. The research presented here has now become part of the literature base which originally began nearly 30 years ago. I approached this topic with three general themes in mind to help me better describe how physical impacts from turbines affect fish. Theme one is best distinguished as applied science content because I sought to add relevant laboratory data to the existing knowledge base using established protocols. That motivation included successfully working with bluegill sunfish (*Lepomis macrochirus*), American eel (*Anguilla rostrata*), rainbow trout (*Oncorrhynchus mykiss*), brook trout (*Salvelinus fontinalis*), American shad (*Alosa sapidissima*), blueback herring (*A. aestivalis*), gizzard shad (*Dorosoma cepedanium*), and paddlefish (*Polyodon spathula*). Dose-response models were created for these species and used to parameterize specialized toolsets to help industry leaders (turbine designers and dam owners/operators) inform design of safer turbines or operations practices. The second theme built upon the first by attempting to quantify how well data from one species may be applied to make inferences about another. More specifically, I directly tested, and provided evidence in support of, using a surrogate species to represent other species at different taxonomic levels (e.g., genus or family). I also showcased how a diverse assemblage of riverine fishes could be grouped together into guilds based on shared functional traits and linked to susceptibility to blade strike impact. These data successfully identified functionally relevant groups of fishes from which surrogates can also be identified. As a result, surrogates—and the creation of guilds they represent—also simultaneously broadens the usefulness and potential application space of dose-response data currently available. Finally, the third theme diverges from the direct study of live fish to the creation of a biomimetic model meant to represent a real fish during a turbine passage event. This theme used laboratory dose-response data to help validate physical model performance during impact testing. In addition, confirmation of surrogacy also suggests the need to create only a handful of actual models that are broadly representative of each functional guild. The following paragraphs summarize blade strike mortality data, describe the utility of dose-response

relationships used to model these data, address data limitations with respect to our industry partners specifically, and suggest additional applications of traits-based approaches for other anthropogenically linked stressors causing disturbances in fish communities.

Results of laboratory experimentation suggests there are useful trends in these data but also revealed contradictory trends and knowledge gaps for a few notable species. Impacts from thinner blades moving at faster velocities are always more detrimental, but the exact impact velocity range describing 0 to 100% mortality is species dependent. Perpendicular impacts relative to the lateral surface between the operculum and anal fin causes the most severe injuries and instances of death across species. Trauma from these strikes is likely more detrimental because of the marked and complete bending of the body around the blade when contact occurs, which is followed by elastic recoil to a neutral position in < 10 milliseconds. Injuries to soft tissues were also more likely to occur from these strikes because most organs are found within this area that also coincides with center of gravity as well (except American eel). For example, one of the more common injuries was observed as visceral hemorrhaging or clotting in the abdominal cavity, though it was usually not possible to link hemorrhaging to a specific organ. Organ injuries including hemorrhaging, clotting, and lacerations were more common in American eel compared to other species, which were likely the result of less skeletal protection (i.e., no ribs) in this species. Rupture or avulsion of the gall bladder, spleen, or swim bladder were only observed in a few individuals across all the species tested suggesting these injuries are rare. The most common injuries were linked with skeletal fractures including the ribs or vertebral column, which also lead to secondary injuries to the musculature found near the fracture sites as well. I suspect that these fractures were also the cause of visceral hemorrhaging/clotting observed in most species as well. Strikes to the caudal region posterior to the anal fin, or shallow angled impacts that deflect away from the center of mass, are less injurious overall and expected mortality was also low. Head strikes were generally less injurious for most species and smaller individuals within a species because they often result in deflections away from the blade. This trend is likely not true for paddlefish which are morphologically distinct

and have an elongate rostrum which may change the inertial effect of bending of the body relative to the head and rostrum. Severe fractures and amputation of the rostrum is possible from blade strike specifically and this trauma was usually not lethal. A notable exception in susceptibility trends among fishes is the nebulous relationship between size and mortality. Contrary trends may be the result of a species × size interaction affect, linked to methodological differences used in the two most prominent testing facilities, or a combination of both. I suspect the contrary trends are actually biologically significant, which indicates that species and size range must be identified so that the correct dose-response model is used. American eel must be tested at velocities of 20 to 30 m/s to determine if impacts from turbine blades are sufficient enough to cause the whole-body amputations observed in the field. Pinching and grinding are the most likely cause of this injury which is quite frequent with some turbine designs and operational regimes. Confirmation of rostrum amputation from blade strike impact for paddlefish would be especially useful information for relicensing efforts associated with for dams on the Missouri and Mississippi Rivers. Finally, catostomid fishes have not been studied in any capacity which is the most glaring weakness because of their unique body shapes, marked species diversity, and extensive range within impacted systems. Comprehensive testing of all impact scenarios is not possible or necessary; however, additional trials would help provide support for the trends that are currently applied to some species with little if any laboratory response data.

The usefulness of these data is undeniable, but caution is advised with model application because some uncertainty exists in these data linked to experiment design and how responses were defined. The biggest uncertainty is actually linked to the fact that researchers know next to nothing about the exact exposure conditions fish experience passing through a turbine. Some hydraulic data have been provided by sensor packages, but information on turbine blade leading edge thickness and more precise estimates of realized strike velocity have yet to be outlined. Obviously, these data are closely guarded trade secrets or proprietary information, but a model is only as good as the data used to build it. Furthermore, to derive useful data we must be able to design the correct experiments that control the dose (turbine characteristics) in order to estimate a

repeatable and appropriate response (mortality). Additional uncertainty is linked to the inherent variation in biological responses and the mathematical models we apply to response data. Mortality is a useful binary response metric, but how it is defined will also greatly impact how the response model is interpreted. For example, fractured vertebrae are the mostly likely cause of death but it is often not lethal and, in many cases, must be confirmed post mortem. This observation necessitated creation of a functional index that signified ecological death even if the fish survived initial impact. Thus, a combined mortality rate provided a more prudent and conservative estimate of mortality because it includes both types of "death". Delayed mortality, caused by less severe vertebral fractures, soft tissue damage, or blood loss, may also be possible and undoubtedly occur at even lower doses than direct and functional mortality. Behavioral impairment could be used to confirm functional death and estimate delayed mortality in the field where necropsies may not always possible. More specifically, indices of behavioral impairment (i.e., lack of eye roll or startle response) are generally easy to measure and replicate, making these indices ideal for field confirmation of functionally dead individuals. Ideally, all mortality types would be estimated so the functional (combined) mortality response curve would be bound by the delayed (behavioral impairment) and observed mortality curves at lower and higher exposure velocities, respectively (Figure 50). The proposed bounds would create a more realistic range of responses and also highlights the inherent biological variation associated with each species.

Uncertainty is also found within model predictions of mortality which complicates interpretation and applicability of these data for our industry partners. The confidence range of mortality estimates is greatly affected by sample size of the treatment groups used to build each dose-response model. In many cases, power analyses suggest that hundreds of fish are needed for each treatment group to have sufficient power to detect a biologically significant treatment effect. Samples sizes of this magnitude undoubtedly limit uncertainty of model predictions which is also of great importance to the target industry defined by precision engineering. However, the time and effort required to produce these numbers can be especially prohibitive because laboratory research on live animals is quite rigorous. I have always advocated that decreasing

sample size in order to cover more treatment scenarios is an equally powerful technique because it allows researchers to assess a much larger range of biological responses. The difference in approaches using 400 fish could result in as little as four (n = 100/group), to as many as 16 (n = 25/group), treatment conditions being evaluated during experimentation. In this way, decreasing sample size has actually decreased uncertainty because more pertinent exposure conditions have been assessed compared to the alternative which only covered ¼ of the possible scenarios. This is especially important for blade strike experiments because the number of possible exposure scenarios is nearly infinite. In addition, laboratory experimentation is defined by the ability to control the dose consistently across all possible treatment conditions such that measurement error is minimized. Neither approach is perfect and the needs of our industry partners will direct which method is best to address passage concerns at each dam. Furthermore, biological variation is always present regardless of sample size or the rigorous experimental controls used to generate data from living organisms. Within these inherent limitations, the current response models should be especially useful to an industry that needs biologically relevant data to better inform turbine design.

Rates of injury and mortality from blade strike represents just one aspect of turbine passage that must be considered by dam owners/operators when estimating the population-level effects of passage. To determine the overall risk to the population, one must also consider entrainment risk and probability of stressor interaction in addition to the rates of injury and mortality from each stressor. While blade strike was the focus of this dissertation, the risk of injury from barotrauma, shear stress, turbulence, or pinching/grinding must be addressed as well. Exact passage conditions are also a function of hydropower dam operations that often differ with seasonal changes in water level and flow rates, which in turn affects the exact exposure level of each stressor during a passage event. Habitat degradation, pollution, and recreational fishing pressue not directly linked with dams or hydropower production, may also affect year-to-year variability of the fish populations within impounded systems. The risk of adverse interaction during turbine passage must also acknowledge that differential survival within a population has been linked with age (or stage) classes as well. Clearly, the population-level effects of turbine

passage are complex and represents a multiplicative probability that includes dam-related stressors and natural population demographics. The risk of entrainment has been estimated for communities of fish based on life history characteristics and fish size. Likewise, the probability of exposure to passage stressors has been estimated using computational fluid dynamics models and sensors capable of detecting hydraulic conditions of an active turbine. Blade strike biological response data have been further developed to create a single, whole-species response curve that accounts for all possible exposure scenarios (location, orientation, and angle of impact) into a single mathematical model. These whole-species response models have been combined with other stressor response models to parameterize new software like the Biological Performance Assessment (BioPA) tool and Hydropower Biological Evaluation Toolset (HBET). These toolsets provide the best estimates of adverse passage risk but would need to be incorporated into Leslie (age-based) or Lefkcovitch (stage-based) models (or matrix) to properly account for changes in riverine fish populations caused by turbine passage (Figure 51). To my knowledge, no such connection between hydropower toolsets and population models is available but would be certainly be useful for species within impounded systems. To that end, the hydropower toolsets and biological response models discussed here represent the most valuable assets available to turbine manufacturers or dam owners to assist with mandatory relicensing efforts.

Quantitative support of surrogacy and creation of anatomorphic functional guilds increase the utility of biological response data and suggests these methods can be applied to other applications as well. Confirmation of surrogacy allows the response model of one species to realistically represent multiple species, which significantly increases the application space of a single dose-response model. Creation of novel anatomorphic functional guilds for the same riverine fish communities also suggests that surrogacy can be applied across taxonomic levels in some instances. These general considerations have only been confirmed for blade strike impact, but I suspect that other passage stressors would also benefit from traits-based approaches as well. In addition to targeted industry partners, confirmation of both surrogacy and guilds suggests far fewer physical fish models would need to be created to accurately investigate community responses to

turbine passage. This is important because more time and financial assets can be directed to develop a few models that maximize biofidelity and data acquisition capabilities. As innovation continues on model development, opportunities to study more live fish are also likely which will allow trends in mortality to be confirmed. If needed, a physical model can be created for any species so that the unique needs of one impacted system are better represented during relicensing efforts. In reality, relicensing requires dam owners and operators to provide environmental assessments of both upstream and downstream passage concerns which dramatically increases the financial burden. Use of traits-based methods for other passage concerns at hydropower dams is also needed so that more effective fishway passage structures can be implemented as well. Eco-hydraulics and swimming performance characteristics are equally important considerations when designing fishway passage structures. In most cases, the most economically valuable and imperiled species receive the most support, while other species (e.g., catostomids) remain mostly untested compared to salmonids and anguillids. Successfully using AFGs for downstream passage and potential "fishway passage guilds" for upstream passage concerns may help design more effective fishways to better restore connectivity for the entire riverine fish community. Lastly, I also argue that creating similar guilds based on shared traits in fish thermal physiology, respirometry, and bioenergetics (among others) would also have climate modeling applications. Many climate models are based on combination of historical trends in species occurrence relative to previous and projected changes in climate only, but does not assess actual physiological limitations (neither lethal nor sub-lethal) placed on species as a result of temperature fluctuations. Creation of such guilds could simultaneously incorporate physiological data into the model and more accurately predict the effects of climate change on an entire fish community.

Gelfish development will also benefit from analyses of relative flexibility which identified many anatomorphic traits that can help focus its innovation moving forward. One essential trait is inclusion of a surrogate vertebral column with approximate dimensions and maximum range of motion that is similar to the species being mimicked. Inclusion of a vertebral column will provide additional biofidelity by maintaining the structural integrity and biomechanical responses of the model during impact. For

example, I observed the tail of Gelfish unnaturally stretch and lag behind the body as the simulated turbine blade made contact with the model. The unnatural lag and stretch was followed by elastic recoil of the tail back to the body as the impact event ended. In contrast, the tail of an actual fish did not lag and generally followed the head and body regardless of where the live fish was struck. The Gelfish also wrapped more completely around the blade (i.e., was more flexible) compared to rainbow trout, which may be linked to the absence of a vertebrae column that would resist bending. The presence of a surrogate vertebrae would help ensure the Gelfish model responded more naturally by providing resistance to bending and additional structural integrity. More rigorous mechanical testing is also needed for the Gelfish model using established static or quasi-static dynamic tests to quantify maximum flexibility. Fish are generally highly flexible organisms when considering swimming performance and C-start (predator escape) behavior observed in most riverine fishes. Alternatively, flexibility may not be the most important biomechanical aspect to measure compared to loading rates or mechanical deformation of the fish body. During impact, the fish body may wrap completely around the blade and return to its natural position in ~ 5 ms, which is comparable to C-start behavior observed in comparably inflexible species as well. However, curvature observed during C-start behavior is the result of muscular contraction within biological limits, whereas blade strike impact exposes the fish body to unnaturally high levels of acceleration and force. Finally, it also appears that the anatomical and biomechanical features of the integument are also important considerations for newer Gelfish models. My traits assessment suggested that scale imbrication significantly influenced relative flexibility and was notably different between AFGs as well. Additional mechanical testing of biological limits would also help separate the exact roles that scales and integument have on the biomechanical properties of the entire organism as well. Regardless, the AFGs and functional relevant traits identified previously suggest that a few biomimetic models can represent multiple species and will help create new versions of the Gelfish model with quantifiably higher biofidelity.

Appendix

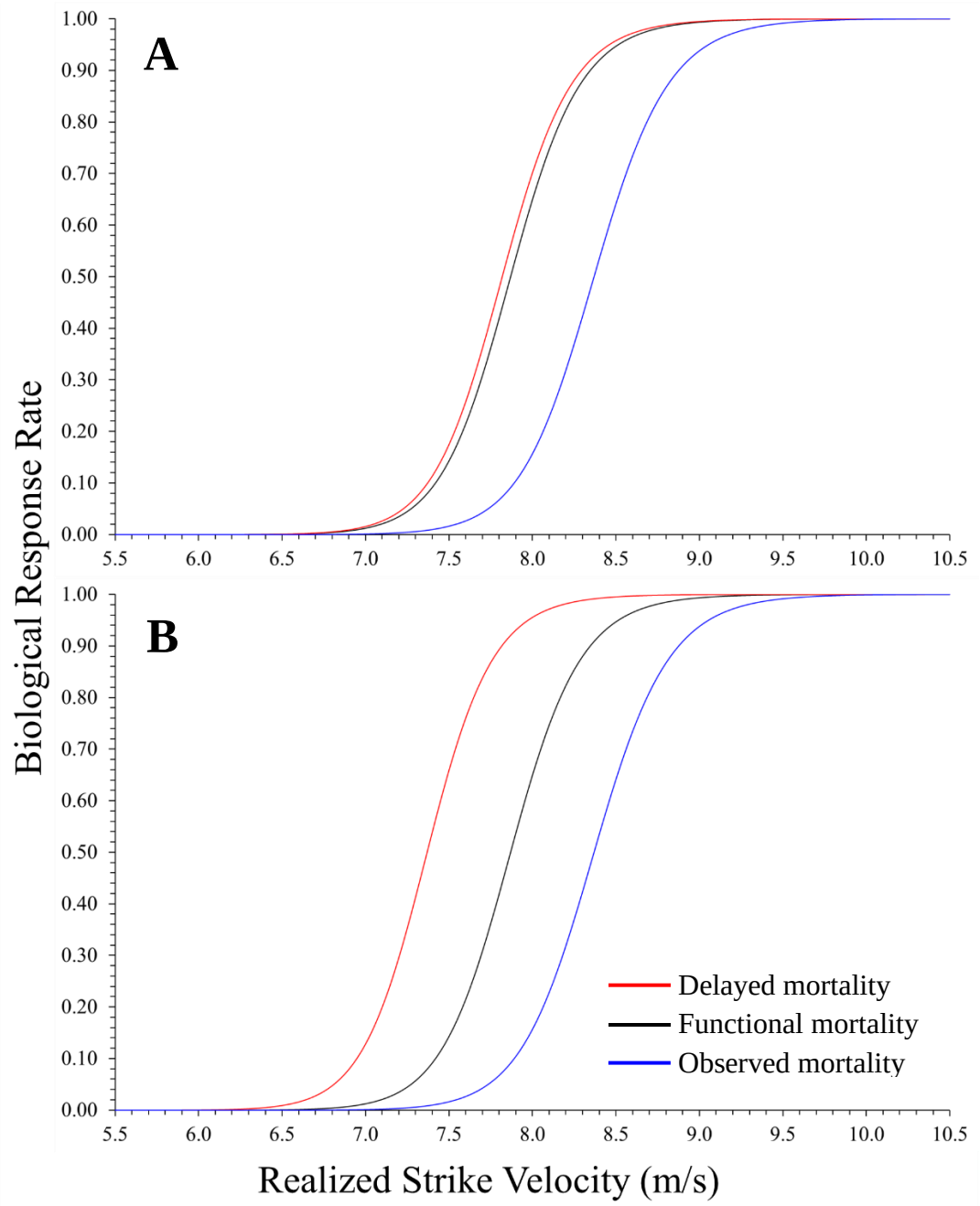

Figure 50. Hypothetical biological response curves for delayed (or behavioral impairment), functional (combined), and observed (instantaneous) mortality rates that provide a "biological confidence interval" for each species in response to blade strike impact. Scenario (A) assumes that delayed and functional mortality rates are approximately the same, whereas scenario (B) highlights delayed mortality occurring at noticeably lower velocities compared to functional mortality.

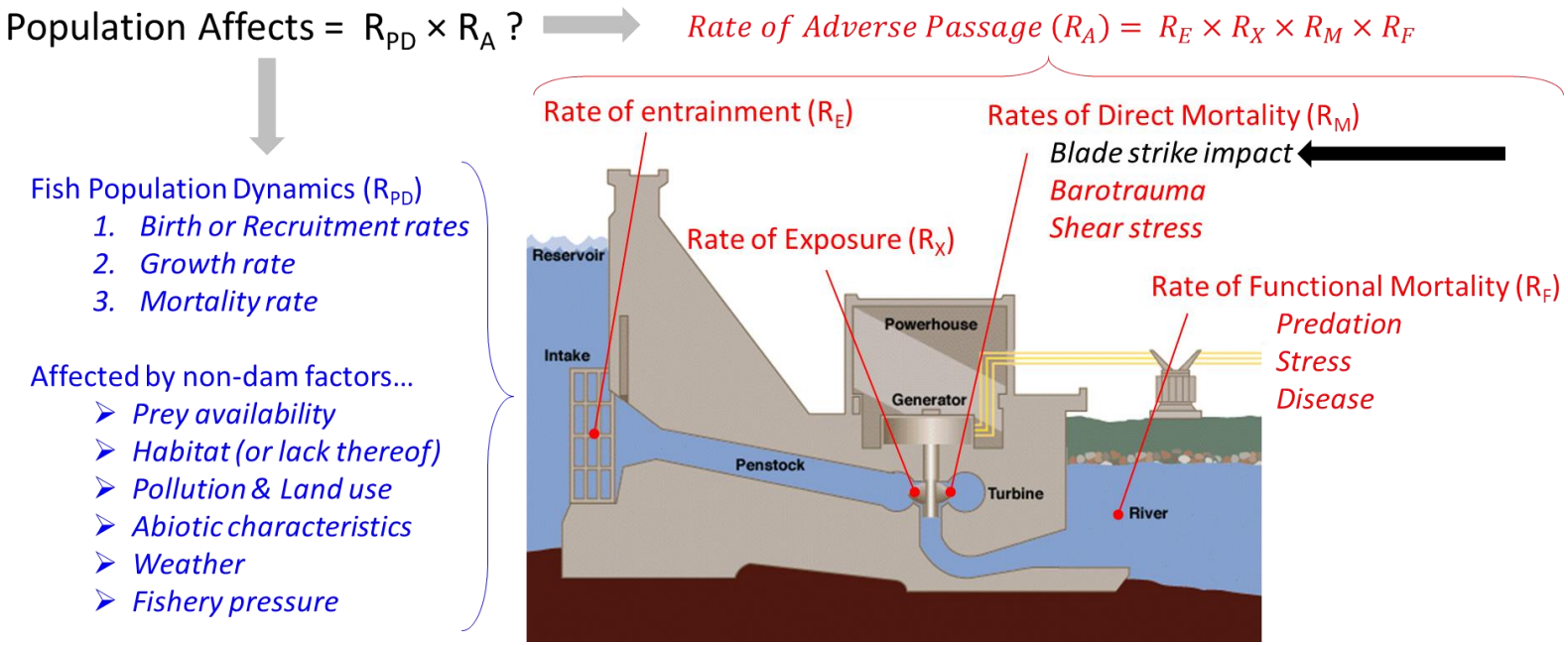

Figure 51. Theoretical calculation of population-level effects of adverse turbine passage for a susceptible riverine species. Natural fish population dynamics (and recreational fisheries) are also a major consideration for an impounded system which may also be affected by a variety of non-dam related factors. Rate of adverse passage through a turbine is a multiplicative probability that accounts for rates of entrainment, exposure, direct mortality, and functional mortality. The exact method for which to calculate the population-level effects of turbine passage for a species is unresolved, but could be connected to Leslie or Lefkovitch population models that also track age or stage groups, respectively as well. The black arrow (and text) represents the stressor that was the focus of this dissertation – i.e., impacts from hydropower turbine blades.

VITA

Ryan Saylor was born in rural town called Salisbury in southwestern Pennsylvania. He graduated from Salisbury-Elk Lick Highschool in 2001, and joined the undergraduate program at University of North Carolina at Wilmington in August of that year where he earned a double bachelor's degree in Marine Biology & Chemistry in 2005. Following graduation, he interned as an aquarist at the South Carolina Aquarium in Charleston for six months, worked as a field technician studying bull trout populations in eastern Oregon for three months, and assisted a PhD student as a fisheries technical studying ecology of non-native northern snakehead in the Potomac River for about one year. Following these field-related experiences, he pursued and eventually completed, a master's degree in Biology from the University of West Florida in 2013 where he studied the thermal physiology of non-native Asian swamp eel. Following his master's degree, he worked as a thermal stress modelling consultant with Mark Bevelhimer (his current PhD adviser) for six months. Following the consultant work, Ryan was encouraged to join the Aquatic Ecology Laboratory at Oak Ridge National Laboratory and pursue his PhD through the Bredesen Center for Interdisciplinary Research and Graduate education at the University of Tennessee. Ryan officially joined the Bredesen Center in August of 2015 to pursue a PhD in Energy Science and Engineering with a concentration in Environment & Climate Sciences.